Technical Report Documentation Page

1. Report No. FHWA/TX-07/0-5132-1	2. Government Accession No.	3. Recipient's Catalog No.
4. Title and Subtitle Recommendations for Reducing Superpave Compaction Effort to Improve Mixture Durability and Fatigue Performance		5. Report Date October 2006 6. Performing Organization Code
7. Author(s) Jorge A. Prozzi, Jose P. Aguiar-Moya, Andre De F. Smit, Maghsoud Tahmoressi, Kenneth Fults		8. Performing Organization Report No. 0-5132-1
9. Performing Organization Name and Address Center for Transportation Research The University of Texas at Austin 3208 Red River, Suite 200 Austin, TX 78705-2650		10. Work Unit No. (TRAIS) 11. Contract or Grant No. 0-5132
12. Sponsoring Agency Name and Address Texas Department of Transportation Research and Technology Implementation Office P.O. Box 5080 Austin, TX 78763-5080		13. Type of Report and Period Covered Technical Report September 2004–August 2006 14. Sponsoring Agency Code
15. Supplementary Notes Project performed in cooperation with the Texas Department of Transportation and the Federal Highway Administration.		

16. Abstract

The Texas Department of Transportation (TxDOT) has recently established Hamburg Wheel Tracking Device (HWTD) specification criteria for Superpave mixtures (Item 344). This step has introduced a performance-related feature into an otherwise volumetric mix design approach structured to ensure asphalt mixtures with high shear resistance to rutting. The Superpave mixture design procedure is itself geared toward the production mixtures with high rutting resistance. This, together with the new HWTD criteria, tends to promote "dry" mixtures with lower binder contents than before. While this shift is advantageous for rutting resistance, some reports show that these mixtures are prone to cracking, which is becoming the single largest problem for hot-mix asphalt (HMA) pavements in Texas.

In an attempt to produce mixes with higher binder contents to alleviate cracking problems, this research study investigated the possibility of modifying the current design criteria established for Superpave mixtures. The initial findings of this study indicate that the current compaction effort expressed by the number of design gyrations (N_{design}) could be lowered from 100 to 85 without significantly compromising the rutting resistance of the mixes, while improving cracking resistance and durability.

An extensive experimental program has been devised to investigate the performance characteristics of asphalt mixtures designed using the revised N_{design} levels and to account for the nominal maximum aggregate size and the concentration of coarse aggregate in the mix. The experimental matrix included two aggregate types (limestone and gravel), three binder grades (PG 64, 70, and 76), and three nominal maximum aggregate size (9.5, 12.5, and 19 mm). Although the testing was extensive, the recommendations in this report should be considered preliminary until more experimental evidence is gathered.

In addition, by reducing the compaction effort (for the same target density) the voids in the mineral aggregate (VMA) increase, thus making it easy to meet VMA specifications and ensuring a performing mixture.

17. Key Words	18. Distribution Statement
Superpave, optimum binder content, compaction effort, gyratory compaction	No restrictions. This document is available to the public through the National Technical Information Service, Springfield, Virginia 22161; www.ntis.gov.

19. Security Classif. (of report)	20. Security Classif. (of this page)	21. No. of pages	22. Price
Unclassified	Unclassified	190	

Form DOT F 1700.7 (8-72) Reproduction of completed page authorized

Recommendations for Reducing Superpave Compaction Effort to Improve Mixture Durability and Fatigue Performance

Jorge A. Prozzi
Jose P. Aguiar-Moya
Andre De F. Smit
Maghsoud Tahmoressi
Kenneth Fults

CTR Technical Report:	0-5132-1
Report Date:	October 2006
Project:	0-5132
Project Title:	Analysis of Laboratory Compactive Effort to Optimize the Durability of Superpave Mixture Design
Sponsoring Agency:	Texas Department of Transportation
Performing Agency:	Center for Transportation Research at The University of Texas at Austin

Project performed in cooperation with the Texas Department of Transportation and the Federal Highway Administration.

Center for Transportation Research
The University of Texas at Austin
3208 Red River
Austin, TX 78705

www.utexas.edu/research/ctr

Disclaimers

Author's Disclaimer: The contents of this report reflect the views of the authors, who are responsible for the facts and the accuracy of the data presented herein. The contents do not necessarily reflect the official view or policies of the Federal Highway Administration or the Texas Department of Transportation (TxDOT). This report does not constitute a standard, specification, or regulation.

Patent Disclaimer: There was no invention or discovery conceived or first actually reduced to practice in the course of or under this contract, including any art, method, process, machine manufacture, design or composition of matter, or any new useful improvement thereof, or any variety of plant, which is or may be patentable under the patent laws of the United States of America or any foreign country.

Notice: The United States Government and the State of Texas do not endorse products or manufacturers. If trade or manufacturers' names appear herein, it is solely because they are considered essential to the object of this report.

Engineering Disclaimer

NOT INTENDED FOR CONSTRUCTION, BIDDING, OR PERMIT PURPOSES.

Project Engineer: Randy B. Machemehl
Professional Engineer License State and Number: Texas Number 41921
Research Supervisor: Jorge A. Prozzi

Acknowledgments

The authors express appreciation to Richard Izzo (Construction Division), Thomas Saenz (El Paso District), Alberto Pardo (Corpus Christi District), and Luis C. Peralez (Pharr District) for their commitment to the goals of this research project, and for generously sharing their time and expertise in pursuit of those goals.

Products

This report contains Product 1 as Appendix A, Product 2 as Appendix B, and Product 3 as Appendix C.

Table of Contents

List of Figures

List of Tables

1. Introduction

The Superpave mix design method was developed as a result of the Strategic Highway Research Program's (SHRP) Asphalt Research Program, which took place between 1987 and 1993. The concept behind this method was that of incorporating performance, environmental conditions, load factors, and material characterization in one design or evaluation process in order to improve the performance of asphalt pavement structures by reducing rutting, thermal cracking, and fatigue cracking.

Several years after the Superpave mixtures were used in numerous states and with the introduction of performance-related tests such as the Hamburg Wheel Tracking Device (HWTD) and the Asphalt Pavement Analyzer (APA), it was observed that, while the mixtures are performing well in terms of rutting resistance, some of the pavement structures had begun to crack relatively early. One possible reason for this occurrence is that the Superpave volumetric mix design method and the performance requirements for tests like the HWTD are promoting asphalt mixtures that have low asphalt content in order for the mixtures to have superior rutting resistance.

Currently, the Texas Department of Transportation (TxDOT) has established HWTD specification criteria for Superpave mixtures. This has introduced a performance-related feature to an otherwise volumetric mix design approach structured to ensure the rutting performance of asphalt mixtures. The Superpave mixture design procedure is itself geared toward the production of rut resistant mixtures, which, together with the new HWTD performance criterion, tends to promote mixtures with lower binder contents. While advantageous for rutting resistance, these mixtures are reportedly prone to cracking, which is becoming the single largest problem for Hot Mix Asphalt (HMA) pavements in Texas.

In an attempt to produce mixes with higher binder contents to alleviate cracking problems, TxDOT has investigated the possibility of modifying the current design criteria established for Superpave mixtures. Initial research investigating the influence of lowering the 4% voids in the mix criterion to 3% and even 2.5% has resulted in increased optimum binder contents but lowering the voids has proven detrimental for those mixtures using softer binders; however, research findings from the NCAT test track indicate that more asphalt could be placed into mixtures that have highly polymer-modified binders. The Superpave mixture design method does not account for mixes with extremely stiff polymer-modified asphalts currently being used. Furthermore, the concentration of coarse aggregate in the mix and the influence of nominal maximum aggregate size are not accounted for.

In contrast to the Marshall and Hveem methods, the Superpave mix design method does not include a standard test such as mixture stability and flow. The Superpave mixture design method relies entirely on the volumetric properties of the mix, originally conceived for asphalt mixtures to be used in lower volume roads. For the design of asphalt mixtures meant to be used on higher volume roads, the method originally required that the asphalt mixture's potential for permanent deformation, fatigue cracking, and low-temperature cracking be evaluated.

The main tool in volumetric mix design is the Superpave Gyratory Compactor (SGC). A satisfactory mix design is one that meets rigorous volumetric requirements at initial and design levels of gyration (N-initial and N_{design}, respectively); these levels are, in turn, determined by the total traffic, expressed in equivalent single axle loads (ESALs), expected on the pavement over its projected service life (usually 20 years).

Based on these criteria, it is expected that the SGC densification curves correlate with pavement performance and, in particular, with permanent deformation, which has been analyzed in previous research conducted by the National Cooperative Highway Research Program (NCHRP). But as mentioned previously, by promoting asphalt mixtures with low asphalt content, the design criteria and specifications are simultaneously promoting stiffer, less flexible asphalt mixtures that do not perform well in the long run, specifically under fatigue cracking. This has been one of the biggest challenges in asphalt pavement mixture design: how to obtain an asphalt mix that performs well at high temperatures or slow-moving traffic (rutting) and that simultaneously performs adequately at lower temperatures (fatigue and thermal cracking).

1.1 Problem Statement

The challenge in formulating an optimum asphalt mixture is achieving an acceptable balance between often-opposing mixture properties (resistance to plastic deformation and fracture) and accounting for environmental, functional, and economic considerations. All mixture designs are based on this premise and have the same objective. It is the methods employed to achieve this objective that differ, be it through empirical approaches, volumetric design, performance based/related, or even analytical methods. The ultimate goal is a mixture that will perform according to design expectations in the field.

The Superpave mix design method as employed by TxDOT (Specification Item 344) is essentially a (level 1) volumetric approach. A mixture design process can be defined as volumetric if the choice of design binder content and aggregate gradation is obtained by analyzing the proportional volumes of air voids (VIM), binder and aggregates for mixes that have been compacted using a test procedure that attempts to reproduce in the laboratory the in-situ compaction process. The advantage of this approach is that specification criteria can be established to judge the quality and control of asphalt mixtures during the manufacturing process and during construction in the field. The disadvantages of this approach are that the mix designer is restricted when adjustments to the volumetric properties are desired (e.g., adjusting the voids in the mineral aggregate or VMA) but, more importantly, the performance of the mixture is not explicitly considered as part of the design process. TxDOT has responded to the latter by including HWTD criteria in the latest Superpave mix specifications. This in itself is a step in the right direction since it directly addresses the problem of rutting in asphalt mixtures. What the approach fails to address, however, is the fatigue or cracking resistance that is reportedly becoming the more severe problem. Research is currently underway to incorporate the TTI Overlay Tester to address this aspect.

In an effort to address fatigue cracking of pavements, previous research has lowered the target air void content in the laboratory from 4% to 3% and even 2.5% to increase optimum binder content. While this approach has proven detrimental to mixes with softer binder, research conducted at the National Center for Asphalt Technology (NCAT) indicates that it may be feasible for mixes with highly polymer-modified binders. For instance, one option is to drop voids in the mix (VIM) criterion from four to a lower level (as represented by Approach 1 in Fig 1.1), while another option would consist of lowering the compaction N_{design} levels currently recommended (as represented by Approach 2 in Fig 1.1). While these two approaches are both viable and appear analogous, they are fundamentally different. Moreover, any other approach resulting from a combination of Approaches 1 and 2 is also feasible (i.e., quadrant between Approaches 1 and 2 in Fig 1.1). The approach that this research project follows corresponds to Approach 2 because it is considered consistent with TxDOT mix design philosophy and because

current Superpave volumetric criteria established at the 4% VIM design level may still be feasible. Besides, Approach 1 has proven problematic with softer binders such as PG 64-22.

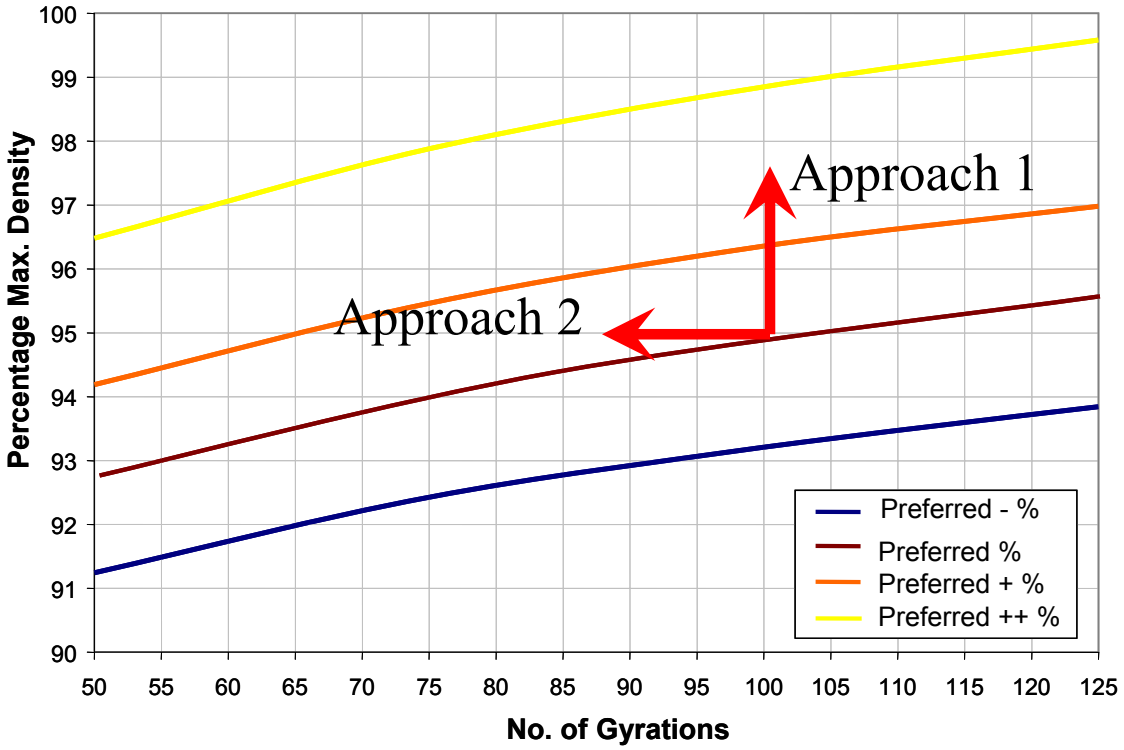

Figure 1.1: Selection of optimum AC content based on current VIM and Ndesign criteria

TxDOT is in the process of establishing Superpave design levels that correspond with their vast knowledge on the behavior of typical Texas type mixes designed using the Texas gyratory compactor (TGC). Problems relating to the compactibility of mixtures designed using the Superpave method have been encountered. It is stated that the source of these problems is related to fundamental "flaws" in the current mix design procedures (quoted from the project statement, Button et al. 2004):

1) All mixtures are designed at 4% air voids (i.e., 96% Gmm) regardless of the nominal maximum aggregate size (NMAS) used.
2) The concentration of the coarse aggregate in the mixture is not considered.
3) Design procedures do not account for the extremely stiff polymer-modified asphalt currently being used.

TxDOT expressed concerns that existing specifications cannot maximize strength and minimize permeability for all dense-graded mixtures. This has a negatively impact on the durability and service life of HMA. TxDOT requires new specifications that allow N_{design} to vary with NMAS and allow VMA to change with coarseness of gradation. Furthermore, TxDOT's VMA specifications are slightly different from those used in other states.

The procedure used in this research project addresses TxDOT's concerns. The procedure is based on a performance-related approach that allows definition of Superpave volumetric

criteria. The basis of the approach is simple: *"To use as much binder in the mix as possible without compromising its rutting performance."* By following this philosophy, not only is fatigue resistance improved but mix durability is also enhanced. Expected rutting resistance was evaluated by means of the HWTD. On the other hand, Indirect Tensile Strength (ITS) and Third-Point Bending Beam were evaluated in order to assess cracking resistance.

The procedure consists of designing a Superpave mixture using the current approach, e.g. determining the optimum binder content such that 96% of the theoretical maximum density (TMD) is achieved at 100 gyrations (Fig 1.1). Three other alternative asphalt contents are then determined at a different number of gyrations and specimens are prepared at all four binder contents. After defining the optimum binder content for a specific mix that simultaneously satisfies both required performance criteria (rutting and cracking), the "new" N_{design} level that ensured 4% VIM were back calculated (i.e., following Approach 2 in Fig 1.1).

A brief discussion of the Superpave mix design method and underlying volumetric principles and criteria that form the basis of the Superpave method follows.

1.2 Superpave Mix Design

The compaction method and procedure used to prepare specimens is critical because it attempts to reproduce, in the laboratory, the compaction in the field during construction and in service. The SGC measures specimen height during compaction. This allows an estimation of specimen density during compaction that may be indirectly related to field compaction. The difficulty with the Superpave mixture design method has been identifying the level at which the density would stabilize in the field, depending on the level of traffic and pavement temperature conditions, and then designing accordingly.

Optimum binder contents of mixtures are selected to ensure that the mix has sufficient VMA during its design life. This is achieved conservatively by controlling the VIM at 4% at laboratory design compaction levels, based on widely publicized research that indicates asphalt mixtures lose stability when voids levels drop below 3%, especially those mixes with soft binders.

Originally, design levels of compaction were specified in the so-called "N_{design} Table" suggesting compaction efforts based on design traffic levels and average high air temperature. The N_{design} Table was determined on the basis of limited laboratory compaction and in-place density data from different traffic levels in different climatic zones (Blankenship et al., 1994). Post-SHRP research evaluated this table, concluding that the design (N_{design}) gyratory compaction level may be too high, at least for lower traffic (Brown et al., 1996). It should be emphasized, however, that the current level of N_{design} results in a mix with adequate resistance to rutting but reduced resistance to cracking. Furthermore, research on test sections on six different highways in five different states (Alabama, Idaho, New Mexico, South Carolina, and Wisconsin) has shown that the number of design gyrations required should be reduced in general and, in cases of low traffic level, by as much as 30 gyrations (Brown and Mallick, 1998).

More recent research under NCHRP Project 9-9 (NCHRP, 1999) supports this reduction and recommended consolidation of the N_{design} compaction matrix to exclude temperature levels and only four traffic levels. The recommended revision of the N_{design} Table is shown in Table 1.1 (Note: this table has higher N_{design} levels than those applied in Tex-241-F for design traffic greater than 30 million ESALs).

Table 1.1: NCHRP recommended consolidation of N_{design} Table (NCHRP, 1999)

Design ESALs (millions)	N-initial	N_{design}	N-max
< 0.1	6	50	75
0.1–1	7	75	115
1–30	8	100	160
> 30	9	125	205

Superpave distinguishes between different compaction levels as shown in the table, defined as follows:

1) N-initial: The initial compaction level used to assess the compactibility of the mixture; it represents mix behavior during breakdown rolling.
2) N_{design}: The design compaction level anticipated after several years of in-service traffic and the anticipated compaction level at the end of a 20 year design period (as per NCHRP 9-9 revision).
3) N-max: The maximum compaction level at the end of the design period;it is set to safeguard against underestimating the design traffic.

Different state agencies are adopting variations of the N_{design} Table to suit specific needs. An example is the recommendation of the Virginia Department of Transportation that an N_{design} of 65 gyrations for specific mixes used on low volume roads and for base layers (Prowell and Haddock 2002). NCHRP (1999) comments on the gyratory compaction of large stone (HMA having nominal aggregate size of 37.5 mm (1.5 in.). The research points out that for asphalt base mixes, the design number of gyrations may be reduced from those shown in Table 1.1 to account for the reduced vertical pressure and lower temperatures at increased depths within the pavement structure. To understand why these levels were selected as part of the Superpave method it is necessary to consider the volumetric principles upon which the method is based.

1.3 Volumetric Criteria

Volumetric parameters used to define the spatial composition of HMA include VMA, VIM or Va, and voids filled with asphalt (VFA). VIM consists of the small air spaces between the bitumen-coated aggregate particles. VMA are the intergranular voids between the aggregate particles in a compacted mix that includes VIM and the effective binder content (Vbe), expressed as a percentage of the total volume. VFA are the voids in the mineral aggregate that are filled with bitumen, not including the absorbed bitumen. The mix parameters VMA, VFA, and VIM are not independent but are related as follows:

$$VFA = 1 - \frac{VIM}{VMA} \qquad \text{(Eq 1.1)}$$

Moreover, for a given binder content:

$$VFA = \frac{Pb \cdot Gsb}{Gb} \cdot \left(\frac{100 - VMA}{VMA} \right) \qquad \text{(Eq 1.2)}$$

The relationship between the volumetric properties VIM (Va), Vbe, VMA, and VFA can also be charted using the so-called *universal volumetric chart* as shown in Figure 1.2.

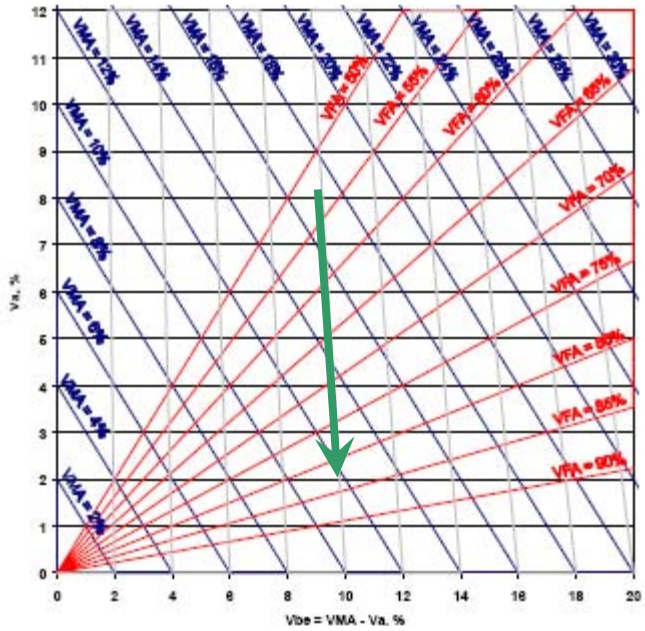

Figure 1.2: Universal volumetric chart (Coree, 1998)

Figure 1.2 presents a linear plot that represents all three volumetric components of a mixture, which is universal in application, i.e., it is independent of differing relative densities and can be used without modification for any mixture. The *y*-axis represents the voids in the mix (VIM or Va). The *x*-axis represents the percent effective binder volume (Vbe) and is calculated as the difference between the VMA and VIM.

The diagonal lines are lines of equal VMA. Since VMA = VIM + Vbe, lines connecting equal values on the two axes are VMA of those magnitudes. The lines radiating from the origin are lines of equal VFA. A further series of lines is shown, sloping slightly left-to-right off the vertical. These are referred to as trajectories. Trajectory lines are constructed by joining any point on the plot (Vbe, Va) to the point (0, 0). These trajectories indicate the path along which the volumetric properties of a mixture change with compaction—as indicated by the thicker vector on the plot.

The mix design chart illustrates the dynamic nature of the volumetric properties of an asphalt mix with compaction. Figure 1.3 shows the mix design chart with actual gyratory compaction data. The mix was compacted at four different binder contents: 4.5%, 5.0%, 5.5%, and 6.0%. The trajectory lines indicating these binder contents are shown on the chart. At each of the binder contents, the volumetric properties of the mix are plotted at three compaction levels: 50, 150, and 250 gyrations. Notice that the trajectory lines at each of the binder contents pass through the points at the different compaction levels as expected. The *x*-axis has been truncated to save space but the parallel lines running top to bottom from left to right are lines of equal VMA. The lines running from bottom to top from left to right actually pass through the origin and are lines of equal VFA. The corresponding VMA and VFA values for the lines have been

included using a slightly smaller font size. The shaded area indicates the region with acceptable Superpave N_{design} volumetric criteria in terms of VMA and VFA.

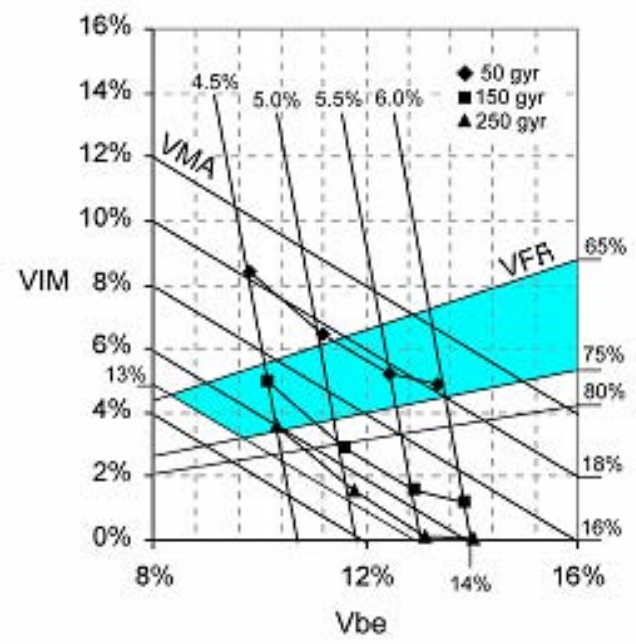

Figure 1.3: Mix design chart with laboratory compaction data

Figure 1.3 sheds light on the Superpave philosophy, which is not always very clear. It can be inferred that the minimum VMA criteria are established to ensure sufficient binder content for durability and workability. The upper VFA criterion (75%) places a limit on the binder content or restricts the use of too high a binder content and the lower VFA criterion (65%) sets the traffic capacity of the mix. The figure also indicates how restrictive the Superpave approach is. Consider, for example, the selection of an optimum binder content to satisfy the 4% VIM criterion at an N_{design} compaction level of 100. Figure 1.3 demonstrates that the designer is restricted to binder contents of approximately 5%. Moutier (1993) points out that the use of volumetric criteria in mix design is often disadvantageous in that, if certain criteria are restrictive, the design mix will quite often be difficult to obtain. According to Moutier, mix design criteria should therefore be chosen with consideration given to the interdependency between volumetric parameters.

Coree (1998) states that in the process of mix design or production, it is frequently necessary to seek to change the magnitude of VIM, VMA, or VFA, but it is not always clear what effect such a change might have on the other parameters nor if that change might in itself compromise compliance in another direction. He emphasizes that no such change in any one parameter should ever be contemplated without checking the effects on the other two. The mix design chart allows the effects of changes in volumetric properties to be evaluated. For instance, the formulation of VMA criteria is complicated since the VMA of a mix depends on the packing characteristic of the aggregates. This is influenced not only by aggregate size, but also by the gradation, shape (angularity), and surface texture of the aggregate (Lefebvre 1957).

Aschenbrenner and McKean (1994) examined laboratory mixes to study the effects of different variables on VMA. They found that gradation played a role in influencing VMA but

obtained such poor correlation that VMA could not effectively be predicted from gradation. They found that filler content has a significant effect on VMA, particularly for gradations on the fine side of the maximum density line. They recommended that the fine aggregate be kept well off the maximum density line. They found that aggregate angularity substantially affected the VMA, with crushed aggregates providing more VMA than rounded aggregates. The fine aggregate angularity had a greater effect on coarse mixes or mixes following the maximum density line than on mixes on the fine side of the maximum density line.

Mallick et al. (2000) looked at an alternative approach for specifying VMA for dense-graded HMA Superpave mixes. (Note: This addresses to an extent the problem faced by TxDOT regarding VMA and NMAS.) They pointed out that coarse graded Superpave mixes (with gradations significantly below the restricted zone), if designed with the minimum VMA criteria based on nominal maximum aggregate size, could result in mixes with very thick binder film because these mixes have relatively lower surface area. Consequently, these mixes may have low resistance to rutting. They concluded that substantial differences in VMA exist among different (Superpave) permissible gradations of mixes with the same nominal maximum aggregate size. They postulate that a more rational way of specifying the minimum design VMA would be to specify VMA based on the percent passing the 2.36 mm sieve rather than the nominal maximum aggregate size. This will ensure about equal binder film thickness in all mixes regardless of gradation to ensure reasonable durability of the mixes. It was recommended that minimum VMA requirements, some of which are shown in Table 1.2, be followed for specifications. The VMA values for the different mixes are given based on the percent passing the 2.36 mm sieve and 4.0% air voids in compacted mix. It was suggested that the VMA in the design mix should not exceed the minimum specified VMA by more than 2.0% to minimize a potential rutting problem. This approach is yet to be validated.

Table 1.2: Recommended design VMA for dense-graded mixes with nominal maximum aggregate size (Mallick et al. 2000)

Passing 2.36 mm	Max size 19.0 mm	Passing 2.36 mm	Max size 25.0 mm	Passing 2.36 mm	Max size 37.5 mm
49-44	14.0	45-40	13.8	41-36	13.6
44-39	13.7	40-35	13.4	36-31	13.2
39-34	13.4	35-30	13.1	31-26	12.8
34-29	13.1	30-25	12.7	25-21	12.2
29-23	12.7	25-19	12.3	21-15	11.7

The reason for adopting alternative measures against which to specify VMA is the reported problems experienced in meeting current Superpave minimum VMA requirements, particularly for coarse graded mixes passing below the restricted zone. Kandhal et al. (1998a) suggest that some of these problems may be caused by the increased compactive effort of the Superpave gyratory compactor. Given the problems experienced, some researchers have found that minimum VMA requirements are restrictive (Hinrichsen and Heggen 1996) and suggest that rigid enforcement of a minimum VMA criterion should be discouraged (Coree and Hislop 1999). Other researchers have opted to drop minimum VMA criteria in place of a minimum average film thickness (Kandhal et al. 1998a, 1998b).

One of the factors that influences the optimum binder content and has a significant impact on overall performance of the mixtures is the absorption of asphalt into the aggregate.

Many of the aggregate sources used in Texas are very absorptive and have high demand for asphalt. The optimum binder content determined in the design process and subsequently used during mixture production is influenced by short-term aging (curing) of the mix prior to compaction. Currently, all mixes undergo 2 hours of curing at compaction temperature prior to laboratory compaction. However, mixtures often spend a substantially longer period of time in the silo and in trucks on the way to the job site. Absorption takes place while the mix is maintained at very high temperatures and the mixture may be effectively low on asphalt content by the time it is laid and compacted.

2. Literature Review

2.1 Introduction

This literature review addresses Superpave Gyratory Compaction (SGC) research studies. The focus is on gyratory compaction effort as it relates to the Superpave N_{design} Table. A review of the French and Australian design procedures is also given, both of which employ gyratory compaction. The experience of various state departments of transportation (DOTs) to increase the binder contents of their Superpave mixes is discussed, as well as research undertaken as part of TxDOT Project 0-4203. A comparison of laboratory and field compaction is provided with emphasis on observed densification trends and efforts undertaken as part of the NCHRP 9-9 project and research at the National Center for Asphalt Technology (NCAT).

2.2 Superpave Gyratory Compaction

The basis for the SGC was a Texas gyratory compactor (TGC) modified to use the compaction principle of a French gyratory compactor. The SGC was developed for the following:

1) Realistically compact trial mix specimens to densities achievable under actual pavement climate and loading conditions
2) Accommodate large aggregates
3) Afford a measure of compactibility so that potential tender mix behavior could be identified, and,
4) Be portable to allow quality control and assurance on site.

Table 2.1 shows the original Superpave gyratory compactive effort table or the N_{design} Table. It shows gyratory compactive efforts for different design traffic levels and average design high air temperatures (ADHAT). From the table it can be seen that the compactive effort increases as the design traffic increases and when the average design high air temperature increases.

The N_{design} Table was determined on the basis of limited laboratory compaction and in-place density data from different traffic levels in different climatic zones. Blankenship et al. (1994) reported on the research done to ascertain the N_{design} levels shown in Table 1.1. This research has received some criticism, which is addressed later in the report. Included in the study were two pavements in Texas (a base and surfacing layer), 13 and 20 years of age, with low and medium design traffic volumes, respectively. Cores taken from the evaluation pavements were broken down, the aged binder extracted, and the mix re-compacted using unaged AC-20 asphalt cement. Two cores were extracted from each pavement section.

Table 2.1: Superpave N_{design} gyratory compactive effort (after McGennis et al. 1994)

Design ESALs (million)	ADHAT (°C)			
	< 39	39–40	41–42	43–44
< 0.3	68	74	78	82
0.3–1	76	83	88	93
1–3	86	95	100	105
3–10	96	106	113	119
10–30	109	121	128	135
30–100	129	139	146	153
> 100	142	158	165	172

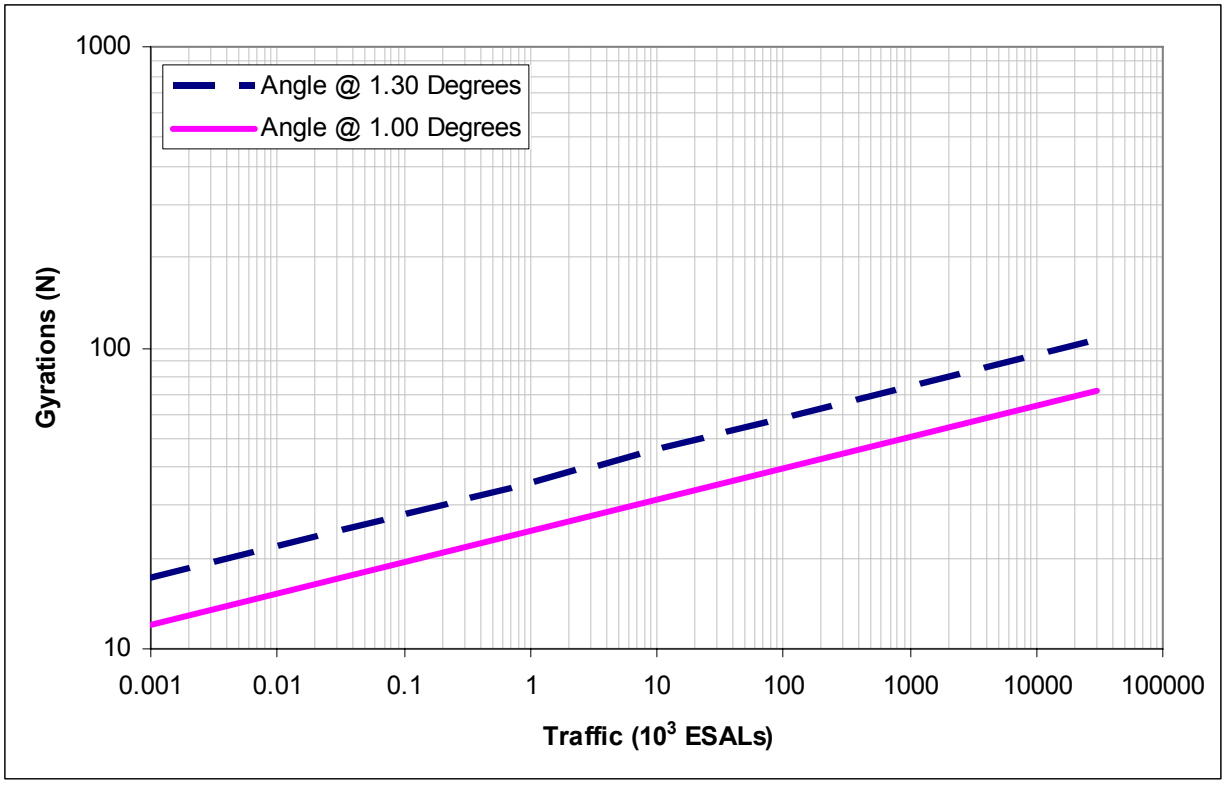

Figure 2.1: Average N_{design} vs. traffic (after Blankenship 1994)

Figure 2.1 shows a graph from Blankenship's master's thesis (Blankenship 1994), which indicates results of gyratory compaction testing using two different gyratory compaction angles. Figure 2.1 illustrates that the difference between the N_{design} values determined from the 1.3- and the 1.0-degree angle increases with an increase in the traffic level. A decision was made in the study to provide N_{design} levels based on the 1.0-degree gyration angle data, primarily because the SHRP gyratory specification (at the time) called for a 1.0-degree angle. The N_{design} levels

obtained from this study, using the 1.0-degree gyration angle results, were used to create the original N_{design} compaction matrix, provided previously in Table 2.1. The SHRP specification changed to a 1.25-degree angle after the study, clearly necessitating a decrease in the number of gyrations at the N_{design} level.

Post-SHRP research was done to re-evaluate the N_{design} Table, which indicated that the N gyratory compaction level might be too high, at least for lower traffic (Brown et al. 1996). Furthermore, research has shown that the number of design gyrations required should be reduced and in cases of low traffic level by as much as 30 gyrations (Brown and Mallick 1998). Brown and Mallick (1998) conducted research in which specimens were compacted in the Superpave gyratory compactor at different gyration levels and then were compared with the density of in-place cores obtained from pavement test sections at various levels of cumulative traffic. Project work consisted of obtaining cores from six test pavements (two in Alabama, one in the states of Idaho, South Carolina, New Mexico, and Wisconsin) with different levels of known traffic. The cores were taken immediately after construction and after 1, 2, and 3 years of service. The air void content and the density of the cores were established. Two sets of specimens were then compacted using the SGC. One set of specimens consisted of original plant produced material that was reheated and then compacted (this set is referred to as compacted reheated). The other set consisted of using the aggregate and asphalt cement that was used in the mixture (this set is referred to as laboratory prepared). Results from the study provide the following conclusions:

1) The gyrations required to achieve the 1-year and 2-year in-place density were below 100 for all mixtures evaluated.
2) For similar gyration levels, the density of compacted reheated specimens and laboratory prepared specimens varied about 1% on average.
3) The N_{design} gyration level may be too high for low traffic volume roadways. This will be further evaluated in the future after the 3-year in-place density is recorded. This conclusion is illustrated in Figure 2.2.
4) The values of voids at N-initial and N-max were lower than the specified values based upon the laboratory data obtained from the project.
5) The density of laboratory prepared samples was approximately 1% greater than the density of the compacted-reheated samples at similar gyration levels. The difference became less as the gyration level increased.

Research under NCHRP Project 9-9 (Brown and Buchanan 2001a) supported a reduction in N_{design} compaction levels and recommended consolidation of the N_{design} compaction matrix to exclude temperature levels and only four traffic levels. The recommended revision of the N matrix is shown in Table 2.2. They also recommended changes to density requirements at the N-initial level for mixes with lower design traffic as shown in Table 2.3.

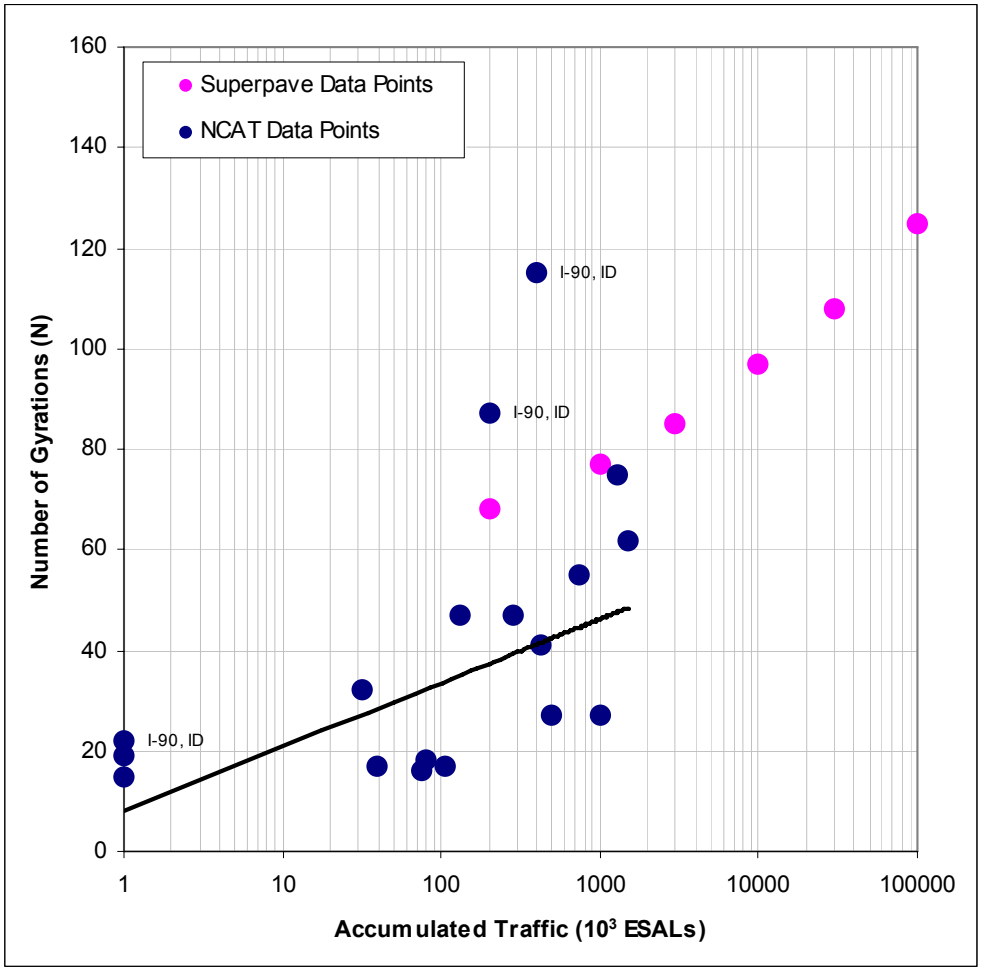

Figure 2.2: N_{design} vs. traffic (after Brown and Mallick 1998)

Table 2.2: NCHRP 9-9 recommended consolidation of N_{design} matrix

Design 20 yr ESALs (million)	N-initial	N_{design}	N-max
< 0.1	6	50	74
0.1–1	7	70	107
1–30	8	100	158
> 30	9	130	212

Table 2.3: NCHRP 9-9 revised Superpave density requirements

Density Requirement	Density Level	Comment
C initial	< 89	Original requirement
C initial	< 91.5 (<0.1 Million ESALs)	Revised requirement
C initial	< 90.5 (0.1 < 1 Million)	Revised requirement
C initial	< 89 (>= 1 Million)	Revised requirement
C design	= 96	Unchanged
C max	= 98	Unchanged

McGennis et al. (1996) evaluated a number of issues pertaining to Superpave gyratory compaction. His research found that the mold diameter had a significant effect on densification of mixes. Also within the 12.5 mm nominal maximum size, mold size affected the densification of coarser mixes more often than it affected that of slightly finer mixes. The effect of compaction temperature on specimen volumetric properties was also investigated. A gap graded mixture was compacted using two binders (a PG 64-28 unmodified and a PG 76-28 modified binder). The results indicated that variations in compaction temperature did not substantially affect the volumetric properties of the unmodified binder mixes but did affect those of the modified binder mixes. They found that short-term oven aging significantly influences specimen volumetric properties. Four different gyratory compactors were evaluated: Pine SGC, Troxler SGC, modified TGC, and the Rainhart SGC. They found significant differences between the compactors for six different aggregate blends. The modified TGC and the Pine SGC produced mixes with lower air voids and therefore lower optimum asphalt contents than the Rainhart SGC and the Troxler SGC.

Cominsky et al. (1994a, 1994b) investigated the ability of the SGC to verify or control mix production. The study was designed to evaluate the effect on the compaction characteristics in the gyratory compactor resulting from changes in the asphalt content, percent passing the 0.075 mm sieve, percent passing the 2.36 mm sieve, aggregate nominal maximum size, and the percentage of natural and crushed sand. One particular mix was used in the study—a coarse-graded (below the restricted zone) 12.5 mm nominal maximum size mix from Milwaukee, Wisconsin. Compaction of all samples in the study was completed using a gyration angle of 1.14 degrees, a vertical pressure of 600 kPa, and a rotational speed of 30 rpm. Notice that the gyratory angle differed from the now specified 1.25 degrees. They found that a 0.02 degrees variation in gyratory angle resulted in an average air voids variation of 0.22% at 100 gyrations. This resulted in an average 0.15% change in the determined optimum asphalt content for a 19 mm mixture. After compaction, response variables of %Gmm at N-initial, %Gmm at N-max, gyratory compaction slope, air voids, VMA, and VFA were calculated and evaluated. The results indicate that all volumetric properties (air voids, VMA, and VFA) were significantly influenced by changes in asphalt content, percent passing the 0.075 mm sieve, and the percent natural sand. Less significant changes were shown in the percent passing the 2.36 mm sieve. Furthermore, the nominal maximum aggregate size did not significantly change volumetric properties of the mixes. Asphalt content and the percent passing the 0.075 mm sieve have the greatest effect on the gyratory compaction response variables, with the percent passing the 2.36 mm sieve and the percent natural sand having a lesser effect. The nominal maximum aggregate size did not have a

significant effect on the compaction response variables. Epps and Hand (2000) reemphasized the sensitivity of particularly coarse Superpave mixtures to AC content and filler content.

Anderson et al. (1995) found that the SGC appeared to be extremely sensitive to changes in asphalt content. Anderson et al. (1998) evaluated the effects of component proportions on mixture properties using the SGC with a 19 mm nominal maximum size blend of crushed limestone and natural sand with a PG 64-22 asphalt binder. A fractional factorial experiment was employed and results of the study indicated that the interaction of asphalt content and fine gradation had the most significant effect on the volumetric and densification properties. The main effect of coarse aggregate gradation, asphalt content, the interaction of asphalt content and fine gradation, and the interaction of asphalt content and coarse gradation caused significant changes in the %Gmm at N-initial. The densification slope of the SGC curve was affected by the fine gradation, the intermediate gradation, the interaction of asphalt content and coarse gradation, and the interaction of asphalt content and fine gradation. It was further shown that the asphalt content had an effect on all volumetric and densification properties with the exception of the densification slope.

Vavrik and Carpenter (1998) investigated the inaccuracies in both mix design and quality control testing resulting from back-calculation of gyratory specimen density at N_{design} from densities obtained at N-max. Differences in back calculated densities at N_{design} and those compacted to N_{design} varied between 0.5% and 1.5%. Due to these differences, the state of Illinois developed the "locking point" concept. The locking point is defined as the point at which three consecutive gyrations produce the same specimen height. Up to the locking point, the densification curve is linear in nature—and non-linear past the locking point. The results of the evaluation indicated that values of 100, 75, and 50 gyrations were specified as typical values to provide 96 %Gmm for high, medium, and low volume traffic pavements.

Mallick et al. (1998) found that the use of a single correction factor in the evaluation of corrected densities is incorrect but that the factor varies with compaction. Based on the findings, the authors recommend that all specimens be compacted to N_{design} in the volumetric mix design procedure.

Forstie and Corum (1997) revisited the original SHRP research for the following reasons:

1) The angle of gyration used by SHRP researchers to develop the current N_{design} was 1.0 degrees, while the angle now specified in AASHTO TP-4 is 1.25 deg. In addition, an angle of 1.3 deg was used unknowingly for a portion of the N_{design} study due to a manufacturer error.
2) The N_{design} experiment was conducted using 100 mm diameter specimens, not the currently used 150 mm diameter specimens.
3) The mixes in the N_{design} experiment were predominantly fine-graded mixes, not the coarse-graded mixes that are most commonly used today
4) The result of the experiment (Table 2.1) is based on limited testing.

Based on their study it was concluded that the N_{design} compaction levels shown in Table 2.1 should be revised in magnitude. The researchers point out that mixes designed at the original N_{design} levels will likely have higher laboratory densities (lower asphalt content). This over compaction could lead to compaction problems during lay-down and also resistance to traffic densification down to designed 4% air voids level.

Hafez and Witczak (1995) found that as the compactive effort N_{design} for the SGC is decreased from 119 to 67 gyrations, an increase of approximately 1.0% asphalt content occurred for a number of different mixes evaluated, i.e., 20 different mixes including conventional, open graded, polymer modified, and asphalt rubber.

Parker et al. (2000) report greater variability of mixture density properties of Superpave designed mixtures compared to those designed using the Marshall method. Asphalt contents for Superpave mixes, particularly for high ESAL ranges, are lower than asphalt contents for comparable Marshall mixes. Effects of gyratory compactor use, mix design ESAL range, and maximum aggregate size were investigated to justify such a difference. Although few consistent trends were observed, all these factors seem to affect the variability and accuracy of air voids and mat density of Superpave mixes.

Bahia et al. (1998) looked to predict densification under construction and traffic using the Superpave gyratory compactor for the Wisconsin DOT, evaluating several gradations and asphalt contents using one aggregate source and one PG58-28 asphalt binder. Asphalt mixes for high volume and medium volume roads were designed. The high volume mixes were compacted to N-max of 150 gyrations and the medium volume mixes to N-max of 129 gyrations. Six different aggregate blends passing above and below restricted zone were evaluated. An analysis of the volumetric properties of the mixes showed the following:

1) Mixes with higher %Gmm at N-initial do not necessarily show higher %Gmm at N-max. In fact, the opposite seems to hold true.
2) Values of %Gmm at N-initial were very close to greater than the maximum limit of 89% of Gmm for blends above and through the restricted zone for both the high and medium volume mixes. The %Gmm at N-initial for aggregate blends below the restricted zone is well below the 89% maximum limit.
3) The %Gmm at N-max was close to the 98% for all aggregate blends. The %Gmm for coarser mixes is closer to the limit than the %Gmm for the finer mixes. This indicates that coarser mixes would be more susceptible to densification beyond the 2% air void limit.

A recent article in *Better Roads* (September 2005) magazine addressed the issue of why and how some states in the U.S. are increasing the binder content in their Superpave mixes. Although there is a general consensus among state DOTs that Superpave has addressed the rutting problem, indications are that Superpave mixtures are prone to durability issues, segregation, fatigue, and cracking, and, in some cases, permeability problems, especially with coarse-graded mixes. These problems point to inadequate binder in the mix and different strategies to increase the binder content in Superpave mixes have been adopted.

Alabama DOT reduced N_{design} for high volume roads from 125 to 100 and then further to 85 gyrations to increase the binder content of Superpave mixes. Not satisfied with the performance of mixes designed using 85 gyrations, they revised the N_{design} level based on the locking point concept described previously. This defines the point at which the aggregate structure in a mixture "locks up" or has reached its maximum compaction in the gyratory compactor. Beyond this point, further compaction leads to degradation of the aggregate. Alabama found that most of their mixes "locked up" in the range of 45 to 55 gyrations. The DOT set the minimum N_{design} at 60 gyrations. Compared to mixes designed at 85 gyrations, the binder content of the new N-60 mix increased 0.2% to 0.4% on average.

Colorado DOT has the option to reduce design air voids content from 4% to 3% during production. However, mixes are still designed at 4%. The DOT reports that a 1% decrease in air voids will result in a 0.1%–0.3% increase in binder content. This approach was followed based on in-house research that indicated Superpave pavements were not densifying to the 4% level as originally anticipated.

Maryland DOT has reduced design air voids from 4% to 3.5 % and in some cases 3%. The DOT encourages the use of Superpave Level 1 mixes with an N_{design} of 50 gyrations. Virginia DOT uses a lower design compaction level--65 gyrations--regardless of design traffic level. Binder "bumping" is used to address higher design traffic, i.e., a stiffer binder is used. Virginia reports that 65 gyrations are still too high when compared to their Marshall designed mixes. To address this problem, they increased the Voids Filled with Asphalt (VFA) criteria and shifted the production mix Voids in Total Mix (VTM) to the low side.

TxDOT Research Project 0-4203

Button et al. (2004) reported on the use of the SGC for the design of traditional TxDOT dense-graded mixtures in place of the TGC. The specific goal was to recommend a design number of gyrations (N_{design}) using the SGC for TxDOT HMA mixtures including Type A, Type B, Type C, Type D, Type Course Matrix High Binder CMHB-C, and Type CMHB-F. Several types of aggregates (gravel, limestone, sandstone, and quartzite) and asphalt binders (with and without lime and other anti-stripping agents) made up the experimental design.

The number of SGC gyrations that most closely simulated the TGC design for each mixture type was recommended. The research results showed that the TGC and the number of SGC gyrations to match the TGC were producing mixtures with comparatively low asphalt contents. The study made the point that, given the difference in gyration compaction angle between the SGC (gyration angle = 1.25°) and TGC (gyration angle = 5.8°), it did not appear likely that adjusting only the number of gyrations of the SGC could produce specimens basically identical to those produced by the TGC. The lower angle of the SGC imparts significantly less mechanical energy into the specimen during each gyration. Different gyration angles have different influences on the orientation of the aggregates, particularly the larger aggregates. The differences between specimens (air void structure, aggregate orientation, voids in the mineral aggregate [VMA], and density gradient) prepared using the TGC and SGC are not likely to be consistent because these differences depend on the shear resistance of the mixture (i.e., maximum particle size, particle size distribution, binder and mastic rheology, and other probable factors).

As part of Phase II of the project, Hamburg Wheel Tracking tests were conducted. The results revealed that mixtures indicating good performance in the Hamburg test could be designed using a considerably lower number of SGC gyrations than the number that matched optimum asphalt contents from the TGC. (Phase II included TxDOT Type A, Type B, Type C, Type D, and CMHB-C mixes; limestone aggregate; river gravel aggregate; and binder types PG64, PG70, and PG76.) The researchers contend that the final recommended SGC design gyrations (shown in Table 2.4) should accommodate adequate asphalt in the mixture to improve resistance to cracking, raveling, and aging, as well as decrease permeability while providing acceptable rutting resistance. The recommended SGC N_{design} levels are considerably higher than those currently being used by other state DOTs around the country.

Table 2.4: TxDOT Project 0-4203 final recommendation on SGC N_{design} levels

Mixture Type	No. of SGC Gyrations
Type A	90
Type B	90
Type C	120
Type D	120
CMHB-C	120

2.3 International Mix Design Procedures Based on Gyratory Compaction

This section discusses the French and Australian mix design procedures, both of which use variations of gyratory compaction.

2.3.1 French (Laboratoires des Ponts et Chaussées) Mix Design Procedure

The Superpave Gyratory Compactor is based on the French Gyratory Compactor. The French system of asphalt mix design has been performance-orientated for almost 20 years. The French bituminous mix design method is documented by Moutier (1993) and more recently by Corté and Serfass (2000). This method makes use of the Gyratory Shear Press (GSP) to design mixes that are impermeable and offer resistance to rutting.

In the 1930s, the French method developed by Duriez consisted of compacting samples by simple compression that often crushed the aggregates because of the high stresses to which they were subjected. The French started using gyratory shear compactors in the late 1970s when a method was developed that proved to be discriminating in separating the behavior of grading components in the evaluation of compactibility. The main justification for using gyratory compaction was the possibility of selecting mixes having low voids contents and generally having a higher resistance to rutting. To confirm the adequacy of the rutting resistance, the chosen mix can be checked using a rutting tester. The GSP is a mandatory part of any mix formulation study. Moutier (1993) states that mix bitumen contents and the type of bitumen used (centered on 60/70 pen grade bitumen) generally lead to acceptable mechanical strengths (fatigue/modulus) for most mixes, hence mechanical characteristics are not measured systematically.

As a rule, asphalt mixes comprise a granular skeleton consisting of all-crushed single fractions with bitumen content of approximately 4% to 6% by weight. The use of rounded sand fractions is not advised. After compaction by heavy or vibratory rollers, the residual in-situ voids in the surfacing mix must be as close as possible but not less than 4%, the threshold below which the risks of instability increase. Layer thickness must be taken into account since thinner layers are more difficult to compact. To balance voids and binder content in a specific mix, use is made of the following equation, defined by Duriez:

$$Pb = K \cdot \alpha^5 \cdot \sqrt{A} \qquad \text{(Eq 2.1)}$$

Where:
Pb : Binder content
K : Richness coefficient
α : 2.65 / bulk relative density of the aggregates used
A : Conventional specific surface area = 0.25 G + 2.3S + 12s + 135f (G: Proportion by weight of elements larger than 6.3 mm; S = Proportion by weight of elements between 6.3 and 0.315 mm; s = Proportion by weight of elements between 0.315 and 0.08 mm; and f = Proportion by weight of elements smaller than 0.08 mm)

In the Superpave mix design method, for example, the optimum binder contents of mixes are often chosen to ensure 4% voids in the mix. Moutier (1993) points out that this approach is often disadvantageous in that, if certain mix criteria are restrictive, the mix will quite often be difficult to obtain (the choice of binder content may even be incorrect).

These equations allow the relationships between VMA, VFB, and VIM to be illustrated as shown in Figure 2.3 for Gsb = 2.7 and Gb = 1.03. Suppose that, for argument's sake, the mix criteria are such that VFB and (100 - VMA) must be lower than 80% and 85%, respectively, for 4% VIM, then, as shown in Figure 2.4, the mix can only be made with rather high binder contents. This may be incompatible with resistance to rutting measures and, furthermore, the volume of aggregate is confined between 80% and 85%, which may be difficult to achieve.

Moutier (1993) argues that in France, mix choice conditions are less restrictive and may fall, for example, within the shaded area of Figure 2.4 for aggregate densities assumed equal to 2.7. In this case, if VIM must be between 4% and 8%, then for binder contents ranging from 5% to 6%, (100 - VMA) ranges between 79% and 86%. He does point out, however, that attaining the objectives of low void contents or high aggregate volumes with binder contents less than 6% and all-crushed aggregates is a delicate operation that requires optimization of the mix.

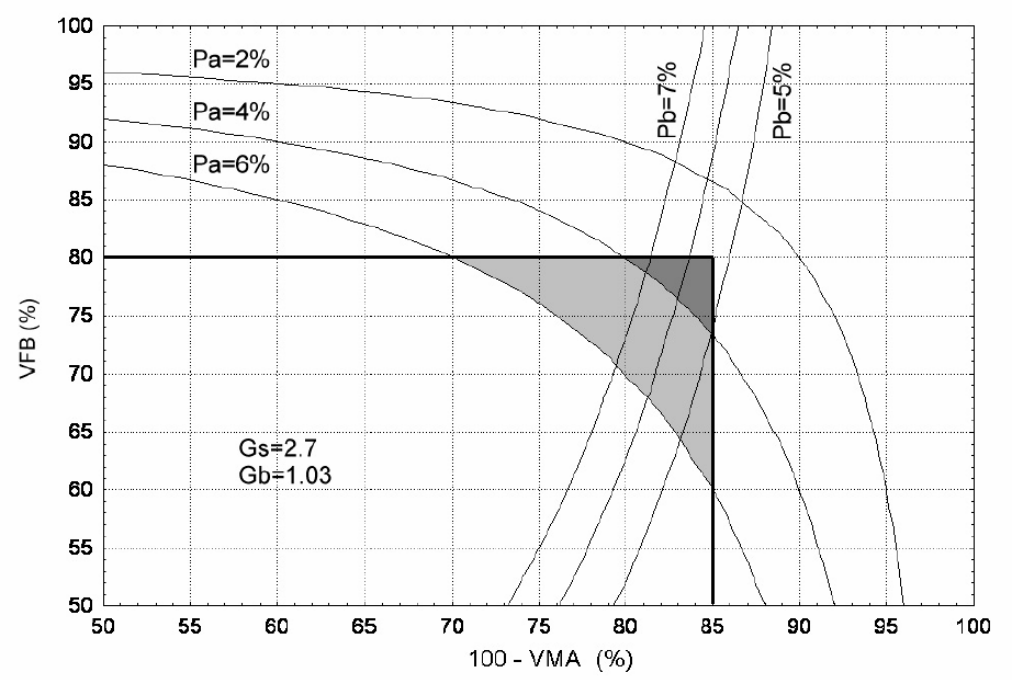

Figure 2.3: Volumetric relationships between VMA, VFB for specified VIM and Pb

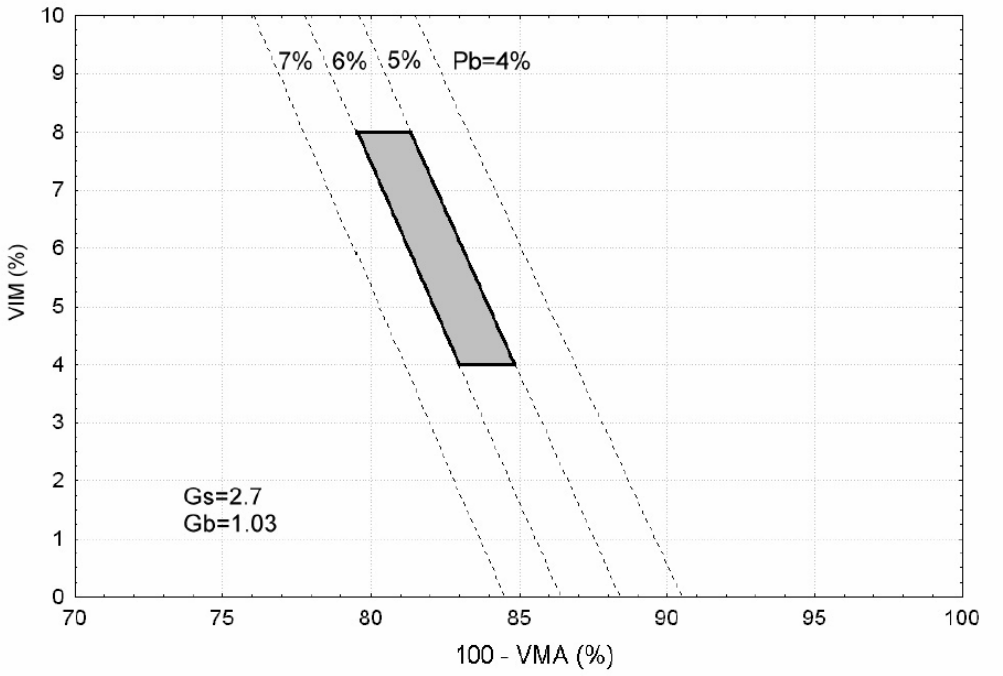

Figure 2.4: Volumetric relationships between VMA and VIM for different Pb

The French Gyratory Shear Press (GSP) differs from the SGC in that an 8 kg mass of sample is compacted, the angle of gyration is 1 degree, and the rate of compaction is 6 rpm. The load applied to the compacted sample is, as with the SGC, kept constant at 0.6 MPa. The suitability of the mix for its intended use is judged by the minimum criteria set in material

standard specifications for VIM at a specific number of gyrations (ng) related to the intended layer thickness of the mixture in the field (e) in centimeters:

$$ng = 10 \cdot e \quad \text{(Eq 2.2)}$$

Moutier (1993) has shown that the number of gyrations (ng) using the gyratory shear press may be related to the number of passes (np) of a pneumatic roller by:

$$ng = K \cdot e \cdot np \quad \text{(Eq 2.3)}$$

Where K depends on the energy expended by the roller and e is the thickness of material placed in one layer (in cm). This relationship allows compaction level predictions if, for a given site, K, e and np are known and if the sample is representative of what is placed.

2.3.2 Australian Mix Design Procedure

The Australian asphalt mix design procedure is well documented (Austroads 1997). The design procedure is arranged in three levels, the extent of testing depending on traffic category as shown in Table 2.5.

Table 2.5: Australian gyratory compaction design levels (after Austroads 1997)

Traffic category	Design level	Gyratory cycles
Light	1	50
Medium	2	80
Heavy	2	120
Very heavy	3	120 + 350

Traffic category is not only based on traffic volume but also on the level of free-flowing vehicles and whether the traffic is stop and start or slow moving as shown in Table 2.6.

Table 2.6: Australian traffic design levels (after Austroads 1997)

Commercial vehicles/lane/day	Structural design level (million ESAs)	Free-flowing vehicles	Stop/start OR climbing lane OR slow moving
< 100	< 0.5	Light	Medium
100–500	0.5–5	Medium	Heavy
500–1000	5–20	Heavy	Very heavy
> 1000	> 20	Very heavy	Very heavy

Using Tables 2.5 and 2.6 as a guide, the appropriate design level based on traffic category is selected. The mix design procedure consists of three levels. During level 1 testing, a composition with suitable volumetric proportions is identified by selecting a target grading and materials combination. Grading specifications are relaxed and trial binder contents are chosen,

either based on past experience with similar mixes or so that a minimum binder film thickness of 7.5 micron or greater is obtained, calculated using the Asphalt Institute method (1993). The binder film thickness procedure gives the minimum binder content and the trial binder content will normally be 0.5% greater.

Batches of the mix are prepared at each of three binder contents: the trial binder content, and the trial binder content plus and minus 0.5% binder. Each batch consists of sufficient material to manufacture five gyratory compaction specimens and provide duplicate samples of loose mix for the determination of maximum bulk density. Mixing time is limited to a maximum of 3 minutes after which excessive oxidation of the binder may occur.

Conditioning of the asphalt mix prior to compaction consists of aging the loose mix in an oven held at 150 °C for 1 hour (Superpave requires 4 hours aging at the mixture compaction temperature). Conditioning simulates the binder hardening that occurs during transportation of the mix from the mixing plant to the construction site and during the first year or two of service. At the completion of the conditioning period, a single specimen is prepared in the gyratory compactor with the following compaction cycles: 10, 50, 80, 120, and 350 cycles. The 350 cycles is applied to obtain a "refusal" or maximum possible density. Voids in the mix must be above 2% at this level. Design binder contents are chosen to achieve an appropriate compaction level that ranges between 3% to 5% air voids depending on mix application. Typically, densities, VIM, VMA, and VFB are calculated at the appropriate gyration cycle as indicated in Table 2.5. For dense-graded mixes to be used on lightly trafficked streets, the general design procedure terminates at this stage. Medium and heavily trafficked mixes will proceed to Level 2 and possible Level 3 testing.

The Australians adopted gyratory compaction in their mix design procedure at about the same time that Superpave was introduced in the United States. They researched the major parameters affecting the development of reduced volume through increasing number of gyrations, gyratory angle, vertical pressure, and speed of gyration.

1) Effect of angle. Butcher (1998), formerly of ARRB Group, Ltd., stated that it is widely acknowledged that gyratory angle has a significant effect on gyratory compaction. In a research project, the gyratory compaction setting used in Europe and by SHRP (1.00/1.25 degree angle, 600 kPa vertical stress and 30 cpm) were compared to those used in Australia (2 degrees for 100 mm and 3 degrees for 150 mm specimens, 240 kPa vertical stress and 60 cpm). The work indicated that there is exponential type decay in the void level of a mix as the angle increased. Similarly, the number of cycles required to generate a specific void value, decreased exponentially as the angle increased. The results demonstrated that the region between a gyratory angle of 2 and 3 degrees is a stable area.

2) Effect of pressure. In comparison to gyratory angle, vertical pressure is not regarded as a highly critical parameter. To investigate this issue, the angle was varied between 0.1 and 3 degrees for pressure values of 400, 200, and 100 kPa (all at 30 cpm). While a voids-pressure relationship appeared to be linear and not of concern, when viewed from a cycles-versus-pressure relationship, a different perspective was obtained. It was reported that for high voids, when the vertical pressure was above 200 kPa, a fairly flat response was obtained. As the voids decreased, however, the response changed so that for 5% voids, a 1% change in pressure around 600 kPa caused a 7% change in cycles. For lower angles, this effect increased and it was estimated that for approximately a 1 degree gyratory

angle a 1% change would at least double the effect to be over a 14% change in cycles. The effect pointed to the need for gyratory angles to be above 2 degrees to keep variations to a minimum and pressure tolerances to be much tighter than the SHRP specification of 18 kPa. With such high tolerances on the vertical pressure, the gain in precision for a tight tolerance set on gyratory angle can be lost. In general, though, there is a voids decrease as the pressure increased. As with angle, the cycles required to generate a specific void value decreased exponentially as the pressure increased.

3) Effect of rate of rotation**.** The effect of the rate of rotation was evaluated with the gyratory parameters held constant with the exception of speed of rotation, which was varied. The speeds of rotation per minute selected were 10, 20, 30, 40, and 60 cpm. The results confirmed previous SHRP work that little variation in response was obtained through different rates of rotation and this appeared to be applicable at any angle. The Australian selection of 60 cpm appears to be advantageous in that less heat is lost during a test and a better production of sample quantity can be achieved. Related research undertaken by Peterson et al. (2003) evaluated a 12.5 mm Superpave mixture comprising a PG 70-22 binder, during which the researchers varied gyratory compaction angle and pressure and compacted specimens to varying heights. This study used mechanical properties measured with the Superpave Shear Tester (SST) to compare field compaction and laboratory compaction. The field compaction consisted of three test sections with different compaction patterns. Results of this study indicate that current gyratory protocol produces specimens with significantly different mechanical properties than field cores produced with the same material and compacted to the same air voids. Results also show that adjustments to certain gyratory parameters can produce specimens that better simulate the mechanical properties of pavement cores. Based on the findings, the researchers recommended using a gyratory angle of 1.5 degrees (instead of 1.25 degrees) and compacting laboratory specimen to a 50 mm height.

2.4 Comparison of Field versus Laboratory Compaction and Densification

The following review focuses on establishing the adequacy of current laboratory compaction criteria to determine the compaction characteristics of mixtures paved in the field. The success of an asphalt mixture in the field depends largely on the degree with which the volumetric performance of the mixture can be predicted in the laboratory during its design. This is particularly true for Superpave mixtures, which are designed to specific void contents anticipated in the field after the application of the design traffic. There are obvious differences in time, temperature and loading regimes between laboratory and field compaction. Furthermore, the mixture in the field is subjected to compaction during construction and in-service compaction or densification over time. A review of literature comparing field and laboratory compaction of asphalt mixtures indicates that:

1) The in-place densities of pavements over time can be related to compaction levels or effort in the laboratory (regardless of compaction procedure).
2) The majority of field compaction occurs within the first year of traffic use with significant compaction occurring within 6 months after construction.

3) Pavements continue to densify after 2 years of service but at a reduced rate.
4) The degree of pavement densification may be related to initial traffic volume, rate of loading, construction density, paving season, temperature, and mixture specific factors such as binder grade and content. Some studies indicate findings to the contrary.
5) The densification of a pavement beneath and between trafficked wheel-paths can be similar.
6) There appears to be a minimum threshold compaction temperature below which the densification of a mixture during construction is impaired. The literature indicates this temperature to be anywhere between 180°F and 220°F depending on binder grade and paving conditions.
7) In-service densification of pavements is related to temperature. Under cooler conditions (less than 104° F), the degree of construction density could influence "stable-state" densities.
8) In general, a linear trend is observed between initial constructed density and final developed density.
9) For low traffic volume roads (<10,000 ADT), densification occurs in the upper 2.5 in. of the surfacing layer. For high traffic volume roads (>50,000 ADT), densification is up to 4 in. within the layer.
10) The Superpave compaction design criteria (as originally established) appear to be too high for low volume roads.

Dillard (1955) compared laboratory Marshall compaction with field densification of sand asphalt and conventional dense-graded mix pavements. For the majority of the pavements analyzed, the Marshall 50-blow procedure appeared to yield significantly higher densities than the in-place densities of the pavements after 16 months, at which time the 30-blow Marshall densities were achieved. The data indicated that the amount of traffic did not have a significant effect on the ultimate densities achieved, which could suggest that a densification "plateau" is reached after which further traffic-induced compaction is negligible.

Field (1958) correlated the densification of 31 dense-graded pavements in Southern Ontario with Marshall 75-blow density. Pavements with varying amounts of traffic volume were evaluated. Findings indicated that the degree of densification of pavements was related to traffic volume, construction density, and the paving season. The majority of mixes constructed during mid-summer were close to the laboratory density at the time of evaluation, which ranged from 2–5 months. Further compaction from traffic can be slow, resulting in the pavement experiencing durability problems before the design lab density is achieved.

Campen et al. (1960) conducted a study on the densification over time of 18 mixes placed between 1955 and 1959 in the city of Omaha, Nebraska. The mixes were all surface mixes and varied in layer thickness from ¾ in. to 2 in. Aggregates used in the mixes consisted of crushed limestone, crusher run gravel, and coarse and fine natural sand. All gradations were dense- to fine-graded with 56% to 76% passing the No. 4 (4.75 mm) sieve. The 50-blow Marshall design procedure was used for each mix and resulted in optimum asphalt contents ranging from 4.5% to 5.3%. The asphalt binders used were 60/70 to 85/100 penetration grade. Traffic on the various

streets ranged from an average daily traffic (ADT) of 6,000 to 35,000 vehicles consisting of passenger cars and trucks, although no breakdown of either was reported. Cores taken from pavements following 1–5 years after construction indicated that the applied traffic generally did not densify the pavement past the densities achieved during the 50-blow Marshall procedure. They found that the ultimate field density is usually attained in a few months during hot weather and the initial field density does not control the ultimate density in the pavement. The authors suggested that the lab design compactive effort should possibly be reduced for light and medium trafficked pavements to allow for more asphalt in the mixes to improve durability.

Graham et al. (1965) looked at the influence of mix composition, thickness, temperature, roller passes, and applied traffic on the in-place density of 47 sections located on 12 construction projects. The mixes used on these projects were conventional dense-graded mixes designed using the 50-blow Marshall procedure. Cores taken from the sections immediately after construction and after 1 and 2 years of service indicated that the pavements densified significantly during the first year but to a lesser degree in the second year. After 1 and 2 years of traffic, approximately 92% and 96% of the sections, respectively, had densities greater than the 50-blow Marshall density. They also found that densification of the pavement between the wheel path can be on par with that in the wheel path as shown in Figure 2.5. Gichaga (1982) and Hughes and Maupin (1987) also report significant densification of asphalt pavement during the first 5–6 months following construction.

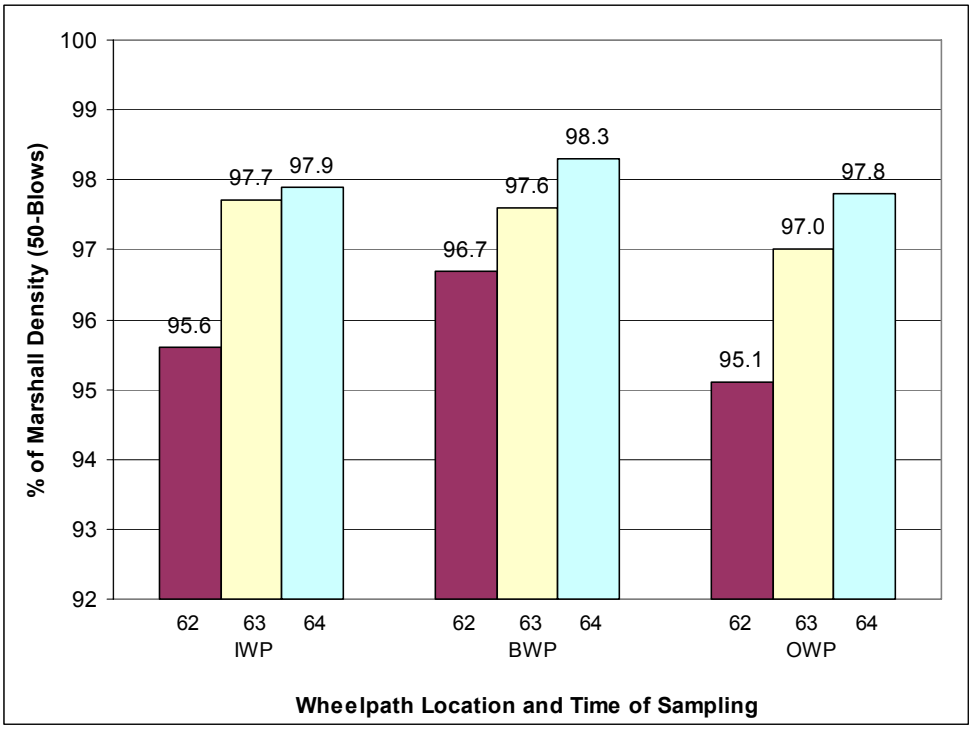

Figure 2.5: In-place density with time for different wheel paths (after Graham et al. 1965)

Serafin et al. (1967) reported on the densification of an experimental road monitored for approximately 12 years. Good relationships between the core bulk densities and time (traffic) over the 12-year period were recorded for the majority of the 24 test sections evaluated. Figure

2.6 shows some of the densification trends observed. Traffic over the evaluation period varied from 7,000–12,000 ADT with 15%–20% commercial vehicles.

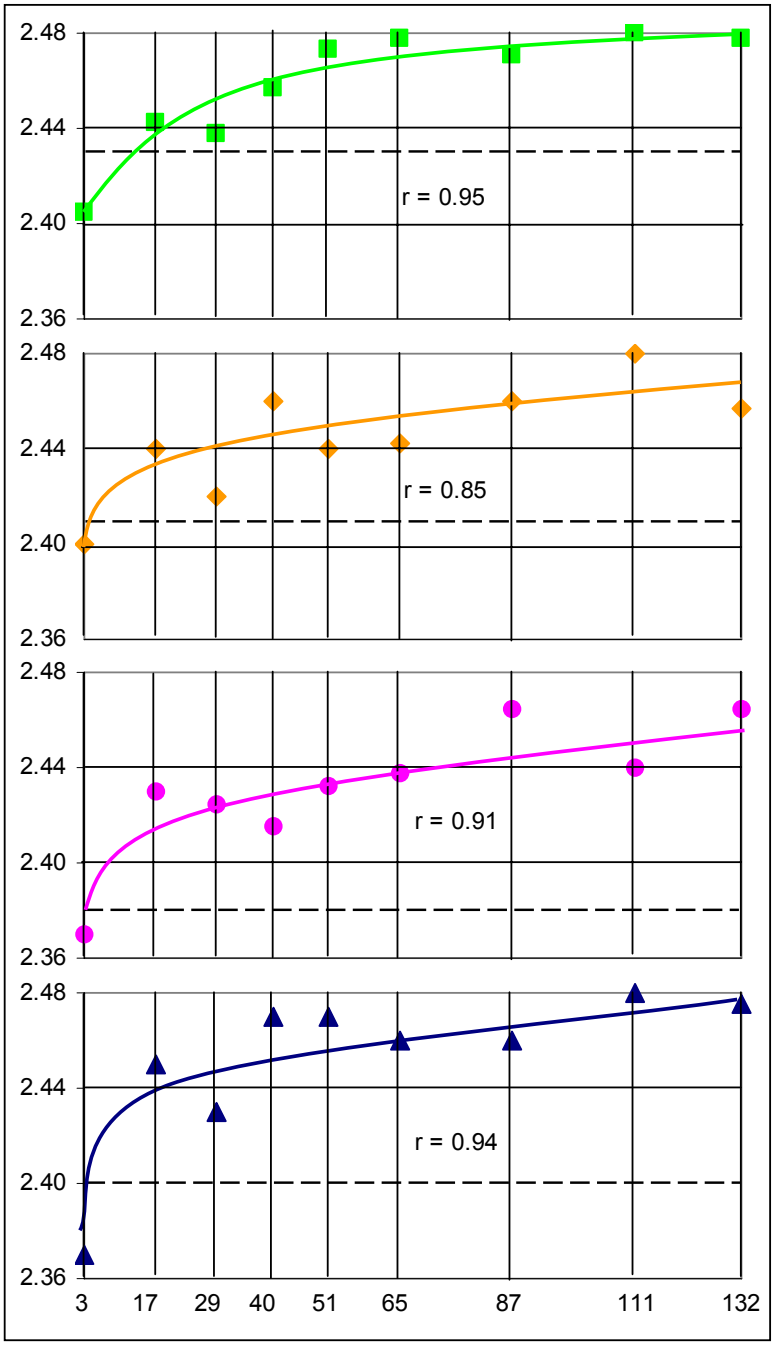

Figure 2.6: In-service densification with time in months (traffic) (after Serafin et al. 1967)

Galloway (1960) compared field densities measured from cores after 9 months following construction of 12 sections in Texas comprised of a variety of aggregates (gravel, limestone, and basalt) with laboratory densities determined using the TGC. Results indicated that densities of five of the sections exceeded the laboratory-achieved density by 1% to 3%. Average in-place

density of the sections after 9 months was determined to be 94.6% with a maximum density of 97.2%. Bright et al. (1967) found that pavements produced with the same mix but placed at different temperatures seemed to reach the same density after 20 months (250 °F–345 °F) regardless of the initial compaction density; the exception was a section paved at a temperature of 225 °F that exhibited a lower density. Palmer and Thomas (1968) researched the in-place density of 47 test sections over the first 5 years of service. It was observed from the data that the first year density increase averaged about half of the total 5 year increase in density. The average gain in the density was 3.5% for the wheel paths and 2.5% between the wheel paths. High volume pavements were seen to have a density increase of approximately twice that of the low and medium volume pavements. Palmer and Thomas concluded that there did not appear to be a good correlation between the applied traffic and the increase in density.

Epps et al. (1970) evaluated 15 field test sections constructed in Texas to determine the relationship between traffic and the in-place air voids over a period of 2 years. Mixes were comprised of gravels, slags, and limestone aggregates with AC-10, AC-20, and 85/100 penetration grade asphalt cements. Eleven of the 15 sections used the AC-20 binder. Sections were constructed to different initial compaction densities. It was found that the initial compaction did not seem to significantly affect the amount of pavement densification (shown in Fig 2.7). The majority of the pavements compacted to densities within 1%–2% of each other after the 2-year analysis period, with a decrease of 4%–6% occurring in air voids. It was concluded that approximately 80% of the average total 2-year densification was obtained during the first year following construction.

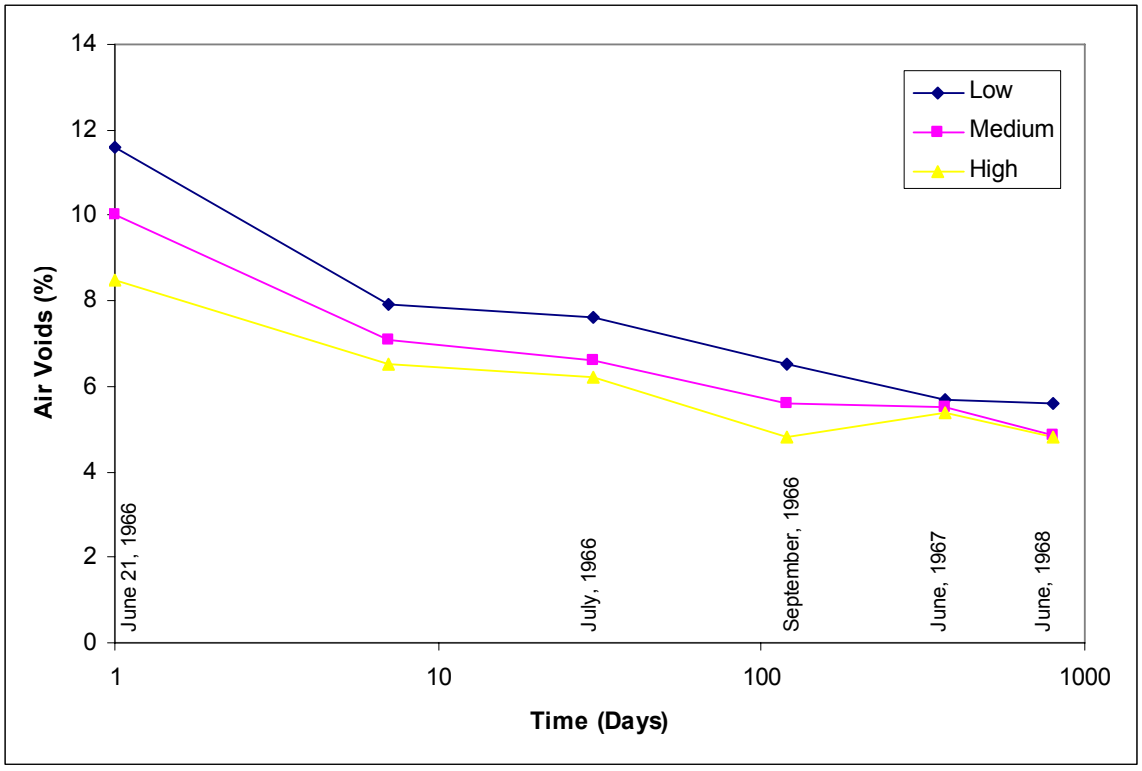

Figure 2.7: Densification for low, medium and high initial compactive efforts (after Epps et al. 1970)

Paterson et al. (1974) reported on densification of 20 accelerated pavement testing (APT) sections comprising varying combinations of asphalt cement type, asphalt content, maximum stone size, lift thickness, tire pressure, and constructed density tested in New Zealand. The mixes used were continuously dense-graded comprising crushed gravel designed using the 75-blow Marshall procedure. A testing vehicle with a 20-kN wheel load made 700 vehicle passes per hour for up to 30,000 total passes. The temperatures at the mid-point in the lift were held constant at 77° F and at 104° F. The results of the study indicated:

1) Temperature greatly influenced the increase in density under traffic while tire pressure influenced the density to a lesser extent.
2) The influence of the construction density depended on the test temperature. For tests at the lower temperature (77° F) the construction density influenced the stable state density but not so at 104° F.
3) The majority of the mixes had densities after testing that ranged from 0.5% to 1% greater than the 75-blow Marshall densities.

Wright and Burgers (1984) reported a linear relationship between initial relative construction compaction density and traffic densification. Brown and Cross (1991) evaluated densification trends on eighteen pavements in six states, thirteen of which had prematurely rutted. They found a poor correlation between pavement densification and traffic applied, indicating that traffic is not the only factor controlling mix densification. Foster (1993) also found that the densification of traffic occurs very quickly immediately following initial placement and loading and slows over time. For the pavements evaluated, research indicated that initial in-place air voids were determined to be the main factor that affects pavement densification over time. Other factors such as climate and rate of loading were also found to have an effect on densification. A summary of the effect of initial in-place voids on pavement densification is shown in Figure 2.8, where VTMd is the developed air voids and VTMc is the construction air voids. The results of 15 pavements evaluated in Texas showed a linear trend. An in-place air void level of 8% was determined to be the void level that generally resulted in approximately 4% (laboratory) voids for the final void level in the pavement.

Hanson et al. (1994) reported on the densification of five asphalt-aggregate mixture analysis system (AAMAS) test sections, one of which was in Texas. The in-place air voids after 5 years were determined to be statistically different from those found after 2 years. A relationship was found between pavement densification and traffic applied but it contained a lot of scatter. It was concluded that:

1) Pavements do continue to densify beyond 2 years of service.
2) Mixes with higher initial in-place voids have higher rates of void changes.
3) The 5-year in-place air voids were generally less than the design air voids.

Newcomb et al. (1997) conducted a research study to evaluate the relationship between traffic and in-place densification on 16 projects completed in 1990 in Minnesota. They found that the majority of densification occurred during the first year of service and that for low traffic volume (< 10,000 ADT) roads, densification generally occurred in the top 65 mm for pavements with little densification below 2.5 in. The authors suggested that the in-place voids immediately

after construction for these lower layers must be close to the design voids to account for the lack of densification. They recommended that the lower layers be designed at 2% lab voids to aid the field compaction. Densification for higher volume pavements (> 50,000 ADT) occurred mostly in the top 4 in. when the initial voids were between 6% and 7%. With initial voids between 9% and 10%, densification was throughout the full depth of the HMA layer.

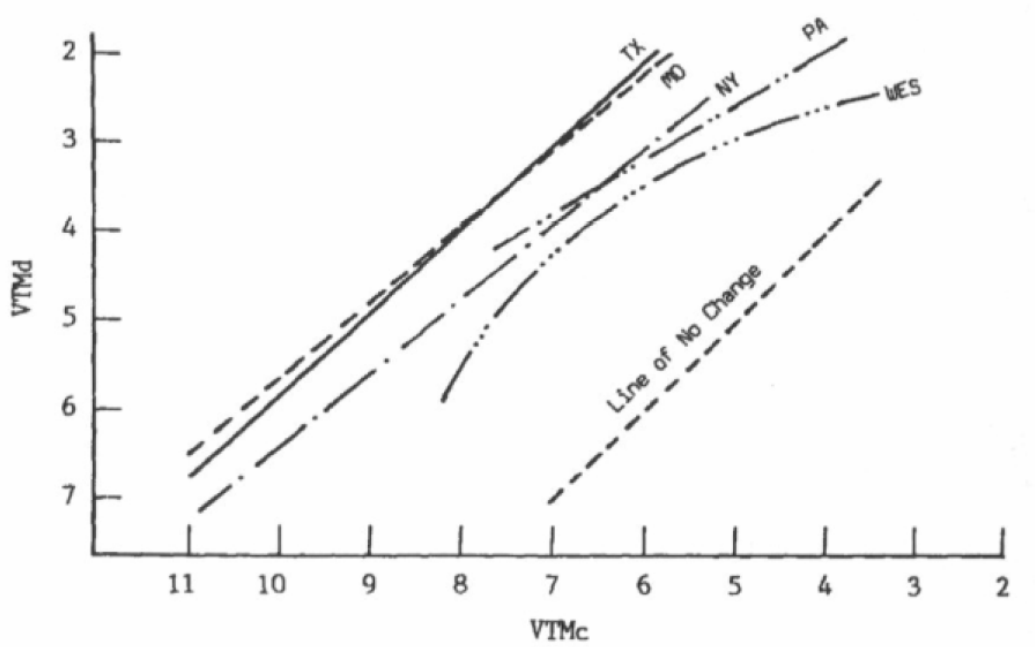

Figure 2.8: Relationship between design and in-place air voids (after Foster 1993)

NCHRP 9-9(1) Verification of Gyration Levels in the N_{design} Table

In a follow-up study to the original NCHRP 9-9 research, Prowell et al. (2003) investigated in-place densification of HMA toward verification of Superpave N_{design}. Densification data were obtained from mixture paved and tested at the NCAT test track in Auburn, Alabama, and from selected sites in the field. Although the research has not been completed to date, some of the preliminary conclusions are:

1) Accelerated testing (at the NCAT test track) indicated a slower rate of densification for mixes containing modified binders that have been "bumped" to provide a higher PG grade.
2) Constructed pavement densities at the accelerated test track were significantly affected by gradation. Nominal maximum aggregate size also had an affect.
3) The data from both the accelerated test track and the field verification projects appear to verify the current specifications for gyrations at design traffic levels of 0.3 to 3 million ESALs.
4) Results have indicated that different brands of Superpave gyratory compactors often provide differences in compactive effort.

5) It appears that the primary difference in compactive effort between different gyratory compactors is caused by differences in the internal angle of gyration as measured with a gauge such as the angle verification kit.

Figure 2.9 indicates densification of HMA mixtures as noted at the NCAT test track. The trends have been determined for PG 67 and PG 76 mixes in the upper and lower lifts of the constructed asphalt layers. Figure 2.10 shows predicted gyrations to achieve the track densities with traffic as back-calculated from gyratory compaction tests done on the field mixtures during construction. Results indicate that the predicted design gyrations level for PG 76-22 to achieve a density of 96% could be lower than for PG 67-22 mixes. Prowell suggests that since densification is decreased with stiffer binders, it may be desirable to consider increasing the asphalt content slightly to promote more durability.

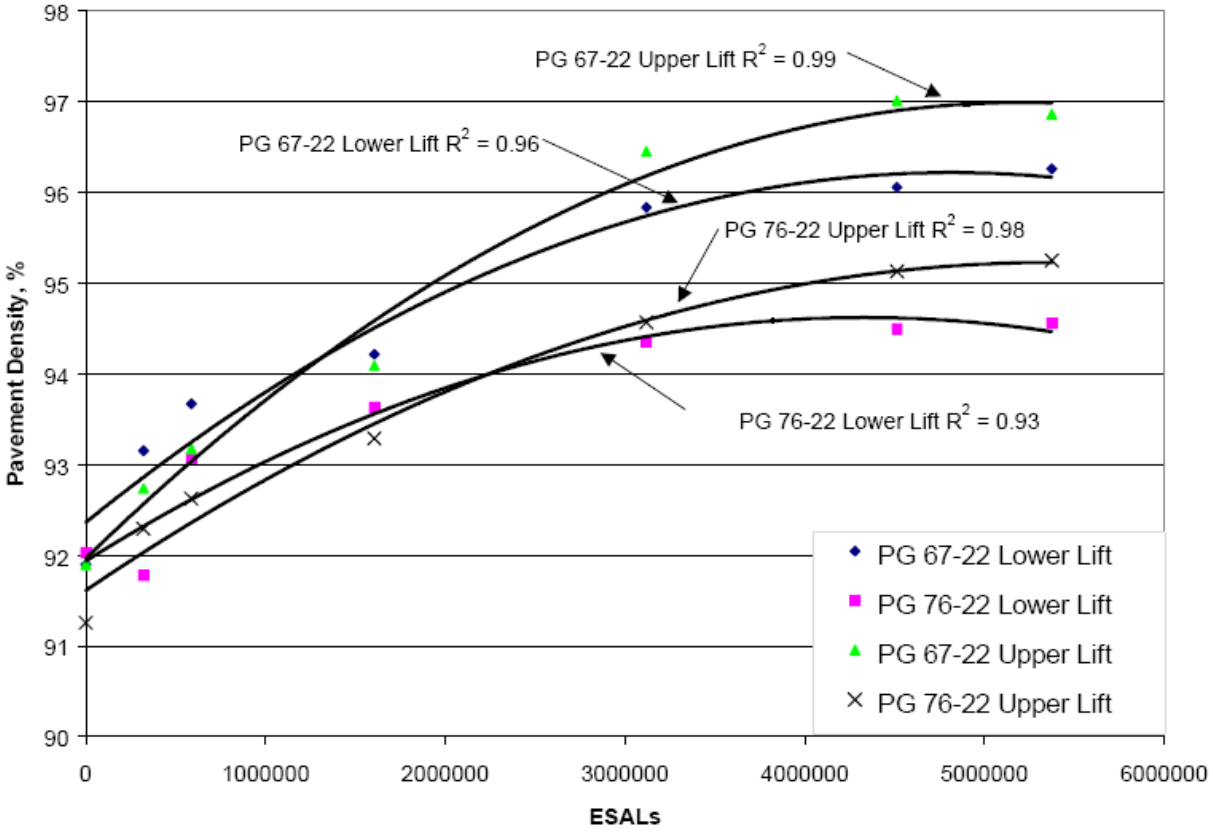

Figure 2.9: Average test track pavement densification (Prowell et al. 2003)

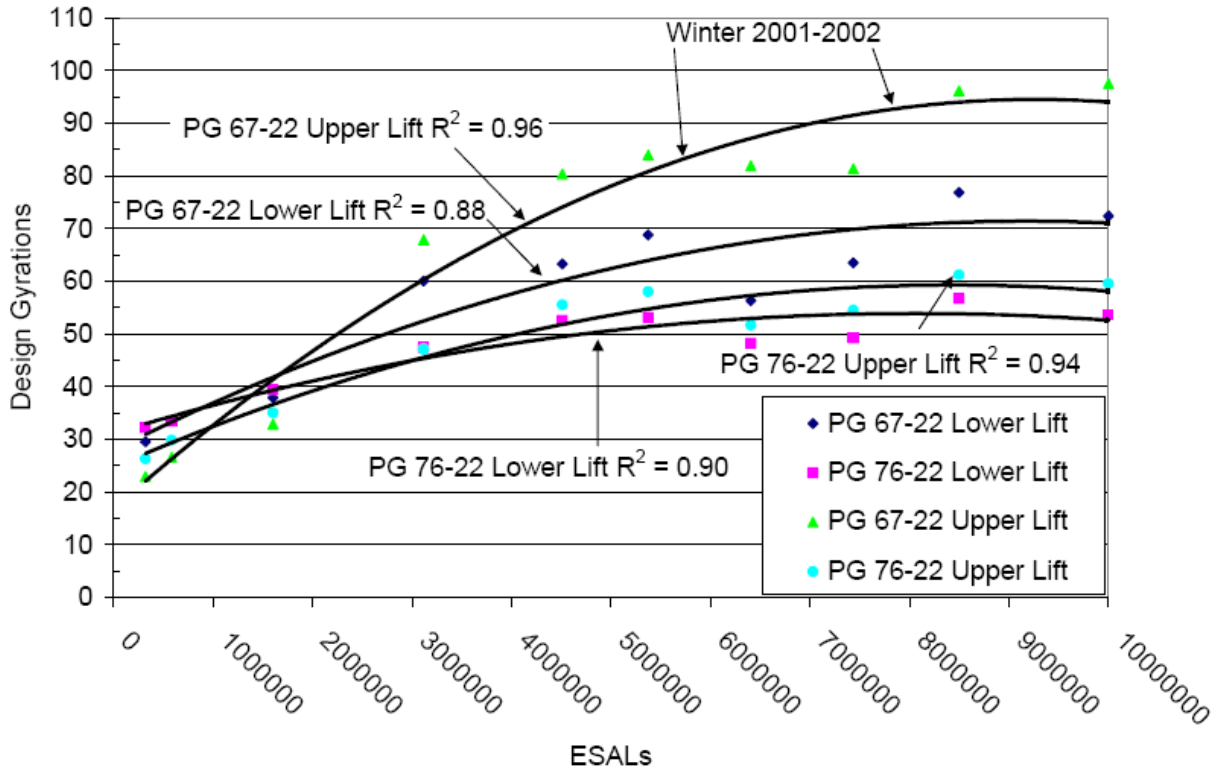

Figure 2.10: Average predicted gyrations to meet field density vs. ESALs (Prowell 2005)

Field verification of the N_{design} Table done as part of the NCHRP 9-9(1) project included monitoring of the densification of 40 pavement sections from various regions around the country over time. Figure 2.11 shows a cumulative frequency plot for in-place density for the sampling periods through 2 years. As can be seen, the majority of densification occurs in the first 3 months after construction. The in-place density representing the 50% frequency increased slightly from 93% to 93.2% between 6 months and 1 year, and then to 94.6% between 1 and 2 years. The month of construction was found to significantly influence densification. The final report on the study is currently under NCHRP review.

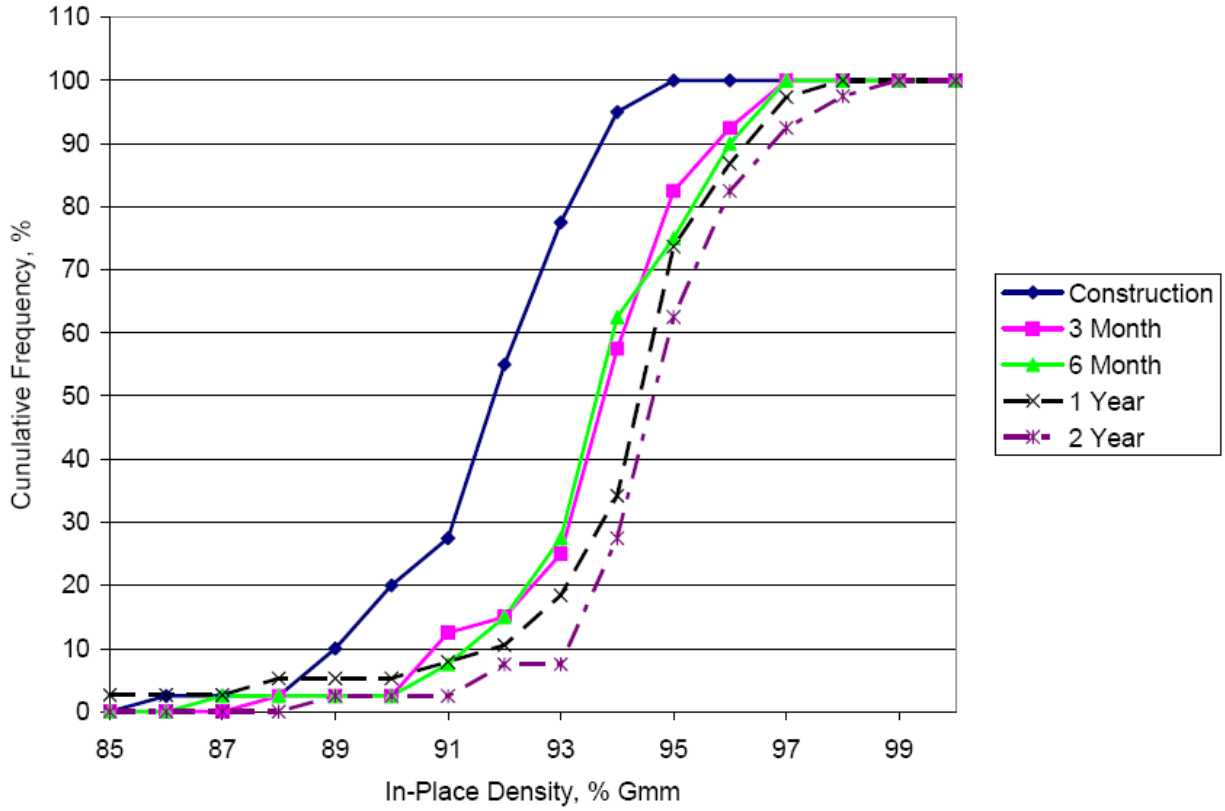

Figure 2.11: Cumulative frequency plot for in-place density by sampling period (Prowell 2005)

3. Experimental Design

3.1 Experimental Approach

A research approach that would allow the selection of the optimal binder content derived from performance-related testing for a given mix was selected for this research study. A number of Superpave mixes commonly used by TxDOT were designed, prepared, and tested. Superpave criteria were used to determine the optimal binder content of the analyzed asphalt mixes: 96% Gmm at current N_{design} (see Fig 1.1). For each mix, the asphalt content was modified such that 96% Gmm was achieved at different N_{design}. For example, three other asphalt contents could be selected for that reference mix such that 96% Gmm would be achieved at 125, 100, 75, and 50 gyrations (i.e., moving along Approach 2 in Fig 1.1).

Each of these four mixes was subjected to performance-related tests to assess their rutting and cracking characteristics. The new specification Item 344, the Hamburg Wheel Tracking Device (HWTD), was used for assessing potential rutting performance, the Indirect Tensile Strength (ITS) test for determining the potential cracking resistance of the mixes, and fatigue testing in order to assess the fatigue resistance in the asphalt mix.

Based on current TxDOT specifications and equivalent specifications from other states and countries, HWTD and fatigue criteria were for the selection of optimum binder content. In principle, a range of binder contents could simultaneously satisfy both criteria (e.g., 3.0% to 4.4% in Fig 3.1) in this case and, based on durability considerations, the maximum possible binder content that satisfied the HWTD criterion was selected.

Once the optimum asphalt binder content was selected, the "new" N_{design} was back-calculated. This innovative approach results in binder content selections that are optimized from a performance point as compared with current Superpave designs. Furthermore, this approach can accommodate different N_{design} for varying environmental and traffic conditions and it allows the designer to tailor mixtures to the lower or higher binder contents depending on whether the concern is rutting or fatigue failure, respectively. Summarizing, the research was based on an approach consisting of the following three steps:

Step 1: Determine reference binder content. Initially, a Superpave mixture is selected and gyratory compacted to Nmax levels at four different binder contents that span the optimum binder content as anticipated. The binder content that allows 4% VIM at a current N_{design} level (100 gyrations) is then determined. This is the reference binder content (Pref).

Step 2: Performance evaluation. This step involves specimen preparation and performance testing. Performance testing includes HWTD tests to assess rutting resistance and ITS and fatigue testing to assess mixture stiffness and cracking or fatigue resistance. For each individual experimental treatment, four different binder contents are selected: Pref - %, Pref, Pref + %, Pref ++ %. These binder contents were selected such that the 96% Gmm criterion was met at 125, 100, 75, and 50 gyrations, respectively. Then asphalt specimens were prepared by gyratory compaction to 7% VIM. It is proposed that 150 mm (6 in.) diameter specimens be prepared to heights of 63 mm (2.5 in.) for the HWTD tests and 50

mm (2 in.) for the ITS. Four specimens were prepared for the HWTD tests and two for the ITS at each of the binder contents. The ITS tests are used to determine the maximum tensile strength of the material being tested. In this case, to analyze fatigue, rectangular samples measuring 63 mm (2.5 in.) by 50 mm (2 in.) by 393 mm (15.5 in.) extracted from larger samples compacted using a vibratory compactor were used.

Step 3: Back-calculate new N_{design}. Having completed the performance tests, the results are evaluated to determine the maximum binder content that gives satisfactory performance. HWTD results are evaluated in light of current specifications related to binder grade (i.e., 12.5 mm at 10k, 15k, and 20k cycles for PG 64, 70, and 76 binders, respectively). Likewise, the mean ITS test result must be in the range of 85 to 200 psi (Item 344). The maximum binder content that satisfies each of the performance criteria will be used to back-calculate a new N_{design} based on the compaction characteristics developed as part of Step 1. Finally, the volumetric criteria of the mix at this new N_{design} compaction level is calculated and compared with current Superpave criteria.

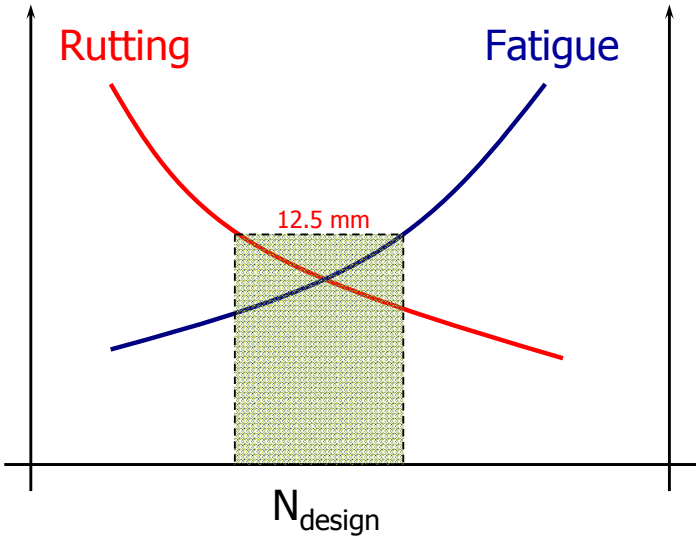

Figure 3.1: Graphical representation of research approach

The previous three steps were performed in order to develop a feasible experimental design that would provide the information required to developed new specifications for the selection of N_{design}. The experimental design carried out within this project was based on testing the following:

1) The evaluated gradations were 19.5 mm (or 12.5 mm NMAS) Superpave B (SP-B), 12.5 mm (or 9.5 mm NMAS) Superpave C (SP-C), and 9.5 mm SP-D (4.75 mm NMAS).
2) The different aggregate gradations were mixed with PG 64-22, PG 70-22, and PG 76-22. The PG 76-22 was obtained from a modification of the PG 64-22 base binder. This selection characterizes the vast majority of mixes used in Texas.

3) Combined blends for the mixtures evaluated were based on gravel and limestone stockpile gradations.
4) Four binder contents were used.
5) For each of the listed combinations, two samples were prepared for rutting, three for indirect tensile strength, four for fatigue, and two for volumetric determinations.

PaveTex Engineering and Testing, Inc., were subcontracted to prepare all samples (gyratory compaction) and to carry out the Superpave volumetric design as well as the HWTD testing as proposed. PaveTex is a laboratory fully accredited by AASHTO Materials Reference Laboratory (AMRL) and TxDOT. PaveTex has extensive experience with TxDOT projects and practices; in fact, the majority of Superpave mixtures currently used in TxDOT projects have been designed by PaveTex for various contractors. The University of Texas at Austin performed the four-point beam loading test to characterize the fatigue performance of the mixtures.

Samples of the various aggregates and blends were collected and evaluated using the Aggregate Imaging System (AIMS). The AIMS system enabled the determination of aggregate statistics that allowed the establishment of correlations between these statistics and mixture performance. Correlations between AIMS statistics and VMA were also evaluated.

Once the laboratory testing was performed, volumetric determinations were made in order to compare relevant volumetrics using the Superpave (level 1) approach as opposed to the performance-related approach recommended in this research. As part of the volumetrics, VMA was calculated for all mixes at the various compaction levels. The calculated information was correlated with the information collected on aggregate characteristics and estimated performance. To determine significant trends from a statistical perspective, a full analysis of variance (ANOVA) and a multiple regression analysis were carried out. The analyses enabled the determination of significant factors that influence the back-calculated N_{design} as well as the quantification of their relative contribution. Subject to the availability of data, multivariate regression analyses were carried out to enhance and corroborate the ANOVA results.

One of the results of these analyses was the quantification of the variability of the test results and their effect of the selection of N_{design}. Thus, it is recommended that a reliability-based approach be used for the selection of N_{design} as a function of expected traffic and environmental conditions. For example, once the N_{design} is recommended based on mean performance (i.e., 50% reliability), if higher traffic volumes are expected (or harsh environmental conditions), the design reliability should be increased.

3.2 Materials

As mentioned previously, the asphalt binders evaluated during this research have the same origin. However, three different PG grades were analyzed: PG 64-22, PG 70-22, and PG 76-22. In accordance with Superpave methodology, the higher the PG number, the higher the stiffness of the asphalt binder at higher temperatures; in other words, the higher the number, the more resistant the asphalt binder is to high temperature distress types such as rutting or shoving. Consequently, the mixes prepared with PG 64-22 were expected to show the highest fatigue resistance and the PG 76-22 mixes were expected to show the highest rutting resistance.

3.2.1 Aggregates

Two aggregate sources have been evaluated during this research project: a gravel and a limestone typical of those found in Texas. All of the gravel stockpiles were mixed in to prepare Superpave Type C gradations, SP-C. The limestone mixes included SP-B, SP-C, and SP-D gradations. The gradations used are shown in Table 3.1.

Table 3.1: Analyzed gradations

Sieve Size	Gravel	Limestone		
	SP-C	SP-B	SP-C	SP-D
2 in.	100.0	100.0	100.0	100.0
1½ in.	100.0	100.0	100.0	100.0
1 in.	100.0	99.0	100.0	100.0
¾ in.	100.0	92.4	100.0	100.0
½ in.	94.6	79.3	90.2	98.0
⅜ in.	81.0	-	69.4	92.7
#4	54.4	41.5	41.7	63.6
#8	32.9	32.6	30.6	49.6
#16	22.4	19.4	16.9	29.2
#30	16.2	12.0	10.3	17.7
#50	11.0	7.2	6.2	10.6
#100	7.6	-	4.4	-
#200	5.5	3.0	2.6	4.2

The gradations in Table 3.1 were obtained by proportioning different aggregate stockpiles. The materials used to develop the desired gradations are shown in Table 3.2.

Table 3.2: Summary of analyzed sieve sizes for each aggregate source

Aggregate Type	Stockpile	Retained Sieve								
		1"	3/4"	1/2"	3/8"	No. 4	No. 8	No. 16	No. 30	No. 60
Gravel	C-Rock			X	X	X	X			
	D/F-Blend				X	X	X	X	X	X
	Sand					X	X	X	X	X
	Screenings (Limestone)					X	X	X	X	X
Limestone	B-Rock	X	X	X	X	X				
	C-Rock			X	X	X	X	X	X	X
	D/F-Blend				X	X	X	X	X	X
	Screenings					X	X	X	X	X

With the aid of the AIMS equipment, properties such as texture, angularity, sphericity, shape, and flatness to elongated ratio were measured. As established by Masad (2005), the following classifications have been selected:

1) Texture (based on wavelet analysis to decompose texture scales):
   a) Polished (< 165)
   b) Smooth (< 275)
   c) Low Roughness (< 350)
   d) Moderate Roughness (< 460)
   e) High Roughness (< 800)
2) Gradient Angularity (based on gradient vectors at each edge point, as well as the vector angle):
   a) Rounded (<2100)
   b) Sub-Rounded (<3975)
   c) Sub-Angular (<5400)
   d) Angular (<10000)
3) Radius Angularity (based on the difference between particle radius and that of an equivalent ellipse):
   a) Rounded (<8)
   b) Sub-Rounded (<10.65)
   c) Sub-Angular (<15.25)
   d) Angular (<20)
4) Sphericity (includes information about three dimensions of the particle, i.e., longest dimension, intermediate dimension, and shortest dimension):
   a) Flat/Elongated (<0.6)
   b) Low Sphericity (<0.7)
   c) Mod. Sphericity (<0.8)
   d) High Sphericity (<1)
5) Shape (used to quantify a particle in two dimensions):
   a) Circular (<6.5)
   b) Semi-Circular (<8)
   c) Semi-Elongated (<10.75)
   d) Elongated (<20)

The results are shown in Table 3.3. It can be observed from the table that the gravel has a texture between polished and smooth, while the limestone is extremely polished. With respect to angularity, and using the gradient method, both aggregate sources appear to be sub-rounded. Based on the radius method, the conclusion is the same, although some of the gravel stockpiles classify as sub-angular (on the lower extreme). It was also determined that both aggregate sources present low sphericity and on average the gravel can be classified as semi-circular, while the limestone can be classified as circular.

Table 3.3: Summary of analyzed properties for each aggregate source

Aggregate Type	Stockpile	Property				
		Texture	Angularity		Sphericity	Shape
			Gradient	Radius		
Gravel	C-Rock	140.333	2778.737	10.603	0.687	7.444
	D/F-Blend	151.768	3577.738	10.983	0.670	8.395
	Sand	152.667	3835.767	11.060	0.693	8.978
	Screenings (Limestone)	318.357	3940.380	10.295	0.667	8.184
Limestone	B-Rock	75.514	2795.085	10.329	0.619	7.280
	C-Rock	74.051	2960.364	10.222	0.610	7.291
	D/F-Blend	77.806	3336.070	10.489	0.668	7.810
	Screenings	52.684	3733.172	10.399	0.623	8.279

More details on the aggregate properties measured using the AIMS equipment are given in Appendix D.

3.3 Tests

As previously discussed, in order to characterize the performance of the analyzed asphalt mixtures, several tests were used: HWDT to evaluate rutting resistance, and ITS and four-point beam testing to characterize the resistance of the asphalt mix to cracking and fatigue.

3.3.1 Hamburg Wheel Tracking Device (HWTD)

The HWTD was originally developed in Hamburg, Germany and later modified. The equipment that was used for this project is illustrated in Figure 3.2. HWTD has been adopted by TxDOT as Tex-242-F specification requirement for bituminous mixtures. The test was originally intended to be run on a slab measuring 260 mm wide, 320 mm long, and typically 40 mm thick (10.2 in. × 12.6 in. × 1.6 in.) that is produced using a linear kneading compactor. Because of the relative difficulty and equipment required to produce such slabs, the test is currently being performed on cylindrical specimens with a 6 in. (150 mm) diameter and a 2.4 ± 0.1 in. (62 ± 2 mm) specimen height. These cylindrical specimens are compacted using the Superpave Gyratory Compactor (SGC) to a 7 ± 1% air void content.

Testing in the HWTD is conducted under water at 122 ± 2° F (50 ±1^{o} C). Loading of samples in the HWTD is accomplished by applying a 158 ± 5 lbs. (705 ± 22 N) force onto a steel wheel with a diameter of 8 in. (203.6 mm) and width of 1.85 in. (47 mm). The steel wheel is then tracked back and forth over two cylindrical test samples previously cut to fit in a mold that will hold the two samples together (as seen on Fig 3.3). Test samples are loaded until 12.5 mm of deformation occur or for 20,000 passes. The travel speed of the wheel is approximately 340 mm per second.

Figure 3.2: Hamburg Wheel Tracking Device

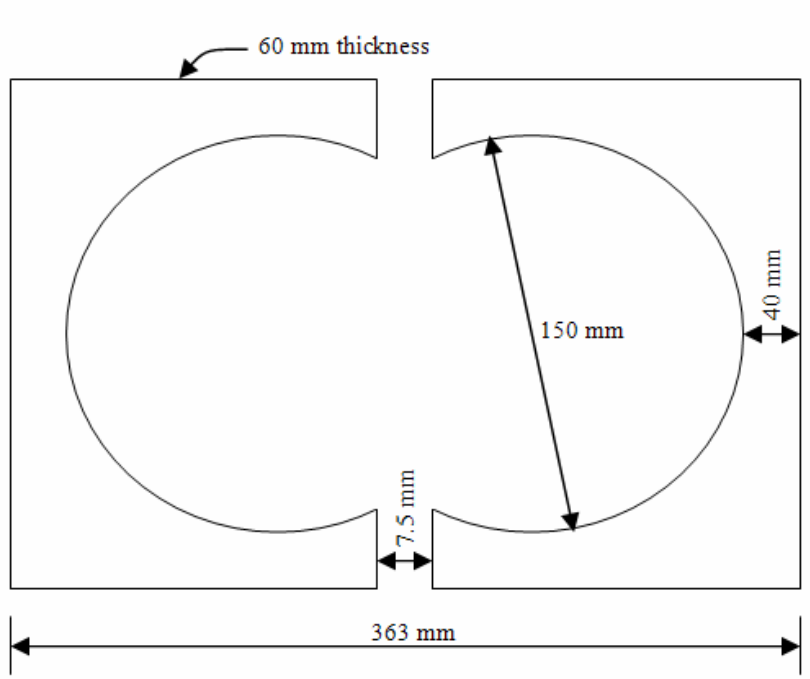

Figure 3.3: Top view of test specimen configuration for the HWTD (not drawn to scale)

As pointed out in Brown et al. (2001b), the results obtained from the HWTD consist of rut depth, creep slope, stripping inflection point, and stripping slope, as seen in Figure 3.4. The creep slope is the inverse of the deformation rate within the linear region of the deformation curve after post compaction and prior to stripping (if stripping occurs). The stripping slope is the inverse of the deformation rate within the linear region of the deformation curve, after the onset of stripping. The stripping inflection point is the number of wheel passes corresponding to the intersection of the creep slope and the stripping slope. This value is used to estimate the relative resistance of the HMA sample to moisture induced damage.

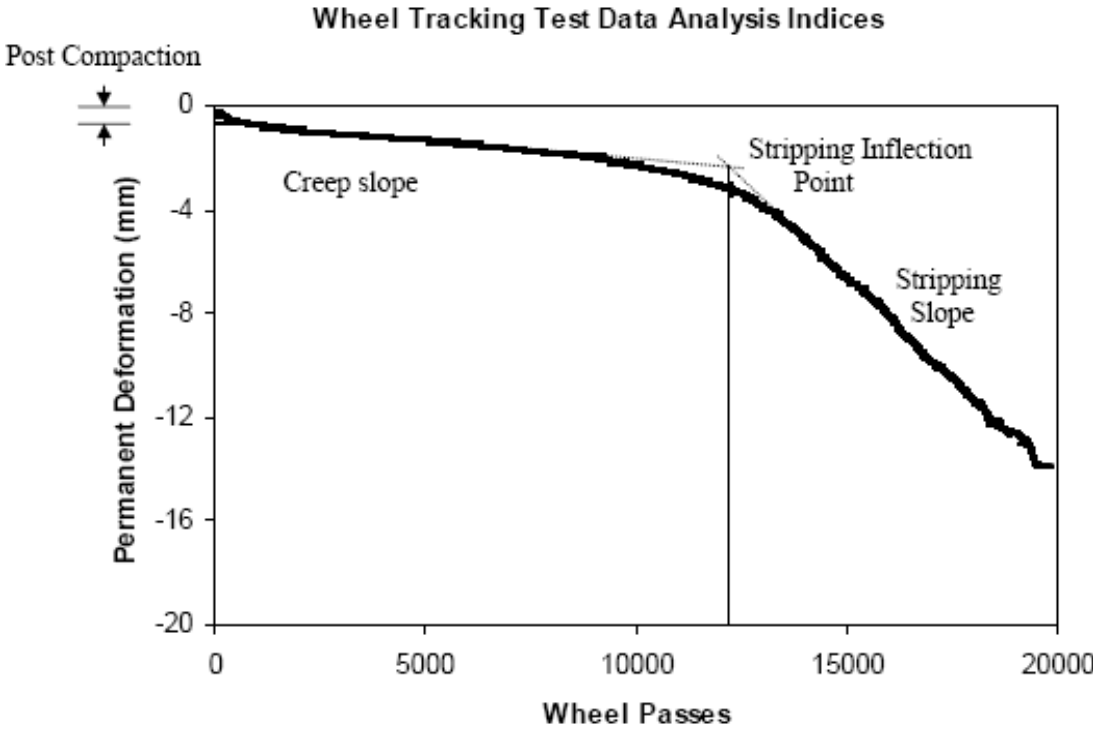

Figure 3.4: Definition of results from HWTD (after Brown et al. 2001b)

3.3.2 Indirect Tensile Strength (ITS)

The ITS test is performed by loading a cylindrical specimen with a single or repetitive compression load to the diametral vertical plane of the cylindrical specimen. The equipment used to perform the tests is shown in Figure 3.5. This type of loading allows a uniform tensile stress perpendicular to the direction of the applied load.

The specimens used for this test are compacted using the SGC to an air void content of 7 ± 1%. The test specimens are then placed in a temperature controlled chamber at 77 ± 2° F (25 ± 1° C) long enough to ensure that the temperature is constant through the entire specimen. A deformation rate of 2 in. (51 mm) per minute is applied to the diametral vertical plane of the cylindrical specimen. The total vertical load at failure of the specimen is then determined and recorded.

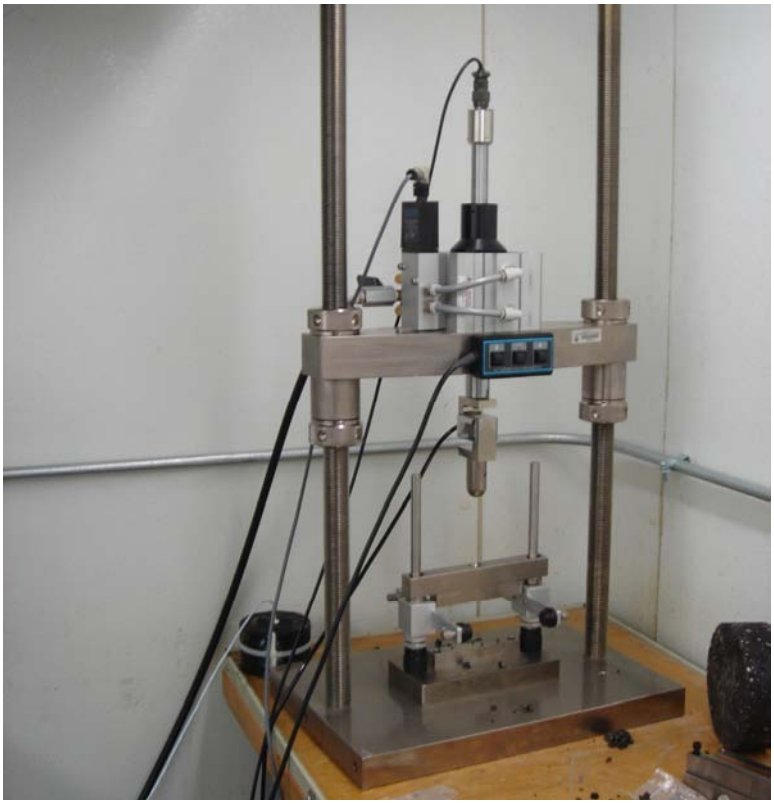

Figure 3.5: Universal Testing Machine used to perform ITS tests

The tensile strength is then calculated as follows,

$$S_T = \frac{2 \cdot F}{\pi \cdot (h \cdot d)} \quad \text{(Eq 3.1)}$$

Where,
S_T = Indirect tensile strength, Pa (psi)
F = Total applied vertical load at failure, N (lb)
h = Height of specimen, in mm (in.)
d = Diameter of specimen, mm (in.).

The tensile strength is generally used to evaluate the cracking potential of the compacted asphalt mix. Asphalt mixes that cannot withstand high strains prior to failure are more likely to crack than asphalt mixes that can resist high strains.

3.3.3 Four-Point Bending Beam (FPBB) Test

Four point bending beam (FPBB) test was used to determine the cracking and fatigue characteristics of the mixtures. The fatigue life that is determined using this test can be used to estimate the fatigue properties of an HMA layer under repeated traffic loading, and thus, pavement life to fracture. The test was performed following AASHTO T321-03 specifications. The test is performed on a beam that is 63 mm wide, 393 mm long, and 50 mm thick (2.5 in. ×

15.5 in. × 2.0 in.). The beams were obtained by using a wet saw to cut previously compacted slabs that were produced using an automatic vibratory compactor (AVC) (refer to Fig 3.6).

Figure 3.6: Vibratory compactor

The testing is performed using a four-point beam loading device like the one shown in Figure 3.7. The beams used for this test are compacted to a target air void content of 7 ± 1%. The test beams are then placed in a temperature controlled chamber at 68 ± 2° F (20 ± 1° C) long enough to ensure that the temperature is constant through the entire beam.

Repeated haversine loads are then applied at the third points of the beam specimen. The loading rate used was 10 Hz, which produces a constant bending moment over the central portion of the beam. This test can be conducted at constant stress or at constant strain. For this research project, testing was performed to a constant strain level (approximately between 250 and 750 μm). Fifty initial load cycles are then applied at the selected strain level and the stiffness of the asphalt mix is determined at this cycle as follows:

$$S = \frac{\sigma_t}{\varepsilon_t} = \frac{\left[\frac{(0.375P)}{bh^2}\right]}{\left[\frac{(12\delta h)}{3L^2 - 4a^2}\right]} \quad \text{(Eq 3.2)}$$

Where,
S = Flexural stiffness (Pa)
σ_t = Maximum tensile strength
ε_t = Maximum tensile strain
P = Load applied by actuator (N)
b = average specimen width (m)
h = average specimen height (m)
δ = maximum deflection at center of beam (m)
a = spacing between inside clamps (0.119 m)
L = length of beam between outside clamps (0.357 m)

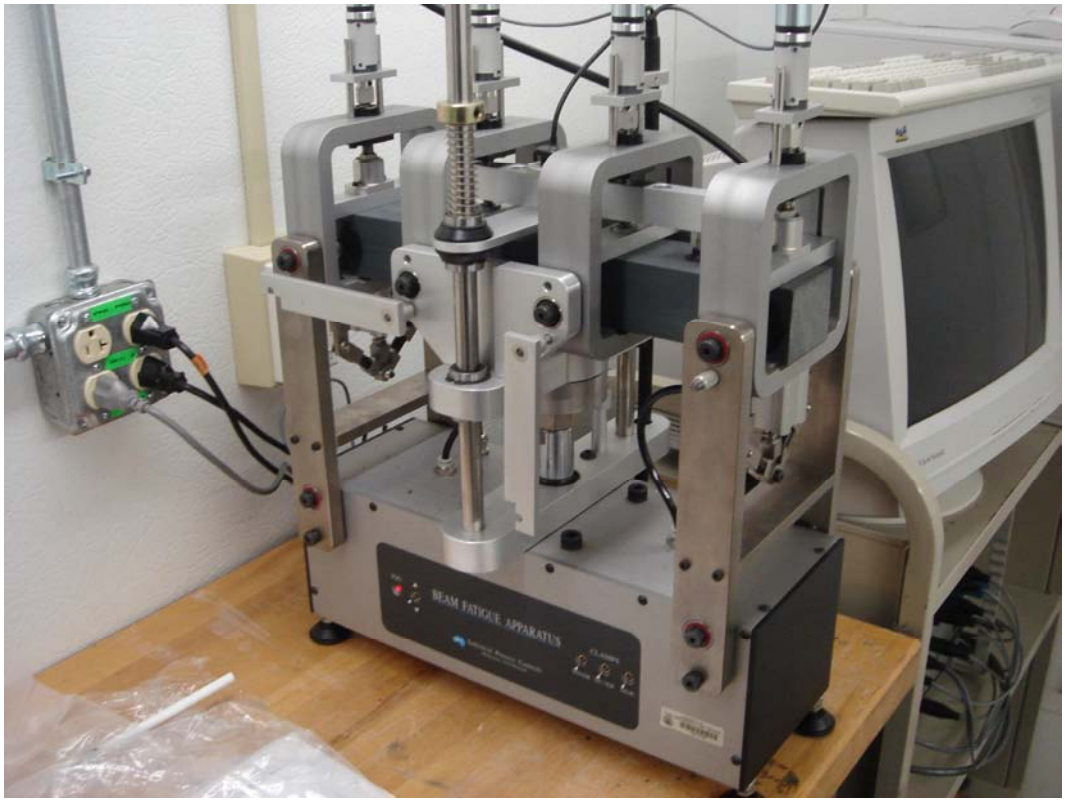

Figure 3.7: Beam fatigue apparatus

The test terminates when the stiffness of the asphalt mix drops below 50% of the initial stiffness. Consequently, the number of cycles that were required for the mix to reach 50% of its initial stiffness is considered as the number of cycles to failure.

4. Results

As mentioned in previous chapters, Hamburg Wheel Tracking Device (HWTD), Indirect Tensile Strength (ITS), and four-point bending beam (FPBB) tests were performed on selected experimental treatments (each at four asphalt contents, which in turn correspond with four selected levels of N_{design} at 50, 75, 100, and 125). The results obtained are described in detail in the following sections.

4.1 Hamburg Wheel Tracking Device (HWTD) Results

TxDOT has recently implemented HWTD specifications, which require asphalt mixes to develop a rut below 12.5 mm at 10,000, 15,000, or 20,000 passes, depending on whether the asphalt mix uses the PG 64, 70, or 76 asphalt binder, respectively. Table 4.1 shows the rut depth for the evaluated experimental treatments and each corresponding asphalt binder content.

Table 4.1: Summary of HWTD results at 10,000, 15,000, and 20,000 passes

Manufacturer	PG Grade	Aggregate Type	Gradation	%AC	Max Deformation		Rut Depth (mm)		
					Cycles to Maximum	Deformation	10,000 Passes	15,000 Passes	20,000 Passes
Valero Asphalt	PG76-22S	gravel	SP-C	5.5%	20,000	5.7	4.8	5.2	5.7
Valero Asphalt	PG76-22S	gravel	SP-C	5.9%	20,000	7.3	6.0	6.7	7.3
Valero Asphalt	PG76-22S	gravel	SP-C	6.3%	20,000	7.2	5.6	6.7	7.2
Valero Asphalt	PG76-22S	gravel	SP-C	6.7%	20,000	9.4	7.2	8.6	9.4
Valero Asphalt	PG70-22	gravel	SP-C	5.5%	20,000	6.7	5.2	6.0	6.7
Valero Asphalt	PG70-22	gravel	SP-C	5.8%	20,000	7.7	6.5	7.1	7.7
Valero Asphalt	PG70-22	gravel	SP-C	6.1%	20,000	7.5	6.0	6.8	7.5
Valero Asphalt	PG70-22	gravel	SP-C	6.5%	20,000	9.8	7.6	8.7	9.8
Valero Asphalt	PG76-22S	limestone	SP-D	4.9%	20,000	3.0	1.3	1.6	3.0
Valero Asphalt	PG76-22S	limestone	SP-D	5.1%	20,000	3.2	2.4	2.8	3.2
Valero Asphalt	PG76-22S	limestone	SP-D	5.4%	20,000	10.1	4.9	7.9	10.1
Valero Asphalt	PG76-22S	limestone	SP-D	5.9%	20,000	8.0	4.0	5.5	8.0
Valero Asphalt	PG64-22	limestone	SP-B	4.2%	7,822	12.5	-	-	-
Valero Asphalt	PG64-22	limestone	SP-B	4.5%	4,950	12.5	-	-	-
Valero Asphalt	PG64-22	limestone	SP-B	4.8%	3,380	12.5	-	-	-
Valero Asphalt	PG64-22	limestone	SP-B	5.2%	2,527	12.5	-	-	-
Valero Asphalt	PG76-22S	limestone	SP-C	5.1%	20,000	3.4	2.8	3.1	3.4
Valero Asphalt	PG76-22S	limestone	SP-C	5.4%	20,000	4.4	4.2	4.4	4.4
Valero Asphalt	PG76-22S	limestone	SP-C	5.8%	20,000	5.3	4.2	4.9	5.3

Table 4.1 Summary of HWTD results at 10,000, 15,000, and 20,000 passes (continued)

Manufacturer	PG Grade	Aggregate Type	Gradation	%AC	Max Deformation		Rut Depth (mm)		
					Cycles to Maximum	Deformation	10,000 Passes	15,000 Passes	20,000 Passes
Eagle Asphalt	PG 64-22S	limestone	SP-C	4.8%	6,300	12.5	-	-	-
Eagle Asphalt	PG 64-22S	limestone	SP-C	5.1%	2,700	12.5	-	-	-
Eagle Asphalt	PG 64-22S	limestone	SP-C	5.5%	5,900	12.5	-	-	-
Eagle Asphalt	PG 64-22S	limestone	SP-C	6.0%	3,500	12.5	-	-	-
Eagle Asphalt	PG 76-22S	limestone	SP-C	5.1%	20,000	7.8	5.0	6.3	7.8
Eagle Asphalt	PG 76-22S	limestone	SP-C	5.4%	16,400	12.5	6.2	10.6	-
Eagle Asphalt	PG 76-22S	limestone	SP-C	5.8%	12,300	12.5	9.1	-	-
Eagle Asphalt	PG 76-22S	limestone	SP-C	6.3%	8,400	12.5	-	-	-
Eagle Asphalt	PG 76-22S	limestone	SP-D	4.9%	15,000	12.5	8.3	12.5	-
Eagle Asphalt	PG 76-22S	limestone	SP-D	5.1%	18,200	12.5	6.3	9.5	-
Eagle Asphalt	PG 76-22S	limestone	SP-D	5.4%	14,900	12.5	7.0	-	-
Eagle Asphalt	PG 76-22S	limestone	SP-D	5.9%	13,900	12.5	8.4	-	-
Eagle Asphalt	PG 64-22	limestone	SP-C	4.8%	5,700	12.5	-	-	-
Eagle Asphalt	PG 64-22	limestone	SP-C	5.1%	8,600	12.5	-	-	-
Eagle Asphalt	PG 64-22	limestone	SP-C	5.5%	5,700	12.5	-	-	-
Eagle Asphalt	PG 64-22	limestone	SP-C	6.0%	7,700	12.5	-	-	-

As can be seen, all experimental treatments that contain gravel aggregate (at all evaluated asphalt binder contents) comply with TxDOT's specification Item 344.4; however, the limestone mixes tested for this study generally did not meet the minimum requirements for most asphalt contents and gradations. As expected, among the limestone mixes tested, the denser mixes (SP-D and SP-C) in combination with the highest viscosity binder used (PG 76-22) show higher rutting resistance.

Figures 4.1 through 4.3 show the deformation on the individual experimental treatments that were evaluated during the research project and they performed adequately according to TxDOT specification. Although the specification requires the asphalt mix to meet the 12.5 mm requirement at a specific number of passes depending on the asphalt binder PG grade used, the figures show the actual deformation at 10,000, 15,000, and 20,000 passes.

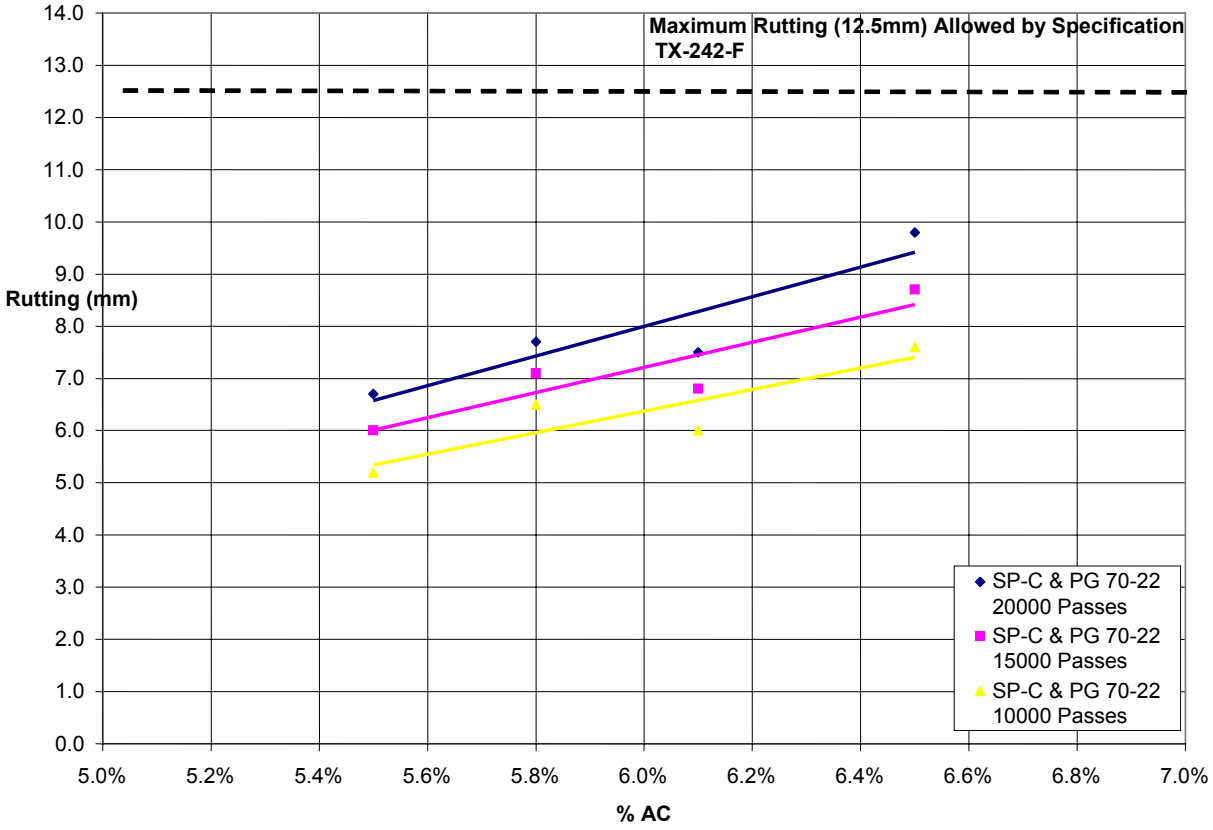

Figure 4.1: Deformation on HWTD (SP-C gravel mix with PG70-22)

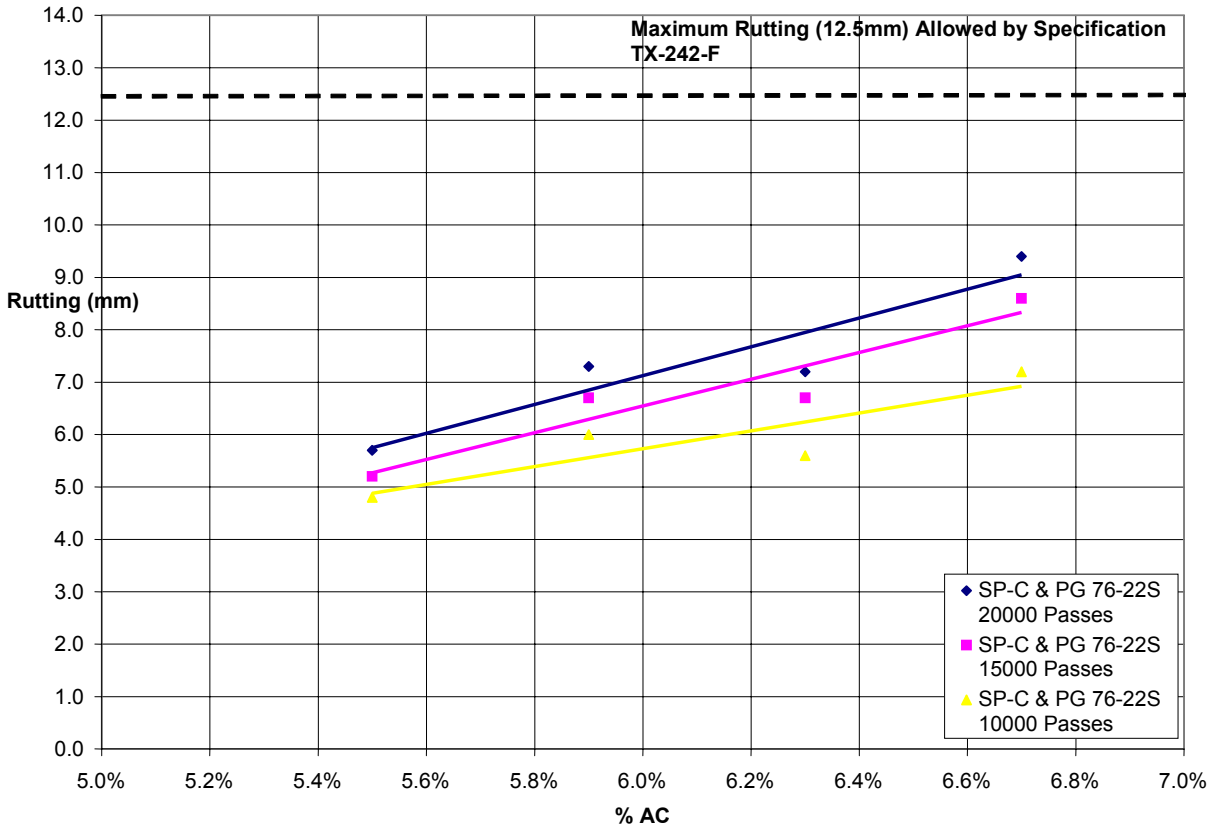

Figure 4.2: Deformation on HWTD (SP-C gravel mix with PG76-22)

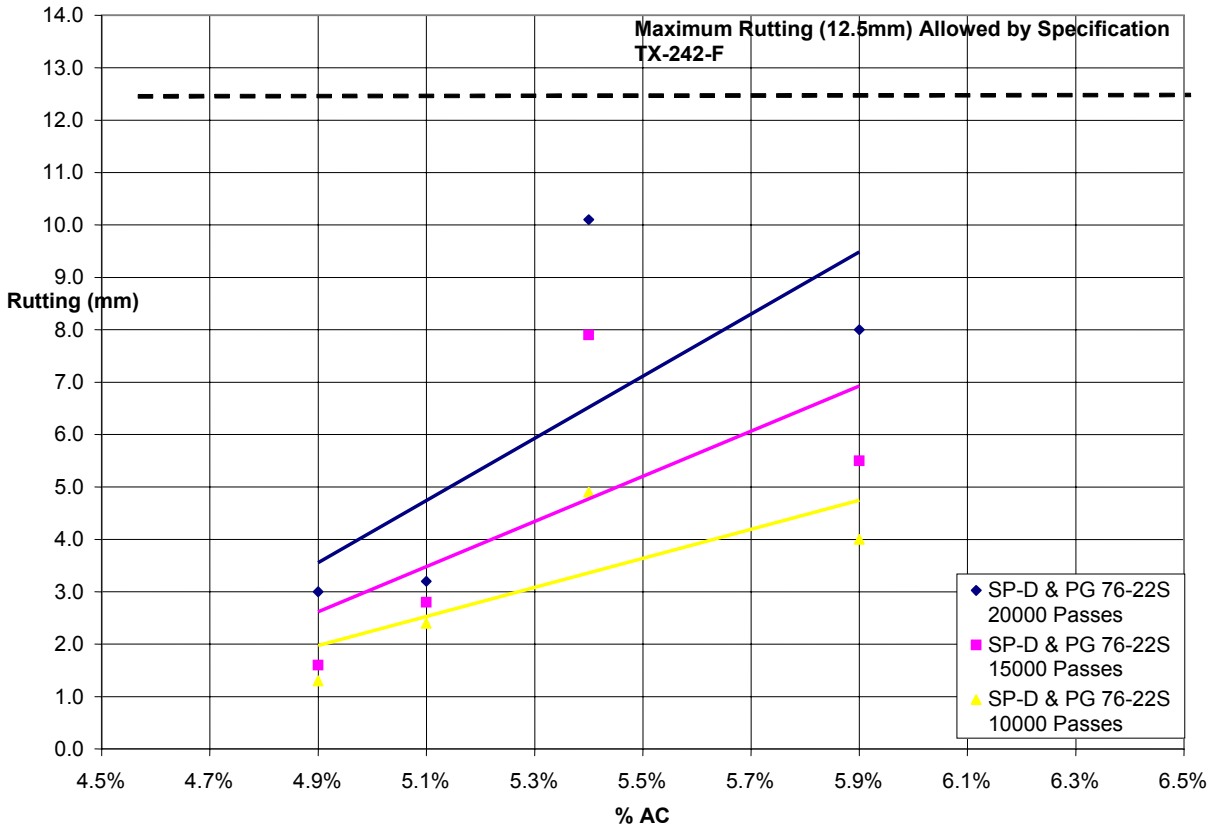

Figure 4.3: Deformation on HWTD (SP-D limestone mix with PG76-22)

A simple analysis of variance (ANOVA) was performed in order to determine the significance of binder manufacturer and PG grade, asphalt cement content, and aggregate type on HWTD results. The results are shown in Table 4.2, which shows that only asphalt cement content and binder manufacturer have a significant effect (90% confidence) on rutting in the HWTD at 10,000 and 15,000 wheel passes. At 20,000 wheel passes, only asphalt binder content is significant.

Table 4.2: ANOVA on HWTD results

Factor	Rut Depth (mm)					
	10,000 Passes		15,000 Passes		20,000 Passes	
	P	Significance	P	Significance	P	Significance
Manufacturer	<.0001	Yes	0.0013	Yes	0.2215	No
PG Grade	0.2319	No	0.6178	No	0.4403	No
Aggregate Type	0.1758	No	0.8811	No	0.3429	No
% AC	0.0076	Yes	0.0645	Yes	0.0169	Yes

4.2 Indirect Tensile Strength Results

Tensile strength has always been thought of as a relatively quick method to evaluate the cracking potential of an asphalt mix. Table 4.3 shows the ITS for the evaluated experimental treatments. It can be seen that the higher the PG grade of the asphalt binder, the higher the tensile strength of the asphalt mix. Figure 4.4 shows that, in general, for any given asphalt mix, the tensile strength is very uniform and generally oscillates within a 20–30 psi range.

Table 4.3: Summary of ITS results

Manufacturer	PG Grade	Aggregate Type	Gradation	%AC	mean ITS (psi)
Valero Asphalt	PG76-22S	gravel	SP-C	5.5%	125.5
Valero Asphalt	PG76-22S	gravel	SP-C	5.9%	111.7
Valero Asphalt	PG76-22S	gravel	SP-C	6.3%	129.6
Valero Asphalt	PG76-22S	gravel	SP-C	6.7%	115.7
Valero Asphalt	PG70-22	gravel	SP-C	5.8%	90.0
Valero Asphalt	PG70-22	gravel	SP-C	6.1%	110.3
Valero Asphalt	PG70-22	gravel	SP-C	6.5%	96.1
Valero Asphalt	PG76-22S	limestone	SP-D	4.9%	133.6
Valero Asphalt	PG76-22S	limestone	SP-D	5.1%	132.9
Valero Asphalt	PG76-22S	limestone	SP-D	5.4%	140.0
Valero Asphalt	PG76-22S	limestone	SP-D	5.9%	150.4
Valero Asphalt	PG76-22S	limestone	SP-C	5.1%	105.8
Valero Asphalt	PG76-22S	limestone	SP-C	5.4%	101.6
Valero Asphalt	PG76-22S	limestone	SP-C	5.8%	98.3
Valero Asphalt	PG76-22S	limestone	SP-C	6.3%	86.5
Eagle	PG 64-22S	limestone	SP-C	4.8%	70.4
Eagle	PG 64-22S	limestone	SP-C	5.1%	84.2
Eagle	PG 64-22S	limestone	SP-C	5.5%	65.9
Eagle	PG 64-22S	limestone	SP-C	6.0%	59.0
Eagle	PG 76-22S	limestone	SP-C	5.1%	100.1
Eagle	PG 76-22S	limestone	SP-C	5.4%	103.0
Eagle	PG 76-22S	limestone	SP-C	5.8%	109.3
Eagle	PG 76-22S	limestone	SP-C	6.3%	100.1
Eagle	PG 76-22S	limestone	SP-D	4.9%	149.9
Eagle	PG 76-22S	limestone	SP-D	5.1%	170.7
Eagle	PG 76-22S	limestone	SP-D	5.4%	142.5
Eagle	PG 76-22S	limestone	SP-D	5.4%	165.5
Eagle	PG 76-22S	limestone	SP-D	5.9%	183.0
Eagle	PG 64-22	limestone	SP-C	5.1%	95.0
Eagle	PG 64-22	limestone	SP-C	5.5%	76.8
Eagle	PG 64-22	limestone	SP-C	6.0%	72.0

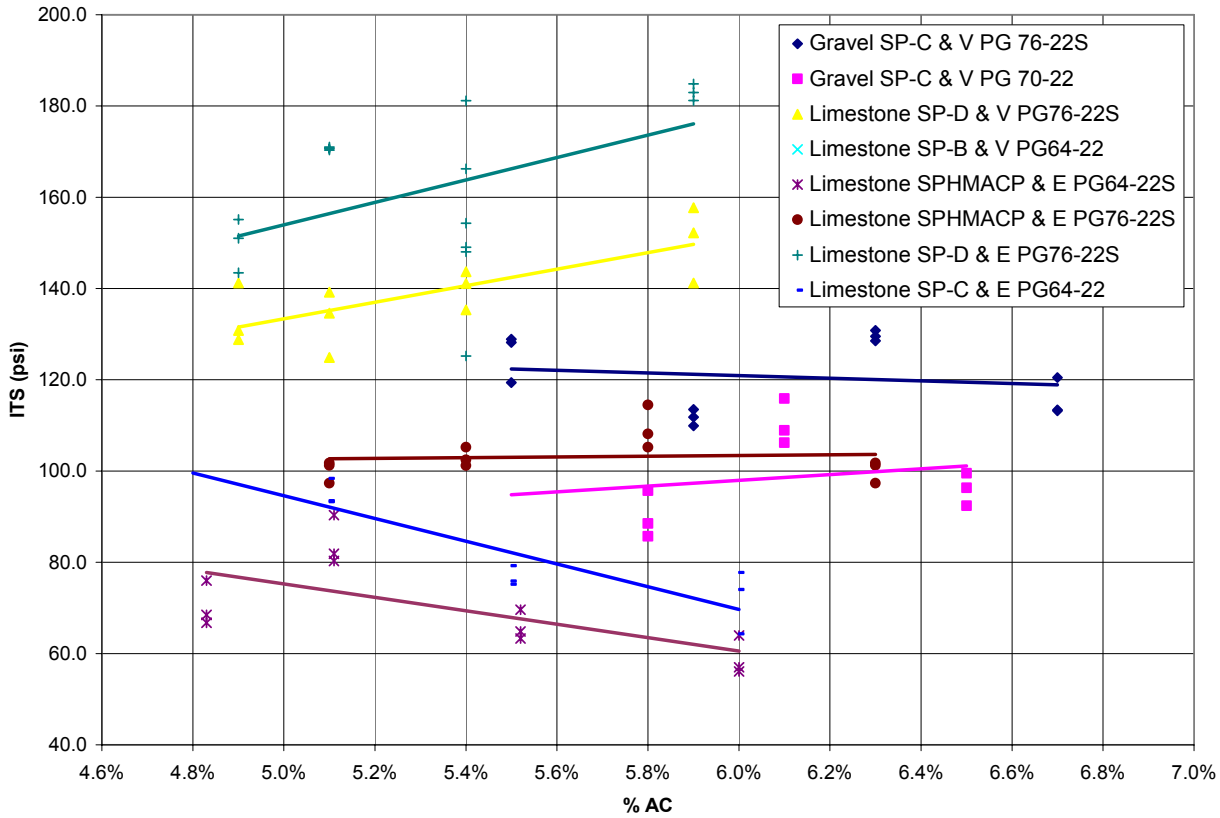

Figure 4.4: ITS of evaluated asphalt mixes

An ANOVA was performed in order to determine the significance of binder manufacturer and PG grade, aggregate type, asphalt cement content, and air void content on ITS. The results are shown in Table 4.4. As mentioned previously and based on the performed ITS tests, only PG grade has a significant effect on ITS (99% confidence).

Table 4.4: ANOVA on ITS results

Factor	ITS (psi)	
	P	Significance
Manufacturer	0.6877	No
PG Grade	<.0001	Yes
Aggregate Type	0.1644	No
% AC	0.2347	No
Air Voids (%)	0.2755	No

4.3 Fatigue Results

Because of the importance of increasing the fatigue life of the asphalt mixes, the four-point loading beam test was performed. Table 4.5 shows the number of cycles that were applied to each beam before it reached 50% of the initial stiffness, at the various strain levels used. The table also shows the initial stiffness (S_{ini}) of each test specimen, an estimate of the modulus of elasticity (E) at 50% of the initial stiffness, and the cumulative dissipated energy through the test.

Table 4.5: Summary of fatigue results

Manufacturer	PG Grade	Aggregate type	Gradation	AC	Va	ε (μs)	N (cycles)	S_{ini} (MPa)	E (MPa)	Cum. Diss. Ener. (MPa)
Valero Asphalt	PG76-22S	gravel	SP-C	5.5%	9.68%	481.33	1475320	4637	2470	459.442
Valero Asphalt	PG76-22S	gravel	SP-C	5.5%	7.66%	481.09	915870	6254	3317	325.753
Valero Asphalt	PG76-22S	gravel	SP-C	5.9%	8.46%	481.38	544360	5712	3029	192.853
Valero Asphalt	PG76-22S	gravel	SP-C	5.9%	7.68%	481.73	812840	6056	3206	302.075
Valero Asphalt	PG76-22S	gravel	SP-C	6.3%	8.61%	481.59	1728690	4835	2581	509.879
Valero Asphalt	PG76-22S	gravel	SP-C	6.3%	8.59%	481.44	1718650	4812	2527	494.722
Valero Asphalt	PG76-22S	gravel	SP-C	6.7%	8.11%	481.26	2161690	4795	2541	589.984
Valero Asphalt	PG76-22S	gravel	SP-C	6.7%	6.87%	481.10	1658060	5063	2685	507.795
Valero Asphalt	PG76-22S	gravel	SP-C	5.5%	8.48%	673.55	86190	6860	3640	64.673
Valero Asphalt	PG76-22S	gravel	SP-C	5.5%	8.30%	673.64	50990	7278	3854	40.624
Valero Asphalt	PG76-22S	gravel	SP-C	5.9%	7.72%	673.30	738950	4041	2142	387.681
Valero Asphalt	PG76-22S	gravel	SP-C	5.9%	-	-	-	-	-	-
Valero Asphalt	PG76-22S	gravel	SP-C	6.3%	7.38%	673.89	207640	5137	2717	127.401
Valero Asphalt	PG76-22S	gravel	SP-C	6.3%	6.40%	673.62	167850	5662	2988	110.633
Valero Asphalt	PG76-22S	gravel	SP-C	6.7%	6.77%	674.05	232450	5091	2689	144.968
Valero Asphalt	PG76-22S	gravel	SP-C	6.7%	6.29%	673.48	489470	5166	2738	297.878
Valero Asphalt	PG70-22	gravel	SP-C	5.5%	7.39%	481.00	787800	6041	3192	279.410
Valero Asphalt	PG70-22	gravel	SP-C	5.5%	7.74%	500.01	891120	3817	2035	223.990
Valero Asphalt	PG70-22	gravel	SP-C	5.5%	9.05%	673.15	238440	4761	2519	136.297
Valero Asphalt	PG70-22	gravel	SP-C	5.5%	9.17%	700.06	124070	2598	1392	45.745
Valero Asphalt	PG70-22	gravel	SP-C	5.8%	8.52%	480.76	2470180	4289	2282	685.934
Valero Asphalt	PG70-22	gravel	SP-C	5.8%	8.61%	673.55	395960	4102	2187	195.256
Valero Asphalt	PG70-22	gravel	SP-C	5.8%	7.97%	500.01	1468480	3300	1748	328.105
Valero Asphalt	PG70-22	gravel	SP-C	5.8%	7.98%	699.98	181800	3030	1589	77.096
Valero Asphalt	PG70-22	gravel	SP-C	6.1%	7.77%	481.29	1772240	4596	2427	497.089
Valero Asphalt	PG70-22	gravel	SP-C	6.1%	7.95%	499.00	2152780	3096	1648	441.231
Valero Asphalt	PG70-22	gravel	SP-C	6.1%	7.06%	674.82	190900	3204	1687	77.438
Valero Asphalt	PG70-22	gravel	SP-C	6.1%	7.49%	700.79	188840	3112	1651	79.870
Valero Asphalt	PG70-22	gravel	SP-C	6.5%	7.64%	481.00	5415290	2763	1451	1205.830
Valero Asphalt	PG70-22	gravel	SP-C	6.5%	7.56%	500.04	2752700	2121	1115	510.901
Valero Asphalt	PG70-22	gravel	SP-C	6.5%	8.43%	698.41	192360	2520	1332	66.155
Valero Asphalt	PG70-22	gravel	SP-C	6.5%	7.49%	700.03	342970	2536	1343	121.186

Table 4.5 Summary of fatigue results (continued)

Manufacturer	PG Grade	Aggregate type	Gradation	AC	Va	ε (μs)	N (cycles)	S_{ini} (MPa)	E (MPa)	Cum. Diss. Ener. (MPa)
Valero Asphalt	PG76-22S	limestone	SP-D	4.9%	11.27%	481.70	483730	5075	2695	134.485
Valero Asphalt	PG76-22S	limestone	SP-D	4.9%	11.15%	499.36	1011070	3699	1967	226.610
Valero Asphalt	PG76-22S	limestone	SP-D	4.9%	11.48%	674.38	24880	5229	2761	14.439
Valero Asphalt	PG76-22S	limestone	SP-D	4.9%	11.06%	698.81	18970	3406	1792	7.962
Valero Asphalt	PG76-22S	limestone	SP-D	5.1%	11.01%	481.55	248270	5635	2985	69.673
Valero Asphalt	PG76-22S	limestone	SP-D	5.1%	10.81%	518.36	168920	3880	2068	39.608
Valero Asphalt	PG76-22S	limestone	SP-D	5.1%	10.04%	676.34	24010	5165	2739	13.909
Valero Asphalt	PG76-22S	limestone	SP-D	5.1%	10.20%	729.10	8940	3679	1948	4.317
Valero Asphalt	PG76-22S	limestone	SP-D	5.4%	9.68%	480.35	412570	5717	3030	122.365
Valero Asphalt	PG76-22S	limestone	SP-D	5.4%	9.18%	494.69	82950	4513	2391	20.532
Valero Asphalt	PG76-22S	limestone	SP-D	5.4%	9.39%	673.36	5340	4115	2172	2.774
Valero Asphalt	PG76-22S	limestone	SP-D	5.4%	9.72%	694.85	32880	3690	1964	14.391
Valero Asphalt	PG76-22S	limestone	SP-D	5.9%	8.61%	483.50	723660	5896	3102	214.932
Valero Asphalt	PG76-22S	limestone	SP-D	5.9%	8.64%	500.55	144000	4576	2443	36.081
Valero Asphalt	PG76-22S	limestone	SP-D	5.9%	7.66%	673.36	98960	5576	2955	60.631
Valero Asphalt	PG76-22S	limestone	SP-D	5.9%	7.77%	699.49	33420	3978	2117	16.019
Valero Asphalt	PG64-22	limestone	SP-B	4.2%	7.55%	290.26	471110	7397	3949	67.446
Valero Asphalt	PG64-22	limestone	SP-B	4.2%	7.12%	293.67	188630	5689	3035	21.130
Valero Asphalt	PG64-22	limestone	SP-B	4.2%	7.64%	480.43	17030	6504	3428	6.221
Valero Asphalt	PG64-22	limestone	SP-B	4.2%	7.67%	477.11	21320	4904	2614	5.832
Valero Asphalt	PG64-22	limestone	SP-B	4.5%	7.19%	288.96	839430	7266	3873	114.964
Valero Asphalt	PG64-22	limestone	SP-B	4.5%	7.25%	383.23	91500	4878	2604	15.407
Valero Asphalt	PG64-22	limestone	SP-B	4.5%	7.20%	480.51	9600	5976	3167	3.382
Valero Asphalt	PG64-22	limestone	SP-B	4.5%	6.85%	477.88	10990	4590	2406	2.909
Valero Asphalt	PG64-22	limestone	SP-B	4.8%	5.99%	291.25	699950	7179	3799	93.089
Valero Asphalt	PG64-22	limestone	SP-B	4.8%	6.20%	300.64	229350	5624	3014	27.068
Valero Asphalt	PG64-22	limestone	SP-B	4.8%	6.70%	482.74	37290	5496	2944	12.280
Valero Asphalt	PG64-22	limestone	SP-B	4.8%	7.00%	480.66	24510	3930	2104	5.871
Valero Asphalt	PG64-22	limestone	SP-B	5.2%	5.83%	290.57	982480	6925	3648	128.718
Valero Asphalt	PG64-22	limestone	SP-B	5.2%	6.00%	300.37	454550	4150	2201	45.102
Valero Asphalt	PG64-22	limestone	SP-B	5.2%	5.42%	490.79	29390	4820	2568	8.439
Valero Asphalt	PG64-22	limestone	SP-B	5.2%	5.46%	492.04	27510	4894	2606	7.942

Table 4.5 Summary of fatigue results (continued)

Manufacturer	PG Grade	Aggregate type	Gradation	AC	Va	ε (μs)	N (cycles)	S_{ini} (MPa)	E (MPa)	Cum. Diss. Ener. (MPa)
Valero Asphalt	PG76-22S	limestone	SP-C	5.1%	10.25%	481.95	141300	5270	2786	39.131
Valero Asphalt	PG76-22S	limestone	SP-C	5.1%	10.32%	487.13	58880	3853	2050	12.487
Valero Asphalt	PG76-22S	limestone	SP-C	5.1%	10.46%	674.44	8600	4982	2644	4.806
Valero Asphalt	PG76-22S	limestone	SP-C	5.1%	10.03%	716.66	14210	3390	1789	6.216
Valero Asphalt	PG76-22S	limestone	SP-C	5.4%	9.03%	480.77	306880	4768	2530	82.571
Valero Asphalt	PG76-22S	limestone	SP-C	5.4%	8.88%	485.10	472590	3343	1765	93.862
Valero Asphalt	PG76-22S	limestone	SP-C	5.4%	8.35%	675.80	26950	5404	2864	16.250
Valero Asphalt	PG76-22S	limestone	SP-C	5.4%	8.54%	680.47	25160	3930	2084	11.025
Valero Asphalt	PG76-22S	limestone	SP-C	5.8%	7.14%	480.43	333260	5483	2915	99.529
Valero Asphalt	PG76-22S	limestone	SP-C	5.8%	6.69%	469.52	256460	4389	2321	58.727
Valero Asphalt	PG76-22S	limestone	SP-C	5.8%	9.12%	688.84	30260	3085	1633	11.870
Valero Asphalt	PG76-22S	limestone	SP-C	5.8%	8.88%	670.92	45770	3245	1714	18.008
Valero Asphalt	PG76-22S	limestone	SP-C	6.3%	6.13%	479.92	1061020	5077	2679	296.158
Valero Asphalt	PG76-22S	limestone	SP-C	6.3%	5.86%	465.09	284710	4053	2161	60.460
Valero Asphalt	PG76-22S	limestone	SP-C	6.3%	7.45%	692.69	111440	3340	1759	45.848
Valero Asphalt	PG76-22S	limestone	SP-C	6.3%	7.17%	673.24	66630	3236	1726	25.350
Valero Asphalt	PG76-22S	limestone	SP-B	4.6%	7.40%	481.36	154140	4858	2560	46.132
Valero Asphalt	PG76-22S	limestone	SP-B	4.6%	8.00%	680.95	31440	2820	1500	11.363
Valero Asphalt	PG76-22S	limestone	SP-B	4.8%	7.73%	483.31	510220	3349	1769	114.452
Valero Asphalt	PG76-22S	limestone	SP-B	4.8%	7.53%	484.87	353270	2782	1471	62.259
Valero Asphalt	PG76-22S	limestone	SP-B	5.1%	6.65%	480.30	2190100	4848	2569	614.979
Valero Asphalt	PG76-22S	limestone	SP-B	5.1%	7.53%	472.05	256940	3234	1726	45.932
Valero Asphalt	PG76-22S	limestone	SP-B	5.6%	8.87%	482.69	3470800	3628	1873	718.801
Valero Asphalt	PG76-22S	limestone	SP-B	5.6%	7.85%	479.46	127820	3096	1656	22.377

Figure 4.5 shows the fatigue curves (obtained by means of linear regression) for all the evaluated experimental treatments at the analyzed strain levels. Figure 4.6 shows the initial stiffness for each evaluated asphalt mixture at the analyzed strain levels. Figure 4.7 presents an estimate of the modulus of elasticity at failure (established at 50% of the initial stiffness). Figure 4.8 shows the cumulative dissipated energy until failure for each of the evaluated asphalt mixtures.

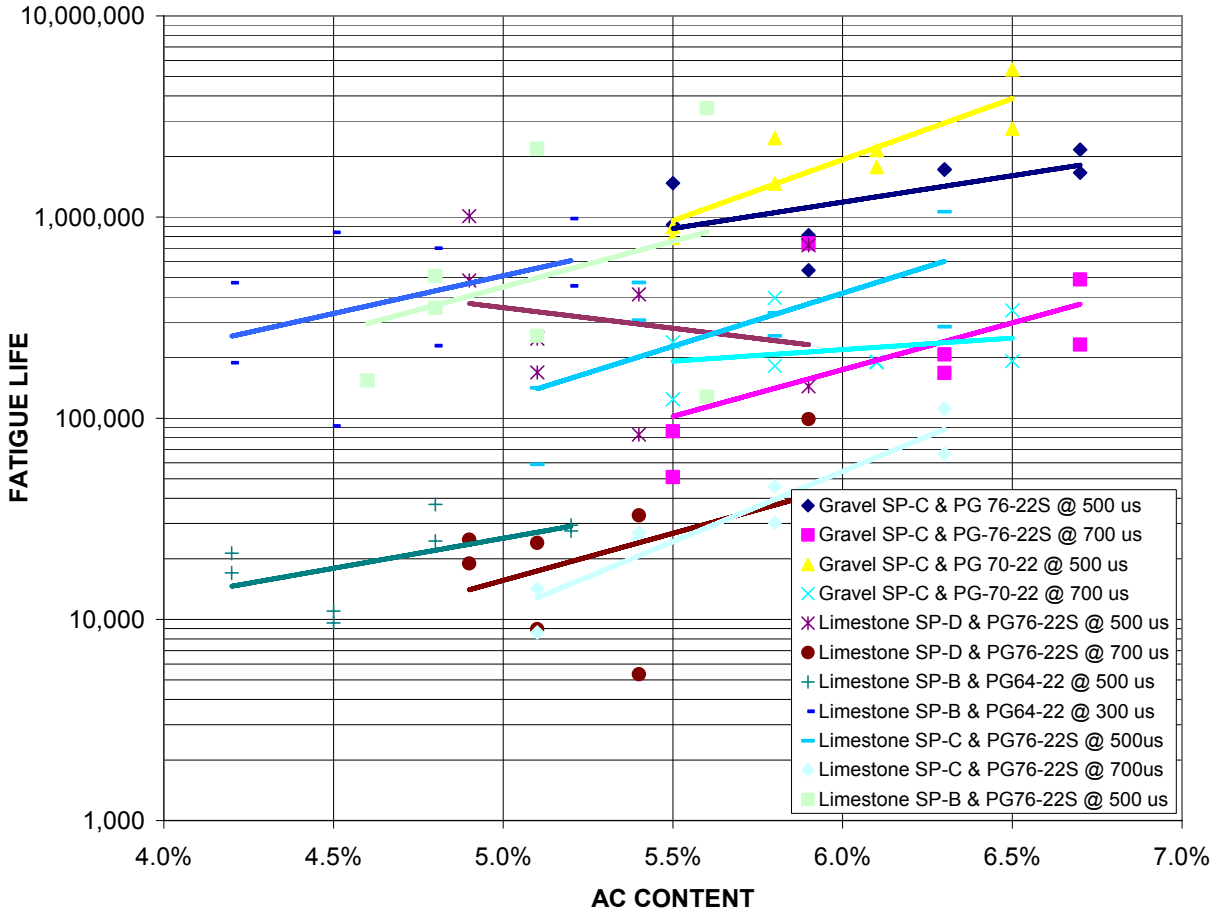

Figure 4.5: Fatigue curves for evaluated asphalt mixes

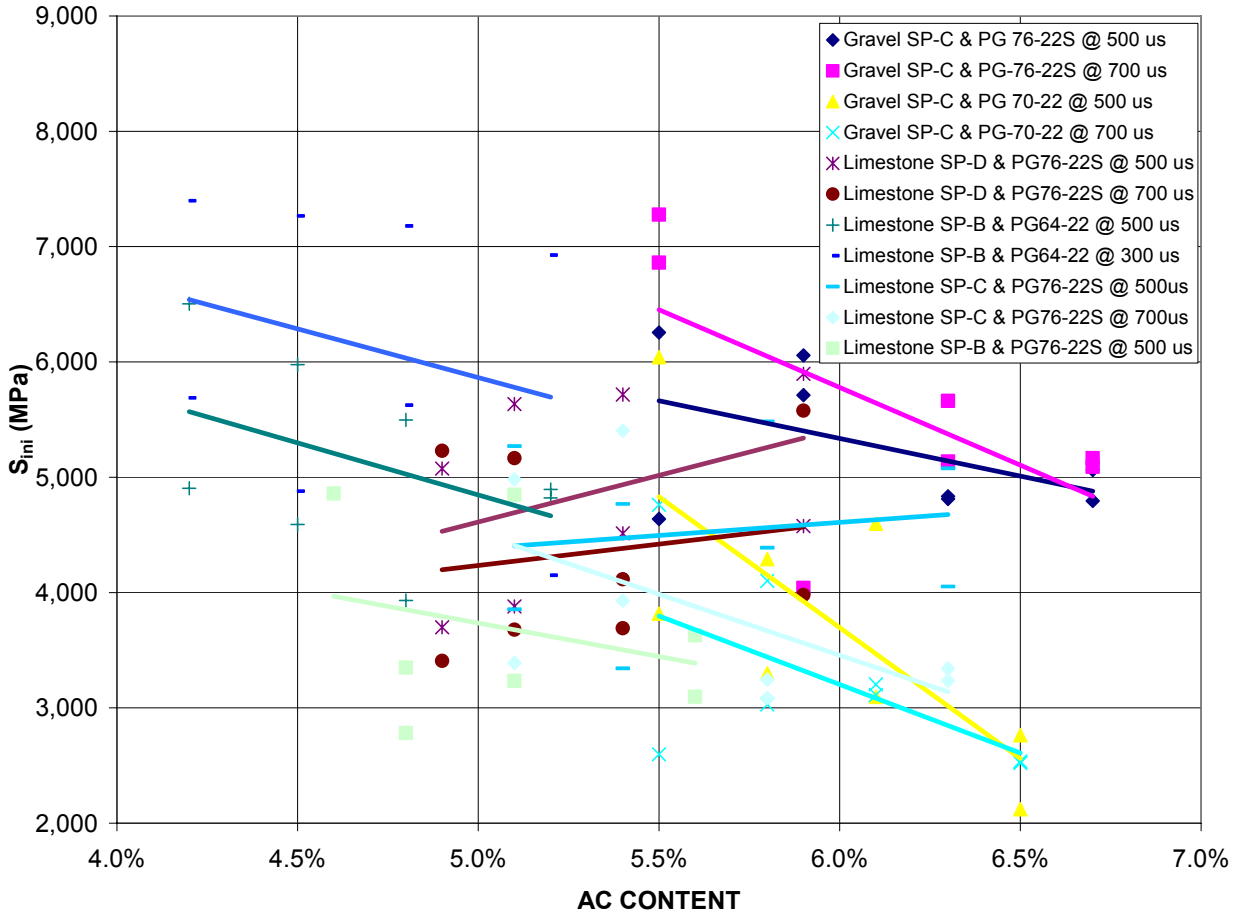

Figure 4.6: Initial stiffness of evaluated asphalt mixes

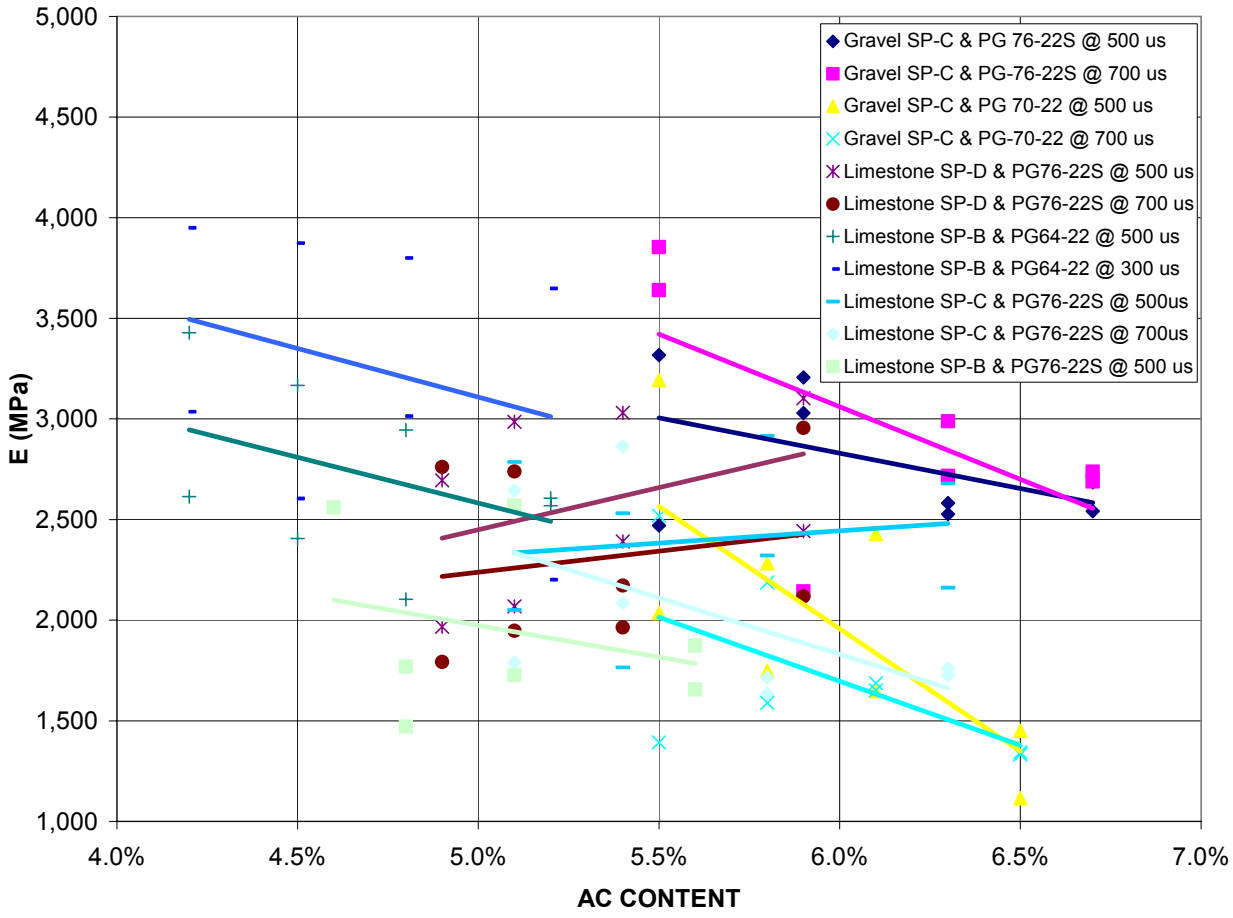

Figure 4.7: Modulus of elasticity (E) at failure

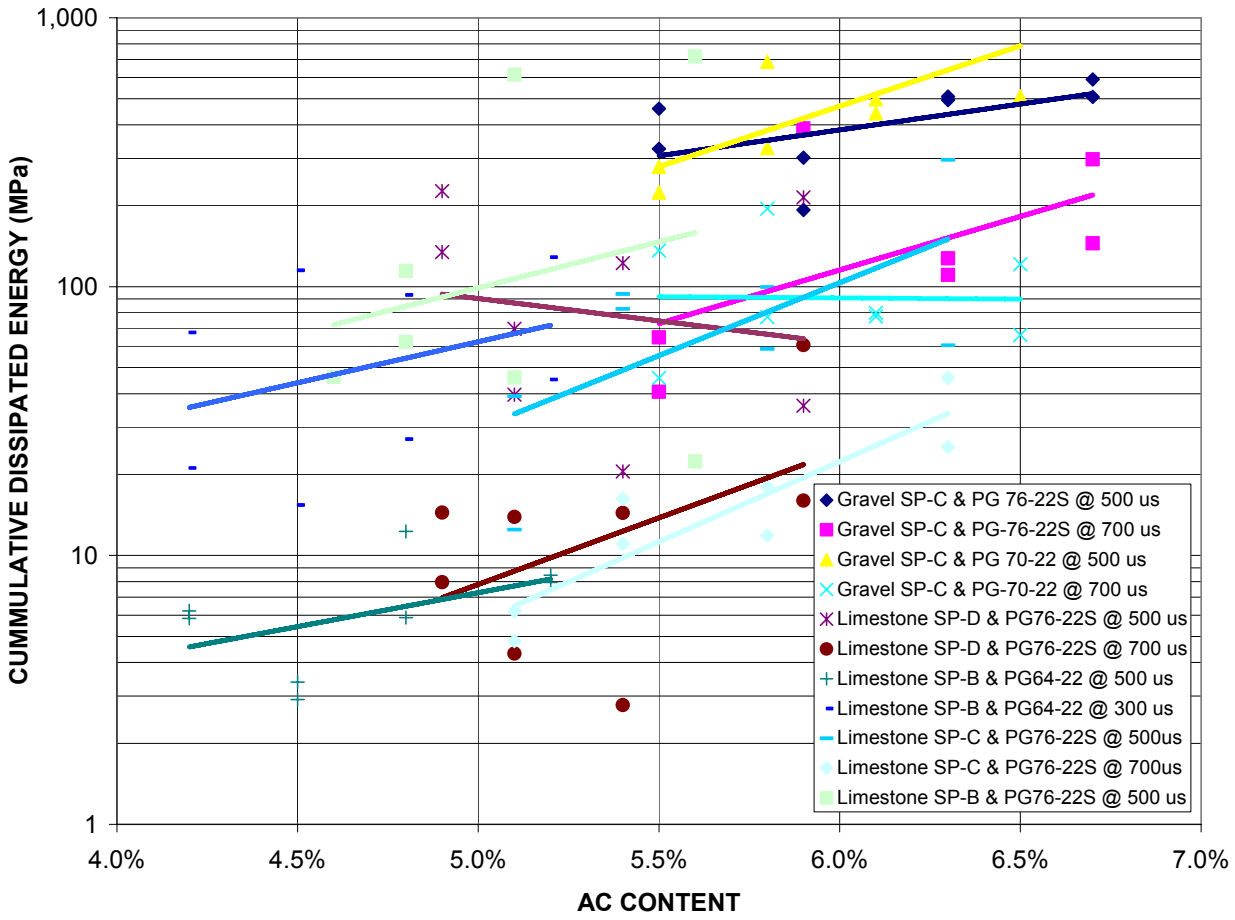

Figure 4.8: Cumulative dissipated energy at failure

An ANOVA was performed in order to determine the significance of PG grade, aggregate type, asphalt cement content, air void content, and the applied strain level on fatigue life, as measured by the FPBB apparatus. The results are shown in Table 4.6. The analysis shows that all the parameters have a significant effect (90% confidence) on initial stiffness and Young's modulus. The analysis also shows that all the parameters except aggregate type have a significant effect on fatigue life and all parameters except PG grade have a significant effect on the dissipated energy.

Table 4.6: ANOVA on fatigue life

Factor	N (cycles)		S_{ini} (MPa)		E (MPa)		Cum. Diss. Ener. (MPa)	
	P	Significance	P	Significance	P	Significance	P	Significance
PG Grade	0.0268	Yes	<.0001	Yes	<.0001	Yes	0.1232	No
Aggregate Type	0.1884	No	<.0001	Yes	<.0001	Yes	0.0021	Yes
Gradation	0.0016	Yes	<.0001	Yes	<.0001	Yes	0.0068	Yes
%AC	<.0001	Yes	<.0001	Yes	<.0001	Yes	0.0002	Yes
Air Voids (%)	0.0017	Yes	0.001	Yes	0.0008	Yes	0.0103	Yes
ε (μm)	<.0001	Yes	0.0009	Yes	0.0008	Yes	<.0001	Yes

Development of a Fatigue Model

Using all the fatigue data, a model to predict fatigue life has been calibrated for the mixes tested for this study. The calibrated model for this study has the following shape:

$$N_f = \beta_0 \cdot \varepsilon^{\beta_1} \cdot S^{\beta_2} \quad \text{(Eq 4-1)}$$

Where,
N_f = number of load cycles to failure (50% of initial stiffness)
ε = strain at the bottom of the asphalt mix layer (μm)
S = initial stiffness of the asphalt mixture (MPa)
β_0, β_1, and β_2 = regression parameters

After performing a regression analysis, the calibrated fatigue model is as follows:

$$N_f = 4.25x10^{19} \cdot \varepsilon^{-3.50} \cdot S^{-1.32} \quad \text{(Eq 4.2)}$$

The model has an F-statistic of 11.5 and a standard error of 0.646.

As expected, the model indicates that as the level of strain in the asphalt mix increases, the number of cycles for the asphalt mix to fail due to fatigue decreases. Likewise, as the stiffness of the asphalt mix increases, the cycles that are needed for the asphalt mix to fail due to fatigue decreases. These tendencies are illustrated in Figure 4.9.

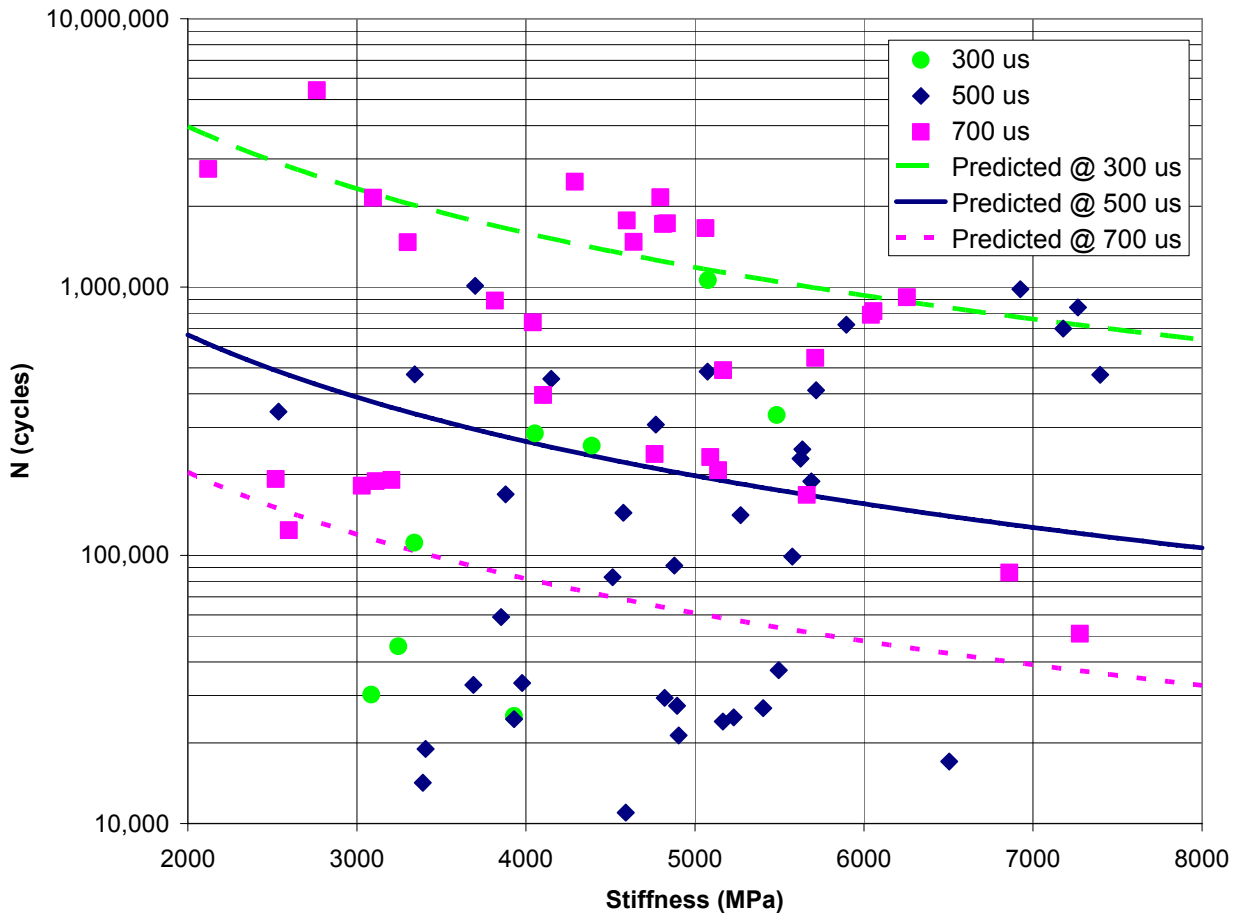

Figure 4.9: Predicted fatigue life at 300, 500, and 700 μm

5. Analysis

As mentioned previously, when the asphalt binder content increases, and consequently the elasticity of the asphalt mix increases, the susceptibility of the asphalt mix to rutting increases and the probability of cracking due to fatigue decreases. Additionally, it has been previously established that there is a relationship between asphalt binder content and number of design gyrations (N_{design}) using the Superpave Gyratory Compactor (SGC). Following these principles, it is easy to see that a decrease in N_{design} generates an increase in fatigue cracking resistance and a reduction in rutting resistance.

5.1 Proposed Method

Based on the previous considerations, the number of design gyrations (N_{design}) can be optimized by minimizing both rutting and fatigue cracking. In order to do this, rutting and fatigue cracking should be measured in some consistent unit. However, when evaluating rutting and fatigue cracking in the laboratory, rutting is generally measured in millimeters of deformation at a given cycle and fatigue cracking is generally measured in numbers of cycles required for the sample specimen to reach a defined stiffness (50% of initial stiffness). Consequently, the ultimate goal is to identify a mixture that will have a low rutting value and a high fatigue life. Nonetheless, as the asphalt content percentage is increased, or equivalently, as the number of design gyrations on the SGC decrease, the asphalt mixtures may exhibit more rutting (lower rutting resistance) but the fatigue resistance of the asphalt mixture will increase.

One way to overcome this difference in units would be to standardize both performance indicators with respect to rutting and fatigue cracking at a specific number of N_{design} gyrations. In other words, define two new performance indicators as follows:

$$RP = \frac{P_{Ndesign=i}}{P_{Ndesign=base}} \qquad \text{(Eq 5.1)}$$

Where,
RP = Relative performance
$P_{Ndesign=i}$ = Performance at i N_{design} gyrations
$P_{Ndesign=base}$ = Performance at base N_{design} gyrations

In this way, both rutting and fatigue cracking are defined as a percentage of the mix performance at a fixed number of gyrations (e.g., 100 N_{design} gyrations) or as a percentage of the number that allows for the optimal performance in either fatigue or rutting. Consequently, for the latter scenario, the "base" number of design gyrations is defined as 50 for fatigue resistance, because within the experimental design, the asphalt mixtures compacted at N_{design} = 50 gyrations (highest asphalt content) achieve the highest fatigue resistance. In contrast, the "base" number of design gyrations is set as 125 for rutting resistance because, within the experimental design, the asphalt mixtures compacted at N_{design} = 125 gyrations (lowest asphalt content) result in the highest rutting resistance.

With the units of both performance indicators standardized, it is possible now to determine an adequate performance range that would increase fatigue resistance with minimal

increase in rutting. In summary, depending on how the "base" number of gyrations is defined, the two new performance indicators are defined as follows for a "base" N_{design} of 100 gyrations:

$$RP_{fatigue} = \frac{P_{Ndesign=i}}{P_{Ndesign=100}} \quad \text{(Eq 5.2)}$$

$$RP_{rutting} = \frac{P_{Ndesign=i}}{P_{Ndesign=100}} \quad \text{(Eq 5.3)}$$

Alternatively, for a "base" number of gyrations that produce the optimal performance at each given distress criteria, the following equations are applicable:

$$RP_{fatigue} = \frac{P_{Ndesign=i}}{P_{Ndesign=50}} \quad \text{(Eq 5.4)}$$

$$RP_{rutting} = \frac{P_{Ndesign=i}}{P_{Ndesign=125}} \quad \text{(Eq 5.5)}$$

Since indirect tensile strength (ITS) is an indicator of fracture strength and captures other properties such as the cohesion of the asphalt mixture, it was included as another performance indicator. However, it has been observed from the different analyzed asphalt mixtures that within the analysis range (50–125 gyrations on SGC), ITS is relatively uniform. This observation was reinforced by the analysis of variance in Chapter 4 that indicated that the asphalt cement content, and hence the number of gyrations, does not have a significant effect on ITS (for the mixtures tested in this study). Figure 5.1 shows the relative performance concept.

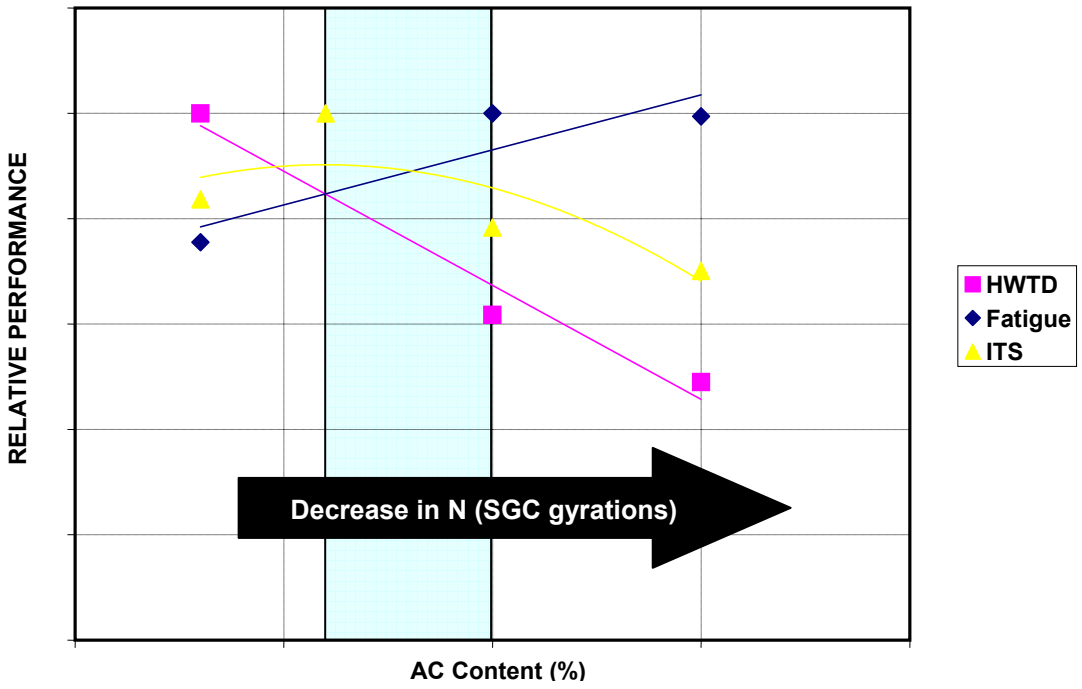

Figure 5.1: Relative performance concept

Standardized fatigue and rutting performance indicator units allow for the optimization of the overall relative performance of the asphalt mix, thereby allowing for the establishment of an overall objective function. This, in turn, allows for the determination of the optimum number of design gyrations required for specific traffic and environmental conditions.

The relative performance can be optimized in many possible ways. Two very distinct methods are proposed in this report:

1) Different weighted combinations of the fatigue and rutting relative performance curves.
2) Assigning different reliability levels to the rutting and fatigue performance curves, allowing for higher probability of attaining a desired performance level, when desired.

Both approaches will be discussed in detail in the following sections.

5.2 Secondary Analysis Parameters

5.2.1 Fatigue Slope ($Z_{fatigue}$)

Because of the variability associated with fatigue testing, even for experimental specimens evaluated under the same experimental conditions, several parameters have been identified and analyzed to adequately characterize fatigue life. These parameters can be obtained either directly from the fatigue test or from subsequent analysis of the test data.

The number of cycles to failure in the four-point bending beam (FPBB) test (generally defined as the number of cycles required for the stiffness of the mix to reach 50% of its initial value, which is specified as the stiffness after 50 load repetitions) is a good choice for a performance parameter because it is measured directly from test and is reported by the testing

equipment. An example of a typical fatigue curve and the number of cycles to failure (as defined previously) can be observed in Figure 5.2.

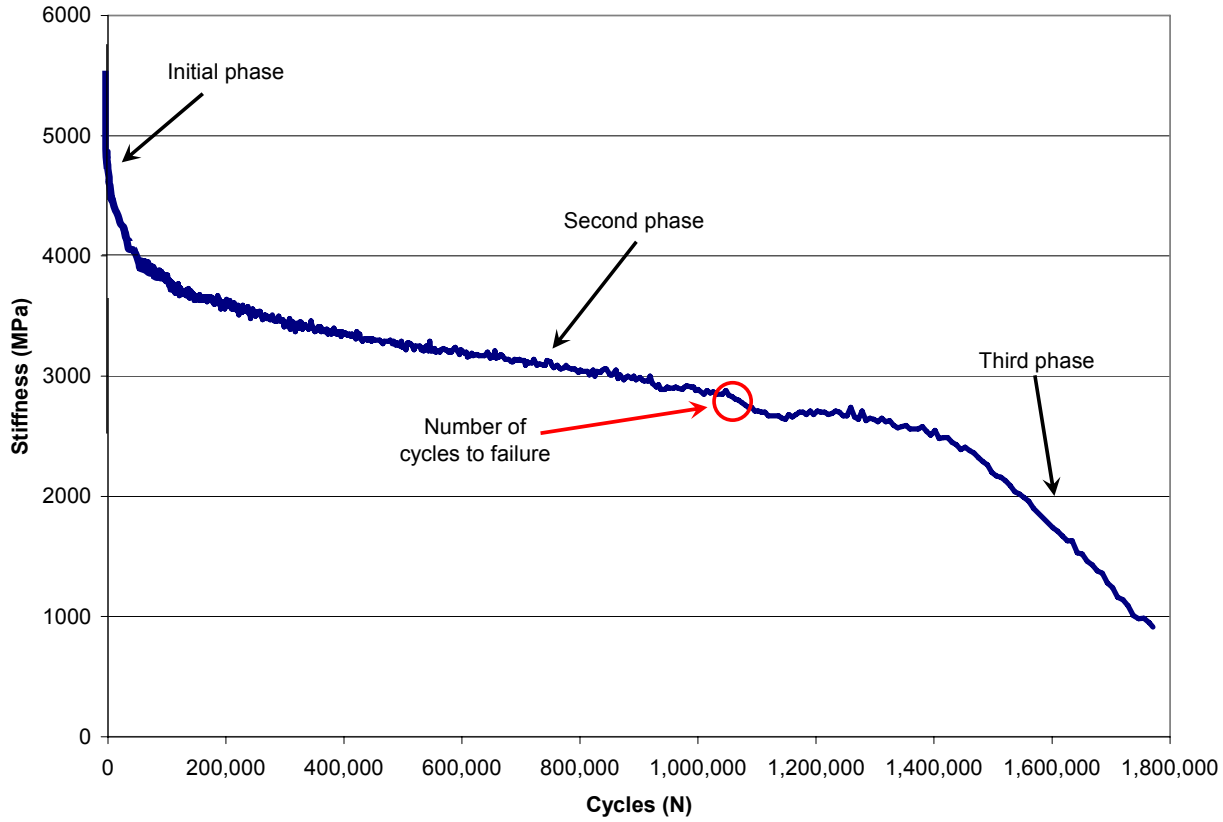

Figure 5.2: Typical fatigue curve of analyzed asphalt mixtures

However, the previous criteria depend on a percentage (generally 50%) of the initial stiffness. Consequently, this factor does not guarantee that the asphalt mixture will reach the third phase in the fatigue life curve (when the asphalt mix starts to crack and lose stiffness at a very rapid rate). It has been observed from the analyzed mixes that the test typically finishes during the second phase, underestimating fatigue life because the asphalt mix has not reached the point where it starts degrading at a faster rate. This underestimation might be considerable for some combinations of binder contents and aggregate types. For these reasons, a logical indicator of fatigue life is a different parameter that, unlike the number of cycles to failure, does not incur this possible underestimation and is more robust or consistent.

After analyzing several alternative indicators, it was determined that the slope ($Z_{fatigue}$) of the second phase of the fatigue curve is a good, consistent indicator of fatigue resistance (refer to Fig 5.3). A small slope (closer to zero) indicates higher fatigue resistance, while a high slope (more negative) indicates an asphalt mixture that is highly susceptible to fatigue damage. Note that Z is not subject to the condition that the asphalt mix specimen reaches the tertiary phase. An added advantage is that the parameter Z is independent of the rapid drop of stiffness observed during the initial phase.

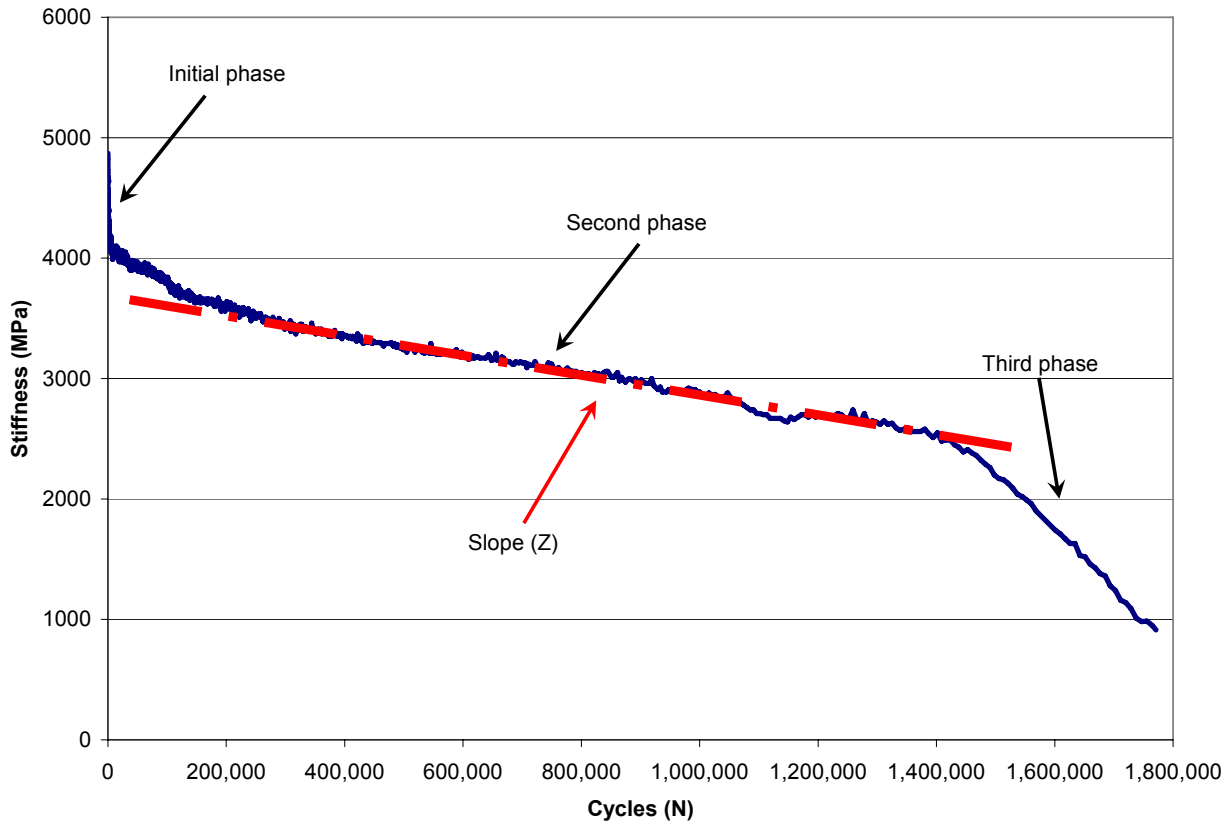

Figure 5.3: Slope ($Z_{fatigue}$) of fatigue curve for second phase

The only problem with the slope parameter ($Z_{fatigue}$) is that it requires additional manipulation of the data obtained from the fatigue test. Nonetheless, the calculations required to determine Z should prove to be relatively simple in any spreadsheet software package such as MS Excel. Appendix A describes a simplified method for determining $Z_{fatigue}$.

5.2.2 Rutting Slope (Z_{rut})

The standard test procedure for evaluating asphalt mixes by the Hamburg Wheel Tracking Device (HWTD), as required by TxDOT (Item 344.4), establishes that the rut depth in the asphalt mix samples should not exceed 12.5 mm at 10,000, 15,000 or 20,000 passes from the steel wheel, depending on the PG grade of the asphalt binder (PG 64, 70, and 76, respectively).

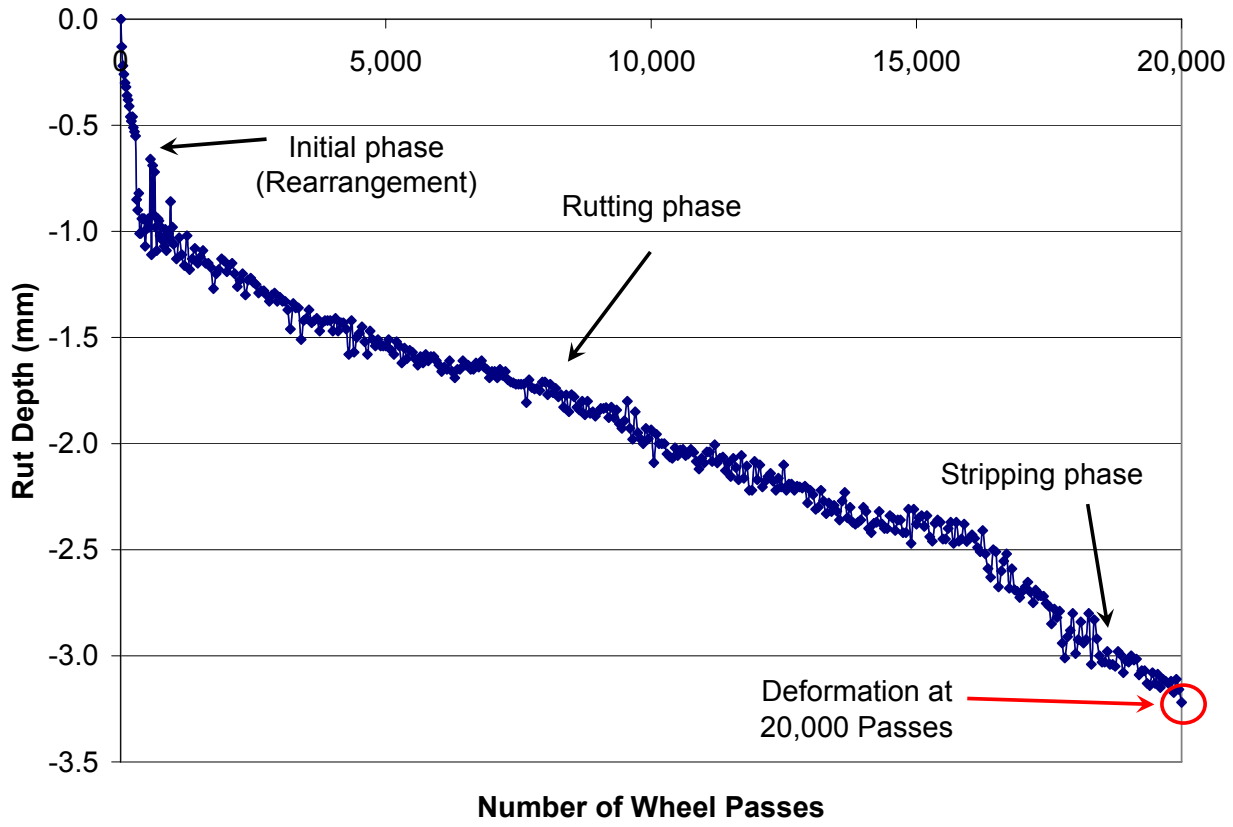

Figure 5.4: Typical HWTD deformation curve

Figure 5.4 shows a typical HWTD output. The parameter that is generally reported (deformation at 20,000 passes) may present high variability, since the measured rut depth is a function of aggregate and binder properties, testing conditions, aggregate structure arrangement, and many other factors. More significantly, this parameter might underestimate rutting resistance because some mixes might finish the HWTD test during the secondary or rutting phase, while weaker mixes might finish during the stripping phase even if the deformations at 20,000 passes are not statistically different.

As was the case with fatigue resistance, it was determined that the slope parameter (Z_{rut}) of the rutting phase of the permanent deformation curve is a good indicator of rutting resistance (refer to Fig 5.5). A small slope (closer to zero) indicates higher rutting resistance, while a high slope (more negative) indicates an asphalt mixture that is highly susceptible to rutting. Also note that Z is not subject to the condition of the asphalt mix specimen reaching the stripping phase and is independent of the inconsistencies of the initial phase.

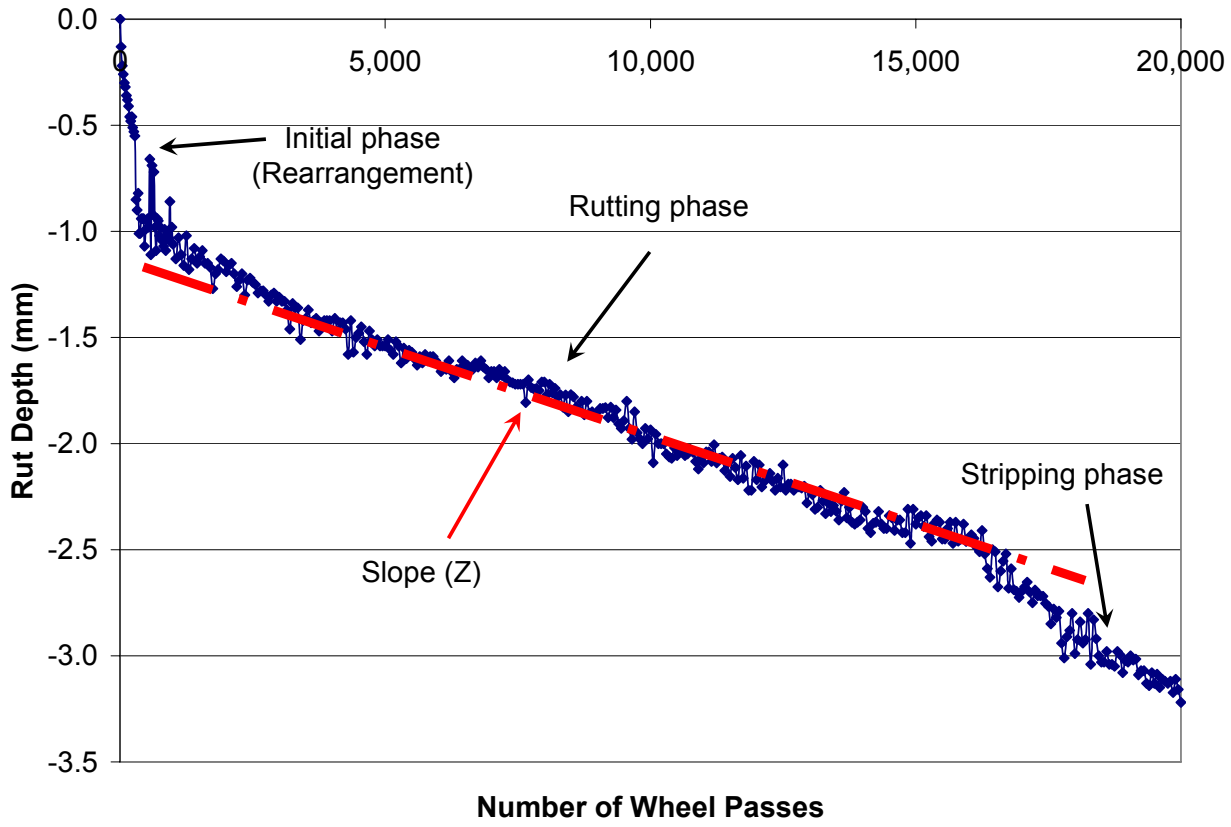

Figure 5.5: Slope of rutting phase (Z) in deformation curve

5.3 Data Analysis

5.3.1 Analysis Based on 100 Design Gyrations

The relative performance of the asphalt mixture with respect to its performance at 100 design gyrations can now be calculated. Table 5.1 shows a summary of the rutting and fatigue indicators; Table 5.2 shows relative performance with respect to 100 design gyrations. In order to determine the relative in rutting, the rut depth at 20,000 wheel passes in the HWTD equipment was used instead of selecting the rut depth at 10,000, 15,000, or 20,000 passes depending on the PG grade of the asphalt binder. This was done to standardize the comparison.

Table 5.1: Summary of analyzed performance indicators

PG Grade	Aggregate type	Gradation	AC	Ndesign	Fatigue		Rutting			
					Final Cycle	Slope (Z)	10,000 Passes	15,000 Passes	20,000 Passes	Slope
PG76-22S	gravel	SP-C	5.50%	125	1,475,320	-0.0008158	4.8	5.2	5.7	-0.0992287
PG76-22S	gravel	SP-C	5.50%	125	915,870	-0.0011933	4.8	5.2	5.7	-0.0992287
PG76-22S	gravel	SP-C	5.90%	100	***1,485,577***	***-0.0007616***	6.0	6.7	7.3	-0.1214101
PG76-22S	gravel	SP-C	5.90%	100	***1,485,577***	***-0.0007616***	6.0	6.7	7.3	-0.1214101
PG76-22S	gravel	SP-C	6.30%	75	1,728,690	-0.0004767	5.6	6.7	7.2	-0.1484449
PG76-22S	gravel	SP-C	6.30%	75	1,718,650	-0.0006951	5.6	6.7	7.2	-0.1484449
PG76-22S	gravel	SP-C	6.70%	50	2,161,690	-0.0002485	7.2	8.6	9.4	-0.1723765
PG76-22S	gravel	SP-C	6.70%	50	1,658,060	-0.0007066	7.2	8.6	9.4	-0.1723765
PG76-22S	gravel	SP-C	5.50%	125	86,190	-0.0140313	4.8	5.2	5.7	-0.0992287
PG76-22S	gravel	SP-C	5.50%	125	50,990	-0.0253903	4.8	5.2	5.7	-0.0992287
PG76-22S	gravel	SP-C	5.90%	100	738,950	-0.0007734	6.0	6.7	7.3	-0.1214101
PG76-22S	gravel	SP-C	6.30%	75	207,640	-0.0035789	5.6	6.7	7.2	-0.1484449
PG76-22S	gravel	SP-C	6.30%	75	167,850	-0.0051042	5.6	6.7	7.2	-0.1484449
PG76-22S	gravel	SP-C	6.70%	50	232,450	-0.0033419	7.2	8.6	9.4	-0.1723765
PG76-22S	gravel	SP-C	6.70%	50	489,470	-0.0022418	7.2	8.6	9.4	-0.1723765
PG70-22	gravel	SP-C	5.50%	125	787,800	-0.0011316	5.2	6.0	6.7	-0.1351088
PG70-22	gravel	SP-C	5.50%	125	891,120	-0.0006942	5.2	6.0	6.7	-0.1351088
PG70-22	gravel	SP-C	5.80%	100	2,470,180	-0.0002735	6.5	7.1	7.7	-0.1478017
PG70-22	gravel	SP-C	5.80%	100	1,468,480	-0.0003170	6.5	7.1	7.7	-0.1478017
PG70-22	gravel	SP-C	6.10%	75	1,772,240	-0.0005369	6.0	6.8	7.5	-0.1477987
PG70-22	gravel	SP-C	6.10%	75	2,152,780	-0.0002278	6.0	6.8	7.5	-0.1477987
PG70-22	gravel	SP-C	6.50%	50	5,415,290	-0.0002054	7.6	8.7	9.8	-0.1679815
PG70-22	gravel	SP-C	6.50%	50	2,752,700	-0.0002694	7.6	8.7	9.8	-0.1679815
PG70-22	gravel	SP-C	5.50%	125	238,440	-0.0032926	5.2	6.0	6.7	-0.1351088
PG70-22	gravel	SP-C	5.50%	125	124,070	-0.0037064	5.2	6.0	6.7	-0.1351088
PG70-22	gravel	SP-C	5.80%	100	395,960	-0.0008736	6.5	7.1	7.7	-0.1478017
PG70-22	gravel	SP-C	5.80%	100	181,800	-0.0031365	6.5	7.1	7.7	-0.1478017
PG70-22	gravel	SP-C	6.10%	75	190,900	-0.0019974	6.0	6.8	7.5	-0.1477987
PG70-22	gravel	SP-C	6.10%	75	188,840	-0.0024904	6.0	6.8	7.5	-0.1477987
PG70-22	gravel	SP-C	6.50%	50	192,360	-0.0015486	7.6	8.7	9.8	-0.1679815
PG70-22	gravel	SP-C	6.50%	50	342,970	-0.0010501	7.6	8.7	9.8	-0.1679815

Table 5.1 Summary of analyzed performance indicators (continued)

PG Grade	Aggregate type	Gradation	AC	Ndesign	Fatigue		Rutting			
					Final Cycle	Slope (Z)	10,000 Passes	15,000 Passes	20,000 Passes	Slope
PG76-22S	limestone	SP-D	4.90%	125	483,730	-0.0007203	1.3	1.6	3.0	-0.0542206
PG76-22S	limestone	SP-D	4.90%	125	1,011,070	-0.0002426	1.3	1.6	3.0	-0.0542206
PG76-22S	limestone	SP-D	5.10%	100	248,270	-0.0014488	2.4	2.8	3.2	-0.0615558
PG76-22S	limestone	SP-D	5.10%	100	168,920	-0.0015402	2.4	2.8	3.2	-0.0615558
PG76-22S	limestone	SP-D	5.40%	75	412,570	-0.0007404	4.0	5.5	8.0	-0.1862284
PG76-22S	limestone	SP-D	5.40%	75	82,950	-0.0041577	4.0	5.5	8.0	-0.1862284
PG76-22S	limestone	SP-D	5.90%	50	723,660	-0.0004891	4.9	7.9	10.1	-0.2093944
PG76-22S	limestone	SP-D	5.90%	50	144,000	-0.0018221	4.9	7.9	10.1	-0.2093944
PG76-22S	limestone	SP-D	4.90%	125	24,880	-0.0293264	1.3	1.6	3.0	-0.0542206
PG76-22S	limestone	SP-D	4.90%	125	18,970	-0.0301956	1.3	1.6	3.0	-0.0542206
PG76-22S	limestone	SP-D	5.10%	100	24,010	-0.0355980	2.4	2.8	3.2	-0.0615558
PG76-22S	limestone	SP-D	5.10%	100	8,940	-0.0761490	2.4	2.8	3.2	-0.0615558
PG76-22S	limestone	SP-D	5.40%	75	5,340	-0.1829725	4.0	5.5	8.0	-0.1862284
PG76-22S	limestone	SP-D	5.40%	75	32,880	-0.0156242	4.0	5.5	8.0	-0.1862284
PG76-22S	limestone	SP-D	5.90%	50	98,960	-0.0065122	4.9	7.9	10.1	-0.2093944
PG76-22S	limestone	SP-D	5.90%	50	33,420	-0.0191259	4.9	7.9	10.1	-0.2093944
PG64-22	limestone	SP-B	4.2%	125	17,030	-0.1037639	-	-	-	-0.6486847
PG64-22	limestone	SP-B	4.2%	125	21,320	-0.0564412	-	-	-	-0.6486847
PG64-22	limestone	SP-B	4.5%	100	9,600	-0.1680770	-	-	-	-0.6861251
PG64-22	limestone	SP-B	4.5%	100	10,990	-0.1113070	-	-	-	-0.6861251
PG64-22	limestone	SP-B	4.8%	75	37,290	-0.0365159	-	-	-	-2.0475997
PG64-22	limestone	SP-B	4.8%	75	24,510	-0.0382160	-	-	-	-2.0475997
PG64-22	limestone	SP-B	5.2%	50	29,390	-0.0317826	-	-	-	-2.1858871
PG64-22	limestone	SP-B	5.2%	50	27,510	-0.0398128	-	-	-	-2.1858871
PG64-22	limestone	SP-B	4.2%	125	471,110	-0.0024496	-	-	-	-0.6486847
PG64-22	limestone	SP-B	4.2%	125	188,630	-0.0028124	-	-	-	-0.6486847
PG64-22	limestone	SP-B	4.5%	100	839,430	-0.0014313	-	-	-	-0.6861251
PG64-22	limestone	SP-B	4.5%	100	***91,500***	***-0.0079507***	-	-	-	-0.6861251
PG64-22	limestone	SP-B	4.8%	75	699,950	-0.0019546	-	-	-	-2.0475997
PG64-22	limestone	SP-B	4.8%	75	229,350	-0.0039698	-	-	-	-2.0475997
PG64-22	limestone	SP-B	5.2%	50	982,480	-0.0011332	-	-	-	-2.1858871
PG64-22	limestone	SP-B	5.2%	50	454,550	-0.0018367	-	-	-	-2.1858871

Table 5.2: Relative performance with respect to performance at N_{design} = 100

PG Grade	Aggregate type	Gradation	AC	Ndesign	Relative performance			
					Relative Fatigue	Fatigue (Slope)	Rutting (Max)	Rutting (Slope)
PG76-22S	gravel	SP-C	5.50%	125	99%	93%	128%	122%
PG76-22S	gravel	SP-C	5.50%	125	62%	64%	128%	122%
PG76-22S	gravel	SP-C	5.90%	100	100%	100%	100%	100%
PG76-22S	gravel	SP-C	5.90%	100	100%	100%	100%	100%
PG76-22S	gravel	SP-C	6.30%	75	116%	160%	101%	82%
PG76-22S	gravel	SP-C	6.30%	75	116%	110%	101%	82%
PG76-22S	gravel	SP-C	6.70%	50	146%	306%	78%	70%
PG76-22S	gravel	SP-C	6.70%	50	112%	108%	78%	70%
PG76-22S	gravel	SP-C	5.50%	125	12%	6%	128%	122%
PG76-22S	gravel	SP-C	5.50%	125	7%	3%	128%	122%
PG76-22S	gravel	SP-C	5.90%	100	100%	100%	100%	100%
PG76-22S	gravel	SP-C	6.30%	75	28%	22%	101%	82%
PG76-22S	gravel	SP-C	6.30%	75	23%	15%	101%	82%
PG76-22S	gravel	SP-C	6.70%	50	31%	23%	78%	70%
PG76-22S	gravel	SP-C	6.70%	50	66%	34%	78%	70%
PG70-22	gravel	SP-C	5.50%	125	40%	26%	115%	109%
PG70-22	gravel	SP-C	5.50%	125	45%	43%	115%	109%
PG70-22	gravel	SP-C	5.80%	100	125%	108%	100%	100%
PG70-22	gravel	SP-C	5.80%	100	75%	93%	100%	100%
PG70-22	gravel	SP-C	6.10%	75	90%	55%	103%	100%
PG70-22	gravel	SP-C	6.10%	75	109%	130%	103%	100%
PG70-22	gravel	SP-C	6.50%	50	275%	144%	79%	88%
PG70-22	gravel	SP-C	6.50%	50	140%	110%	79%	88%
PG70-22	gravel	SP-C	5.50%	125	83%	61%	115%	109%
PG70-22	gravel	SP-C	5.50%	125	43%	54%	115%	109%
PG70-22	gravel	SP-C	5.80%	100	137%	230%	100%	100%
PG70-22	gravel	SP-C	5.80%	100	63%	64%	100%	100%
PG70-22	gravel	SP-C	6.10%	75	66%	100%	103%	100%
PG70-22	gravel	SP-C	6.10%	75	65%	81%	103%	100%
PG70-22	gravel	SP-C	6.50%	50	67%	129%	79%	88%
PG70-22	gravel	SP-C	6.50%	50	119%	191%	79%	88%

Table 5.2 Relative performance with respect to performance at N_{design} = 100 (continued)

PG Grade	Aggregate type	Gradation	AC	Ndesign	Relative performance			
					Relative Fatigue	Fatigue (Slope)	Rutting (Max)	Rutting (Slope)
PG76-22S	limestone	SP-D	4.90%	125	232%	207%	107%	114%
PG76-22S	limestone	SP-D	4.90%	125	485%	616%	107%	114%
PG76-22S	limestone	SP-D	5.10%	100	119%	103%	100%	100%
PG76-22S	limestone	SP-D	5.10%	100	81%	97%	100%	100%
PG76-22S	limestone	SP-D	5.40%	75	198%	202%	40%	33%
PG76-22S	limestone	SP-D	5.40%	75	40%	36%	40%	33%
PG76-22S	limestone	SP-D	5.90%	50	347%	306%	32%	29%
PG76-22S	limestone	SP-D	5.90%	50	69%	82%	32%	29%
PG76-22S	limestone	SP-D	4.90%	125	151%	191%	107%	114%
PG76-22S	limestone	SP-D	4.90%	125	115%	185%	107%	114%
PG76-22S	limestone	SP-D	5.10%	100	146%	157%	100%	100%
PG76-22S	limestone	SP-D	5.10%	100	54%	73%	100%	100%
PG76-22S	limestone	SP-D	5.40%	75	32%	31%	40%	33%
PG76-22S	limestone	SP-D	5.40%	75	200%	358%	40%	33%
PG76-22S	limestone	SP-D	5.90%	50	601%	858%	32%	29%
PG76-22S	limestone	SP-D	5.90%	50	203%	292%	32%	29%
PG64-22	limestone	SP-B	4.2%	125	165%	135%	-	106%
PG64-22	limestone	SP-B	4.2%	125	207%	248%	-	106%
PG64-22	limestone	SP-B	4.5%	100	93%	83%	-	100%
PG64-22	limestone	SP-B	4.5%	100	107%	126%	-	100%
PG64-22	limestone	SP-B	4.8%	75	362%	383%	-	34%
PG64-22	limestone	SP-B	4.8%	75	238%	366%	-	34%
PG64-22	limestone	SP-B	5.2%	50	285%	440%	-	31%
PG64-22	limestone	SP-B	5.2%	50	267%	351%	-	31%
PG64-22	limestone	SP-B	4.2%	125	56%	58%	-	106%
PG64-22	limestone	SP-B	4.2%	125	22%	51%	-	106%
PG64-22	limestone	SP-B	4.5%	100	100%	100%	-	100%
PG64-22	limestone	SP-B	4.5%	100	11%	18%	-	100%
PG64-22	limestone	SP-B	4.8%	75	83%	73%	-	34%
PG64-22	limestone	SP-B	4.8%	75	27%	36%	-	34%
PG64-22	limestone	SP-B	5.2%	50	117%	126%	-	31%
PG64-22	limestone	SP-B	5.2%	50	54%	78%	-	31%

Figures 5.6 and 5.7 show the relative performance of the analyzed mixes with respect to their performance at 100 gyrations on the SGC with different asphalt cement contents. Figure 5.6 uses the number of cycles to failure (50% initial stiffness) as the fatigue performance indicator and the maximum rut depth (measured at 20,000 wheel passes) as the rutting indicator. Figure 5.7 uses the slope of the secondary phase (Z) of the fatigue and rutting curves as the performance indicator. Note that the scatter observed is due to the fact that all mixtures are represented in the figure irrespective of aggregate or binder type.

Figures 5.8 and Figure 5.9 show the relative performance of the analyzed mixes with respect to the performance at 100 gyrations on the SGC, with the difference being that the *x*-axis has been changed to reflect number of gyrations on the SGC. Bear in mind that the experiment was developed so that the four selected asphalt contents for each analyzed asphalt mix corresponds to 50, 75, 100, or 125 gyrations in the SGC.

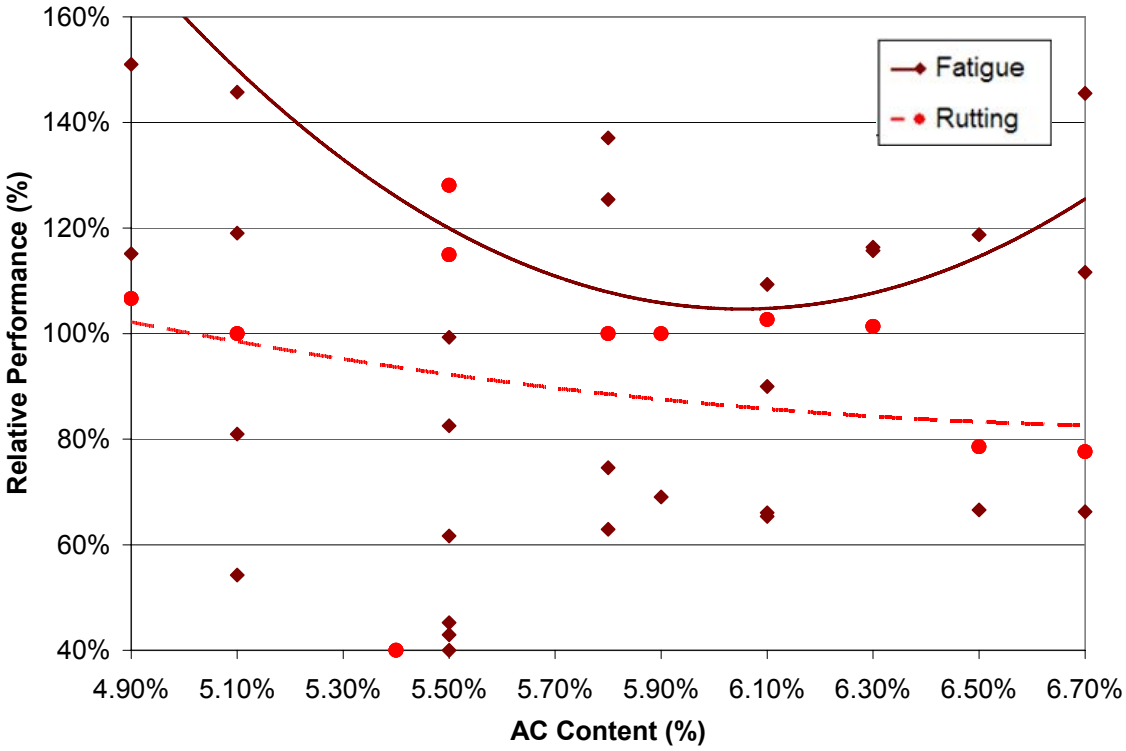

Figure 5.6: Relative performance at N_{design} = 100 versus AC content

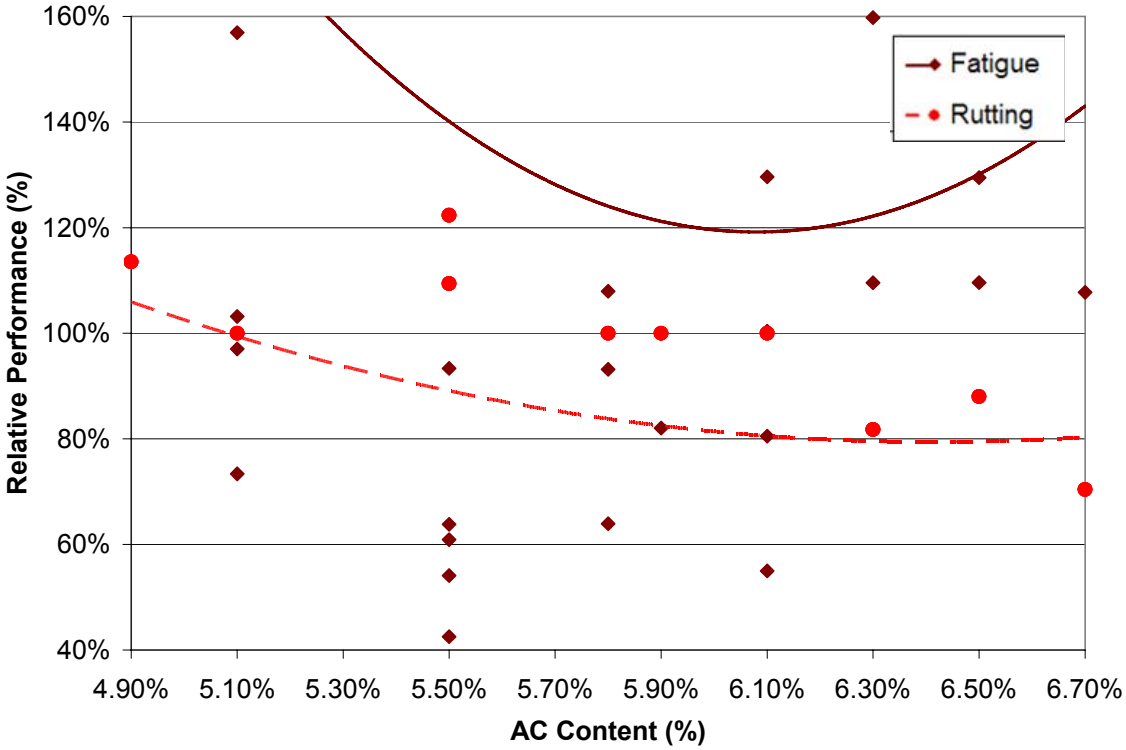

Figure 5.7: Relative performance at N_{design} = 100 versus AC content (using $Z_{fatigue}$ and Z_{rut} as performance indicators)

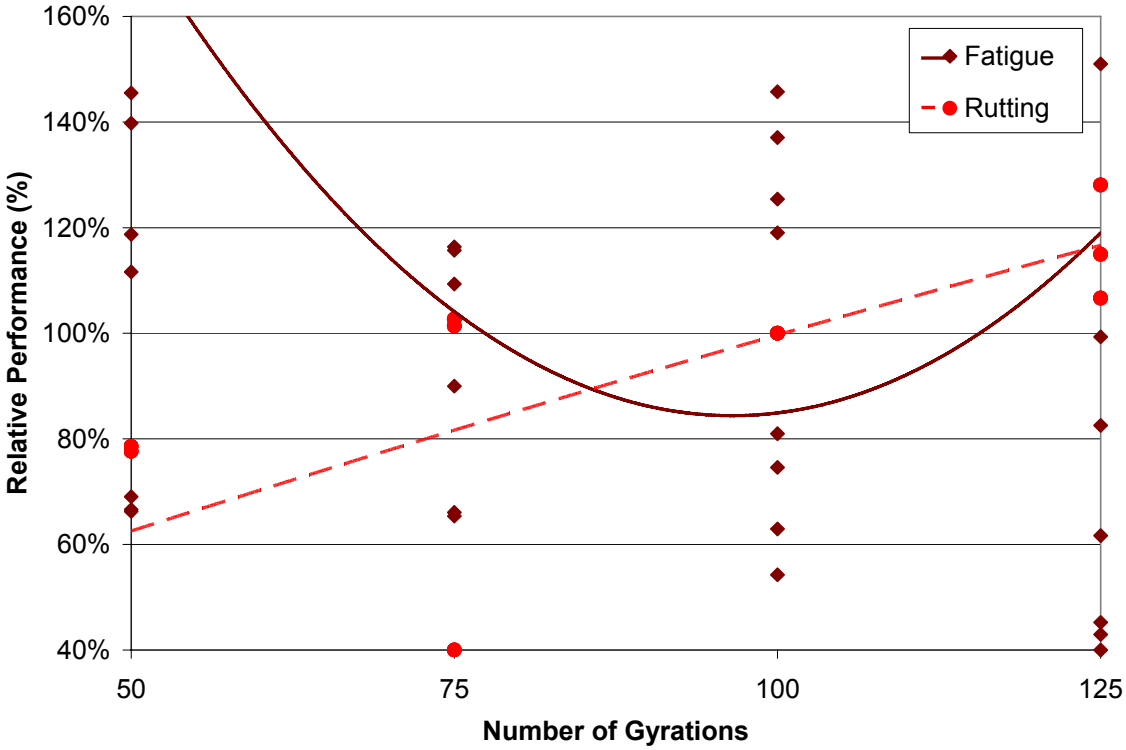

Figure 5.8: Relative performance at N_{design} = 100 versus SGC gyrations

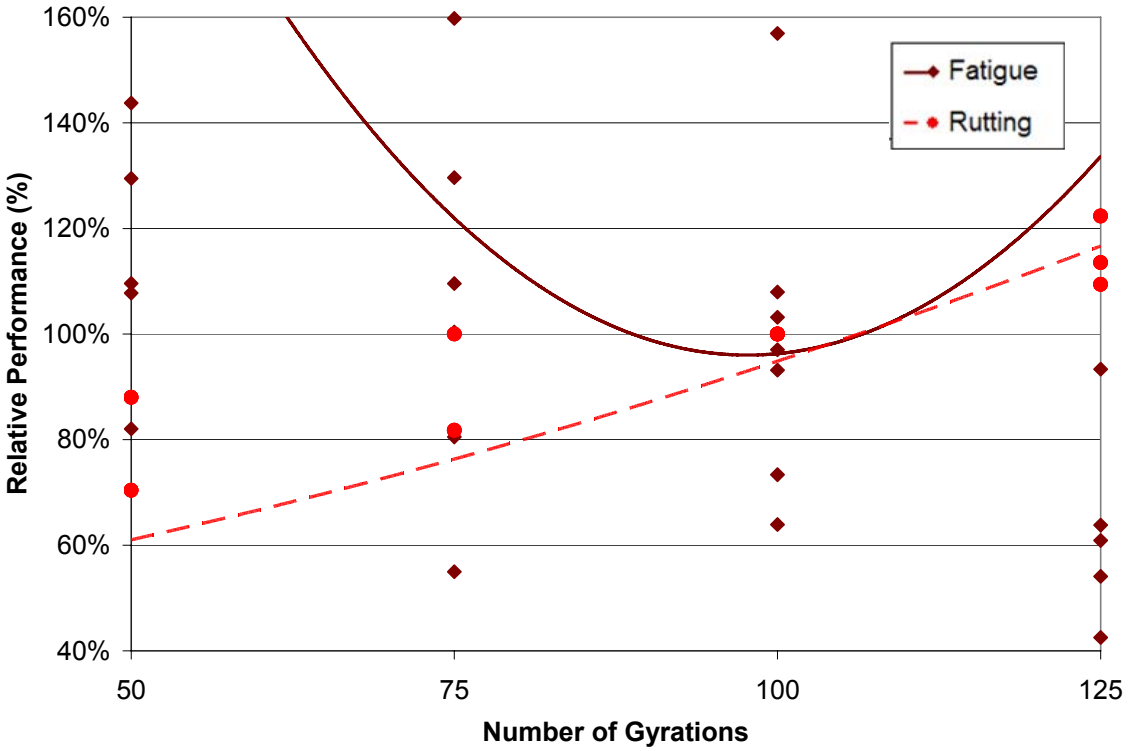

Figure 5.9: Relative performance at N_{design} = 100 versus SGC gyrations (using $Z_{fatigue}$ and Z_{rut} as performance indicators)

The previous figures show that, in general, at a high number of design gyrations the asphalt mixtures tend to show adequate rutting resistance. It can also be seen that at a low number of design gyrations, rutting resistance decreases; however, the asphalt mixture resistance to fatigue damage increases significantly.

If 100 gyrations on the SGC were to be selected as a base indicator, the resulting objective function would consist of a combination of the relative performance in both fatigue and rutting, where the optimum value would be over 100%. This is conceptually more complicated to understand, and "100%" using this definition would not necessarily mean good performance. In some cases, it could actually lead to rather low performance of the asphalt mixture.

This problem can be eliminated by selecting the maximum performance as the "base" performance for both fatigue resistance and rutting resistance. In this manner, 100% performance would indicate the highest resistance in either fatigue or rutting and anything below that would correspond to reduced expected performance. The details of these analyses are presented in the following section.

5.3.2 Analysis Based on N_{design} at Optimal Resistance

The calculation of relative performance of the various asphalt mixtures with respect to the maximum performance in fatigue and rutting (for the range of gyrations tested) is described in this section. As previously discussed, the highest fatigue resistance was obtained at 50 gyrations on the SGC (highest asphalt content) and the highest rutting resistance was achieved at

125 gyrations on the SGC (lowest asphalt content). Accordingly, these two levels of gyrations (50 and 125) were defined as the "base" performance for fatigue and rutting, respectively. In this way, the highest resistance for either rutting or fatigue will be 100%. Table 5.3 shows relative performance with respect to the maximum performance, as explained previously.

As in the previous section, relative rutting has been determined with respect to the rut depth at 20,000 wheel passes in the HWTD equipment, instead of selecting the rut depth at 10,000, 15,000, or 20,000 passes depending on the PG grade of the asphalt binder. This was done in order to standardize the comparison.

Table 5.3: Relative performance with respect to maximum resistance

PG Grade	Aggregate type	Gradation	AC	Ndesign	Relative performance			
					Relative Fatigue	Fatigue (Slope)	Rutting (Max)	Rutting (Slope)
PG76-22S	gravel	SP-C	5.50%	125	77%	59%	100%	100%
PG76-22S	gravel	SP-C	5.50%	125	48%	40%	100%	100%
PG76-22S	gravel	SP-C	5.90%	100	29%	20%	78%	82%
PG76-22S	gravel	SP-C	5.90%	100	43%	31%	78%	82%
PG76-22S	gravel	SP-C	6.30%	75	91%	100%	79%	67%
PG76-22S	gravel	SP-C	6.30%	75	90%	69%	79%	67%
PG76-22S	gravel	SP-C	6.70%	50	113%	192%	61%	58%
PG76-22S	gravel	SP-C	6.70%	50	87%	68%	61%	58%
PG76-22S	gravel	SP-C	5.50%	125	24%	20%	100%	100%
PG76-22S	gravel	SP-C	5.50%	125	14%	11%	100%	100%
PG76-22S	gravel	SP-C	5.90%	100	205%	361%	78%	82%
PG76-22S	gravel	SP-C	6.30%	75	58%	78%	79%	67%
PG76-22S	gravel	SP-C	6.30%	75	47%	55%	79%	67%
PG76-22S	gravel	SP-C	6.70%	50	64%	84%	61%	58%
PG76-22S	gravel	SP-C	6.70%	50	136%	125%	61%	58%
PG70-22	gravel	SP-C	5.50%	125	19%	21%	100%	100%
PG70-22	gravel	SP-C	5.50%	125	22%	34%	100%	100%
PG70-22	gravel	SP-C	5.80%	100	60%	87%	87%	91%
PG70-22	gravel	SP-C	5.80%	100	36%	75%	87%	91%
PG70-22	gravel	SP-C	6.10%	75	43%	44%	89%	91%
PG70-22	gravel	SP-C	6.10%	75	53%	104%	89%	91%
PG70-22	gravel	SP-C	6.50%	50	133%	116%	68%	80%
PG70-22	gravel	SP-C	6.50%	50	67%	88%	68%	80%
PG70-22	gravel	SP-C	5.50%	125	89%	39%	100%	100%
PG70-22	gravel	SP-C	5.50%	125	46%	35%	100%	100%
PG70-22	gravel	SP-C	5.80%	100	148%	149%	87%	91%
PG70-22	gravel	SP-C	5.80%	100	68%	41%	87%	91%
PG70-22	gravel	SP-C	6.10%	75	71%	65%	89%	91%
PG70-22	gravel	SP-C	6.10%	75	71%	52%	89%	91%
PG70-22	gravel	SP-C	6.50%	50	72%	84%	68%	80%
PG70-22	gravel	SP-C	6.50%	50	128%	124%	68%	80%

Table 5.3 Relative performance with respect to maximum resistance (continued)

PG Grade	Aggregate type	Gradation	AC	Ndesign	Relative performance			
					Relative Fatigue	Fatigue (Slope)	Rutting (Max)	Rutting (Slope)
PG76-22S	limestone	SP-D	4.90%	125	112%	160%	100%	100%
PG76-22S	limestone	SP-D	4.90%	125	233%	476%	100%	100%
PG76-22S	limestone	SP-D	5.10%	100	57%	80%	94%	88%
PG76-22S	limestone	SP-D	5.10%	100	39%	75%	94%	88%
PG76-22S	limestone	SP-D	5.40%	75	95%	156%	38%	29%
PG76-22S	limestone	SP-D	5.40%	75	19%	28%	38%	29%
PG76-22S	limestone	SP-D	5.90%	50	167%	236%	30%	26%
PG76-22S	limestone	SP-D	5.90%	50	33%	63%	30%	26%
PG76-22S	limestone	SP-D	4.90%	125	38%	44%	100%	100%
PG76-22S	limestone	SP-D	4.90%	125	29%	42%	100%	100%
PG76-22S	limestone	SP-D	5.10%	100	36%	36%	94%	88%
PG76-22S	limestone	SP-D	5.10%	100	14%	17%	94%	88%
PG76-22S	limestone	SP-D	5.40%	75	8%	7%	38%	29%
PG76-22S	limestone	SP-D	5.40%	75	50%	82%	38%	29%
PG76-22S	limestone	SP-D	5.90%	50	150%	197%	30%	26%
PG76-22S	limestone	SP-D	5.90%	50	50%	67%	30%	26%
PG64-22	limestone	SP-B	4.2%	125	60%	34%	-	100%
PG64-22	limestone	SP-B	4.2%	125	75%	63%	-	100%
PG64-22	limestone	SP-B	4.5%	100	34%	21%	-	95%
PG64-22	limestone	SP-B	4.5%	100	39%	32%	-	95%
PG64-22	limestone	SP-B	4.8%	75	131%	98%	-	32%
PG64-22	limestone	SP-B	4.8%	75	86%	94%	-	32%
PG64-22	limestone	SP-B	5.2%	50	103%	113%	-	30%
PG64-22	limestone	SP-B	5.2%	50	97%	90%	-	30%
PG64-22	limestone	SP-B	4.2%	125	66%	61%	-	100%
PG64-22	limestone	SP-B	4.2%	125	26%	53%	-	100%
PG64-22	limestone	SP-B	4.5%	100	117%	104%	-	95%
PG64-22	limestone	SP-B	4.5%	100	13%	19%	-	95%
PG64-22	limestone	SP-B	4.8%	75	97%	76%	-	32%
PG64-22	limestone	SP-B	4.8%	75	32%	37%	-	32%
PG64-22	limestone	SP-B	5.2%	50	137%	131%	-	30%
PG64-22	limestone	SP-B	5.2%	50	63%	81%	-	30%

Figures 5.10 and 5.11 show the relative performance of the analyzed mixes with respect to their maximum performance in both fatigue and rutting with different analyzed asphalt cement contents. Figure 5.10 uses the number of cycles to failure (50% initial stiffness) as the fatigue performance indicator and the maximum rut depth (measured at 20,000 wheel passes) as the rutting indicator. Figure 5.11 uses the slope of the secondary phase (Z) of the fatigue and rutting curves as the performance indicator.

Figures 5.12 and 5.13 show the relative performance of the analyzed mixes with respect to the maximum performance of the asphalt mix. In these figures the *x*-axis has been changed to reflect number of gyrations on the SGC.

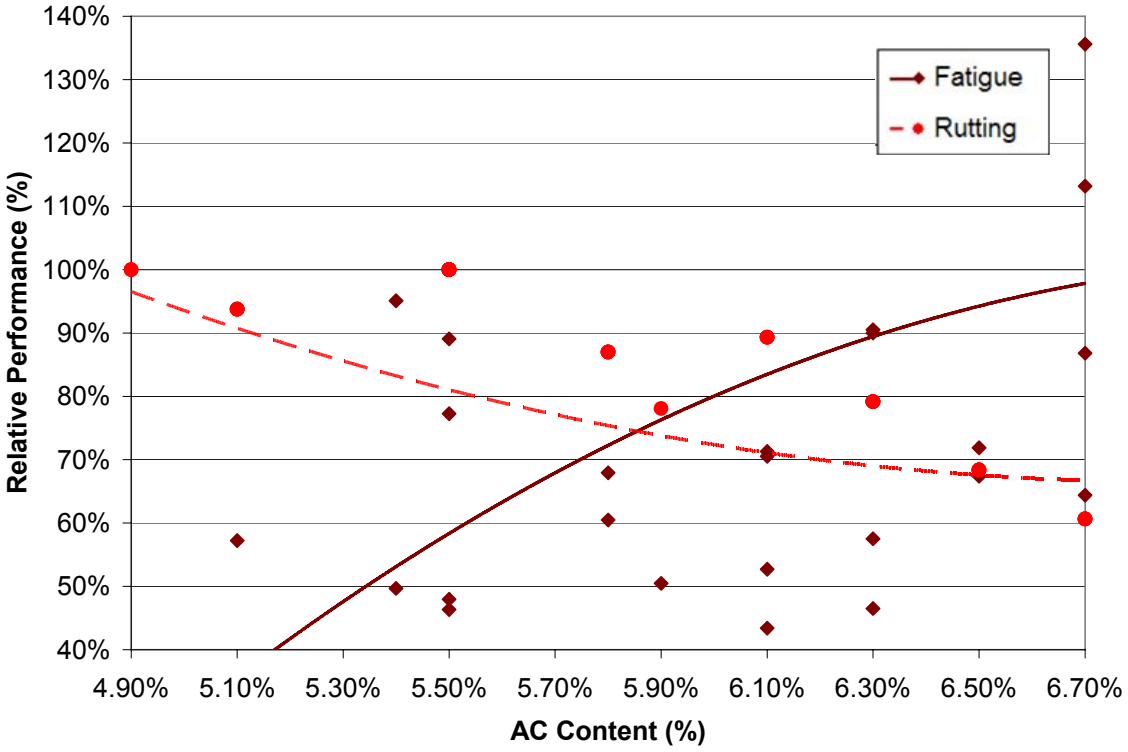

Figure 5.10: Relative performance with respect to maximum resistance versus AC content

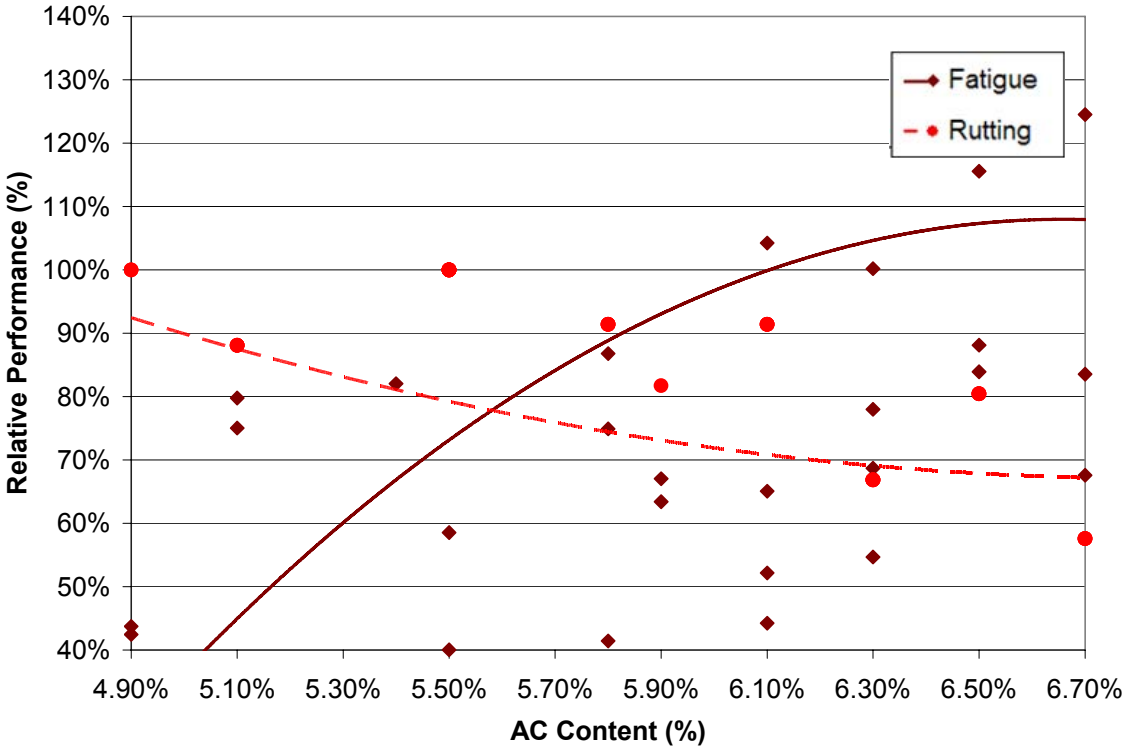

Figure 5.11: Relative performance with respect to maximum resistance versus AC content (using $Z_{fatigue}$ and Z_{rut} as performance indicators)

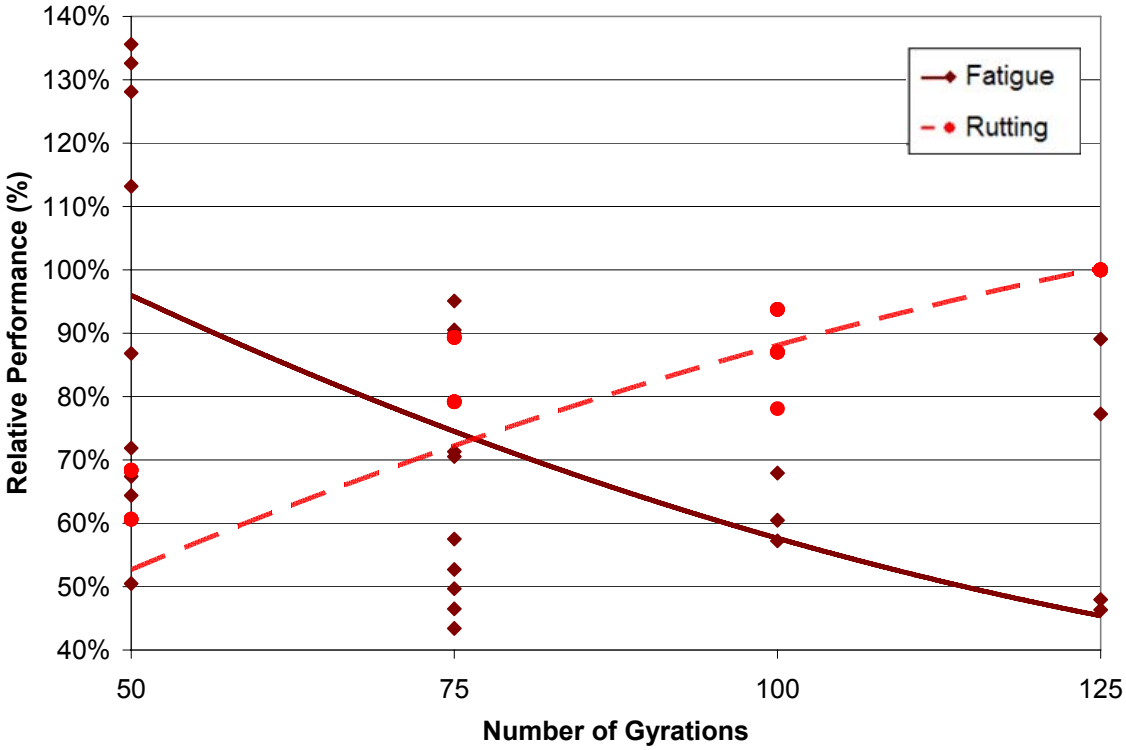

Figure 5.12: Relative performance with respect to maximum resistance versus SGC

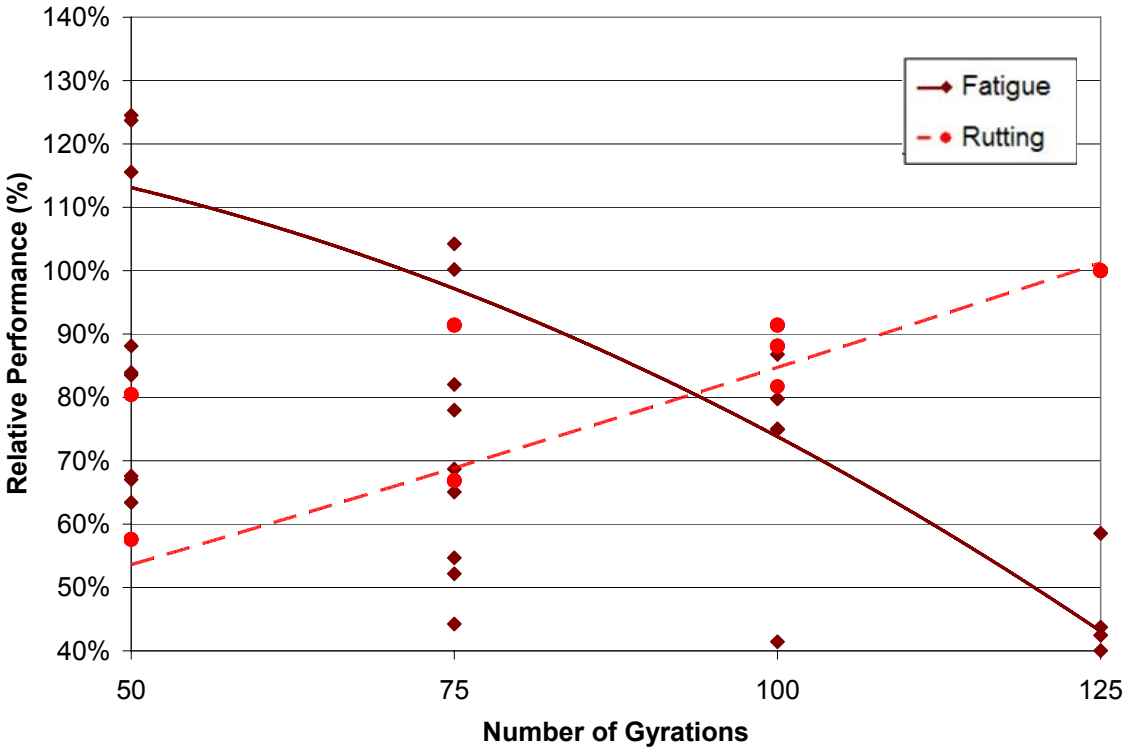

Figure 5.13: Relative performance with respect to maximum resistance versus SGC gyrations (using $Z_{fatigue}$ and Z_{rut} as performance indicators)

As in the previous section, it can be observed from the figures that, in general, the asphalt mixtures adequately resist rutting at a higher number of design gyrations. It can also be seen that rutting resistance decreases at a lower number of design gyrations; however, the asphalt mixture resistance to fatigue damage is high. The main difference is that the new parameters are more consistent and more repeatable for the same mix.

5.3.3 Relative Performance Optimization

The main advantage of standardizing both rutting and fatigue units to relative performance can be observed during the optimization process. This standardization allows for the generation of an objective function that includes both relative performance indicators. In doing so, an optimum number of gyrations on the SGC that allows for the maximization of the combined relative performance can be determined.

The relative performance to rutting and fatigue cracking can be combined in many different ways. One simple way of doing so is using a linear combination of relative rutting performance and relative fatigue performance. One logical way of doing so is by assigning equal weights to both types of damage, i.e., 50% to rutting resistance and 50% to fatigue or cracking resistance. The outcome of this approach is illustrated in Figures 5.14 and 5.15.

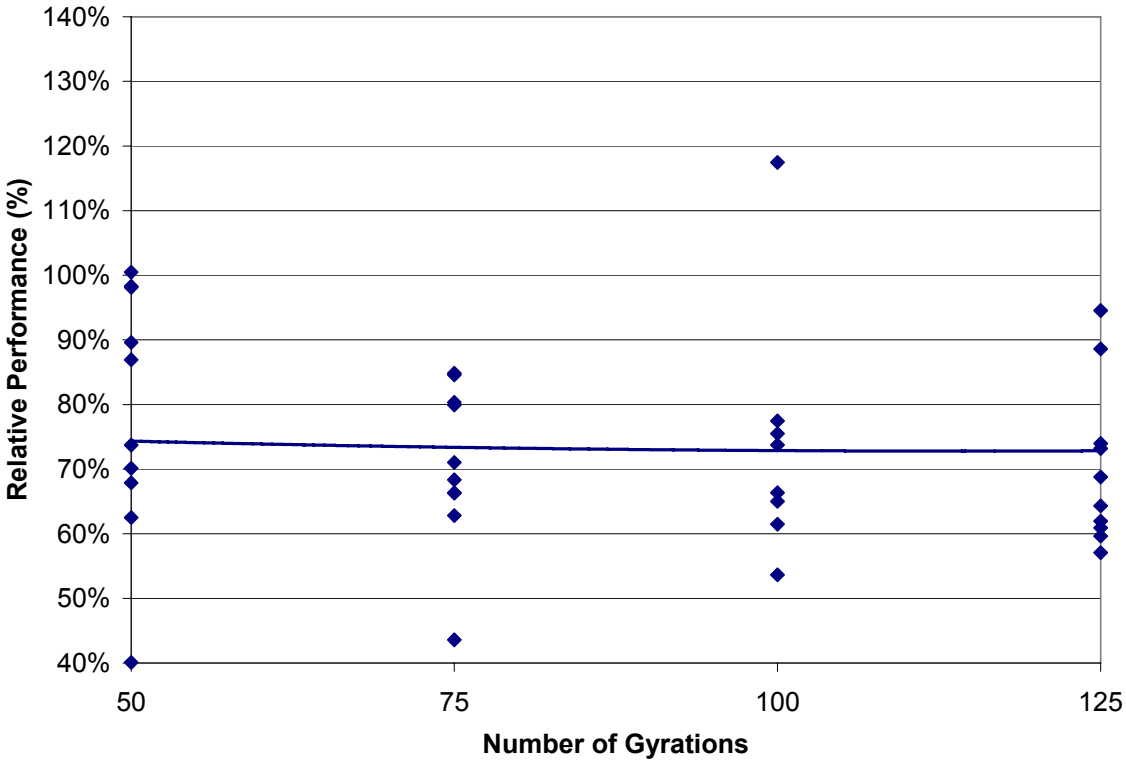

Figure 5.14: Relative performance assigning equal weights to rutting and fatigue

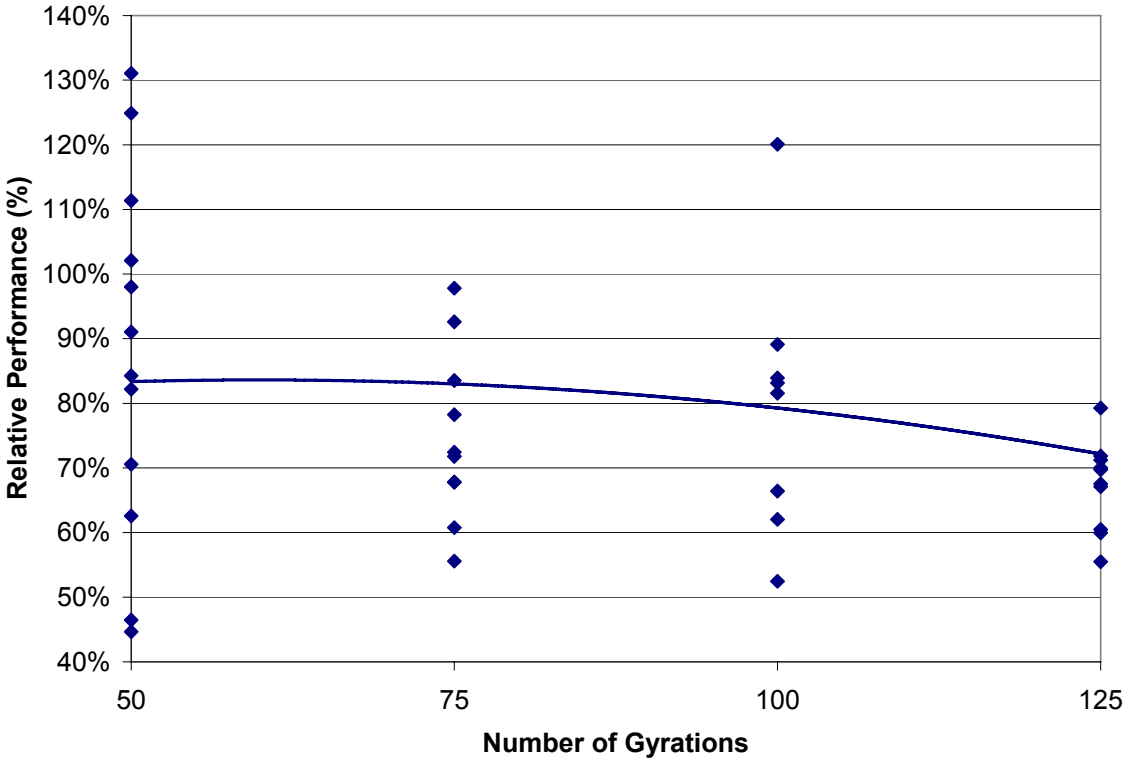

Figure 5.15: Relative performance assigning equal weights to rutting and fatigue based on $Z_{fatigue}$ and Z_{rut} as performance indicators

Based on a linear combination of both relative performance to rutting and relative performance to fatigue and assigning equal weights to both distress types, an optimum number of gyrations can be obtained.

In the case of Figure 5.14, which was obtained by selecting the number of cycles to failure as the fatigue life indicator and the rut depth at 20,000 wheel passes as the rutting indicator, the number of gyrations to achieve an optimal performance is 50 (within the analysis range). In Figure 5.15, which was obtained by selecting the slope of the secondary phase of the fatigue and permanent deformation curve as performance indicators, the number of gyrations required to attain optimal performance (as defined previously—equal weights to fatigue resistance and rutting resistance) is 60.

However, depending on the needs of each specific region, and accounting for traffic, structural, and environmental conditions, the design engineer can choose to assign more weight to either fatigue resistance or to rutting resistance.

Figures 5.16 and 5.17 show examples of several possible weight assignments of fatigue resistance and rutting resistance. In the figures, the weight distribution is indicated as XX/YY, where XX is the assigned weight to fatigue resistance and YY is the assigned weight to rutting resistance.

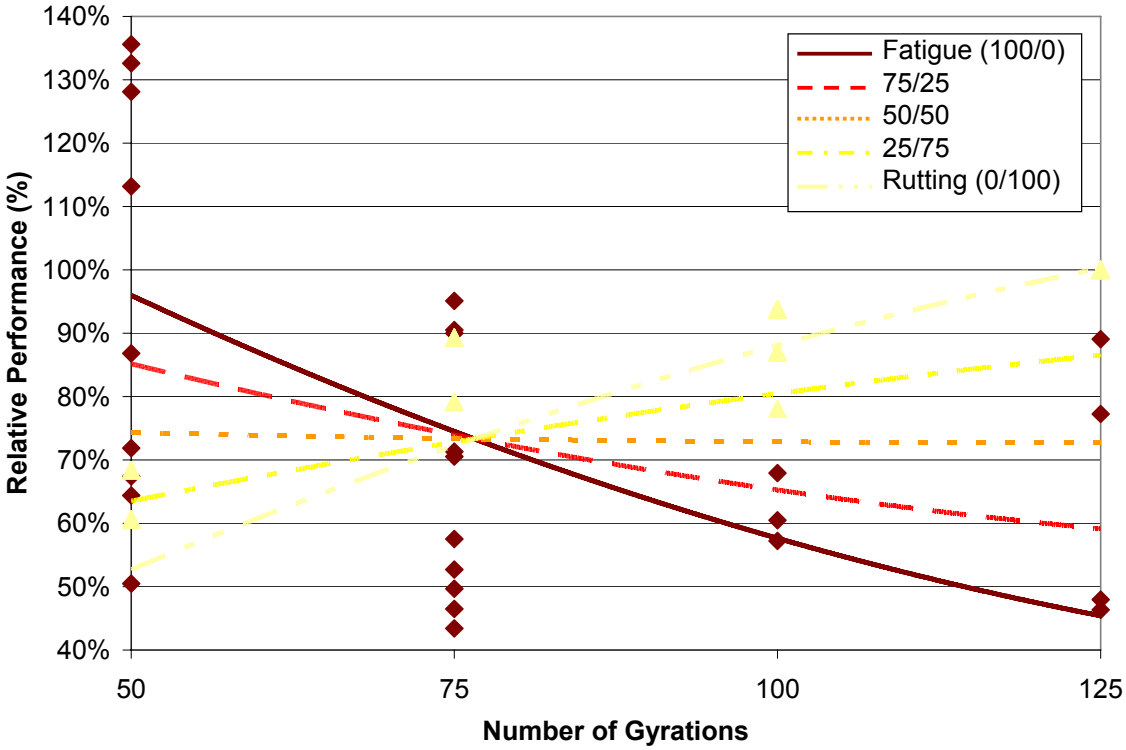

Figure 5.16: Linear combinations of relative performance to rutting and fatigue

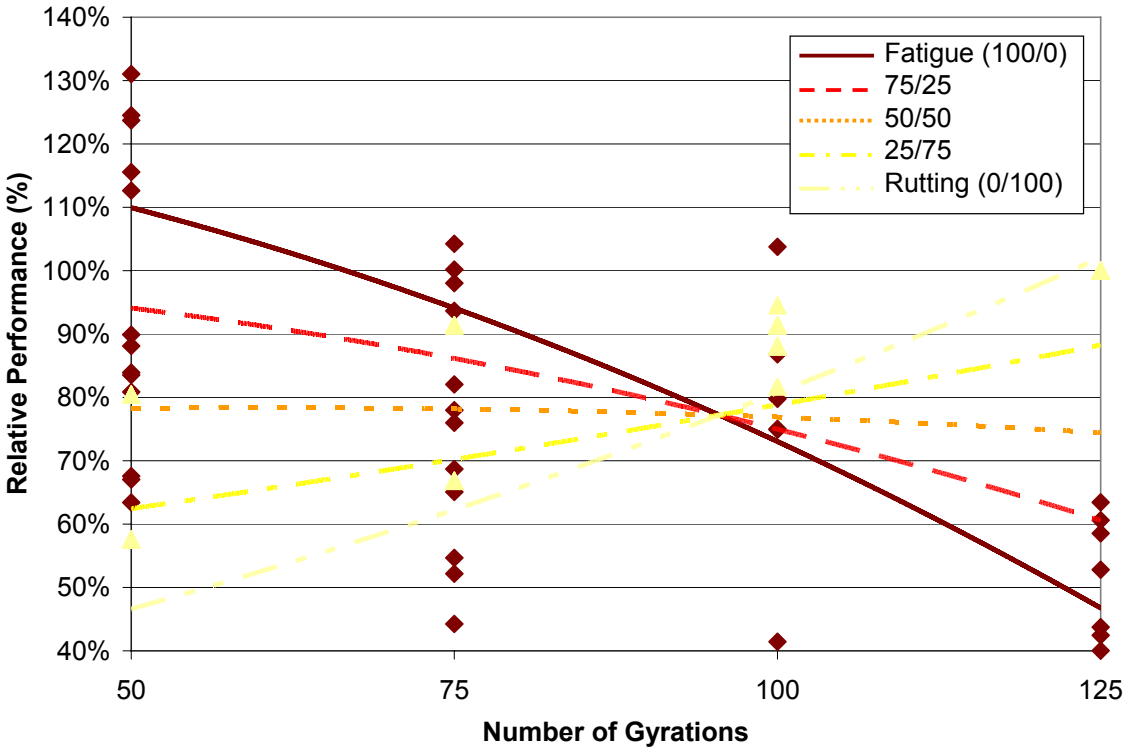

Figure 5.17: Linear combinations of relative performance to rutting and fatigue (based on $Z_{fatigue}$ and Z_{rut} as performance indicators)

Data used to develop the previous figures included information from all the analyzed asphalt mixes, which allowed for determination of generalized trends but also showed high variability owing to differences in the performance of different asphalt mixes. Consequently, similar analyses were performed for each individual asphalt mix and the results are now discussed.

Figure 5.18 shows the relative performance curves for the gravel SP-C mix with PG 76-22 binder. Of all the analyzed mixes, the SP-C mix with PG 76-22 binder showed the highest rutting resistance and one of the highest levels of fatigue resistance. It can be concluded from the average weighted combination of the relative performance curves (i.e., 50/50) that the number of gyrations required to optimize relative performance is 87. However, if, because of project specific considerations, fatigue were the only concern, 73 gyrations on the SGC optimize fatigue resistance according to the 100/0 curve. This selection would place emphasis on fatigue resistant mixes, completely disregarding rutting considerations. On the other hand, if rutting resistance was the only concern, the mix could be designed for 125 gyrations (according to the 0/100 curve).

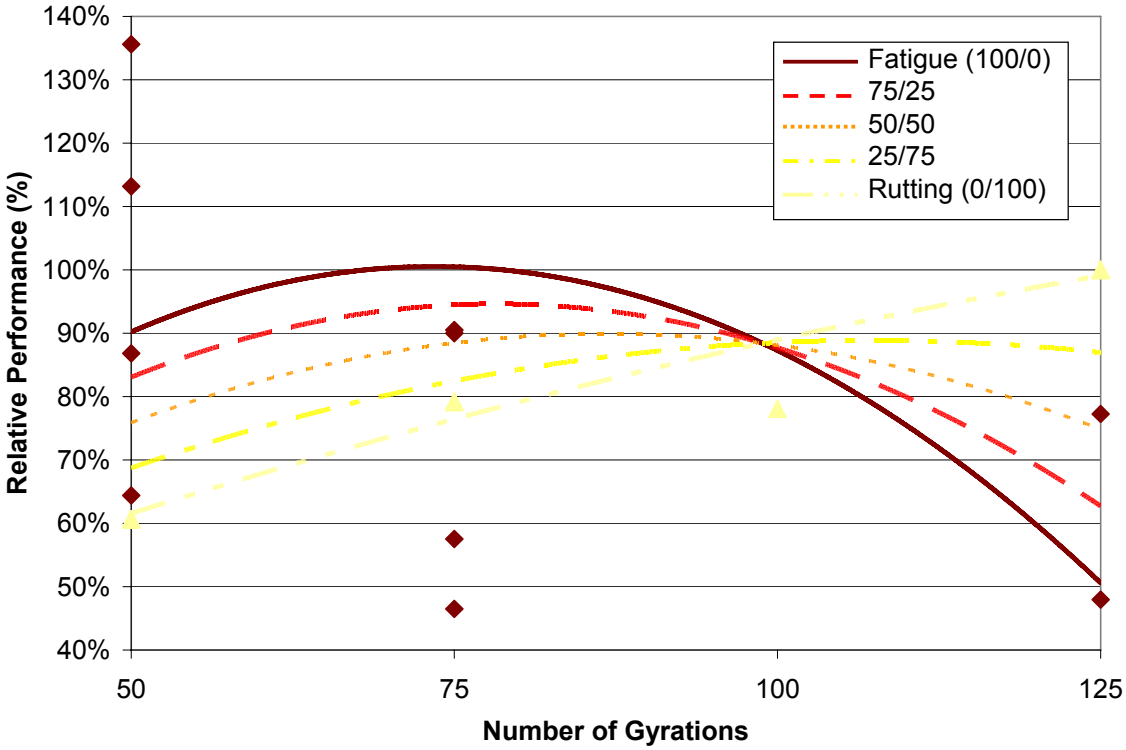

Figure 5.18: Relative performance curves for SP-C gravel and PG 76-22 mix

Figure 5.19 shows the relative performance curves for the gravel SP-C mix with PG 70-22 binder. Of all the evaluated mixes, this one shows the highest fatigue resistance. From the relative performance curves, it can be estimated that less than 50 gyrations optimize the relative performance in both rutting and fatigue for this mix type (equal weight for fatigue resistance and rutting resistance or 50/50).

Figure 5.20 shows the relative performance curves for the limestone SP-D mix with PG 76-22 binder. In general, the limestone mixes showed poorer rutting and fatigue resistance compared with the gravel mixes used in this study.

From the fatigue results obtained for the different samples generated at different numbers of gyrations, it was observed that this mix (for the particular range of analysis: 50–125 gyrations on the SPG) was not significantly sensitive to changes in asphalt binder content. An analysis of variance confirmed that the applied number of gyrations (or resulting binder content) was not statistically significant for fatigue performance. For the range tested, the fatigue performance of this mix was independent of the asphalt content; therefore, the optimum number of gyrations should be selected based on other considerations. For example, rutting performance could be combined with durability considerations.

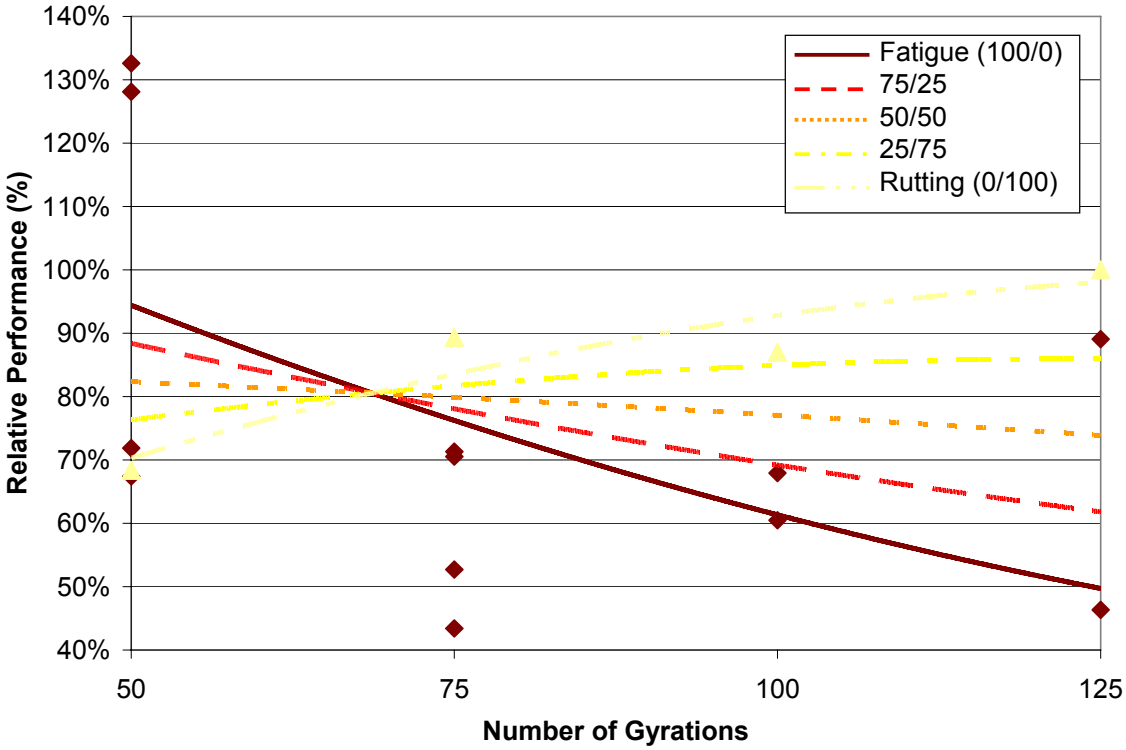

Figure 5.19: Relative performance curves for SP-C gravel and PG 70-22 mix

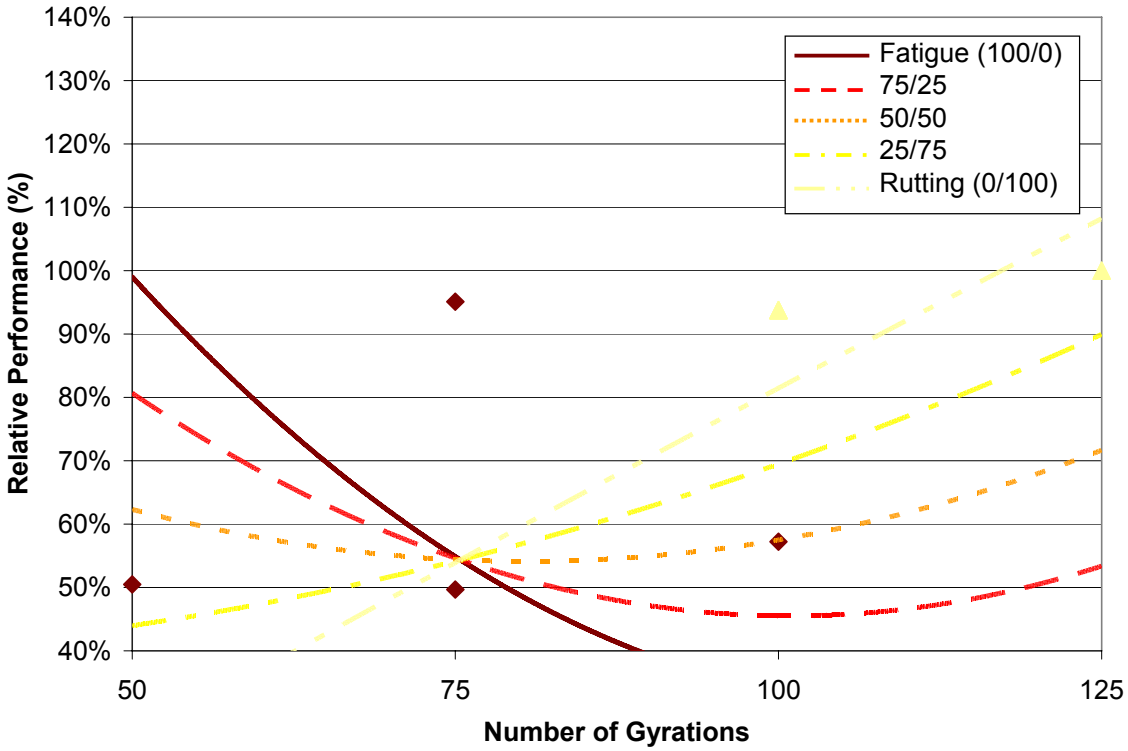

Figure 5.20: Relative performance curves for SP-D limestone and PG 76-22 mix

The limestone SP-B mix with PG 64-22 did not meet the minimal rutting resistance requirements (maximum 12.5 mm rut depth in HWTD); consequently, the relative performance at 10,000 wheel passes could not be determined. In such cases, the importance of alternative parameters, such as the slope Z, becomes evident.

Following the same procedure used with the conventional parameters, relative performance curves were developed using the slope parameters Z_{rut} and $Z_{fatigue}$ defined earlier. Figure 5.21 shows the relative performance curves for the gravel SP-C mix with PG 76-22 binder based on the slope parameters. It can be concluded from the average weighted combination of the relative performance curves that the number of gyrations required to optimize relative performance is 87. However, if fatigue were the only concern, 80 gyrations on the SGC would optimize the design.

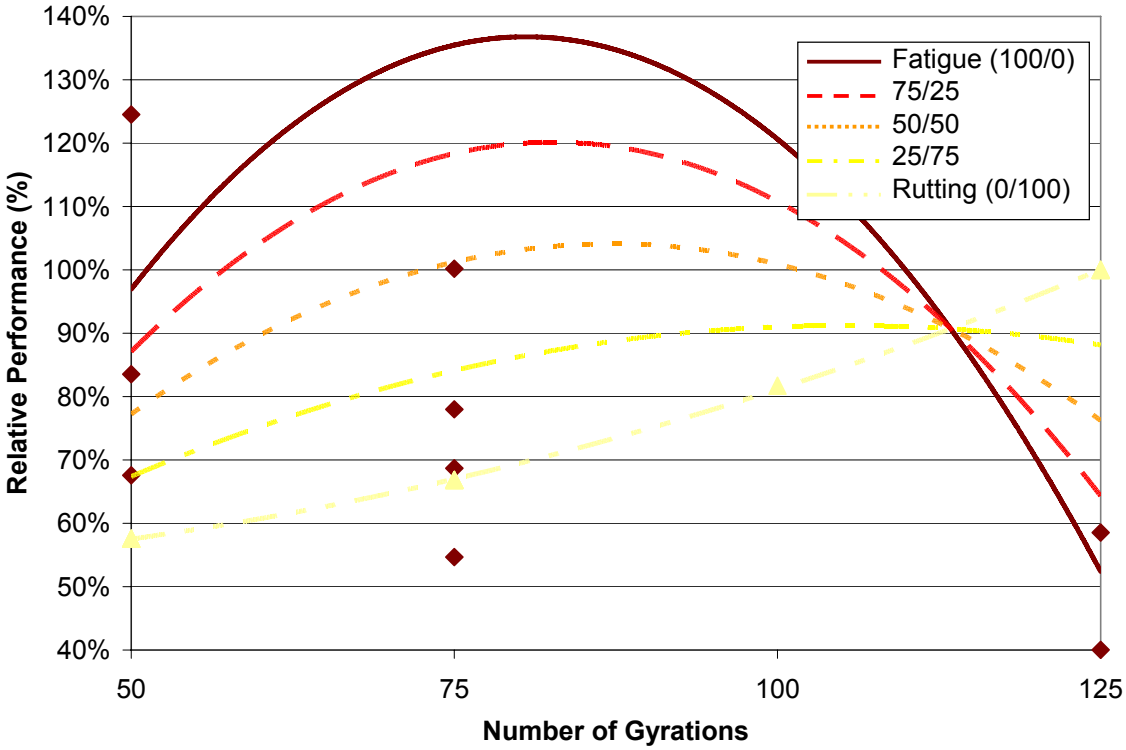

Figure 5.21: Relative performance curves for SP-C gravel and PG 76-22 mix (based on $Z_{fatigue}$ and Z_{rut} as performance indicators)

Figure 5.22 shows the relative performance curves for the gravel SP-C mix with PG 70-22 binder, based on the Z parameters. From the relative performance curves, it can be estimated that 57 gyrations would optimize the relative performance in both rutting and fatigue for this mix type (equal weight for both fatigue and rutting resistance).

Figure 5.23 shows the relative performance curves for the limestone SP-D mix with PG 76-22 binder, based on the Z parameter. As was the case when the same mix was analyzed using the conventional parameters, when equal weight was assigned for fatigue resistance and rutting resistance, the optimal number of gyrations was outside the tested range. Again, this is due to the fact that the fatigue resistance of the mix was not susceptible to changes in asphalt binder content for the range that was tested. This fact was demonstrated through statistical analyses.

Based on the Z parameters, relative performance curves can be generated for the limestone SP-B mix with PG 64-22 binder. Figure 5.24 shows the relative performance curves for this mix. It can be estimated that 125 gyrations optimize the relative performance in both rutting and fatigue for this mix type (equal weight for both fatigue and rutting resistance, within analysis range).

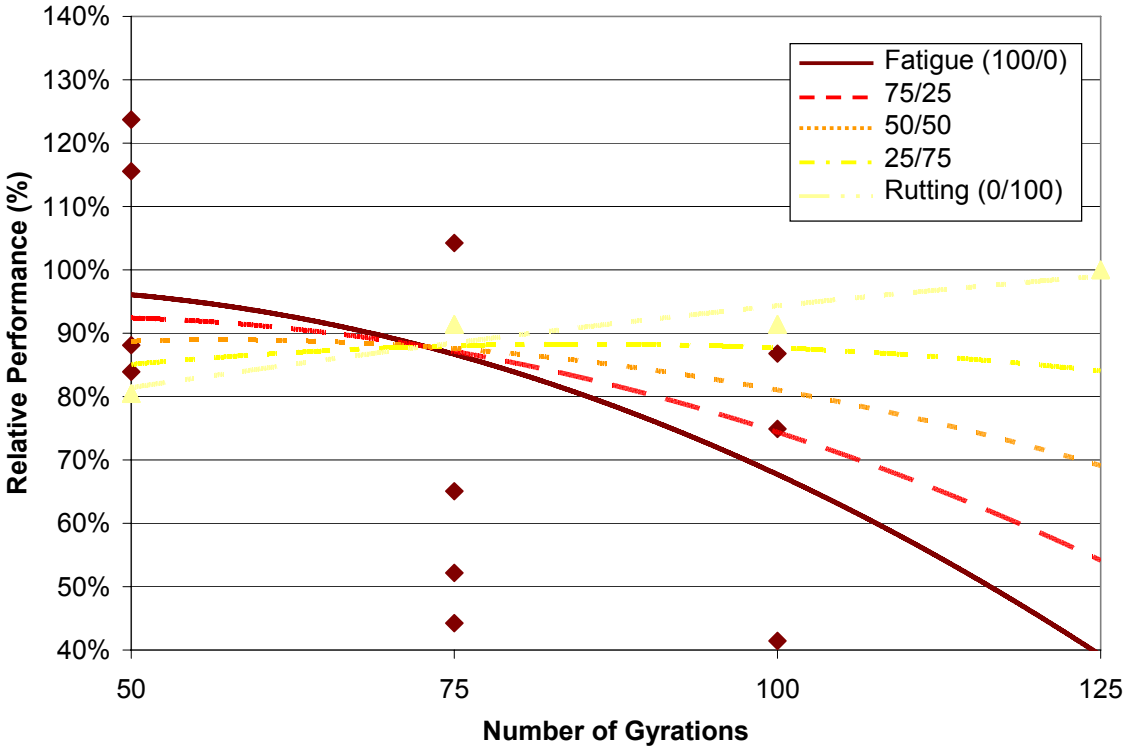

Figure 5.22: Relative performance curves for SP-C gravel and PG 70-22 mix (based on $Z_{fatigue}$ and Z_{rut} as performance indicators)

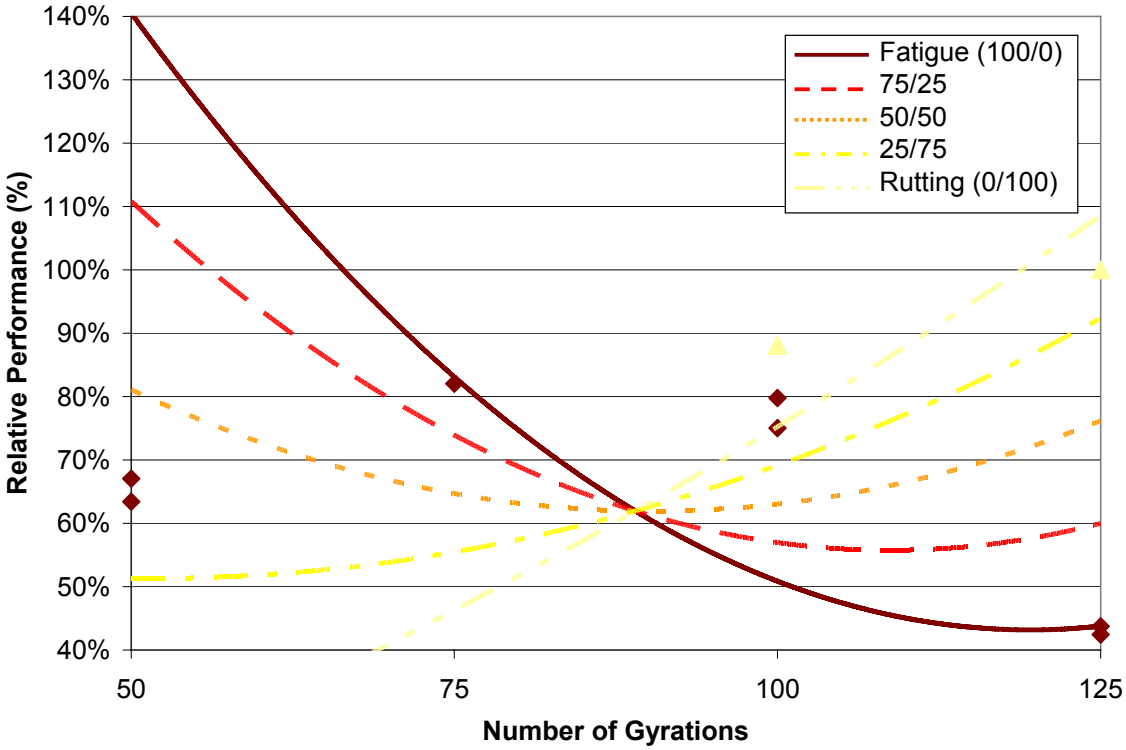

Figure 5.23: Performance curves for SP-D gravel and PG 76-22 mix based on Z parameter

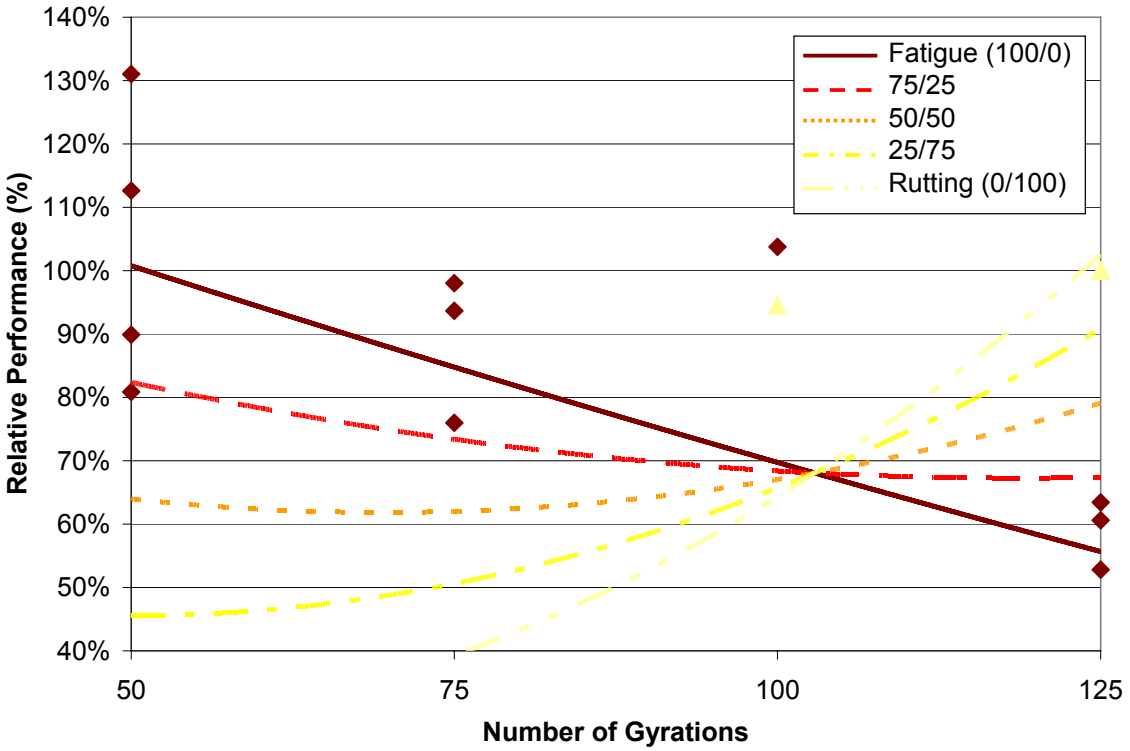

Figure 5.24: Performance curves for SP-B gravel and PG 64-22 mix based on Z parameter

5.3.4 Reliability Approach to Optimizing N_{design}

A second method of selecting an appropriate number of design gyrations requires assigning different reliability levels to the rutting and fatigue performance curves instead of simply using the average curves (50% reliability). By following this approach, the designer could allow for higher probability of attaining a desired performance level when preferred. Another advantage of this method is that the reliability could be increased in term of expected rutting performance, fatigue performance, or both. Thus, the designer could use 50/50 or 90/50 or 90/90. That is, the level of reliability of each distress can be selected independently and according to the requirements of the specific project.

The assignment of different reliability levels also allows, depending on the needs of a specific pavement structure, for more weight to be given to fatigue resistance or to rutting resistance without compromising pavement performance in general, and maintaining the performance of the asphalt mix within reasonable confidence levels. As was the case with the relative performance curves, the analyzed asphalt mixes have been evaluated.

Figure 5.25 shows the relative performance based on the average of all the analyzed asphalt mixes. While combining all the results increases the variability and consequently underestimates the performance of the best performing mixes owing to inclusion of all the information, it can be seen that the optimal relative performance is achieved at 82 gyrations on the SGC. At this number of gyrations, the 50% reliability curves for relative performance in fatigue and rutting intersect.

It can also be observed that, in general, an average increment of five gyrations results in an increase in relative performance to rutting of 3.2%, while the fatigue relative performance decreases by 2.1%.

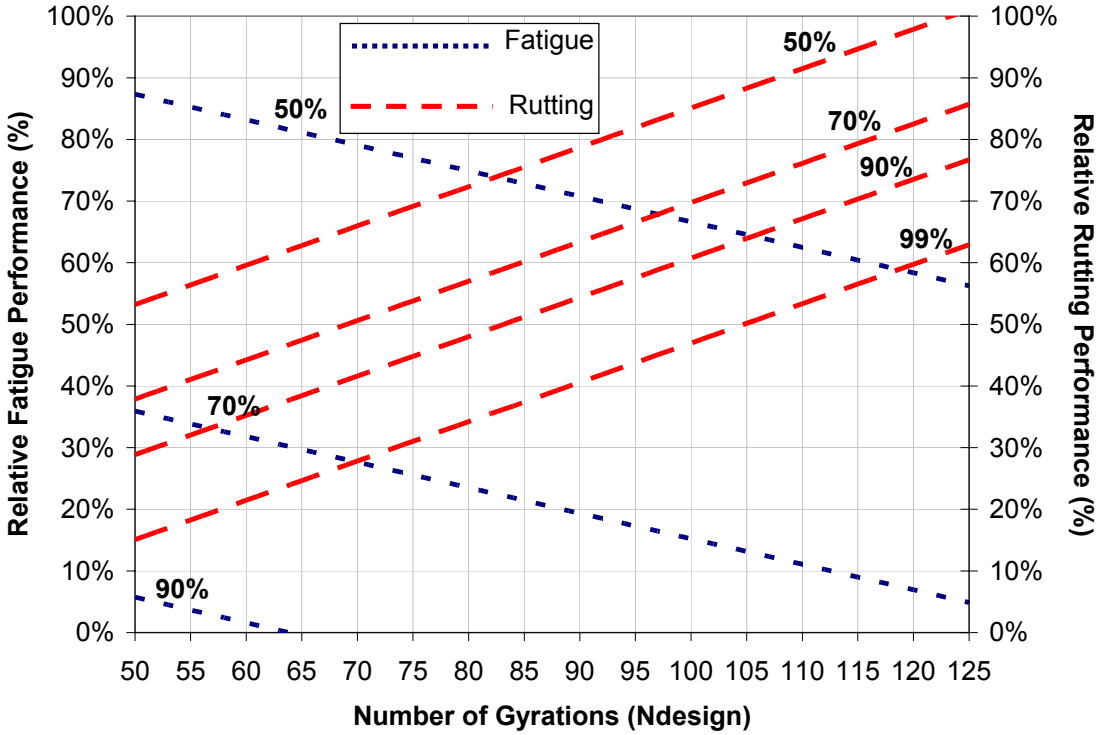

Figure 5.25: Reliability plots combining analyzed asphalt mixes

Since the 50% reliability performance curves are statistically estimated, additional levels of reliability can also be calculated for cases where more confidence is required. Accordingly, Figure 5.25 also includes the 60%, 70%, 80%, 90%, 95%, and 99% reliability performance curves. It can be observed from these curves that, for a given level of relative performance, changes in the number of gyrations or N_{design} result in an increase or decrease in reliability and, consequently, the probability that the desired relative performance will be achieved.

The relative performance in Figure 5.25 was determined based on rut depth at 20,000 wheel passes as the rutting performance indicator and number of cycles to failure (50% of initial stiffness) as the fatigue performance parameter. For the relative performance curves, combining all the asphalt mixes increases variability and is not recommended because it only reveals general trends. Consequently, reliability plots have been developed for each type of asphalt mix to increase the probability that the targeted relative performance is achieved at a given number of gyrations for a given asphalt mix.

Figure 5.26 shows the relative performance curves for the gravel SP-C mix with PG 76-22 binder. Of all the analyzed mixes, this one shows the highest rutting resistance and one of the highest levels of fatigue resistance. It can be concluded from the figure that the number of gyrations that optimize relative performance with 50% reliability (average) is 90. With this number of gyrations, a relative performance of 81% could be achieved. Note that for higher

reliability levels, a different number of gyrations will be optimal but lower relative performance can be expected. For example, if 70/70 reliability was used, the optimum gyrations would be 76 but the expected relative performance would decrease to 73% (refer to Fig 5.26).

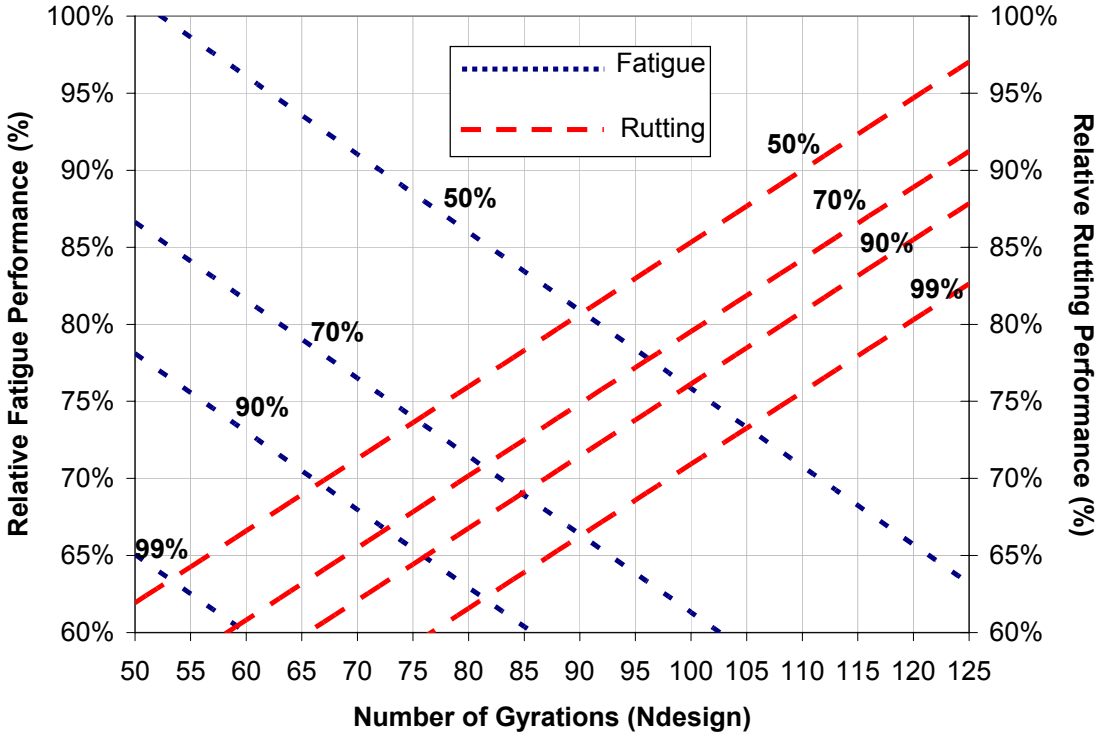

Figure 5.26: Reliability plots for SP-C gravel and PG 76-22 mix

Figure 5.27 presents the relative performance curves for the gravel SP-C mix with PG 70-22 binder; of all the analyzed mixes, this one shows the highest fatigue resistance. It is concluded from the 50% reliability curves that 63 gyrations optimize the relative performance in both rutting and fatigue for this mix type.

Figure 5.28 shows the relative performance curves for the limestone SP-D mix with PG 76-22 binder. In general, the limestone mixes exhibited poor rutting resistance and fatigue life. From the fatigue results obtained for the different samples generated at different numbers of gyrations, it was observed that this mix (for the particular range of analysis: 50–125 gyrations on the SPG) was unresponsive to changes in asphalt binder content. An analysis of variance confirmed that for this mix, the applied number of gyrations is not statistically significant. Because of this, the optimal number of gyrations at a reliability level of 50% is over 125 gyrations (owing to the fact that the fatigue resistance of the mix was not susceptible to changes in asphalt binder content). It should be emphasized that, based on the analysis of variance, the curves representing relative fatigue performance lack meaning but are shown in the figure for the sake of thoroughness.

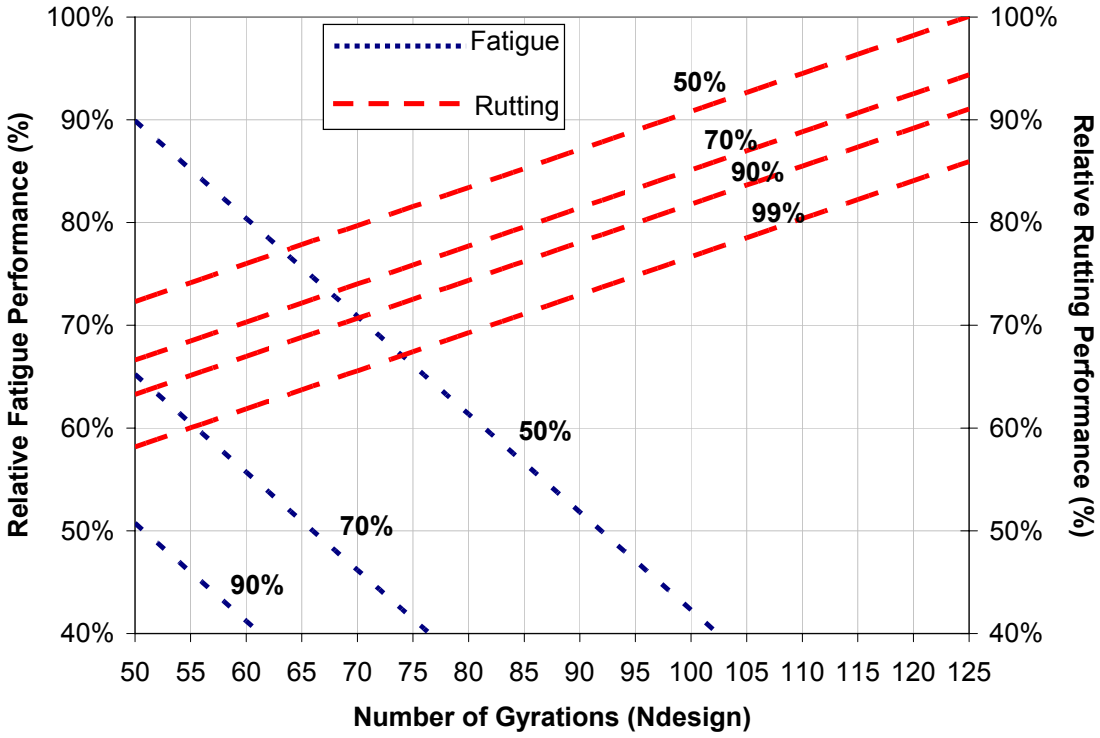

Figure 5.27: Reliability plots for SP-C gravel and PG 70-22 mix

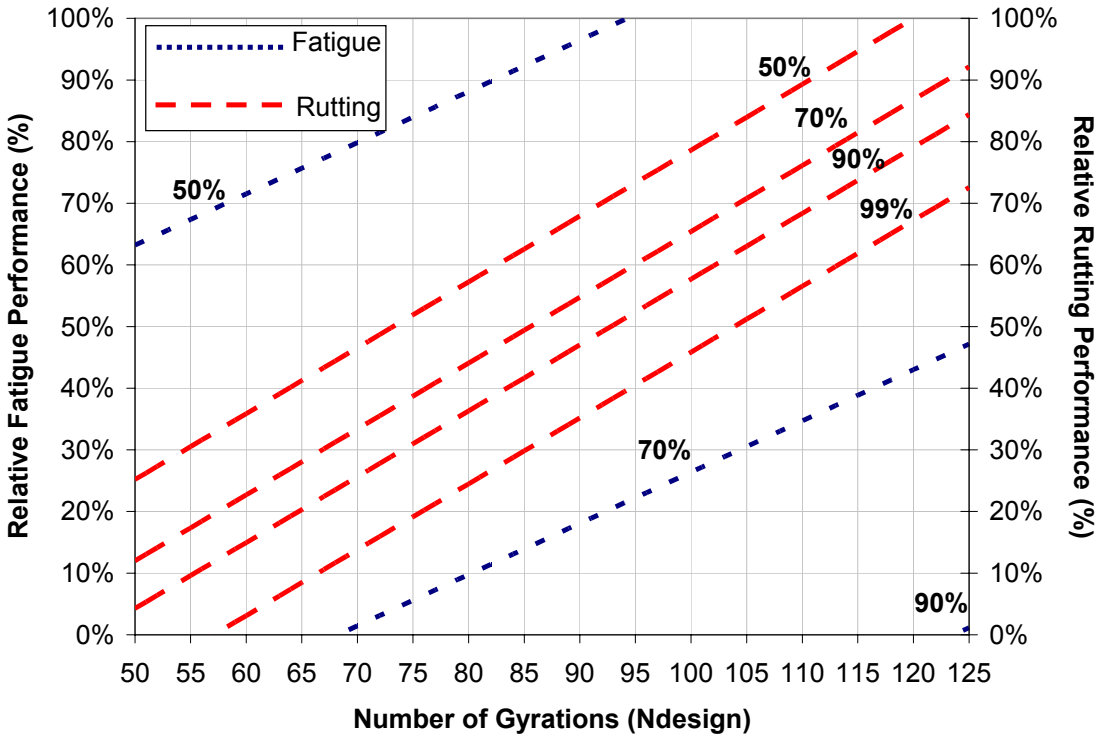

Figure 5.28: Reliability plots for SP-D limestone and PG 76-22 mix

Because the limestone SP-B mix with PG 64-22 did not meet the minimal rutting resistance requirements (maximum 12.5 mm rut depth in HWTD), the relative performance at 20,000 wheel passes could not be determined. Such cases emphasize the importance of parameters such as slope (Z) that are independent of testing protocols.

Following the same procedure as with the conventional parameters, reliability plots were developed using the slope ($Z_{fatigue}$ and Z_{rut}) values. Figure 5.29 shows the relative performance combining all the analyzed asphalt mixes. It can be calculated that the optimal relative performance is achieved at 97 gyrations on the SGC, which coincides with current Superpave specifications; however, the aggregation of the different asphalt mix types is not desirable for establishing N_{design} recommendations. It can also be determined that an average increment of five gyrations results in an increase in relative performance to rutting of 3.8%, whereas the fatigue relative performance decreases by 2.4%. These results agree with those obtained using the conventional rutting and fatigue parameters.

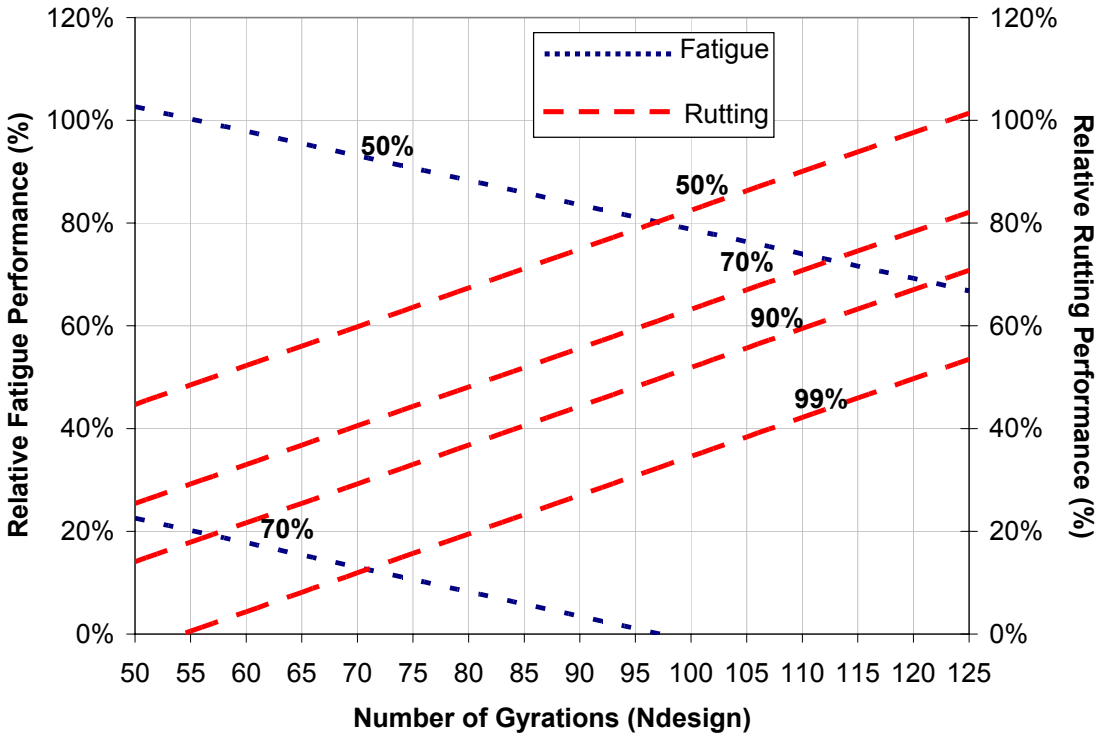

Figure 5.29: Reliability plots combining analyzed asphalt mixes based on Z parameter

Figure 5.30 shows the relative performance curves for the gravel SP-C mix with PG76-22 binder based on the slope (Z) parameter. It can be calculated that 85 gyrations on the SGC optimize the overall relative performance in the asphalt mix.

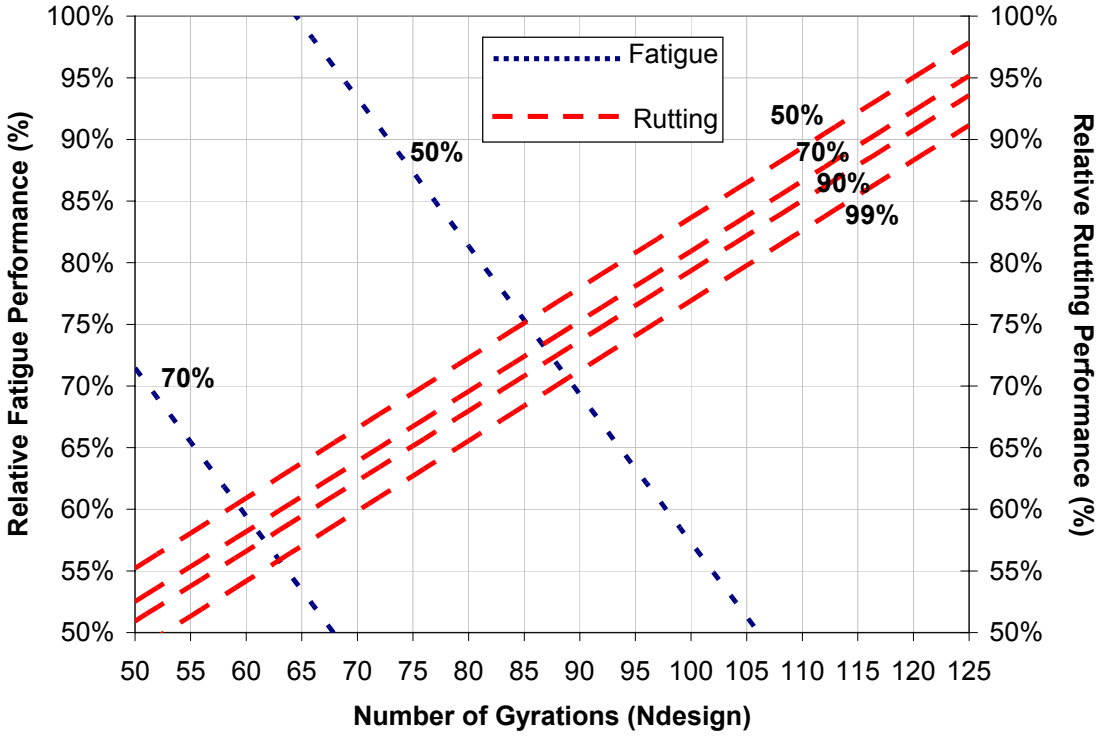

Figure 5.30: Reliability plots for SP-C gravel and PG 76-22 mix based on Z parameter

Figure 5.31 shows the relative performance curves for the gravel SP-C mix with PG 70-22 binder based on the Z parameter. It was determined with 50% reliability that 70 gyrations optimize the relative performance in both rutting and fatigue for this mix type.

Figure 5.32 shows the relative performance curves for the limestone SP-D mix with PG 76-22 binder based on the Z parameter. As was the case when the same mix was analyzed using the conventional parameters, the optimal number of gyrations at a reliability level of 50% is over 125 gyrations (again, this is due to the fact that the fatigue resistance of the mix was not susceptible to changes in asphalt binder content).

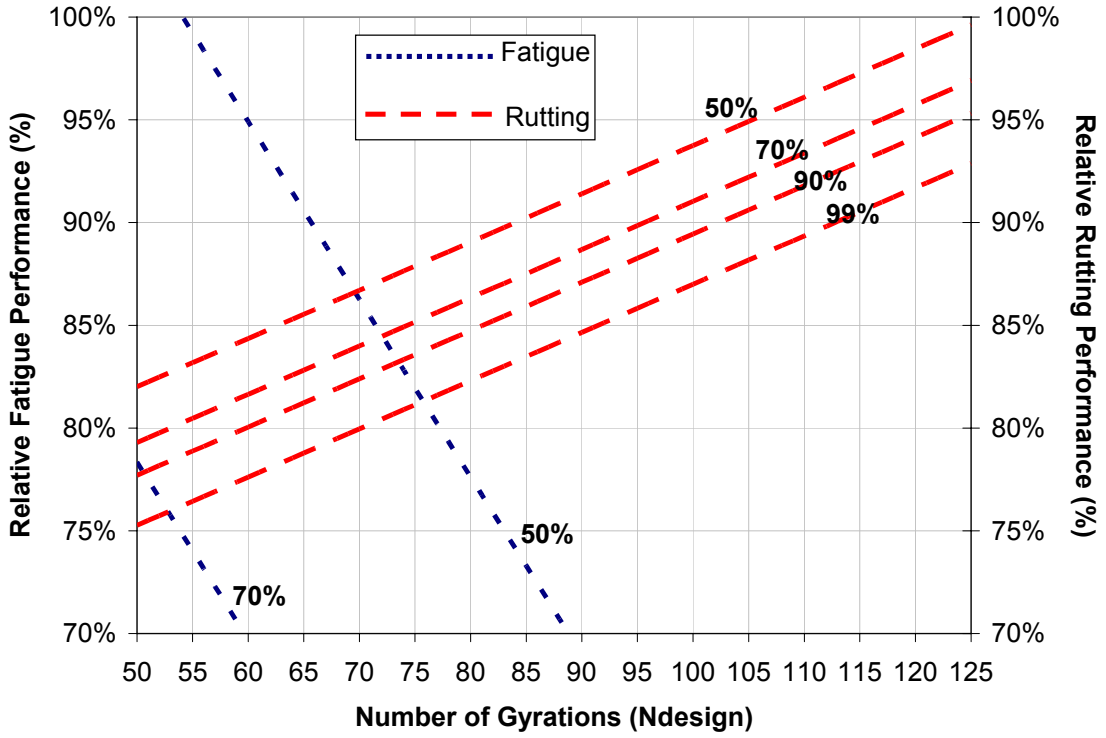

Figure 5.31: Reliability plots for SP-C gravel and PG 70-22 mix based on Z parameter

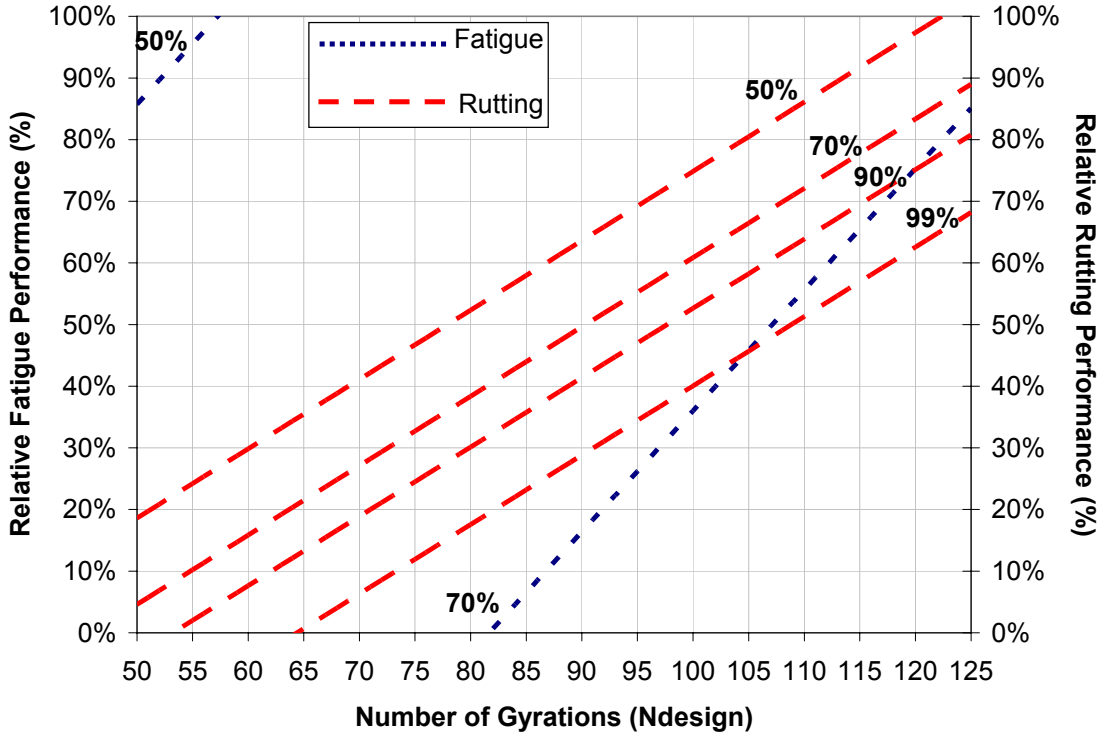

Figure 5.32: Reliability plots for SP-D limestone and PG 76-22 mix based on Z parameter

Based on the Z parameter, reliability plots can be determined for the limestone SP-B mix with PG 64-22 binder. Figure 5.33 shows the relative performance curves for this mix. It can be demonstrated that, on average, 90 gyrations on the SGC maximizes the relative performance to rutting and fatigue for this asphalt mix.

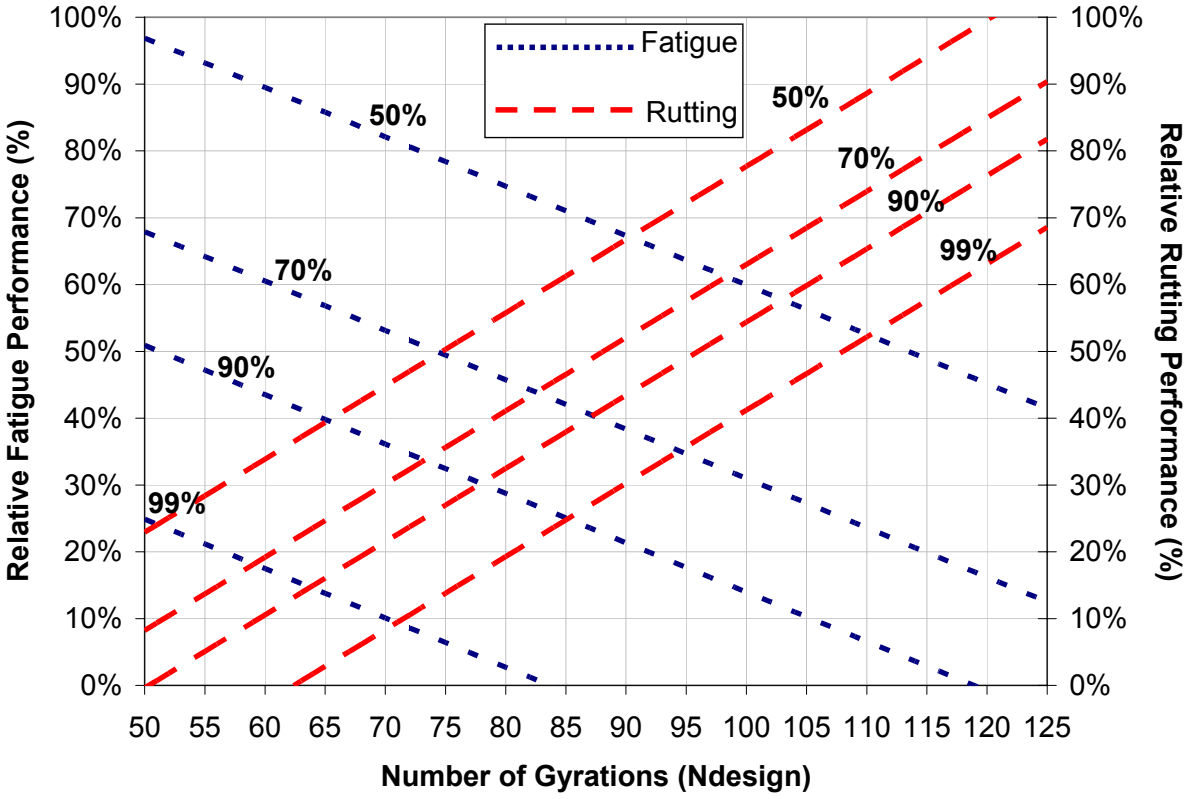

Figure 5.33: Reliability plots for SP-B limestone and PG 64-22 mix based on Z parameter

6. Summary and Conclusions

This study developed a methodology for quantifying the effects on expected rutting and fatigue performance of typical asphalt mixes designed at different N_{design} levels following the Superpave design method. Motivation for the research was based on the fact that mixes originally designed and built in Texas using 100 gyrations have performed well in terms of rutting but have shown premature signs of fatigue cracking. In addition, Texas has recently incorporated Hamburg Wheel Tracking Device (HWTD) specifications that result in highly rutting-resistant mixes that may have compromised fatigue cracking properties. In addition, as the asphalt binder decreases, the durability of the mixes may also be compromised.

6.1 Summary

Two possible methods for determining the modified number of design gyrations (based on Superpave design methodology) have been presented. Both are based on the concept of relative performance. The relative performance parameter, depending on how it is defined, corresponds to the performance at a specific level of compactive effort with respect to the performance of the asphalt mixture at a fixed level of compaction, or "base" performance. During development of the analysis method, it was observed that a convenient level of compactive effort to be selected as "base" level was the one that provided the highest performance within the experimental design (however, this depends on the levels of compaction that are being analyzed). The selection of "base" compactive effort has the added advantage that the relative performance of the asphalt mixture will be maximized at 100% because results are expressed relative to the performance of the best mix tested.

Once the relative performance was determined, two possible methods of analyzing and selecting a more appropriate level of compaction for design were presented. One method consists of the development of performance curves, which are different weighted combinations of the performance curves for rutting and fatigue cracking (as measured by the HWTD and the four-point bending beam (FPBB), respectively). This procedure allows for the selection of an appropriate or "optimal" number of design gyrations in order to achieve the desired performance, depending on how critical the resistance to fatigue and rutting is to a specific project.

The second method consists of assigning different confidence levels to the performance curves to both types of distress. The different confidence levels for both types of distress are then plotted in one figure. From the plots it is simple to determine the effect on rutting performance when a specific confidence level is assigned to a desired level of relative fatigue performance. The opposite problem (effect on fatigue resistance given a specific level of rutting resistance) can be analyzed with the same ease. This second method also allows for the selection of a range of design gyration numbers that in turn provides an acceptable range of both rutting and fatigue resistance levels.

6.2 Conclusions and Recommendations

The following conclusions and recommendations are based on the asphalt mixtures tested and analyzed in this study, and were established as a result of the research project. Implementation of these recommendations may result in Superpave mixes of improved fatigue resistance and durability.

- Both the PG grade and the content of the asphalt binder have a significant effect on rutting resistance (as measured by the HWTD). However, the aggregate source did not show a significant effect on rutting resistance at the 10% level of significance.
- Based on the Indirect Tensile Strength (ITS) results and the analyzed set of asphalt mixtures, only the PG grade of the binder has a significant effect on the ITS of the asphalt mixtures (at the 10% level of significance). However, the ITS was relatively uniform for each specific mix (oscillating in a range of 20 to 30 psi) and thus does not appear to be a good indicator of expected fatigue performance.
- In contrast to rutting resistance, fatigue resistance (as measured by the FPBB apparatus) is significantly affected by both binder PG grade and content, as well as by aggregate source and gradation, all at the 10% level of significance.
- Based on the asphalt mixtures tested and analyzed in this study, the current indicators of rutting resistance (deformation at 10,000, 15,000 or 20,000 wheel passes) and fatigue resistance (number of cycles to failure, defined as reduction in stiffness to 50% of initial stiffness) are not the best indicators of rutting or fatigue resistance, respectively, because they are highly variable and may underestimate the resistance of the asphalt mixtures to both types of distress.
- The slope parameter Z better characterizes the asphalt mixture in both the rutting and fatigue cases, because it is based not only on the measurement at a specific load or wheel pass cycle, but also on the rutting or fatigue history of the asphalt mixture. Slope parameter Z is also a more consistent indicator because it uses more of the information recorded during the HWTD or FPBB test. A small slope (closer to zero) indicates higher rutting or fatigue resistance, whereas a high slope (more negative) indicates an asphalt mixture that is highly susceptible to rutting or fatigue.
- For Texas conditions, the number of design gyrations using the Superpave Gyratory Compactor (SGC) (N_{design}) can be significantly reduced in order to improve the fatigue life of the asphalt mixes, without significantly affecting their rutting performance. This reduction in the compaction effort has the additional benefit of potentially increasing the mix durability in the field. It is unacceptable for relatively new (5–7 year old) pavements to be showing early signs of fatigue cracking. This was confirmed using the relative performance-based approach as applied to two performance-related tests such as the HWTD and the bending beam.
- The fact that Superpave mixes designed in Texas have very good rutting resistance but relatively low fatigue resistance was confirmed in this study using the relative performance approach. At 100 gyrations—the current Superpave specification—the average relative performance of all mixes evaluated is high (85%–95%) when rutting is considered; however, the relative performance in terms of fatigue is typically low (45%–75%).
- From the average relative performance of all the mixes that were tested, it was found that 75 to 85 gyrations on the SGC generally optimize the performance of the asphalt mixes.

- In order to account for different traffic levels and environmental conditions, the different weighted relative performance curves can be used to determine an asphalt mix that will perform adequately for each specific project and circumstance. Based on the limited testing conducted in this study, interim guidelines have been developed in this regard. It should be noted that these guidelines should be updated by testing more mixes and monitoring their field performance.
- The level of reliability should be selected based on previous experience and performance of specific asphalt mixes and the requirements of the specific project.
- The concepts of relative performance and different confidence levels or percentiles should be further evaluated and integrated with environmental and traffic data to calibrate the proposed approach to specific regions. For example, in the Panhandle region, curves higher than 50% in terms of cracking should be used, while the curve for 50% rutting is acceptable. On the opposite side, in the Houston district, for example, curves of 50% in terms of cracking could be used in conjunction with a much higher rutting percentage, e.g., 80%. If the facility is to be subjected to heavy, slow moving loads, this could be further increased to 95%.

6.3 Future Research

It should be noted that the recommendations presented are based on the testing of a limited combination of asphalt binders and aggregates. For this reason, it is recommended that a similar analysis be performed on those asphalt mixes that are most commonly used throughout Texas so that more accurate N_{design} recommendations can be developed for specific aggregate and binder combinations under specific environmental conditions.

Currently, TxDOT is in the process of developing a database that will contain mix design and construction information linked to pavement performance data contained in the TxDOT Pavement Management Information System (PMIS). The data in this database will serve for final calibration and validation of the proposed method.

Although accounting for traffic should be included in this approach and should be the subject of future studies, an increased level of reliability will account for higher design traffic levels as well as severe environmental surroundings. The level of reliability should be selected based on previous experience and performance of specific asphalt mixes.

It is recommended that TxDOT's Flexible Pavement Branch of the Construction Division embark on the development of a database of HWTD test results in conjunction with FPBB tests carried out on the same HMA mixtures. These mixtures could be plant-produced mixes corresponding to ongoing construction projects. With such a database, TxDOT will own a unique library of performance-related information that will be invaluable for making informed decisions on mix type selection and performance.

References

Anderson, M.R., Bosley, R.D., and Creamer, P. A. (1995), Quality Management of HMA Construction Using Superpave Equipment: A Case Study, Transportation Research Record 1513, Transportation Research Board, Washington, D.C.

Anderson, M. R., Cominsky, R. J. and Killingsworth, B. M. (1998), Sensitivity of Superpave Mixture Tests to Changes in Mixture Components, Journal of the Association of Asphalt Paving Technologists, Vol. 67.

Aschenbrenner, T. and McKean, C. (1994), Factors that effect the voids in the mineral aggregate of hot-mix asphalt, Transportation Research Record 1469, Transportation Research Board, Washington, D.C.

Austroads (1997), Selection and Design of Asphalt Mixes: Australian provisional Guide, APRG Report No. 18, Austroads and Australian Road Research Board, Sydney, Australia.

Bahia, H. U, Frieme, T. P., Peterson, P. A., Russell, J. S. and Poehnelt, B. (1998), Optimization of Constructability and Resistance to Traffic, A New Design Approach for HMA Using the Superpave Compactor, Journal of the Association of Asphalt Paving Technologists, Vol. 67.

Blankenship, P. B. (1994), Gyratory Compaction Characteristics: Relation to Service Densities of Asphalt Mixtures, Master's Thesis, University of Kentucky, Kentucky.

Blankenship, P. B., Mahboub, C. K. and Huber, G. A. (1994), Rational Method for Laboratory Compaction of Hot Mix Asphalt, Transportation Research Record 1454, Transportation Research Board, Washington, D.C.

Bright, R., Steed, B., Steele, J. and Justice A. (1967), The Effect of Viscosity of Asphalt on Properties of Bituminous Wearing Surface Mixtures, Proceedings of the Association of Asphalt Paving Technologists, Vol. 36.

Brown, E. R., Hanson, I. R. and Mallick, R. B. (1996), An Evaluation of SHRP Gyratory Compaction of HMA, Paper presented at the Annual Meeting of the Transportation Research Board, Washington, D.C.

Brown, E. R. and Cross, S. A. (1991), Comparison of Laboratory and Field Density of Asphalt Mixes, Transportation Research Record 1300, National Research Council, Washington, D.C.

Brown, E. R. and Mallick, R. B. (1998), An Initial Evaluation of the N-design Superpave Gyratory Compactor, Proceedings of the Association of Asphalt Paving Technologists, Vol. 67.

Brown, E. R. and Buchanan, M. S. (2001a), Verification of the gyrations in the NDESIGN Table, NCHRP 9-9 (1), National Cooperative Highway Research Program, Transportation Research Board, National Research Council, Washington, D.C.

Brown, E. R., Khandal, P. S. and Zhang, J. (2001b), Performance Testing for Hot Mix Asphalt, NCAT Report 01-05, National Center for Asphalt Technology, Auburn, Alabama.

Butcher, M. (1998), Determining Gyratory Compaction Characteristics using Servopac Gyratory Compactor, Transportation Research Record 1630, Transportation Research Board, Washington, D.C.

Button, J. W., Chowdhury, A. and Bhasin, A. (2004), Design of TxDOT Asphalt Mixtures using the Superpave Gyratory Compactor, Project P0-4203, Texas Department of Transportation, Austin, Texas.

Campen, W. H., Smith, J. R., Erickson, L. G. and Mertz, L. R. (1960), The Effect of Traffic on the Density of Bituminous Paving Mixtures, Proceedings of the Association of Asphalt Paving Technologists, Vol. 29.

Cominsky, R., Leahy, R. B. and Harrigan, E. T. (1994a), Level One Mix design: Materials Selection, Compaction, and Conditioning, SHRP A-408, Strategic Highway Research Program, National Research Council, Washington, D.C.

Cominsky, R. J., Huber, G. A., Kennedy, T. W. and Anderson, M. (1994b), The Superpave Mix Design Manual for New Construction and Overlays, SHRP A-407, Strategic Highway Research Program, National Research Council, Washington, D.C.

Coree, B. J. (1998), HMA volumetrics revisited - a new paradigm, Presented to the Annual meeting, Transportation Research Board, Washington, D.C.

Coree, B. J. and Hislop, W. P. (1999), The difficult nature of minimum VMA: A historical perspective, Presented to the Annual meeting, Transportation Research Board, Washington, D.C.

Corté, J. F. and Serfass, J. P. (2000), The French Approach to Asphalt Mixtures Design: A Performance-Related System of Specifications, Association of Asphalt Paving Technologists, Vol. 69.

Dillard, J. H. (1955), Comparison of Density of Marshall Specimens and Pavement Cores, Proceedings of the Association of Asphalt Paving Technologists, Vol. 24.

Epps, J. A, Gallaway, M. and Scott, W. W. (1970), Long Term Compaction of Asphalt Concrete Pavements, Highway Research Record 313, National Research Council, Washington, D.C.

Epps, A. L., and Hand, A. J. (2000), Coarse Superpave Mixture Sensitivity, TRB paper presented at 79th Annual Meeting, TRB, Washington, D.C.

Field, F. (1958), Correlation of Laboratory Compaction with Field Compaction of Asphaltic Concrete Pavements, Proceedings of the Third Annual Conference of the Canadian Technical Asphalt Association, Vol. 3.

Forstie, D. A. and Corum, D. K. (1997), Determination of Key Gyratory Compaction Points for Superpave Mix Design in Arizona, ASTM Special Technical Publication, Vol. 1322, ASTM, Philadelphia.

Foster, C. R (1993), Densification of Asphalt Pavements by Traffic, Proceedings of the Conference on Airport Pavement Innovation, American Society of Civil Engineers.

Galloway, B. M. (1960), Laboratory and Field densities of Hot Mix Asphaltic Concrete in Texas, Highway Research Board Bulletin 251, Asphaltic Concrete Construction-Field and Laboratory Studies, National Academy of Sciences, Washington, D.C.

Gichaga, F. J. (1982), Behaviour of Flexible Road Pavements Under Tropical Climates, Proceedings of the 5th International Conference on the Structural Design of Asphalt Pavements, Delft University of Technology, Vol. 1.

Graham, M. D., Burnett, W. C., Thomas, J. T. and W. C. Dixon (1965), Pavement Density – What Influences It, Proceedings of the Association of Asphalt Paving Technologists, Vol. 34.

Hafez, I. H and Witczak, M. W. (1995), Comparison of Marshall and Superpave Level I Mix Design for Asphalt Mixes, Transportation Research Record 1492, Transportation Research Board, Washington, D.C.

Hanson, D. I., Mallick, R. B. and Brown, E. R. (1994), Five Year Evaluation of HMA Properties at the AAMAS Test Sections, Transportation Research Record 1454, National Research Council, Washington, D.C.

Hinrichsen, J. A. and Heggen, J. (1996), Minimum voids in mineral aggregate in hot-mix asphalt based on gradation and volumetric properties. Transportation Research Record 1545, Transportation Research Board, Washington, D.C.

Hughes, C. S. and Maupin, G. W. (1987), Experimental Bituminous Mixes to Minimize Pavement Rutting, Proceedings of the Association of Asphalt Paving Technologists, Vol. 56.

Kandhal, P. S., Foo, K. Y. and Mallick, R. B (1998a), A critical review of VMA requirements in Superpave, NCAT Report No. 98-1, National Center for Asphalt Technology, Auburn, Alabama.

Kandhal, P. S., Foo, K. Y. and Mallick, R. B. (1998b), Critical review of voids in mineral aggregate requirements in Superpave, Transportation Research Record 1609, Transportation Research Board, Washington, D.C.

Lefebvre, J. (1957), Recent investigations of the design of asphalt paving mixtures, Proceedings of the Association of Asphalt Paving Technologists, Vol. 26.

Mallick, R. B., Buchanan, M. S., Brown, E. R. and Huner, M. H. (1998), Evaluation of Superpave Gyratory Compaction of Hot Mix Asphalt, Transportation Research Record 1630, Transportation Research Board, Washington, D.C.

Mallick, R. B., Buchanan, M. S., Kandhal, P. S. Bradbury, R. L. and McClay, W. (2000), A rational approach of specifying the voids in mineral aggregate (VMA) for dense graded hot mix asphalt, Presented at 79th Annual meeting of the Transportation Research Board, Washington, D.C.

Masad, E. A. (2005), Aggregate Imaging System (AIMS): Basics and Applications, TTI Report No. 5-1707-01, Texas Transportation Institute, College Station, Texas

McGennis, R. B., Anderson, R. M., Kennedy, T. W. and Solaimanian, M. (1994), Superpave Asphalt Mixture Design and Analysis, National Asphalt Training Center, Federal Highway Administration, FHWA-SA-95-003, Washington, D.C.

McGennis, R. B., Anderson, M. R., Perdomo, D. and Turner, P. (1996), Issues Pertaining to the Use of Superpave Gyratory Compactor, Transportation Research Record 1543, Transportation Research Board, Washington, D.C.

Moutier, F. (1993), The French bituminous mix design method, Fifth Eurobitume Congress, Stockholm.

NCHRP (1999), Superpave gyratory compaction guidelines, Research Results Digest, National Cooperative Highway Research Program, Washington, D.C.

Newcomb, D. E., Olson, R., Gardiner, M. and Teig, J. (1997), Traffic Densification of Asphalt Concrete Pavements, Transportation Research Record 1575, National Research Council, Washington, D.C.

Palmer, R. K. and Thomas, J. J. (1968), Pavement Density – How it Changes, Proceedings of the Association of Asphalt Paving Technologists, Vol. 37.

Parker, F., Hossain, M. S. and Song, J., (2000), Analysis of Quality Control / Quality Assurance Data for Superpave Mixes, Paper presented at 79th Annual Meeting, Transportation Research Board, Washington, D.C.

Paterson, W. D. O., Williman, A. and Pollard, J. S. (1974), Traffic Compaction of Asphalt Surfacings, National Institute for Road Research, Pretoria, South Africa

Peterson, R. L., Mahboub, K. C., Anderson, R. M, Masad, E. and Tashman, L. (2003), Superpave Laboratory Compaction Versus Field Compaction, Transportation Research Record 1832, Transportation Research Board, Washington, D.C.

Prowell, B. D. and Haddock, J. E. (2002), Superpave for low volume roads and base mixtures, Association of Asphalt Paving Technologists.

Prowell, B. D., Brown E. R. and Huner, M. H. (2003), In-place densification of hot mix asphalt and verification of Superpave N(design), Third International Conference on the Design of Asphalt Pavements (ISAP).

Prowell B. D. (2005), Progress Report presented at the NCAT Applications Steering Committee, NCAT Test Track Conference, Auburn, Alabama.

Serafin, P. J., Kole, L. L. and Chritz, A. P. (1967), Michigan Bituminous Experimental Road: Final Report, Proceedings of the Association of Asphalt Paving Technologists, Vol. 36.

Vavrik, W. R. and Carpenter, S. H. (1998), Calculating Voids at a Specified Number of Gyrations in the Superpave Gyratory Compactor, Transportation Research Record 1630, Transportation Research Board, Washington, D.C.

Wright, D. F. H. and A. Burgers (1984), Traffic Compaction of Bituminous Concrete Surfacings, Proceedings of the Fourth Conference on Asphalt Pavements for Southern Africa, Cape Town, South Africa.

Appendix A. Method for Calculating the Slope (Z) Parameter

Because the slope (Z) of the secondary phase of either the fatigue or the rutting curve has been proposed as an alternative parameter to characterize fatigue and rutting, a proposed method for determining the slope is shown in this appendix.

The method consists of analyzing the differences between either the fatigue or permanent deformation curve and a line that spans from the initial stiffness or deformation (first recorded measurement during the four point bending beam (FPBB) or Hamburg Wheel Tracking Device (HWTD) test, respectively). Figure A1 shows the differences analysis concept, assuming a continuous response variable y_i. It can be observed from the figure that there are three distinctly separate phases to describe the performance of the asphalt mix. Because the data is continuous, we can define a line from the initial response value (x_1,y_1) to the final response value (x_n,y_n) as,

$$\hat{y} = \frac{x_n - x_1}{y_n - y_1} x_i \qquad \text{Eq. A1}$$

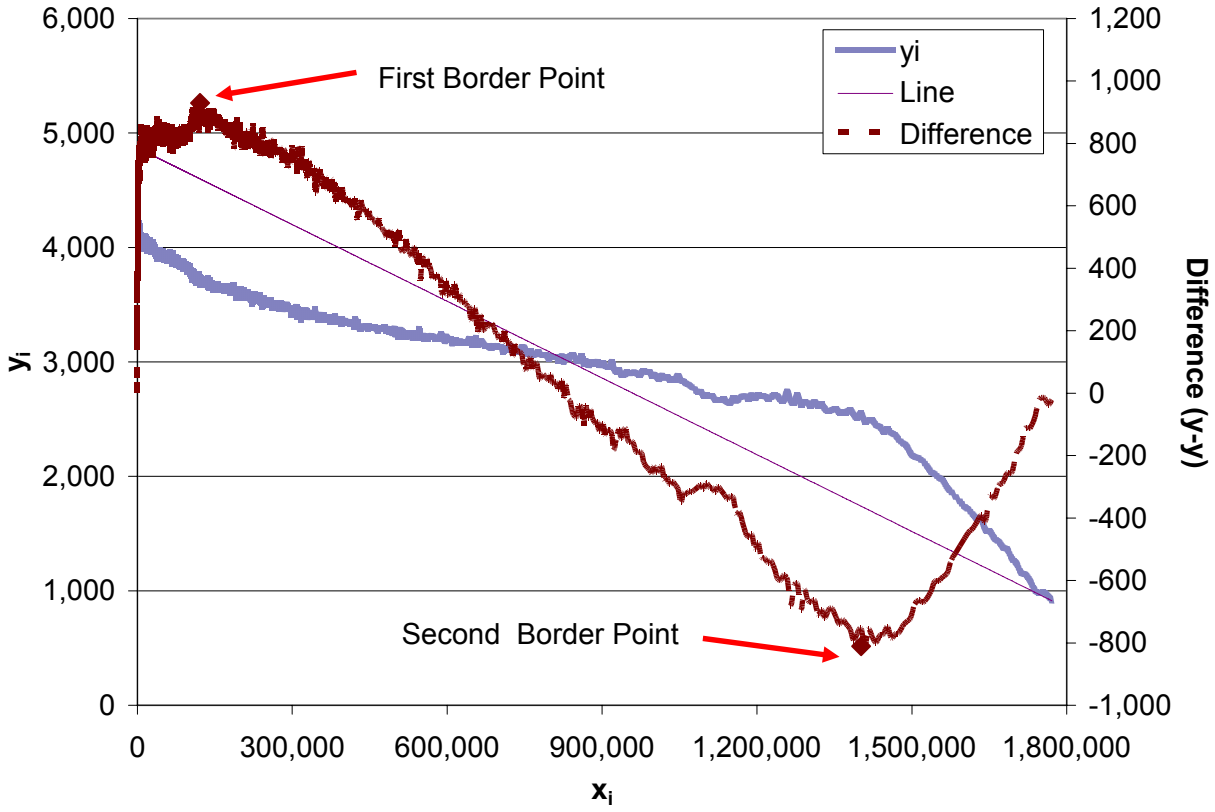

Figure A1. Concept of differences approach to determine slope

In Figure A1, the dashed line represents the difference between the actual performance data and the calculated line ($y-\hat{y}$). Finally, the boundary points can be identified where the difference $y-\hat{y}$ is maximum or minimum (highest positive and negative values). The first boundary point corresponds to the cycle or wheel pass where the initial performance phase stops and the secondary phase starts. Similarly, the second boundary point corresponds to the cycle or wheel pass where the secondary performance phase stops and the tertiary phase starts. In other words, the first and second boundary points correspond to the limits of the secondary performance phase.

Having determined the first and second boundary points, a simple linear regression analysis of the performance data between two boundary points is carried out to determine the slope of the secondary phase of either the fatigue or the rutting curve as measured by the four point beam loading or the HWTD test, respectively.

Appendix B. Guidelines for Adjusting N_{design} as a Function of Traffic and Environment

Since the introduction of the Superpave methodology, the selection of N_{design} has been a function of temperature and traffic. Higher air temperatures require higher N_{design}. Similarly, higher traffic volumes require higher N_{design}.

Based on a historical monthly weather record for Texas (data obtained from the Department of State website), the state's 254 counties have been classified based on the monthly average high temperature and the monthly average low temperature. Additionally, in order to get a better perspective on the high-low temperature contrasts, the counties have also been classified based on the temperature gap or temperature differential between average high temperature and average low temperature. The greater the gap, the more extreme environmental conditions the asphalt mix is subjected to.

Figure B1 shows the high temperature distribution of Texas counties. It can be observed that the southern counties present the highest average high temperatures, while the northern counties show the lowest average high temperatures. Figure B2 shows the low temperature distribution of Texas counties. It can be seen that the southeastern counties present the highest average low temperatures, while the northwestern counties show the lowest average low temperatures.

Figure B3 shows the temperature differential between the monthly average high temperatures and average low temperatures. It is clear that the northwestern counties experience the most extreme environmental conditions.

Based on the percentile classification of average high and low temperatures for the 254 Texas counties and taking into consideration the conclusions of the research project, where the effect of changes in N_{design} were quantified, the guidelines for modifying N_{design} based on the high and low temperature distribution of the Texas counties are presented on Figures B4 and B5.

Finally, combining the effect of changes in the number of design gyrations based on the high and low weather temperatures and considering the effect of traffic volume, the guidelines for modifying the number of design gyrations for the different counties in Texas are shown in Figure B6, based on a "base" N_{design} of 85 gyrations. It should be noted that the guidelines are based on a limited set of analyzed samples, and that local experience should always be considered. The average recommendations per district are shown in Figure B7.

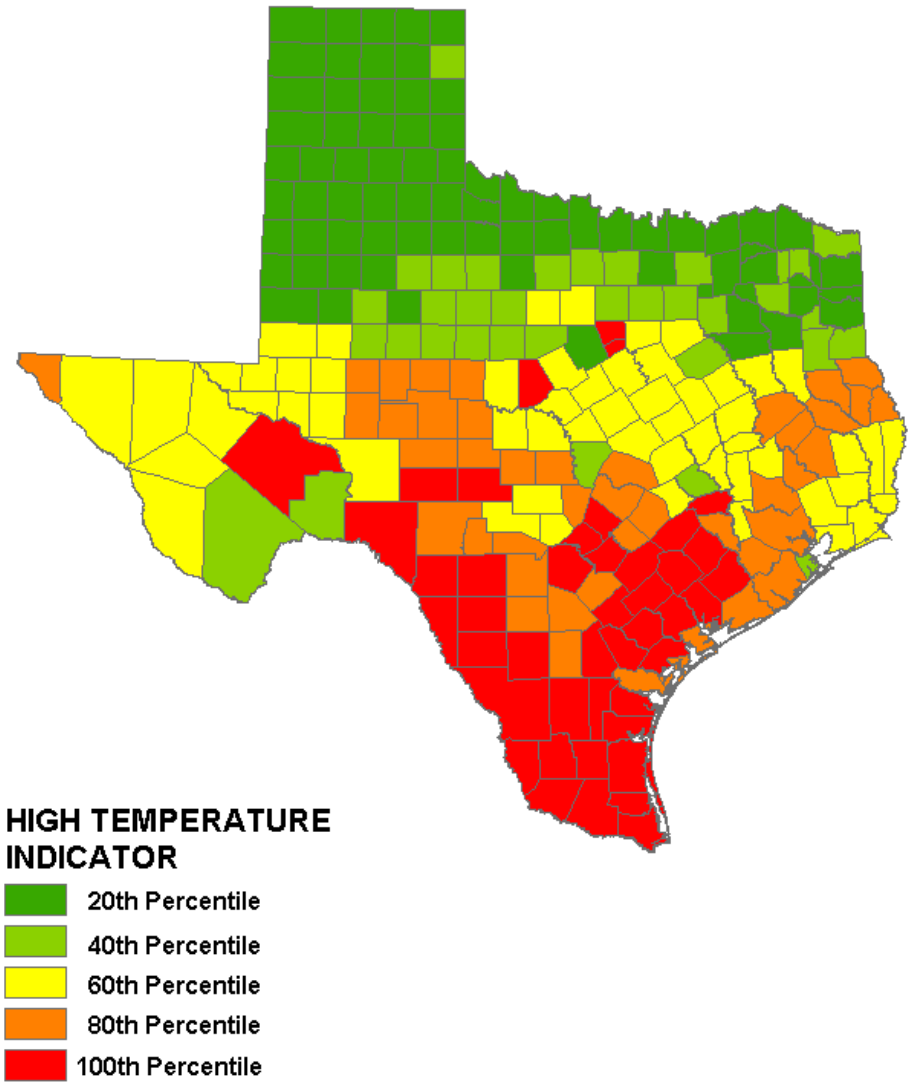

Figure B1. High temperature distribution for Texas

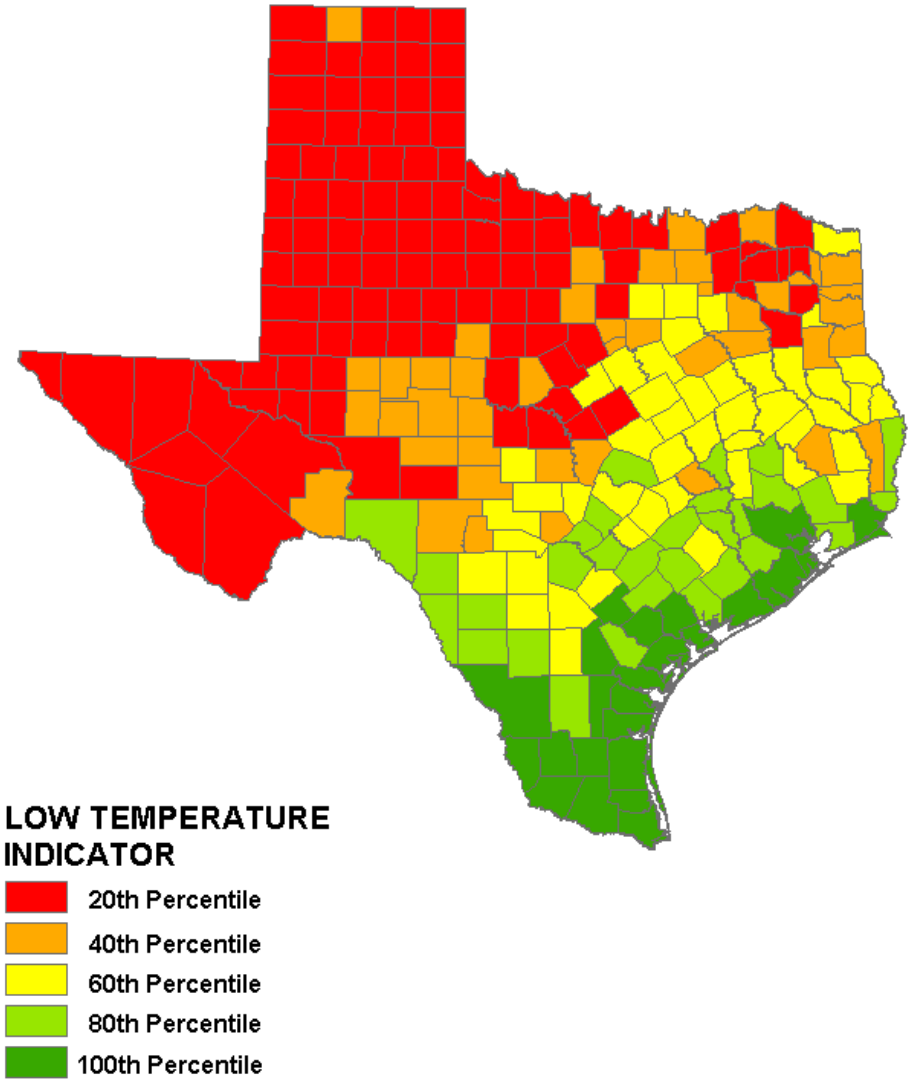

Figure B2. Low temperature distribution for Texas

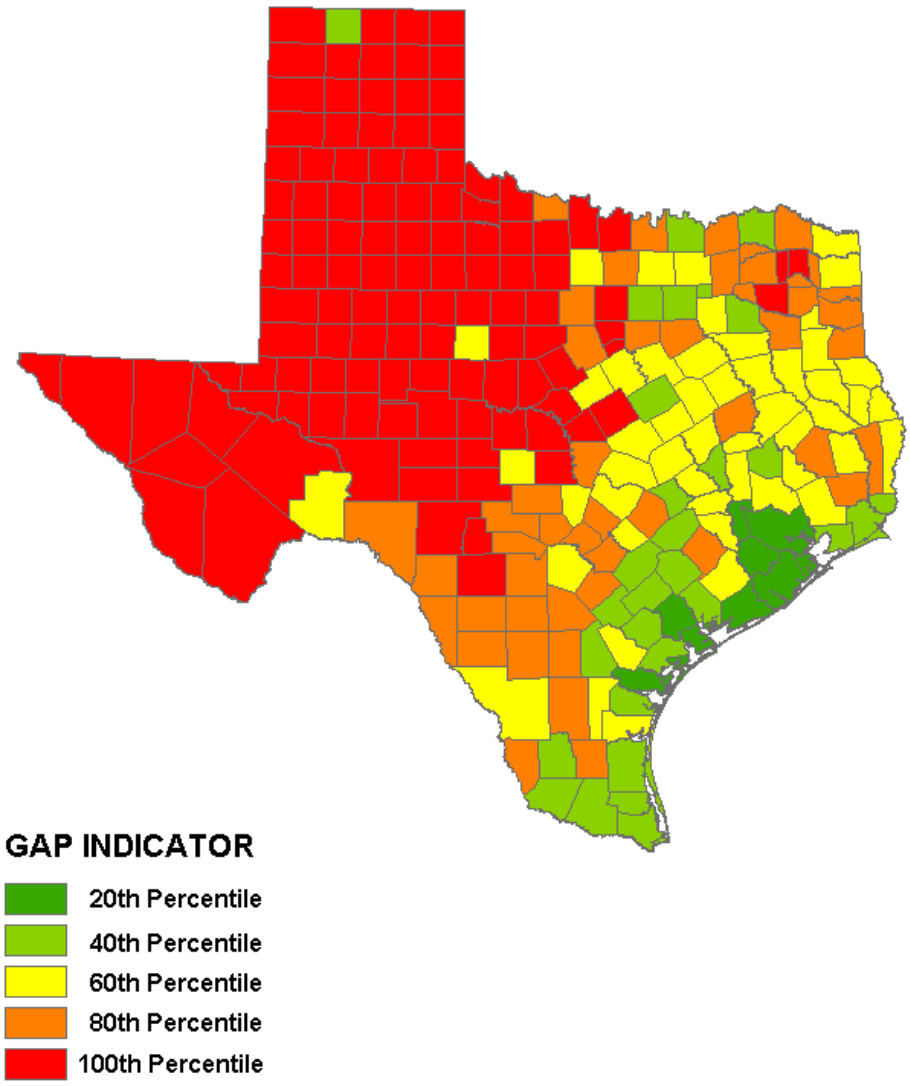

Figure B3. High-low temperature differential distribution for Texas

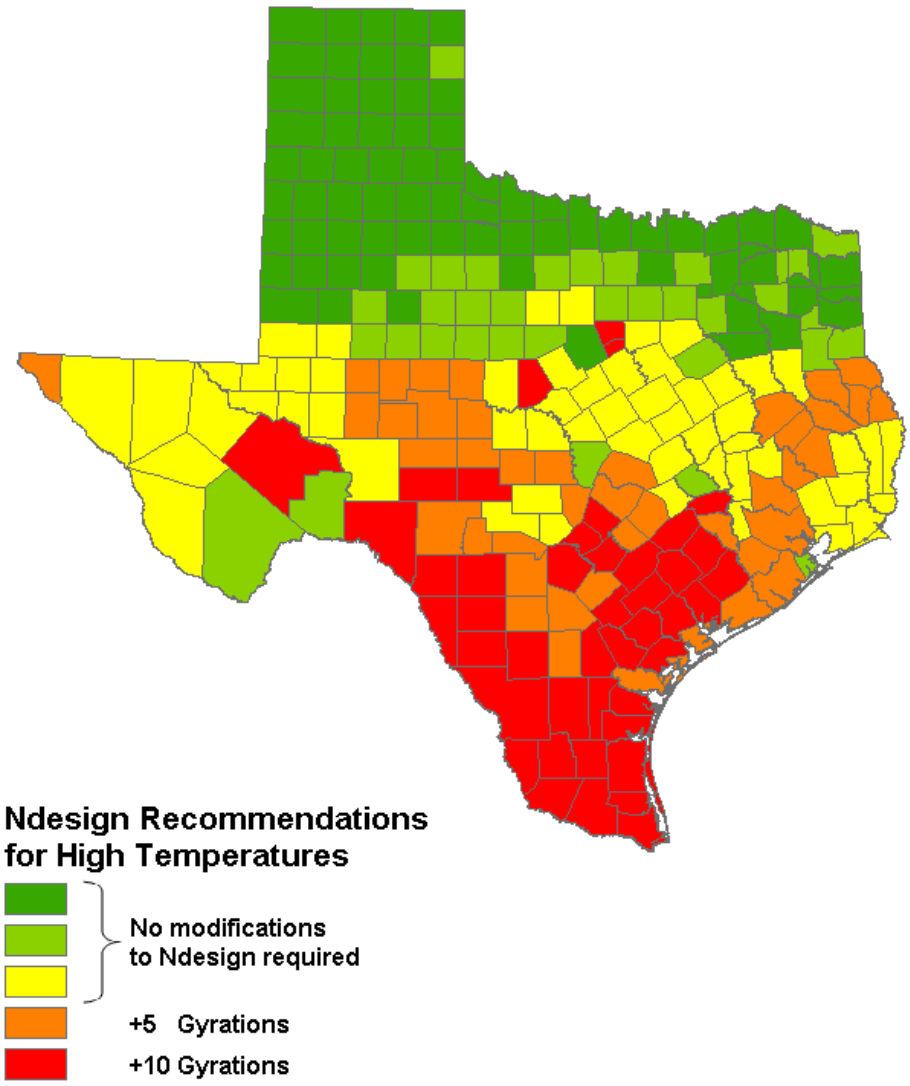

Figure B4. High temperature N_{design} recommendations

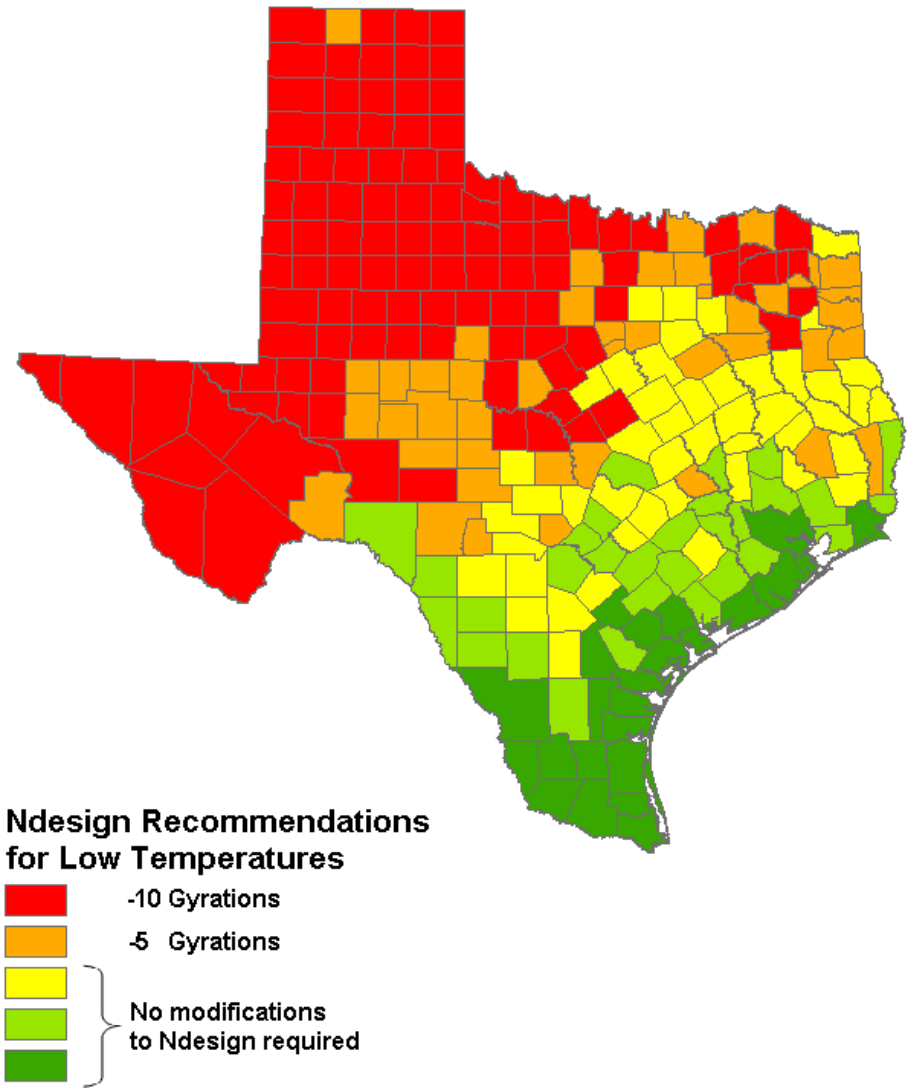

Figure B5. Low temperature N_{design} recommendations

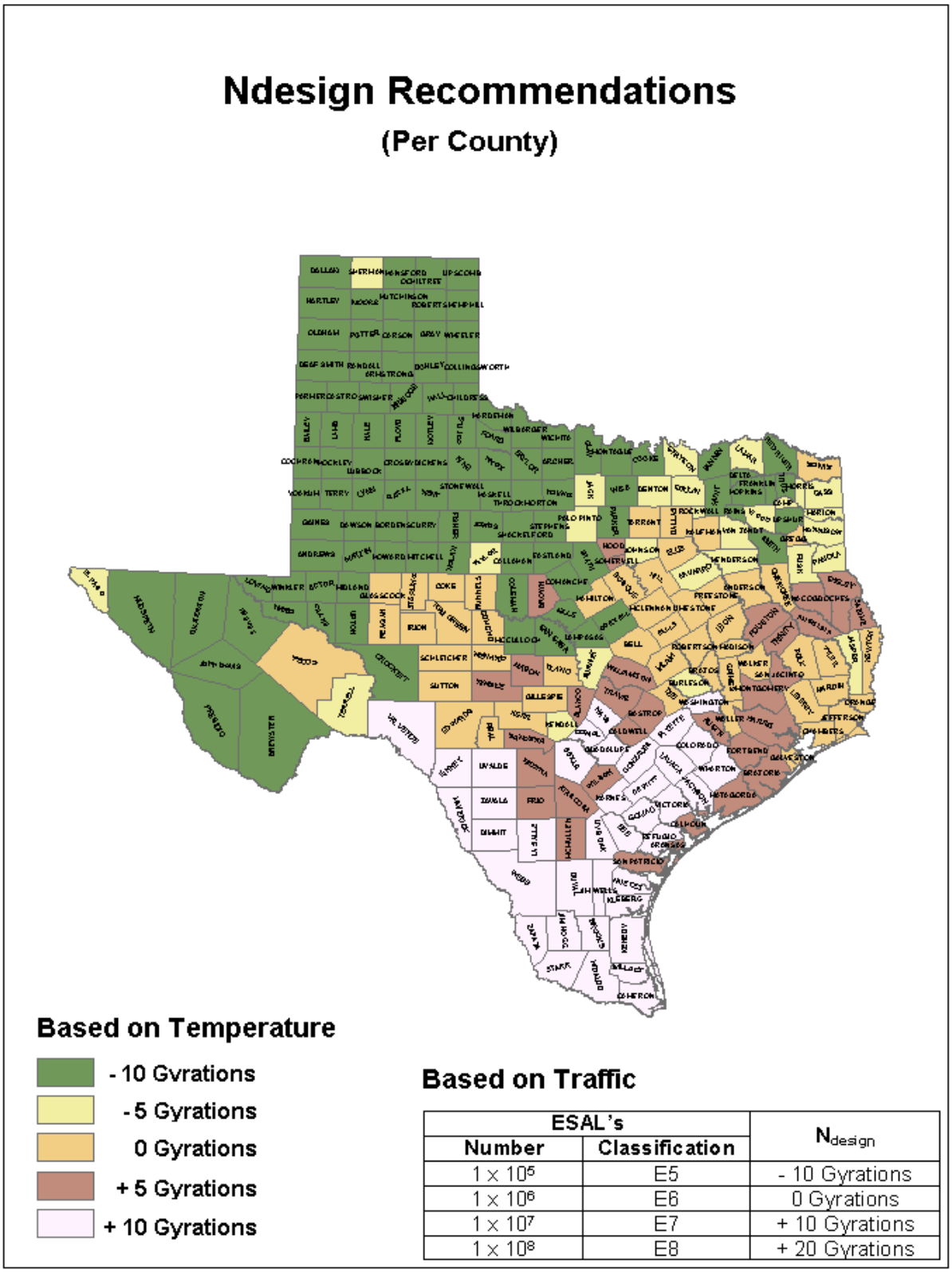

Figure B6. Guidelines for selection of N_{design} for Texas per county (based on temperature and traffic volume)

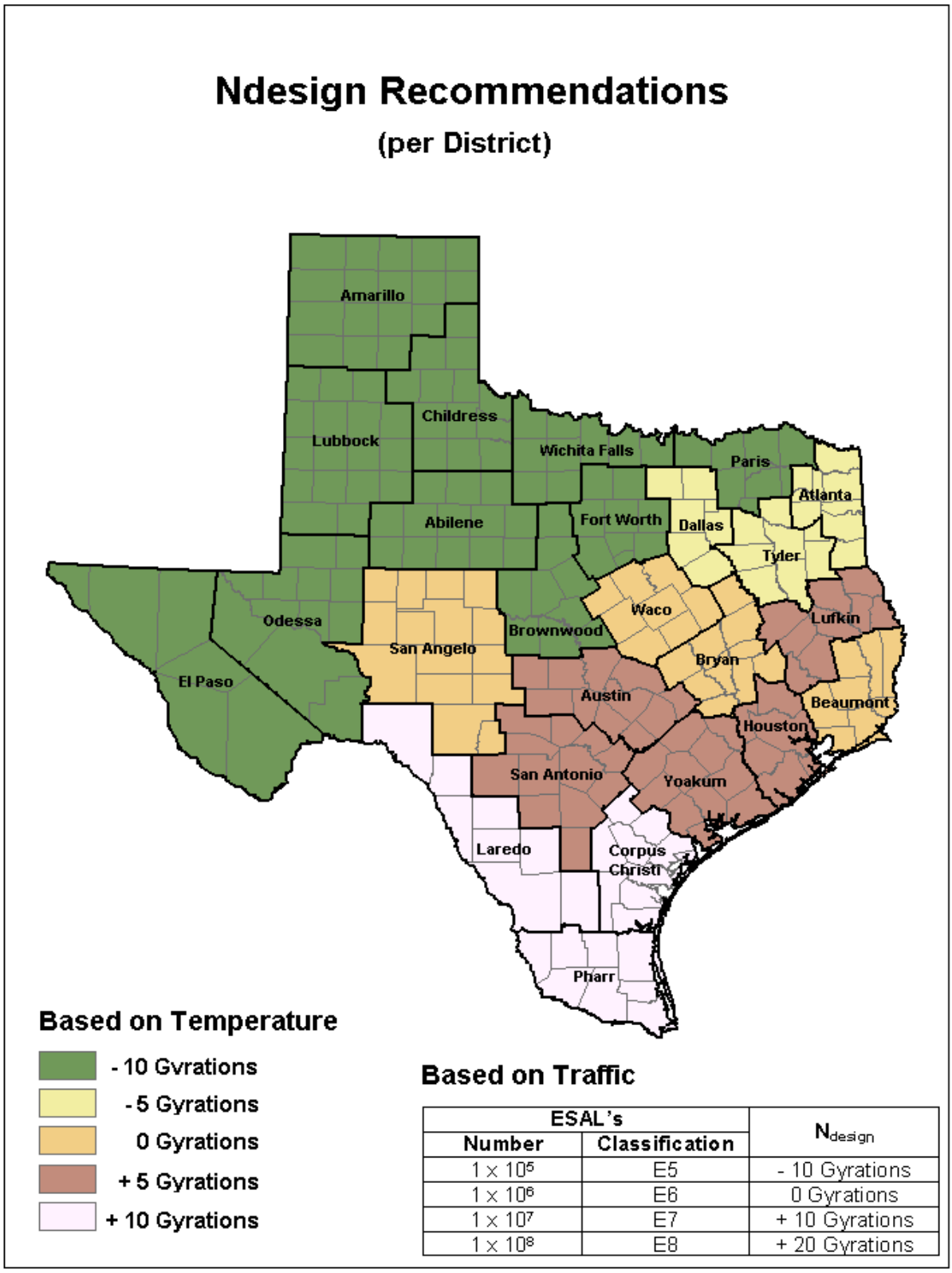

Figure B7. Guidelines for selection of N_{design} for Texas per district (based on temperature and traffic volume)

Appendix C. Criteria for Design and Selection of Superpave Mixes

This appendix presents general recommendations for the selection of Superpave mixtures based on factors such as expected traffic, loading characteristics and desired performance. It is based on experience of TxDOT personnel that has been adapted to the research results. However, previous district and area experience with similar asphalt mixtures should always be taken into account when making the final selection.

Additionally, it has to be considered that asphalt mixtures are generally produced by combining different asphalt binders from different sources and aggregates locally available. Consequently, the selection of an adequate asphalt binder and grade and aggregate combination with the desired consensus properties and characteristics should also be of the utmost importance. Particular importance should be placed on the volumetric characteristics of the mix such as the total voids in the mix (VTM) and the voids in the mineral aggregate (VMA).

With these principles in mind, the following recommended steps should be considered for selecting Superpave mixes. The same concepts were applied for the development of TexSys for the selection of other mix types such as dense mixes (Item 340 and 341), PFCs (Item 342), CMHBs (Item 344) and SMAs (Item 346) (http://pavements.ce.utexas.edu/TexSys).

Step 1: Desired Mix Properties. The first step in the Superpave mix selection is to determine the performance requirements for the particular project, if any are provided. These requirements could be in terms of (i) a desired modulus value, which will control the stresses and strain that develop in the layer as a result of traffic loadings, or (ii) a particular performance requirement such as rutting, cracking or durability.

Step 2: Traffic Characteristics. In Texas, Superpave mixtures are generally used on medium to high traffic roads because of their perceived high cost, especially if cost is measured in terms of initial construction cost without regard to the life cycle. However, the Superpave mix design methodology is appropriate for any level of traffic volume when correctly applied specifying an adequate number of design gyrations (N_{design}), binder grade, and aggregate characteristics. Some of these recommendations are presented in Appendix B. Superpave mixtures also perform well under slow or fast moving traffic when high strength mixes are required.

Step 3: Pavement Layer and Thickness. Generally, Superpave mixtures with smaller nominal maximum aggregate size (NMAS) are used as surface mixtures (e.g. SP-C and SP-D), but mixtures with larger NMAS can be used as base or intermediate layers (e.g. SP-A and SP-B). Table C1 presents recommendations developed by TxDOT personnel for the selection of the Superpave mix type based on layer thickness requirement and layer use. Based on the intended application, the binder content can be adjusted by adjusting N_{design}. Surface layers should be designed to withstand high shear stresses, and rutting resistance should be a primary concern. Lower layers, especially when built on top of softer granular layers, are subjected to higher horizontal tensile strains and, consequently, fatigue resistance should be the main concern. Hence, N_{design} recommendations could also be a function of the position (or depth) of the mix within the pavement structure: the deeper into the pavement structure, the lower the N_{design}.

According to TxDOT's "Standard Specifications for Construction and Maintenance of Highways, Streets, and Bridges," the Department specifies the following Superpave mixtures:

Table C1. TxDOT Superpave mixtures

Mixture Type	Nominal Aggregate Size	Minimum Lift Thickness (in)	Maximum Lift Thickness (in)	Typical Use
SP-A	1 ½"	3.00"	5.00"	Base
SP-B	1"	2.25"	4.00"	Base / Intermediate
SP-C	¾"	1.50"	3.00"	Intermediate / Surface
SP-D	½"	1.25"	2.00"	Surface

Step 4: Aggregate Properties. As mentioned previously, specific aggregate requirements (including consensus properties) have to be met in order for the Superpave mixture to achieve optimal performance. Among the specified aggregate requirements are the following: % deleterious materials, % decantation, % micro-Deval abrasion, % L.A. abrasion, magnesium sulfate soundness (after five cycles), % coarse aggregate angularity, % flat and elongated particles, % linear shrinkage, and % sand equivalent. Additionally, several requirements should be met with respect to the individual gradation of the fines and the mineral filler. The master gradation bands and mix volumetric properties should be as shown in Table C2:

Table C2. Master gradation bands (% passing by weight or volume) and volumetric properties of Superpave mixtures

Sieve Size	SP-A	SP-B	SP-C	SP-D
2”	100	–	–	–
1½”	98–100	100	–	–
1”	90–100	98–100	100	–
¾”	(*)	90–100	98–100	100
½”	–	(*)	90–100	98–100
⅜”	–	–	(*)	90–100
#4	–	–	–	(*)
#8	19–45	23–49	28–58	32–67
#16	1–45	2–49	2–58	2–67
#30	1–45	2–49	2–58	2–67
#50	1–45	2–49	2–58	2–67
#200	1–7	2–8	2–10	2–10
Min. Design VMA (%) (**)	13	14	15	16
Design VFA (%)	65–75	65–75	73–76	73–76

(*) Must retain at least 10% cumulative.
(**) Strict adherence to volumetric requirements will warrant adequate field performance.

Step 5: Binder Selection. The binder selection process is one of the most significant and widely accepted developments of the Superpave methodology. The selection of the binder performance grade (PG) is based on the properties of the binder (primarily G*) at the average 7-day maximum and minimum pavement temperatures expected at the location of the specific project. These grades can be determined by using LTPP Bind software (developed by the Federal Highway Administration) once the importance of the project and the desired reliability are determined. In Texas, the binder recommendations by LTPP Bind have been slightly modified by the TxDOT Construction Division to adapt to local experience. This binder selection could be further modified when traffic speed is expected to be slow or even stationary. When traffic volume or axle loads are expected to be high during the design life, these grades could be increased accordingly.

Step 6: Constructability and Density. When properly designed and constructed (uniformly compacted to the target density), Superpave mixtures generally have a high shear strength, resistance to rutting, and also show reasonable resistance to segregation, raveling, moisture damage, freeze/thaw damage, and durability. These mixtures also show an adequate resistance to cracking, permeability problems, and workability. However, one practical issue with Superpave mixtures is that they can be hard to compact because of the coarse aggregate structure. This aspect can lead to permeability and durability problems,

and consequently to a reduction of the performance life of the asphalt mixture. Superpave mixtures can also be "too dry" with respect to asphalt binder content. This factor increases the potential for durability problems and produces mixes that are susceptible to fatigue cracking.

Step 7: Performance Testing. Asphalt mix tests, such as Hamburg Wheel Tracking Device (HWTD), Indirect Tensile Strength (ITS), and Four point Bending Beam (FPBB) should be performed on the designed Superpave mixtures so that the designer can evaluate a priori whether the in-place mix is expected to perform adequately for the duration of its design life.

Step 8: Cost. Although cost considerations are often based on initial construction costs only, life-cycle cost analysis should be performed to correctly assess the benefit to the Department of using mixes that have higher initial cost but tend to last longer in the field. In addition, Superpave mixtures tend to have higher modulus and therefore may result in reduced layer thickness compared to traditional mixes. This is especially true when thicker surface layers are necessary.

Appendix D. AIMS Output

D.1 Gravel

D.1.1 C-Rock

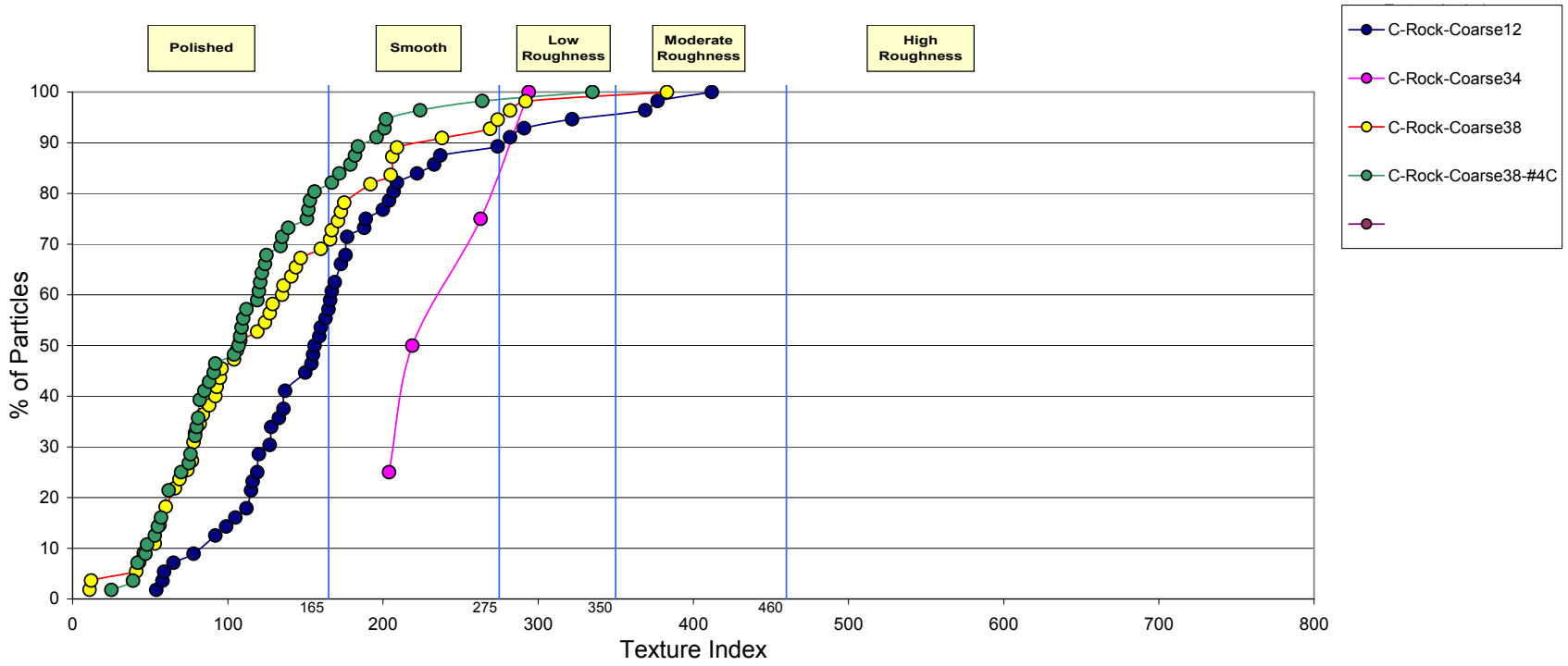

Figure D1. Texture index gravel C-Rock

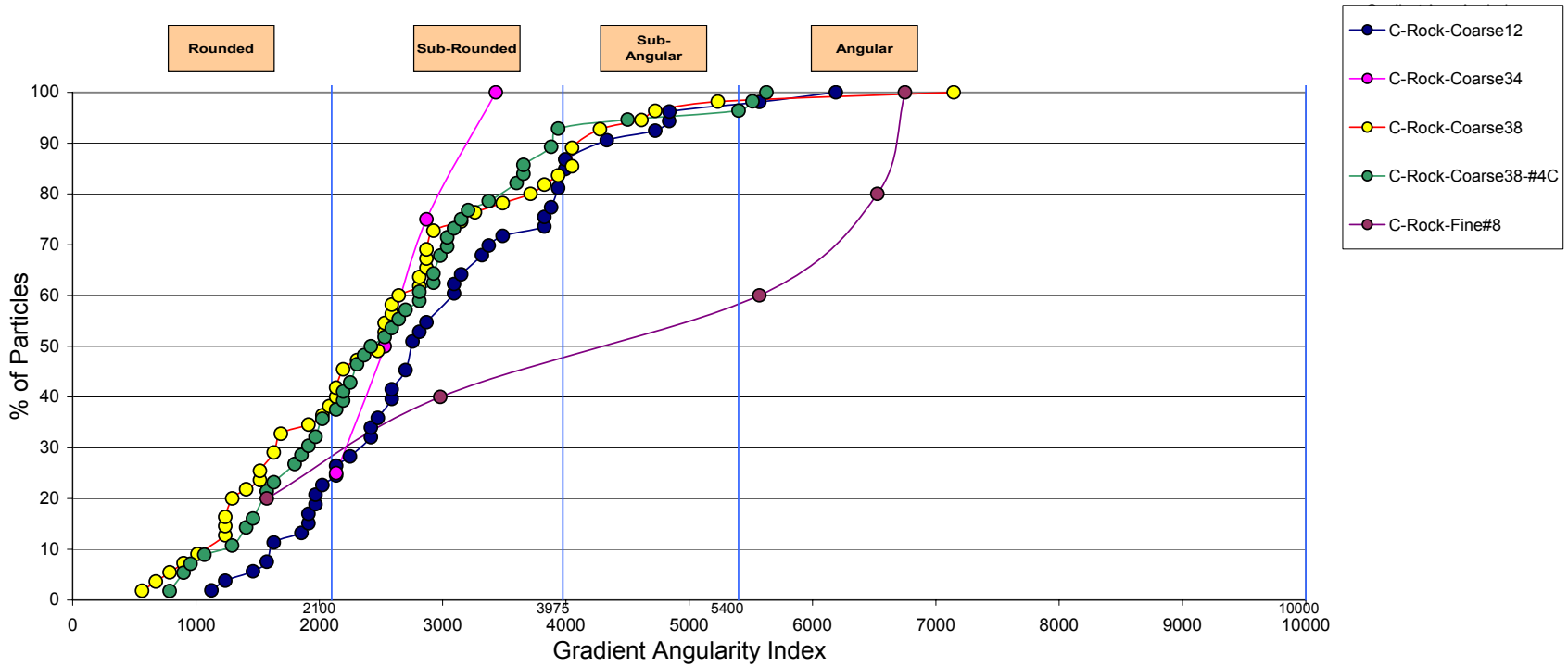

Figure D2. Gradient angularity index gravel C-Rock

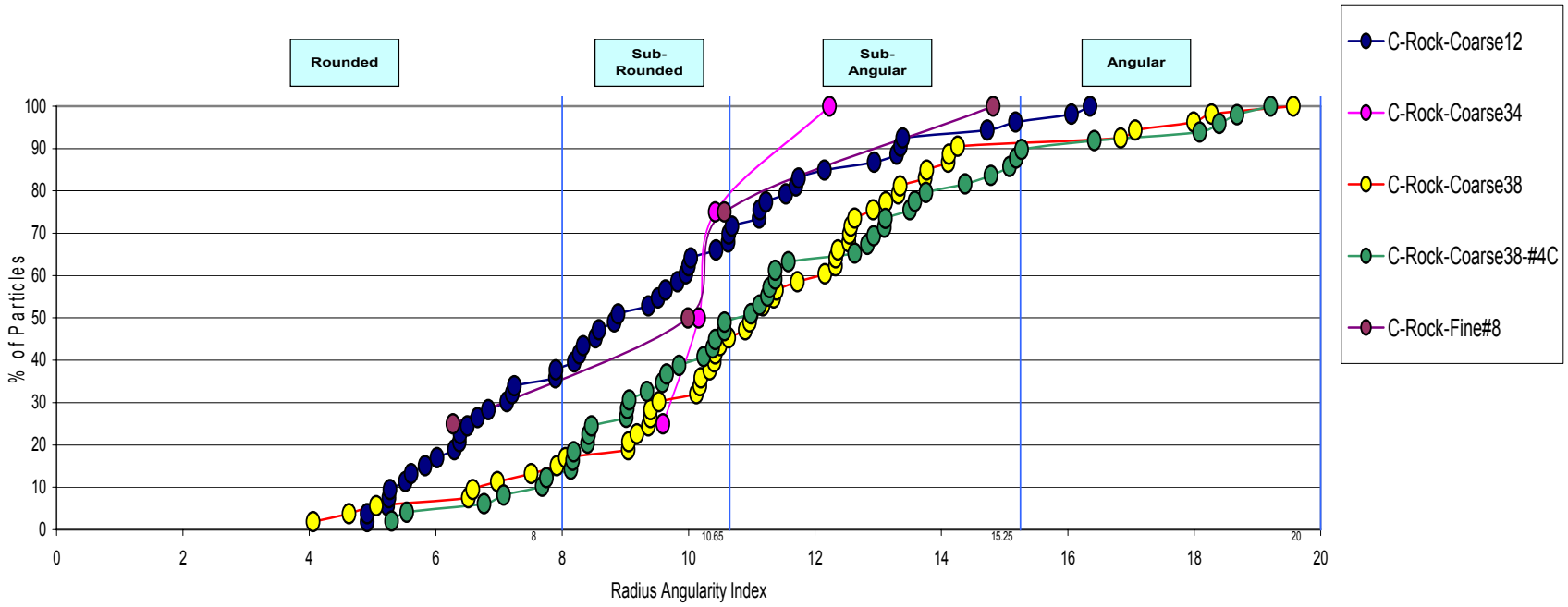

Figure D3. Radius angularity index gravel C-Rock

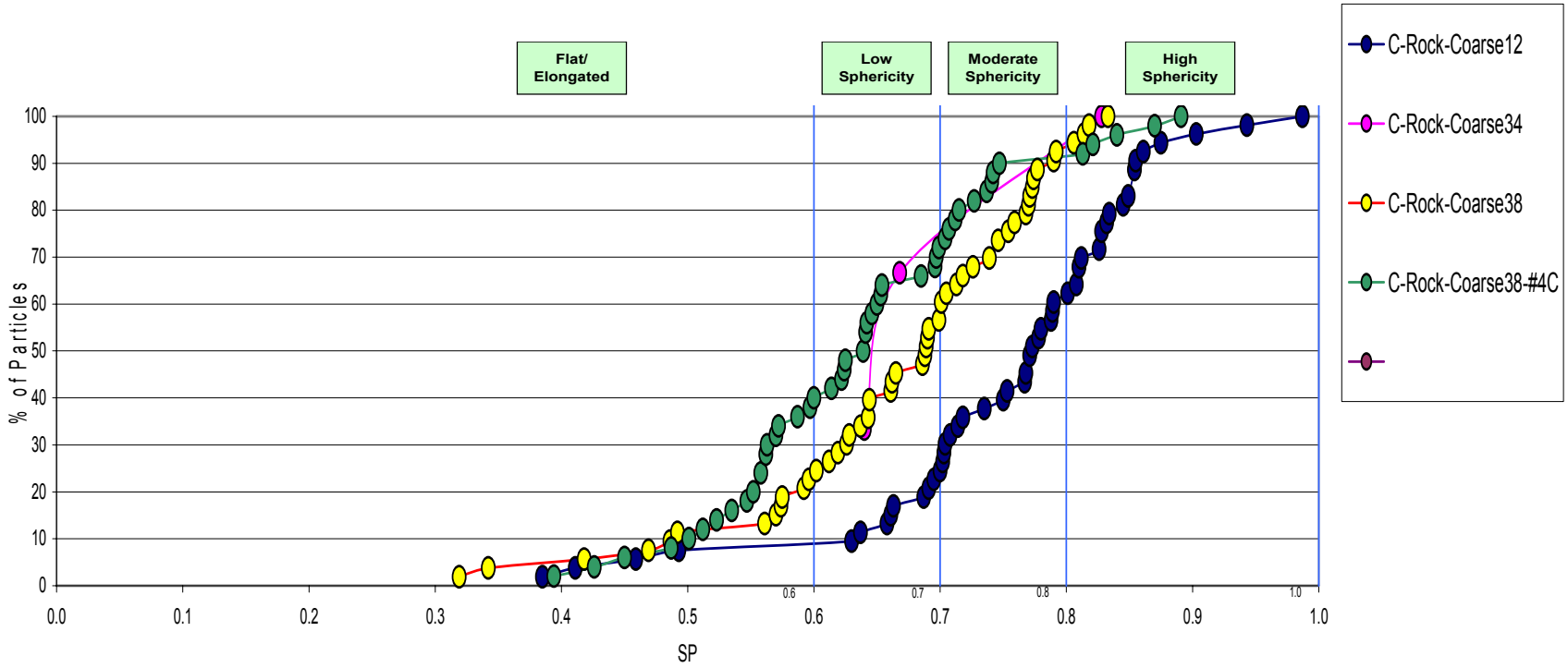

Figure D4. Sphericity gravel C-Rock

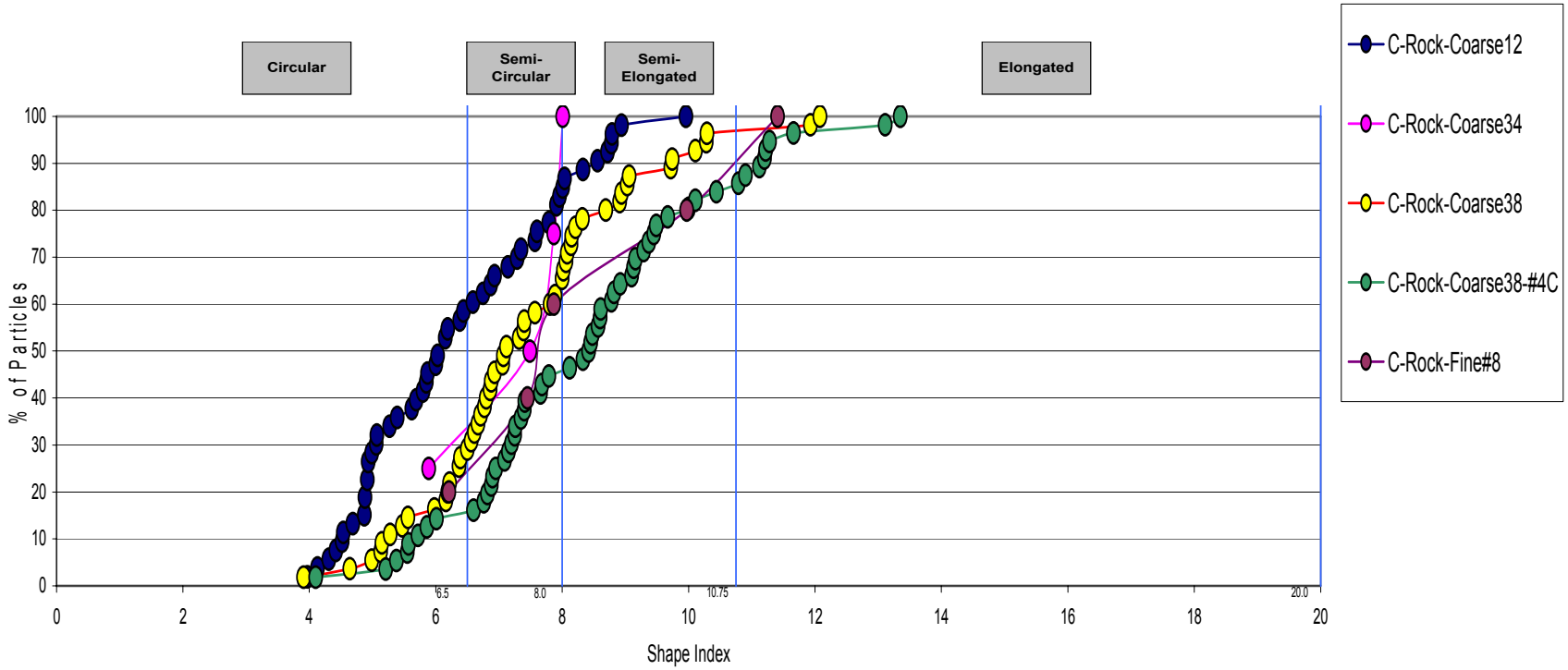

Figure D5. Shape index gravel C-Rock

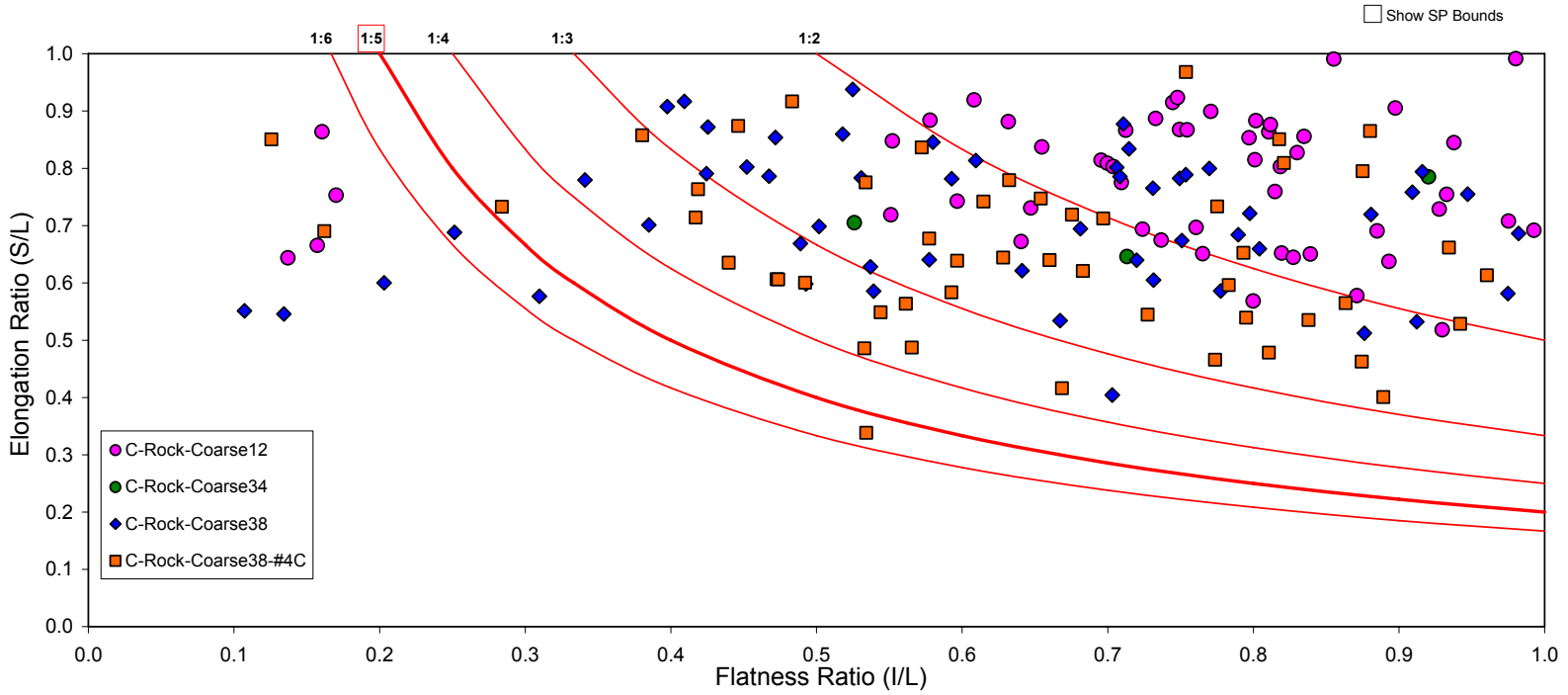

Figure D6. Flat to elongated ratio gravel C-Rock

D.1.2 D/F-Blend

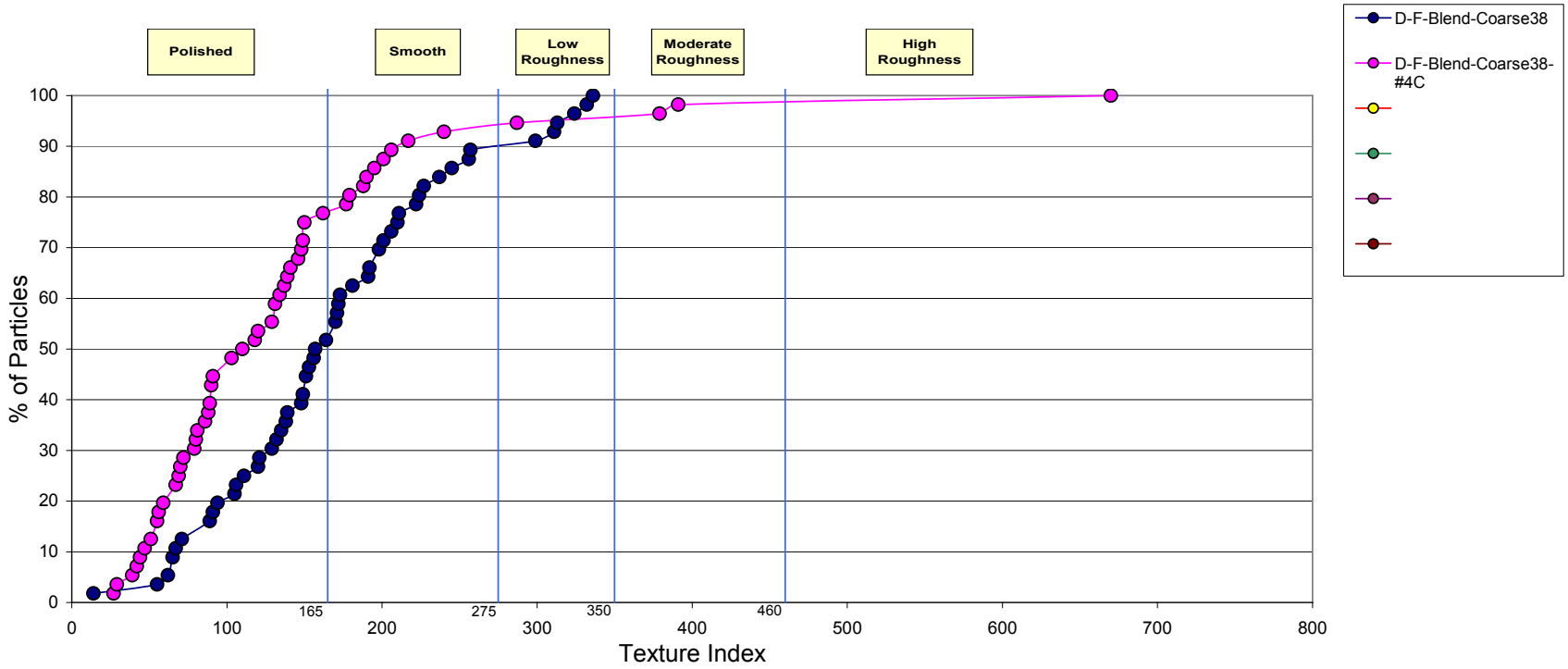

Figure D7. Texture index gravel D/F-Blend

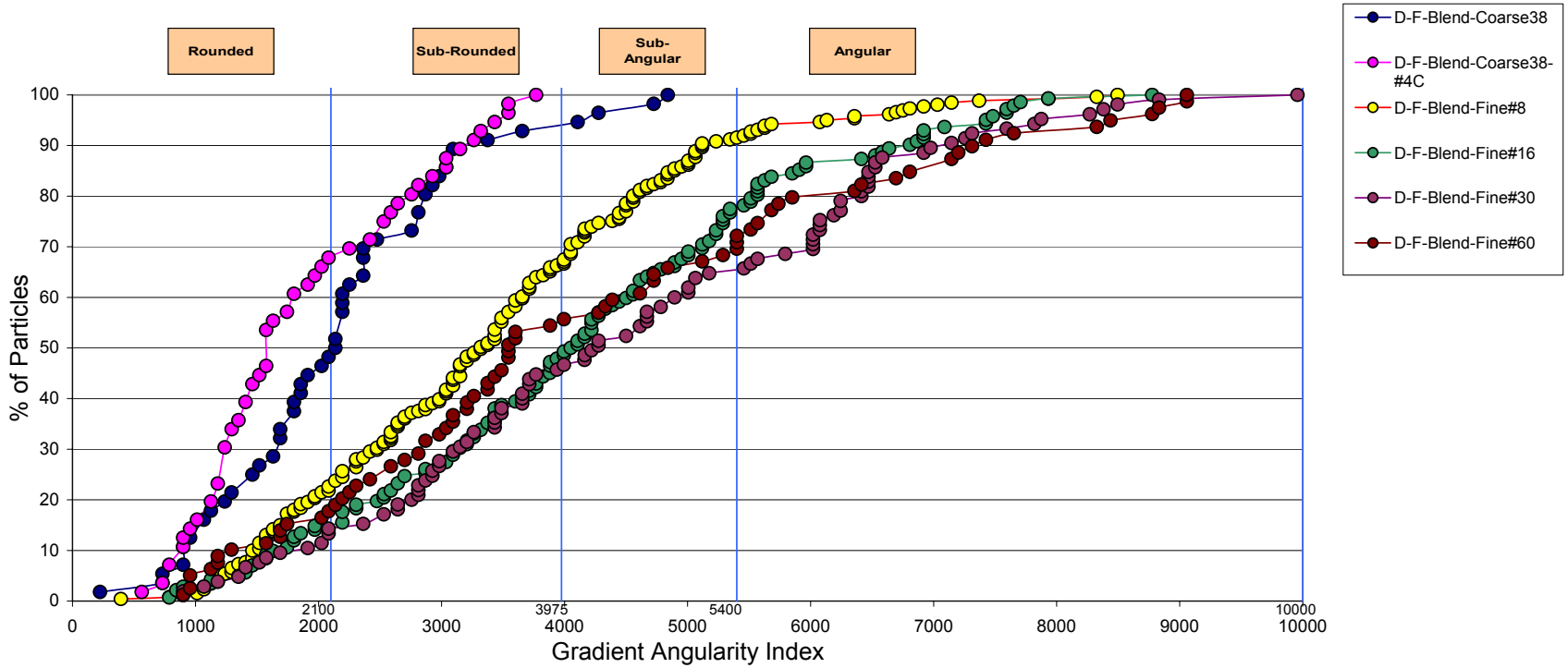

Figure D8. Gradient angularity index gravel D/F-Blend

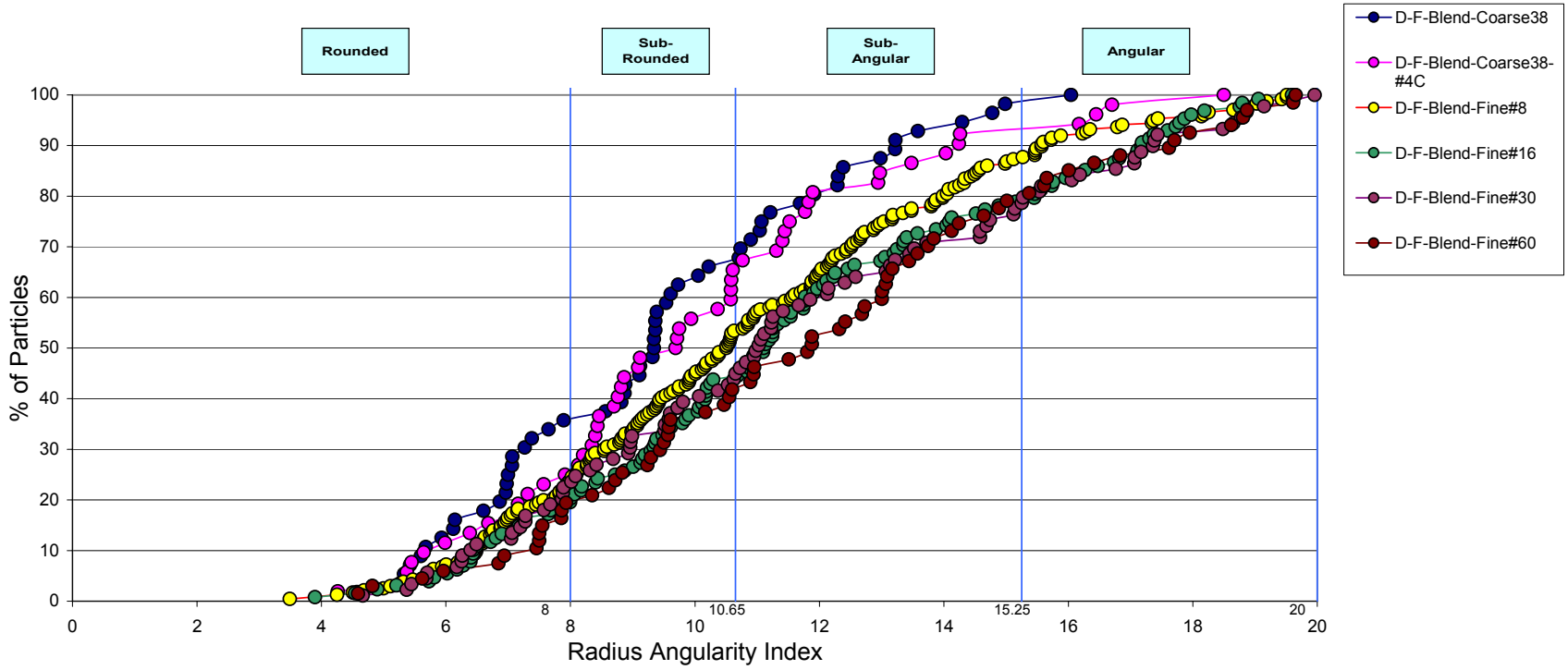

Figure D9. Radius angularity index gravel D/F-Blend

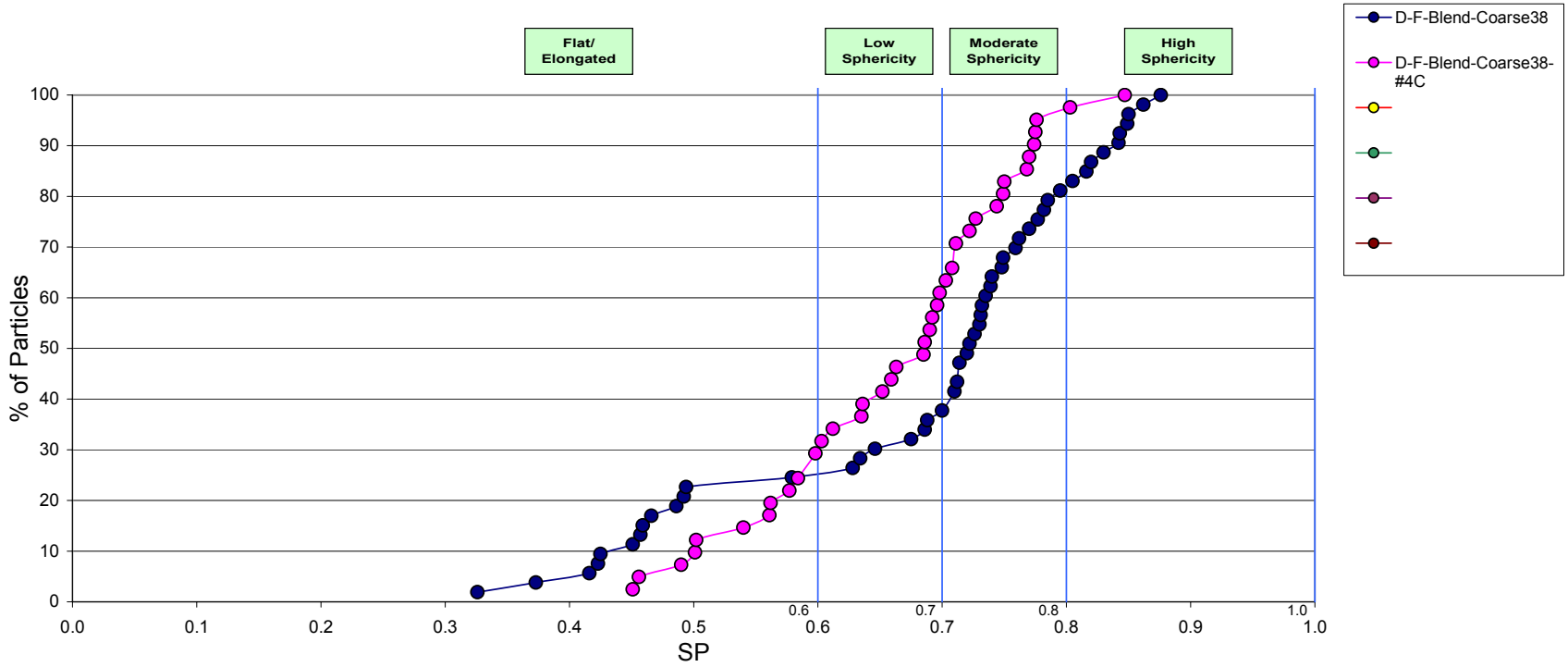

Figure D10. Sphericity gravel D/F-Blend

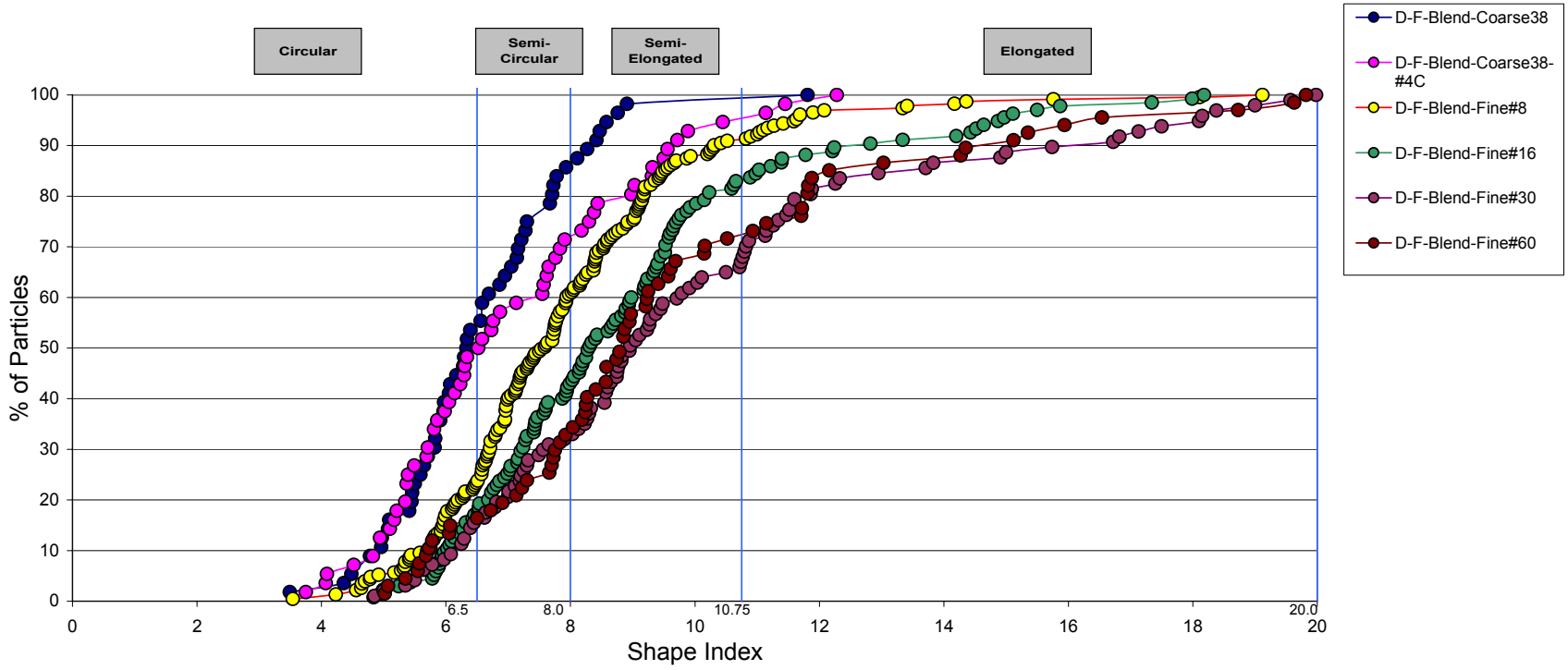

Figure D11. Shape index gravel D/F-Blend

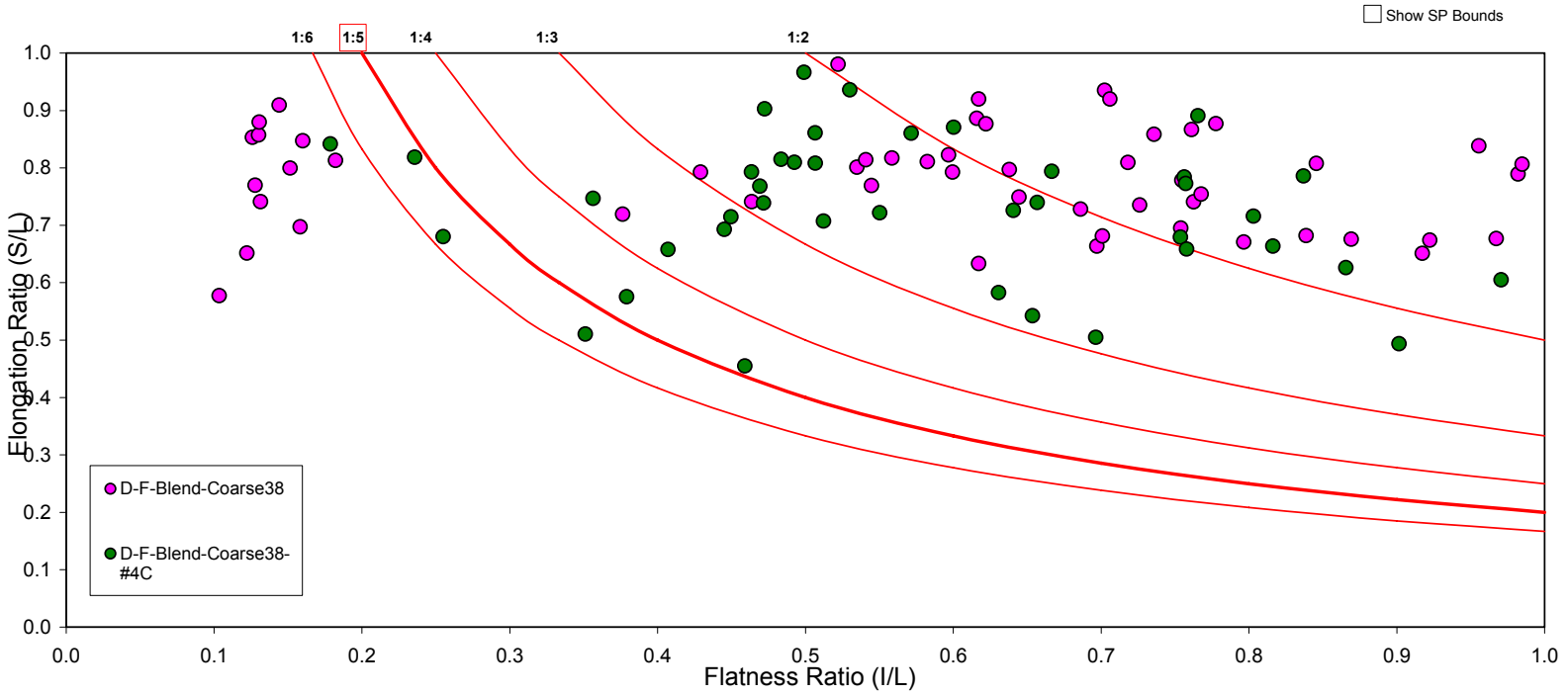

Figure D12. Flat to elongated ratio gravel D/F-Blend

D.1.3 Sand

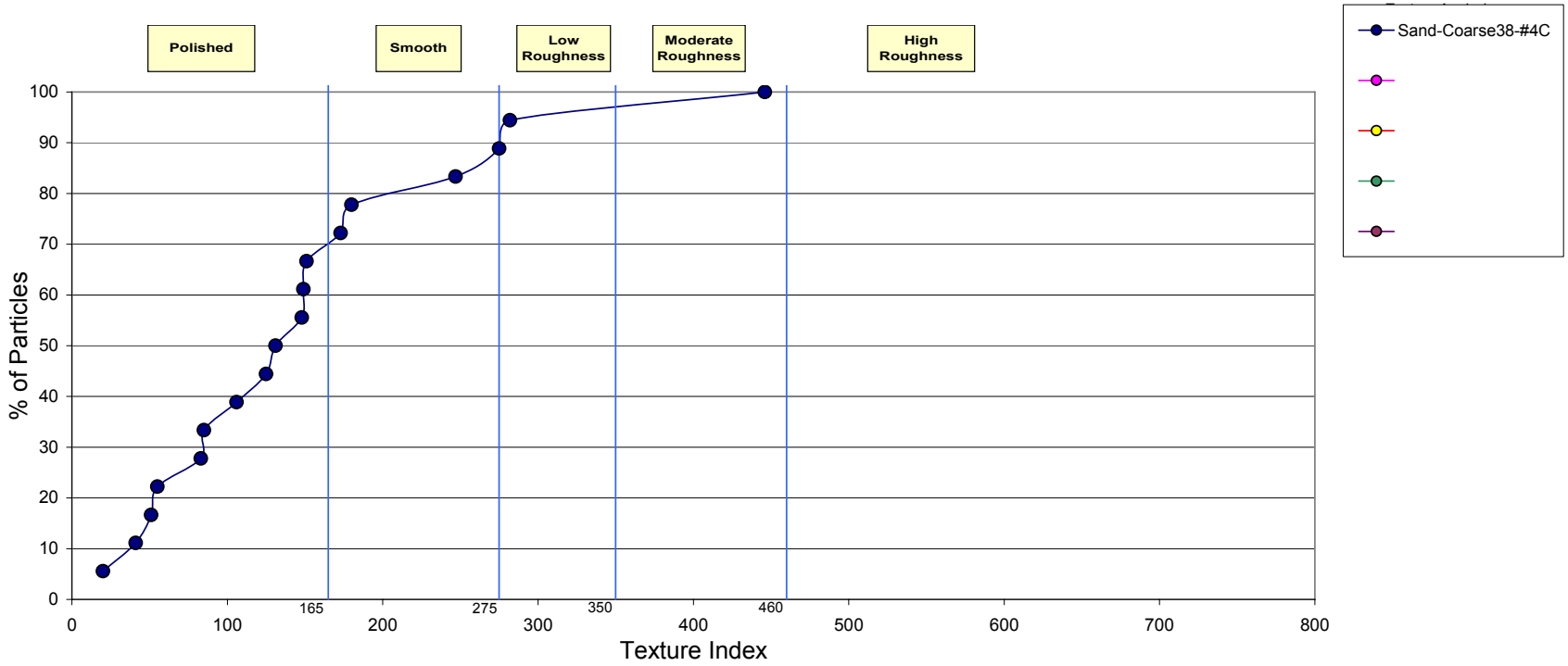

Figure D13. Texture index gravel sand

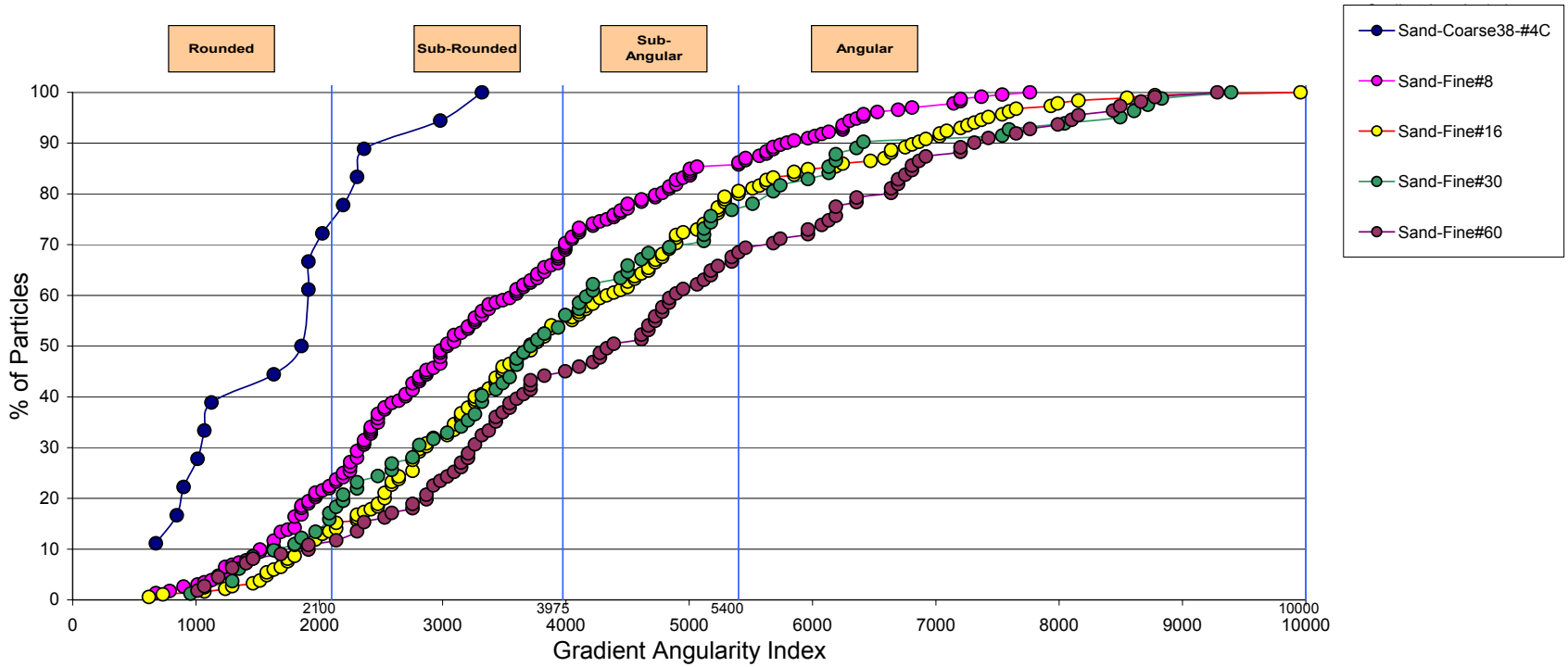

Figure D14. Gradient angularity index gravel sand

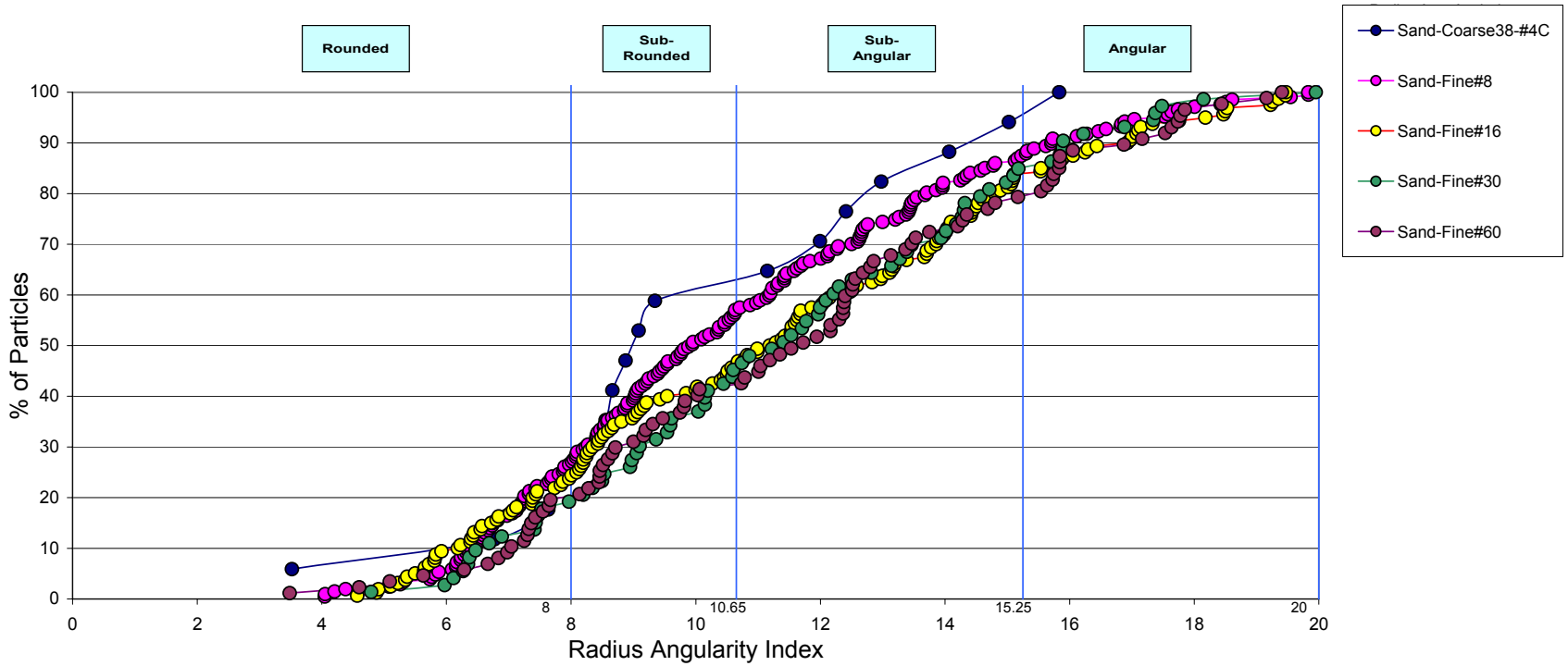

Figure D15. Radius angularity index gravel sand

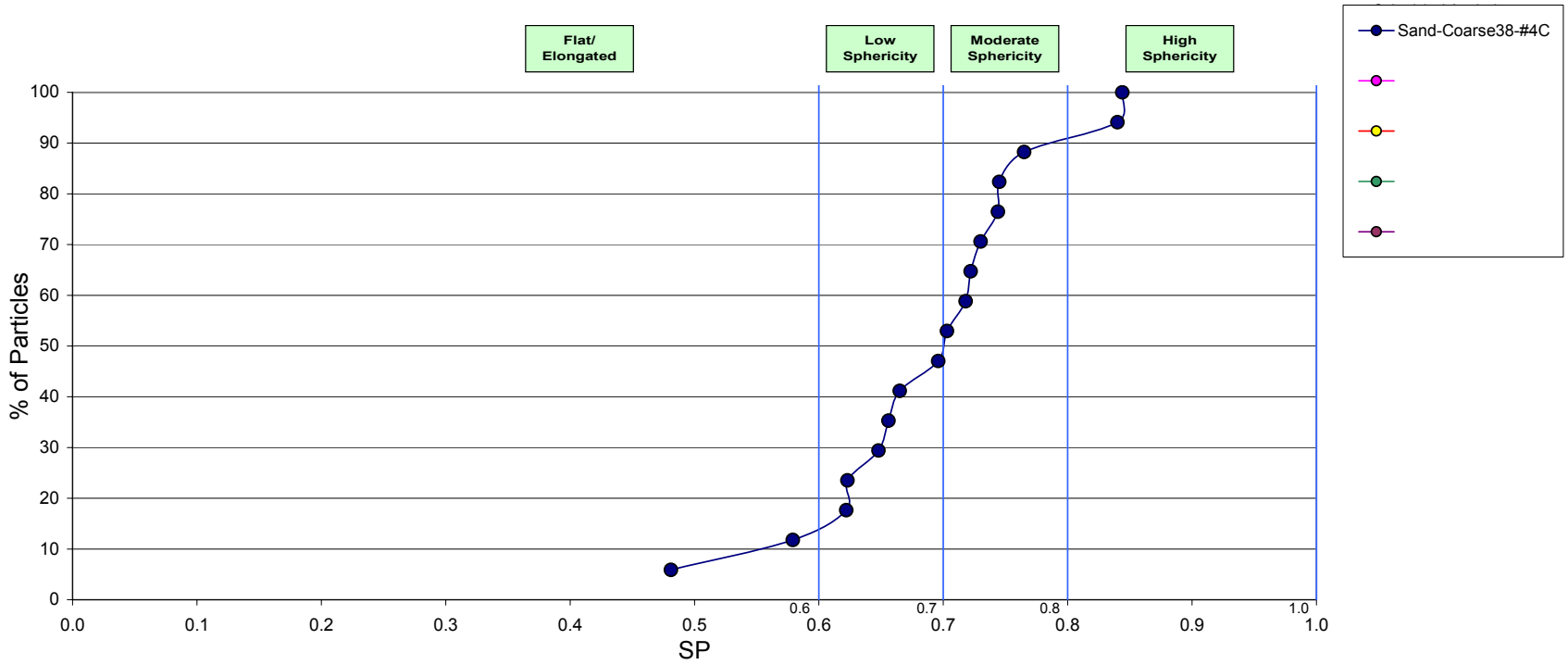

Figure D16. Sphericity gravel sand

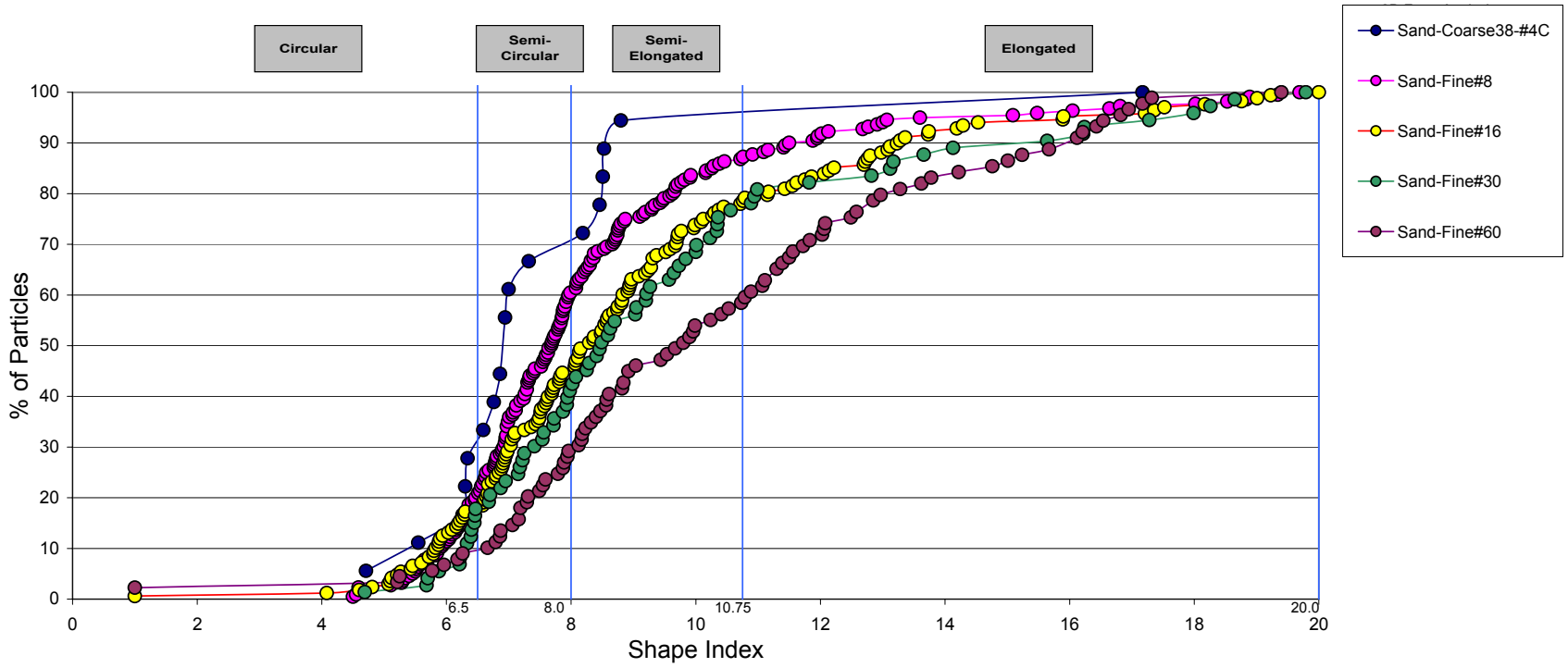

Figure D17. Shape index gravel sand

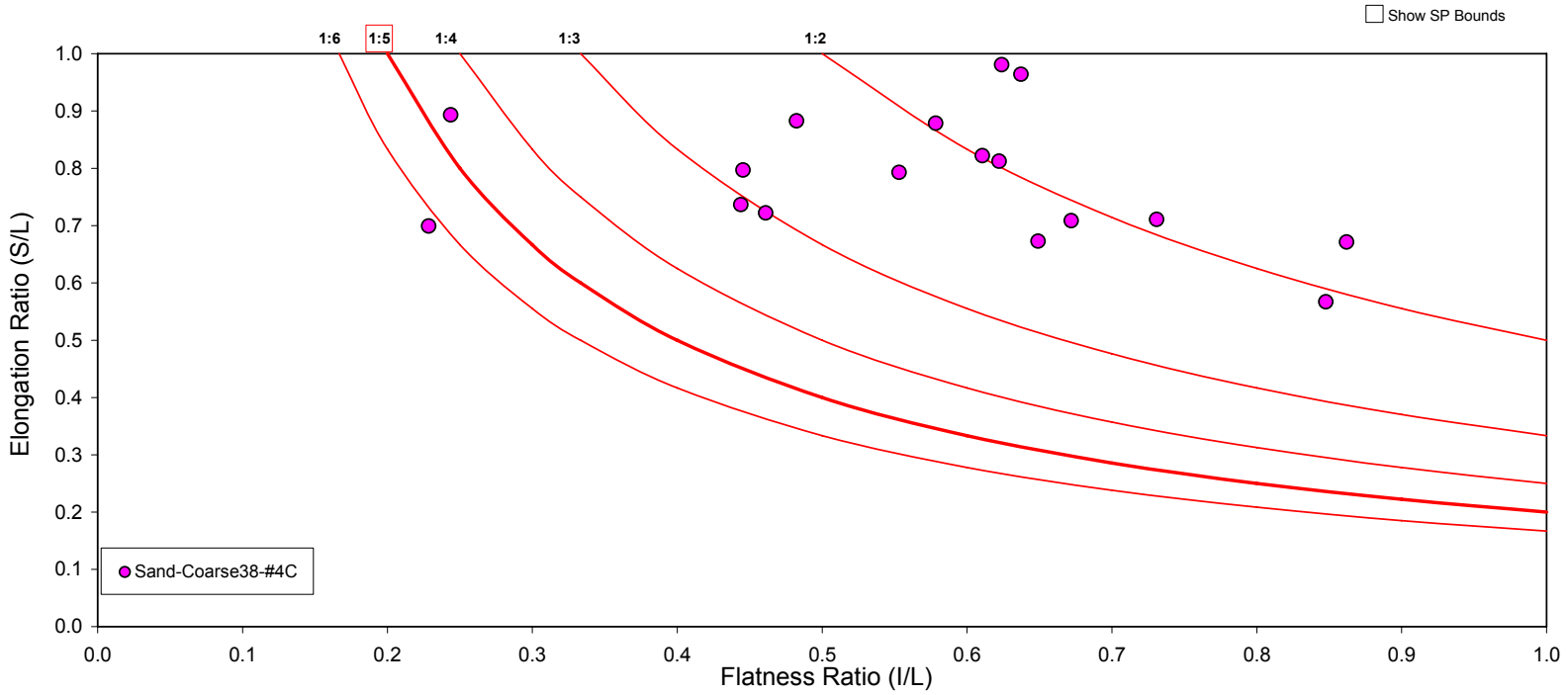

Figure D18. Flat to elongated ratio gravel sand

D.1.4 Screenings (Limestone)

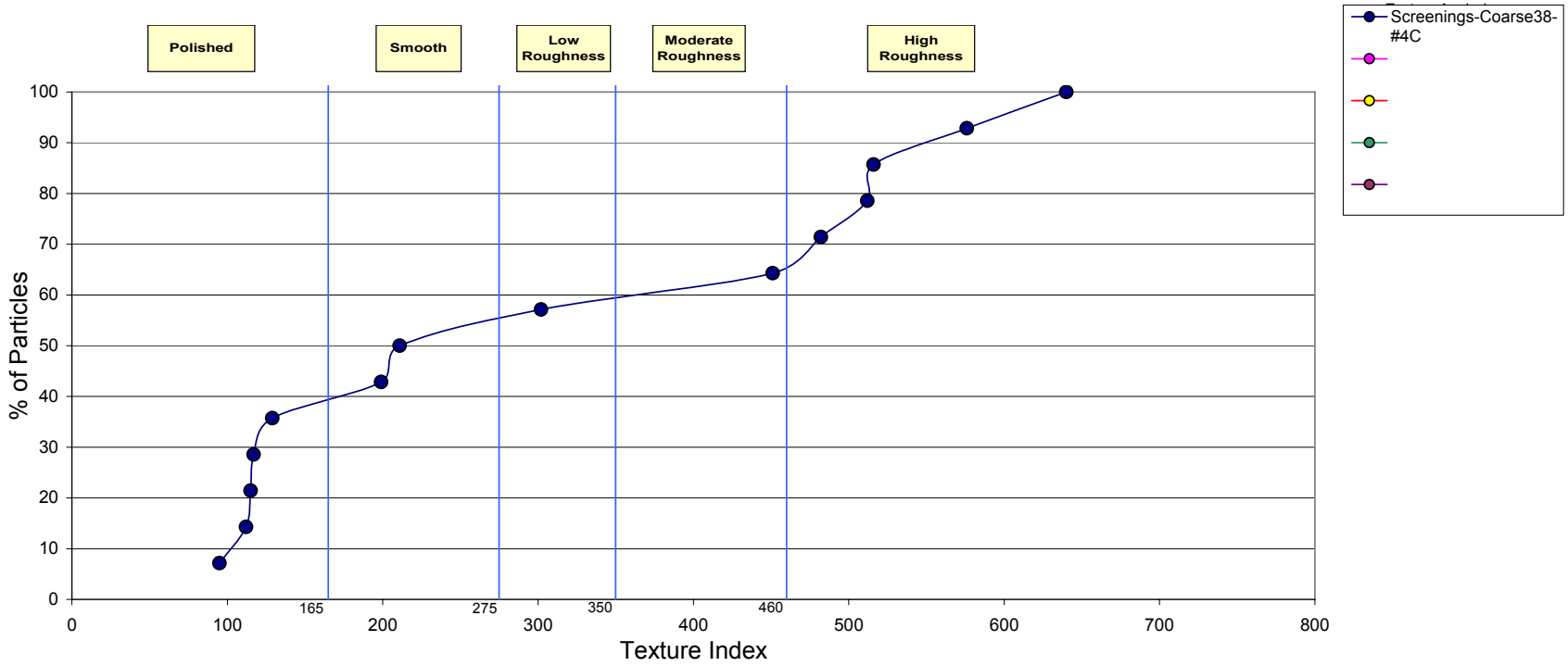

Figure D19. Texture index gravel screenings (limestone)

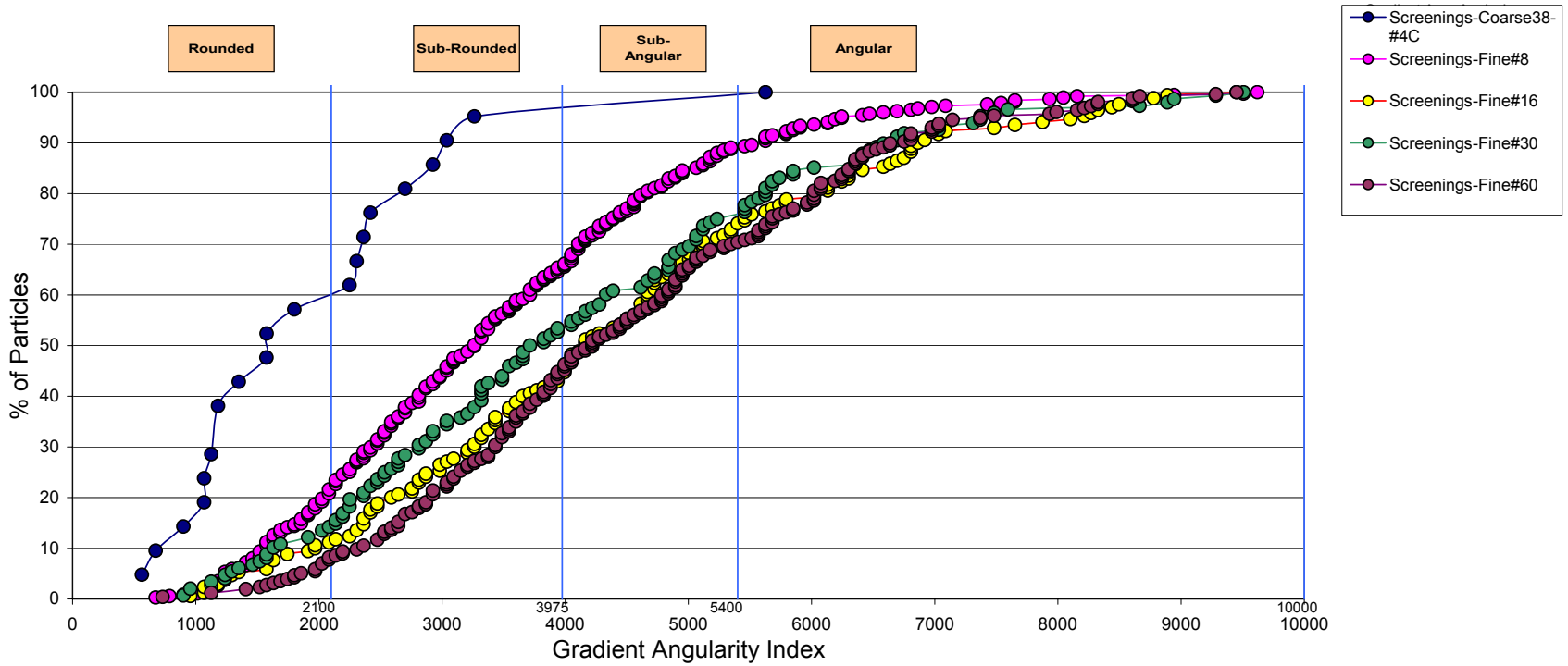

Figure D20. Gradient angularity index gravel screenings (limestone)

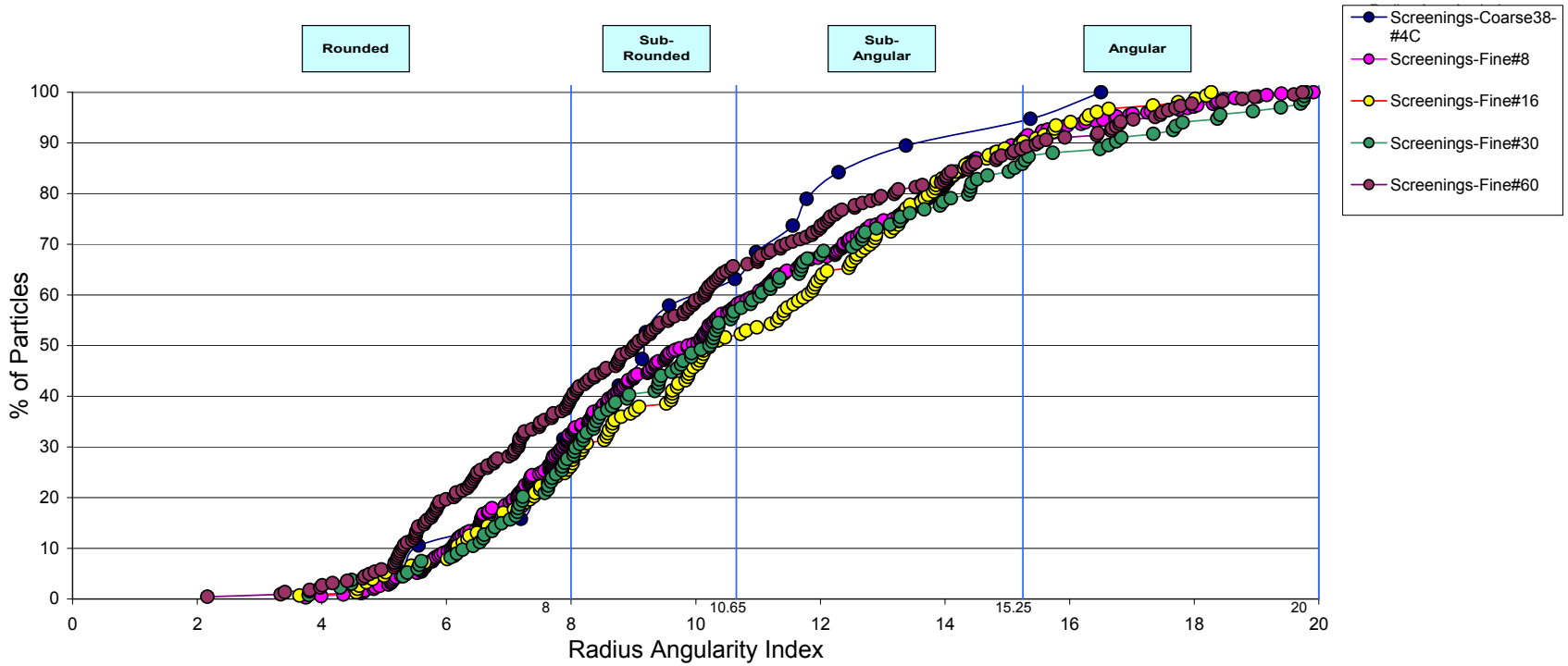

Figure D21. Radius angularity index gravel screenings (limestone)

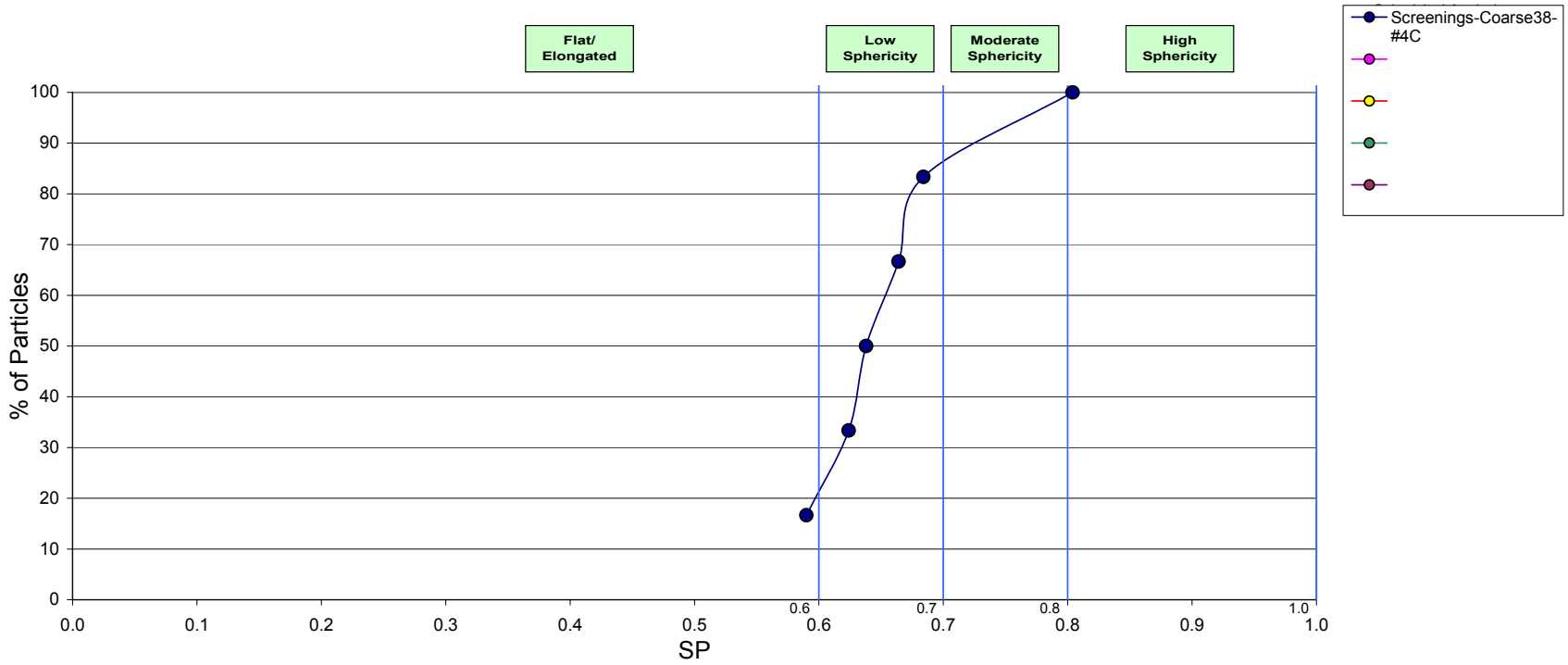

Figure D22. Sphericity gravel screenings (limestone)

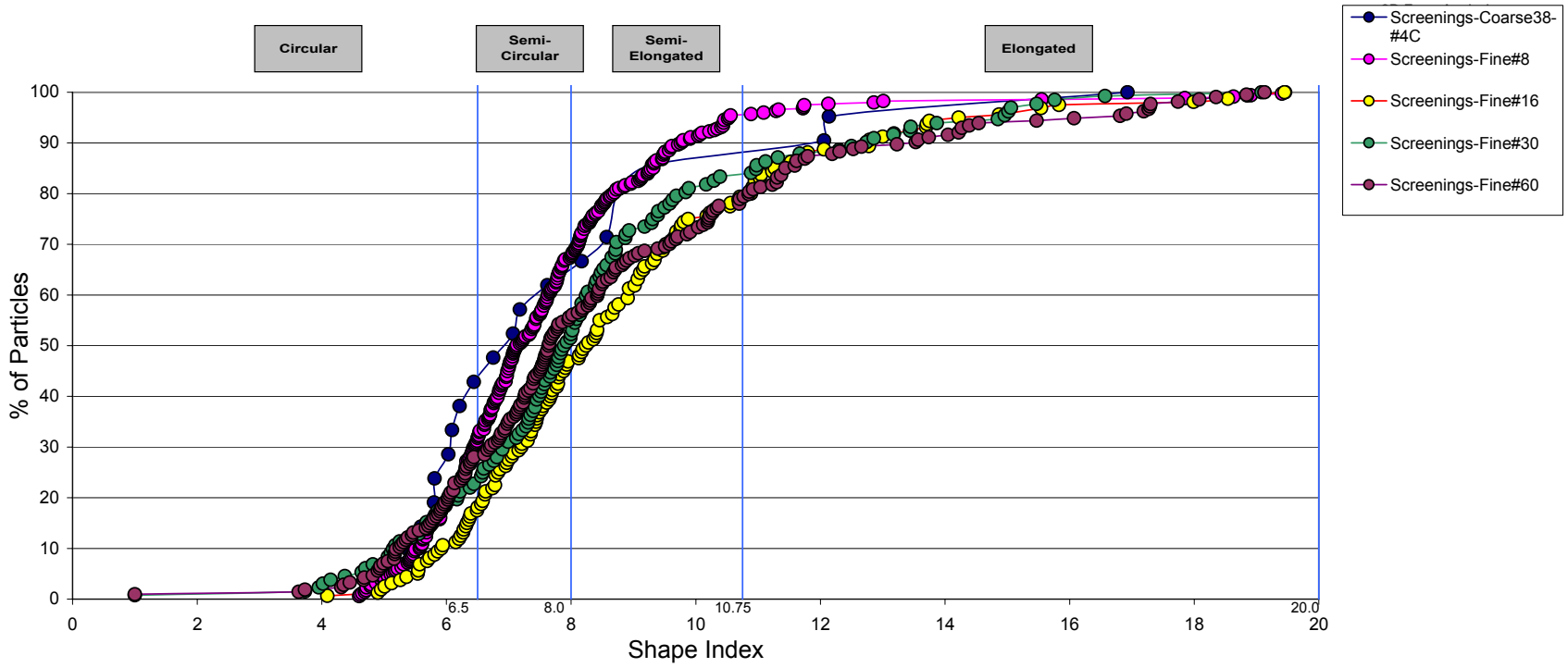

Figure D23. Shape index gravel screenings (limestone)

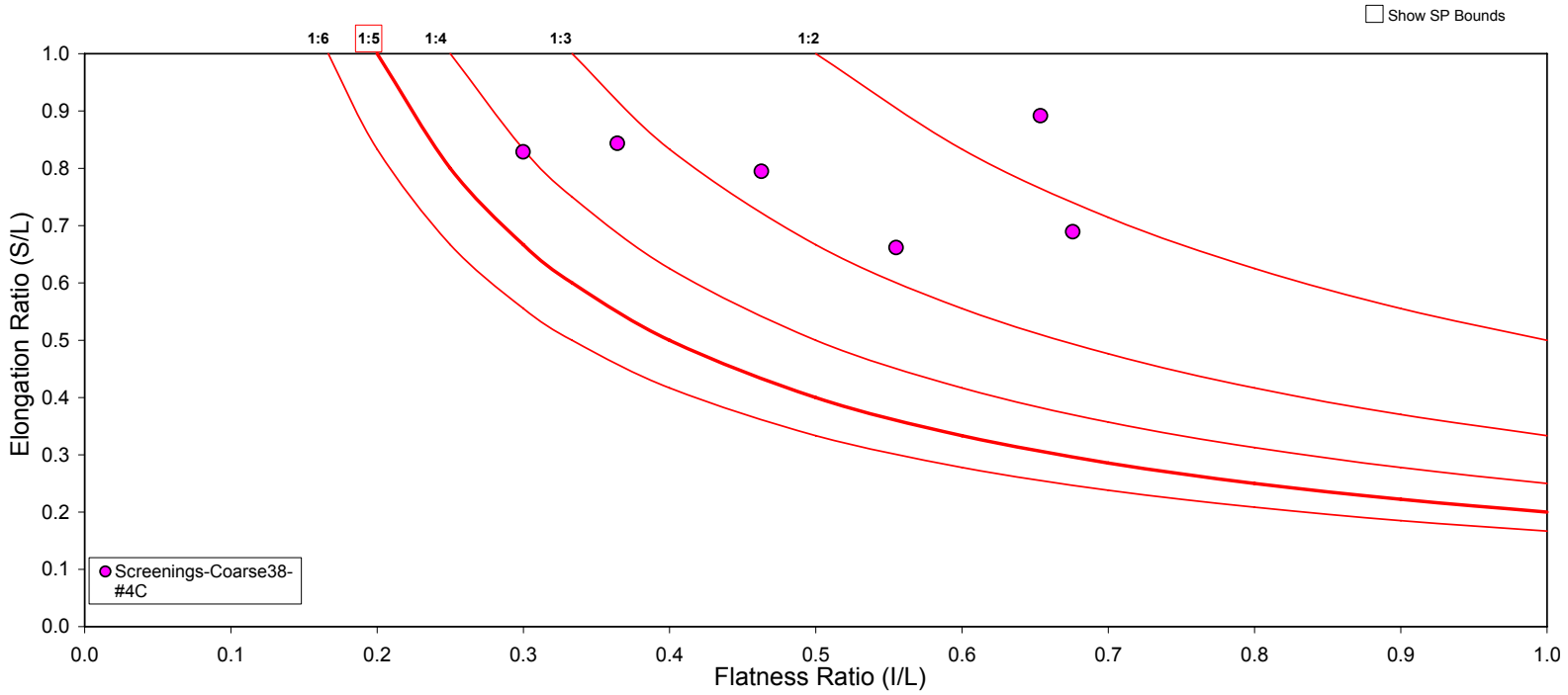

Figure D24. Flat to elongated ratio gravel screenings (limestone)

D.2 Limestone

D.2.1 B-Rock

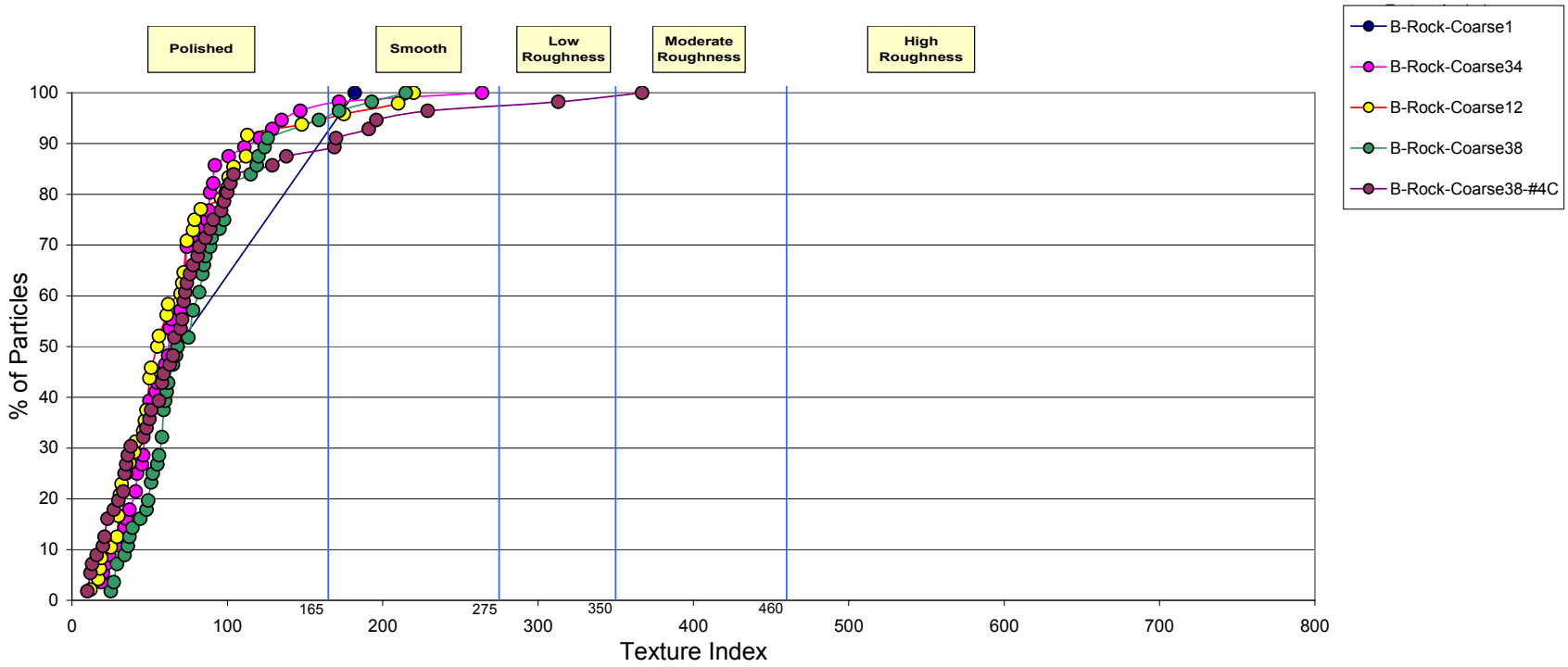

Figure D25. Texture index limestone B-Rock

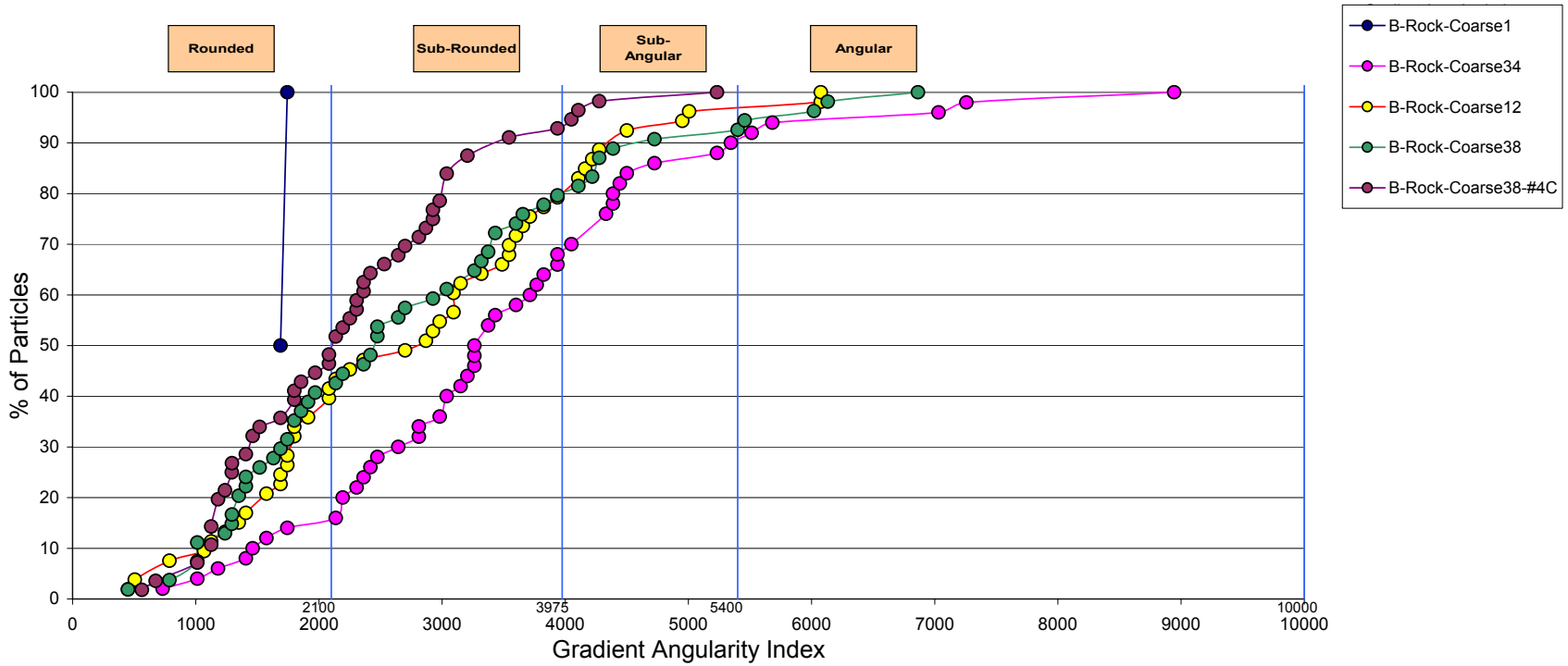

Figure D26. Gradient angularity index limestone B-Rock

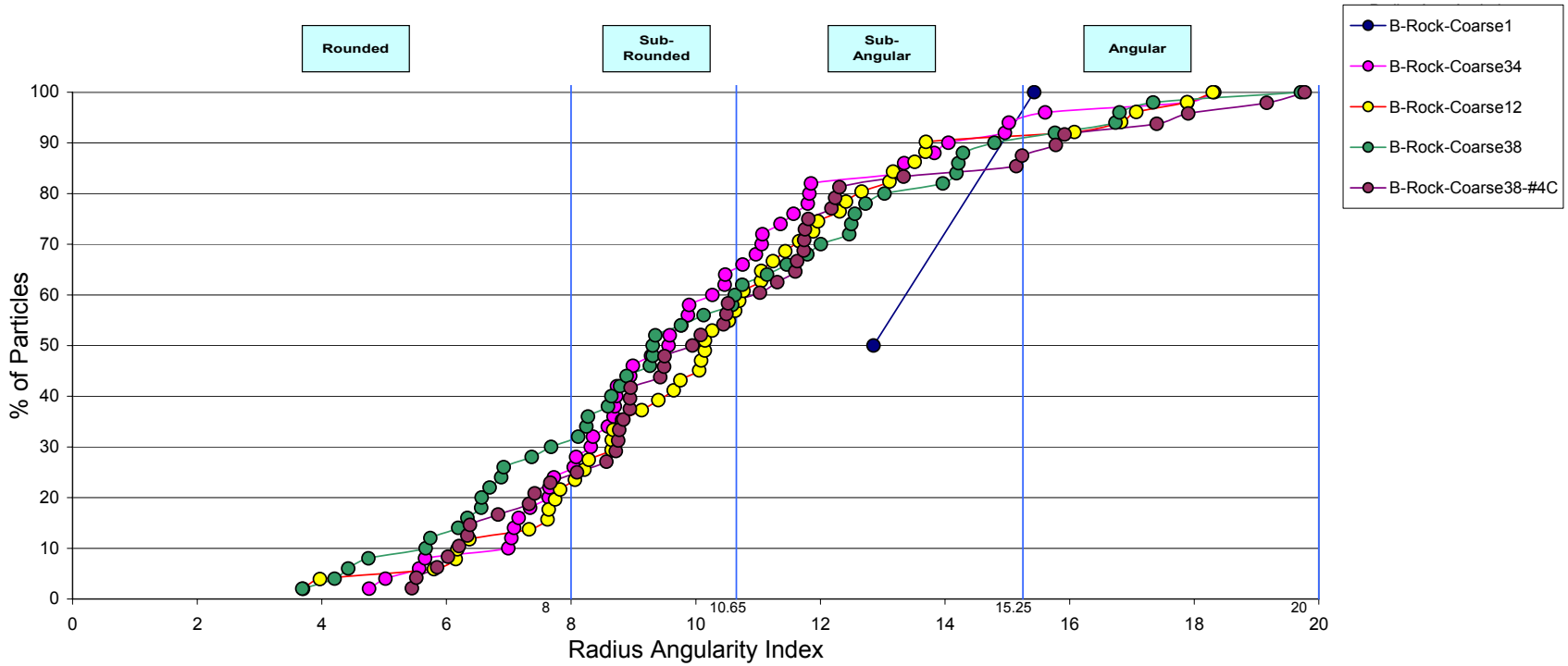

Figure D27. Radius angularity index limestone B-Rock

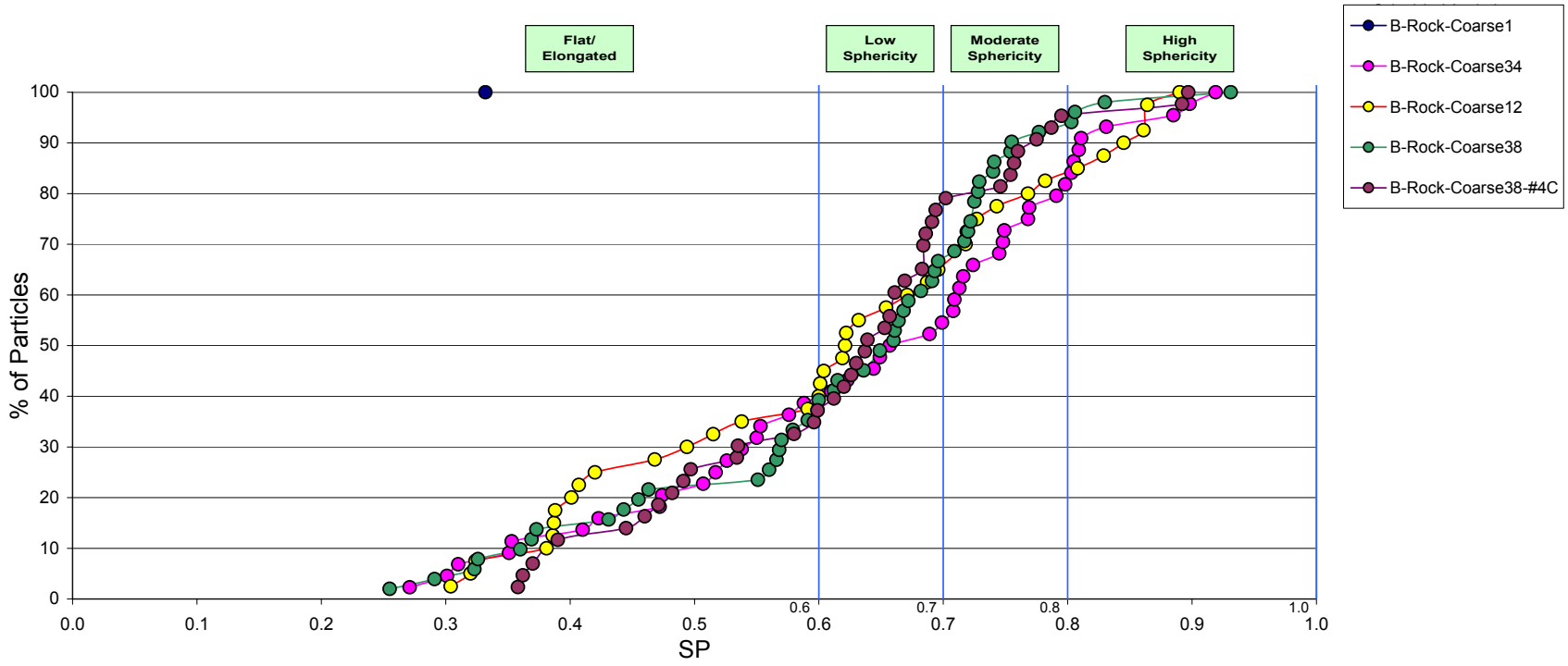

Figure D28. Sphericity limestone B-Rock

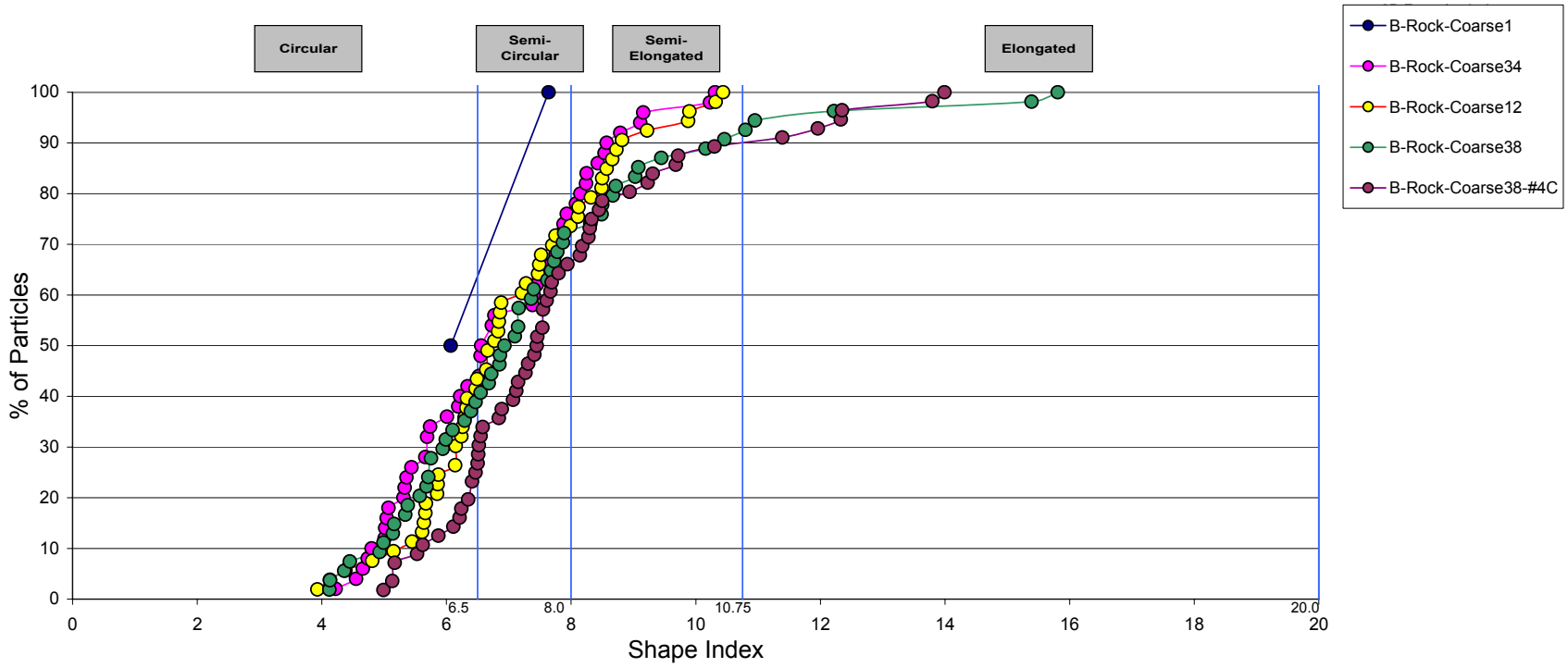

Figure D29. Shape index limestone B-Rock

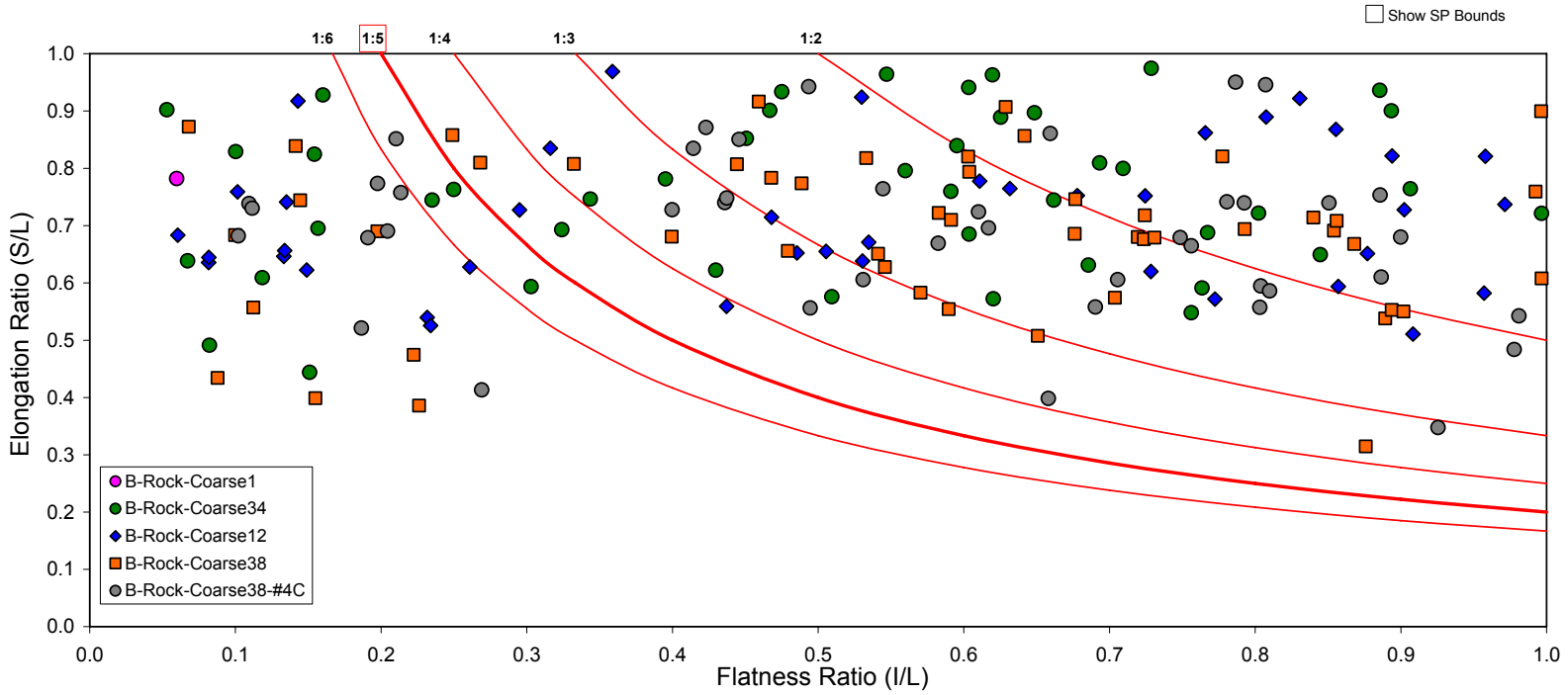

Figure D30. Flat to elongated ratio limestone B-Rock

D.2.2 C-Rock

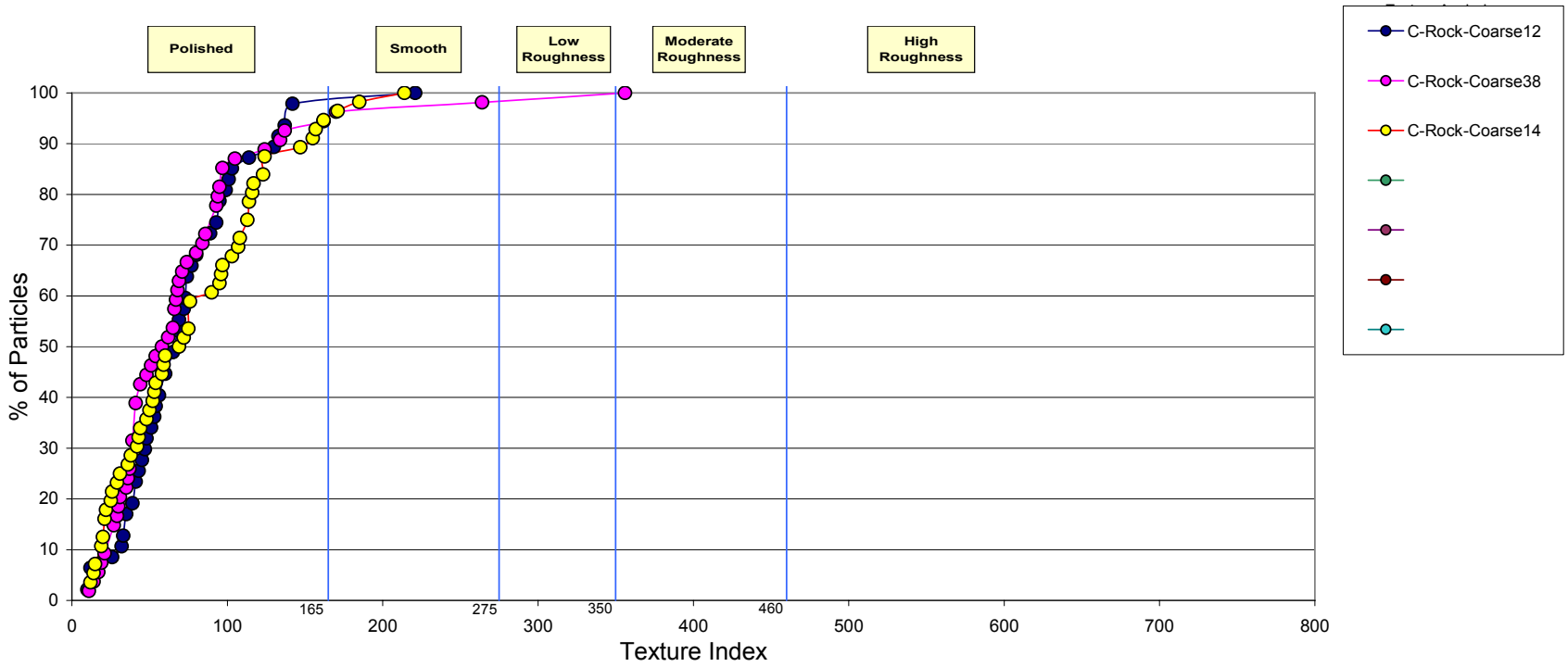

Figure D31. Texture index limestone C-Rock

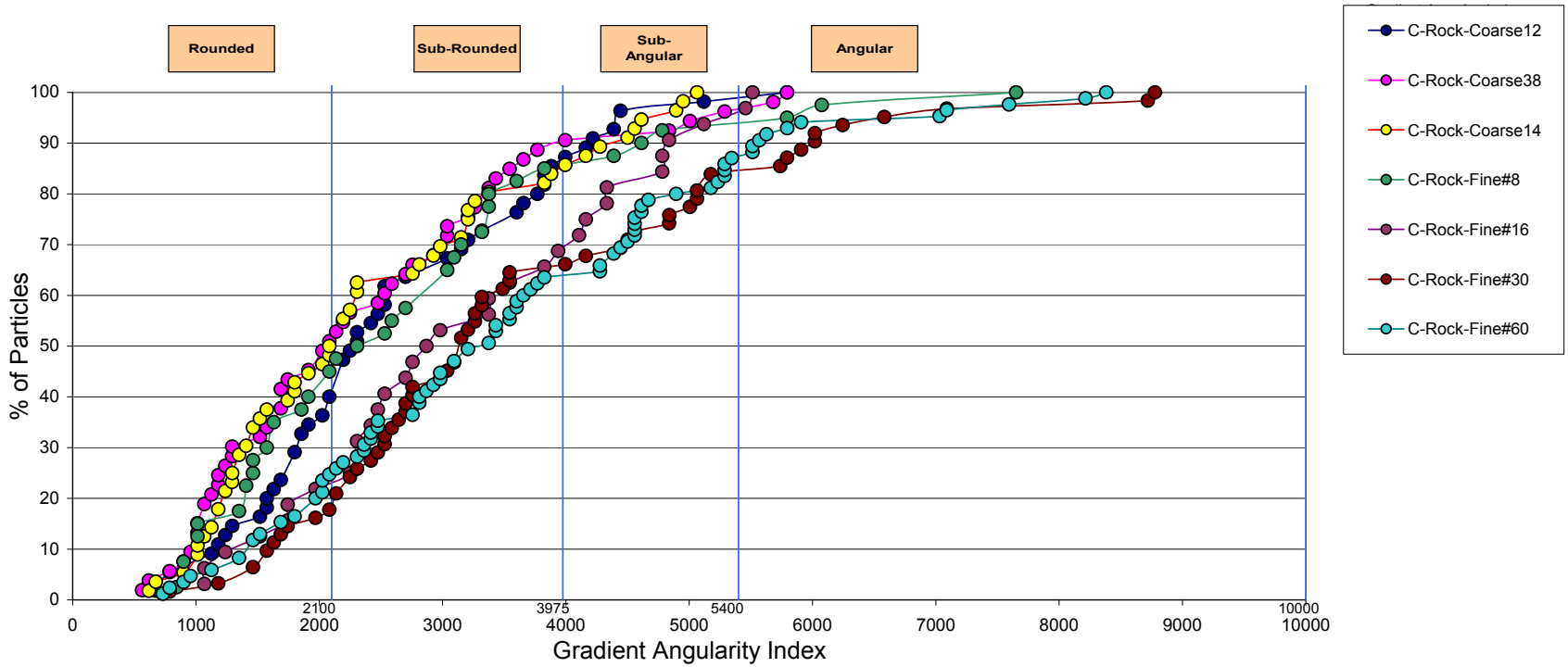

Figure D32. Gradient angularity index limestone C-Rock

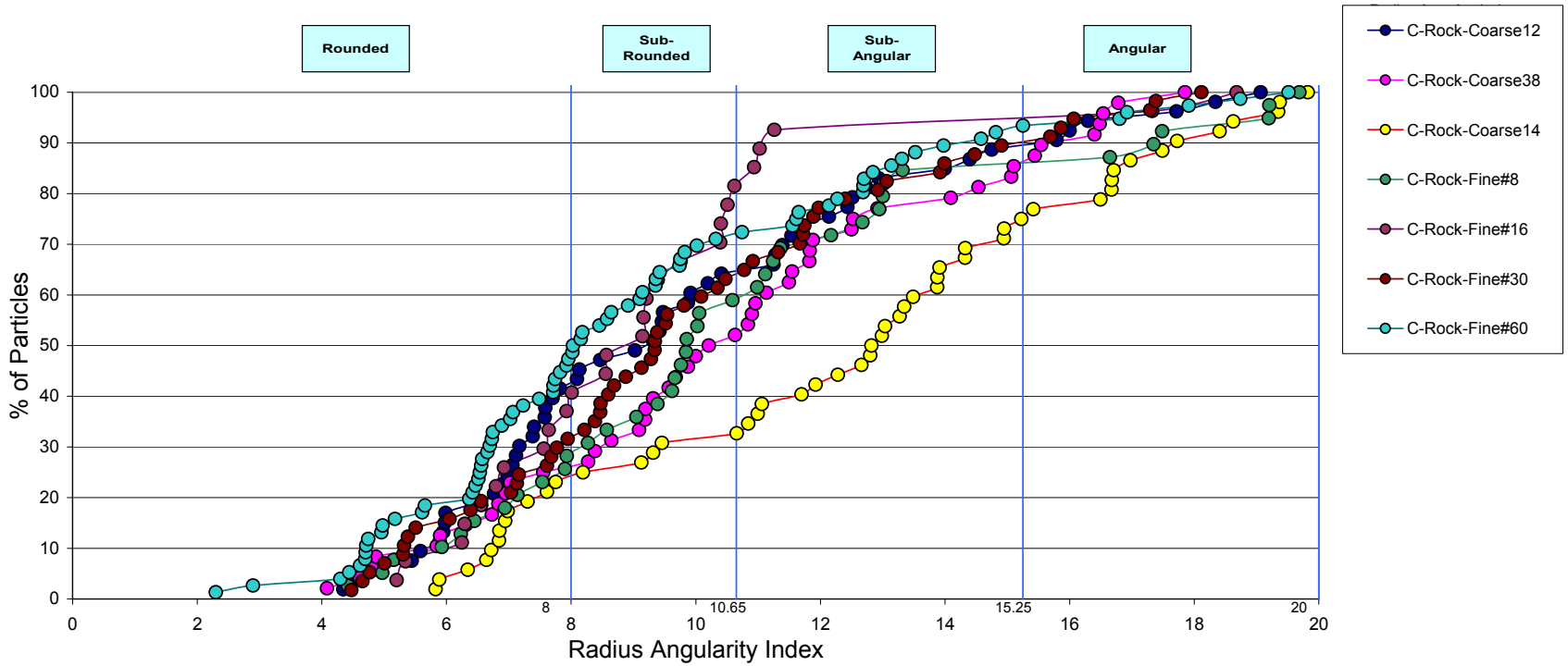

Figure D33. Radius angularity index limestone C-Rock

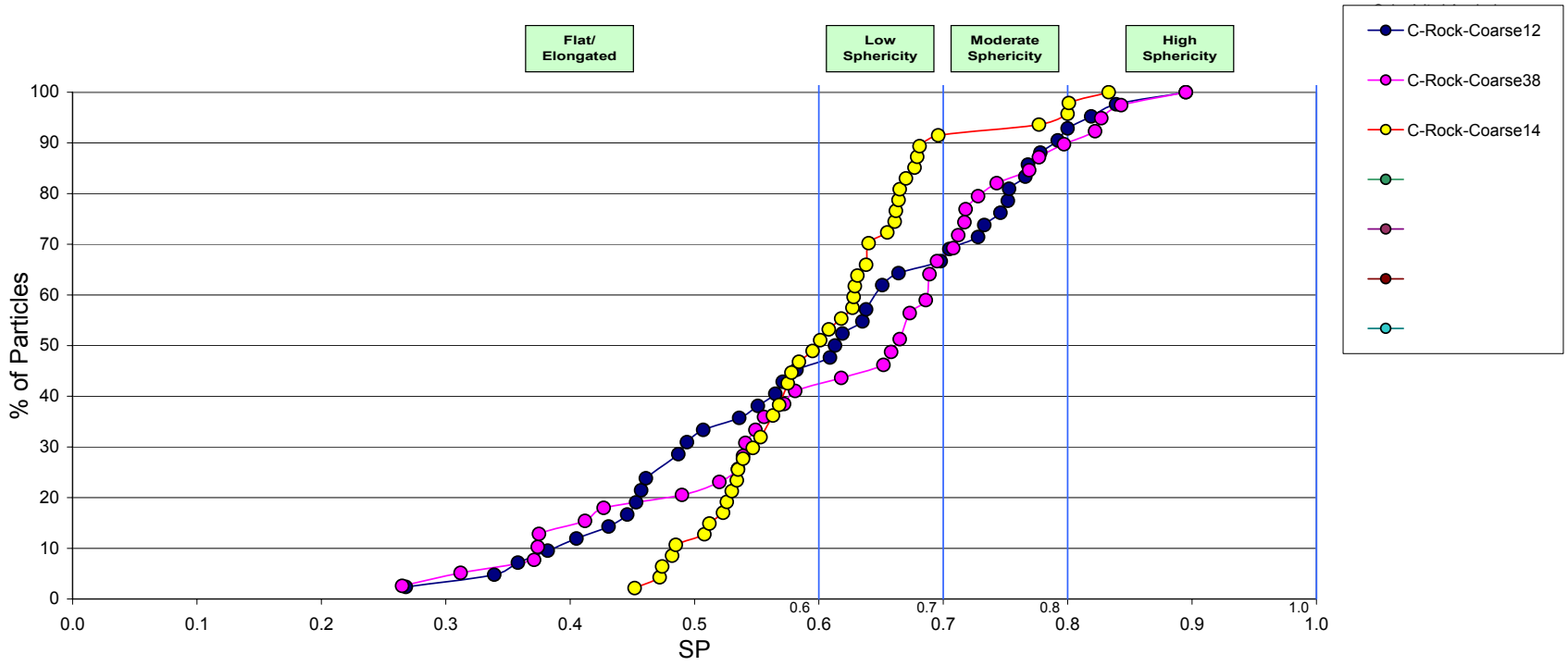

Figure D34. Sphericity limestone C-Rock

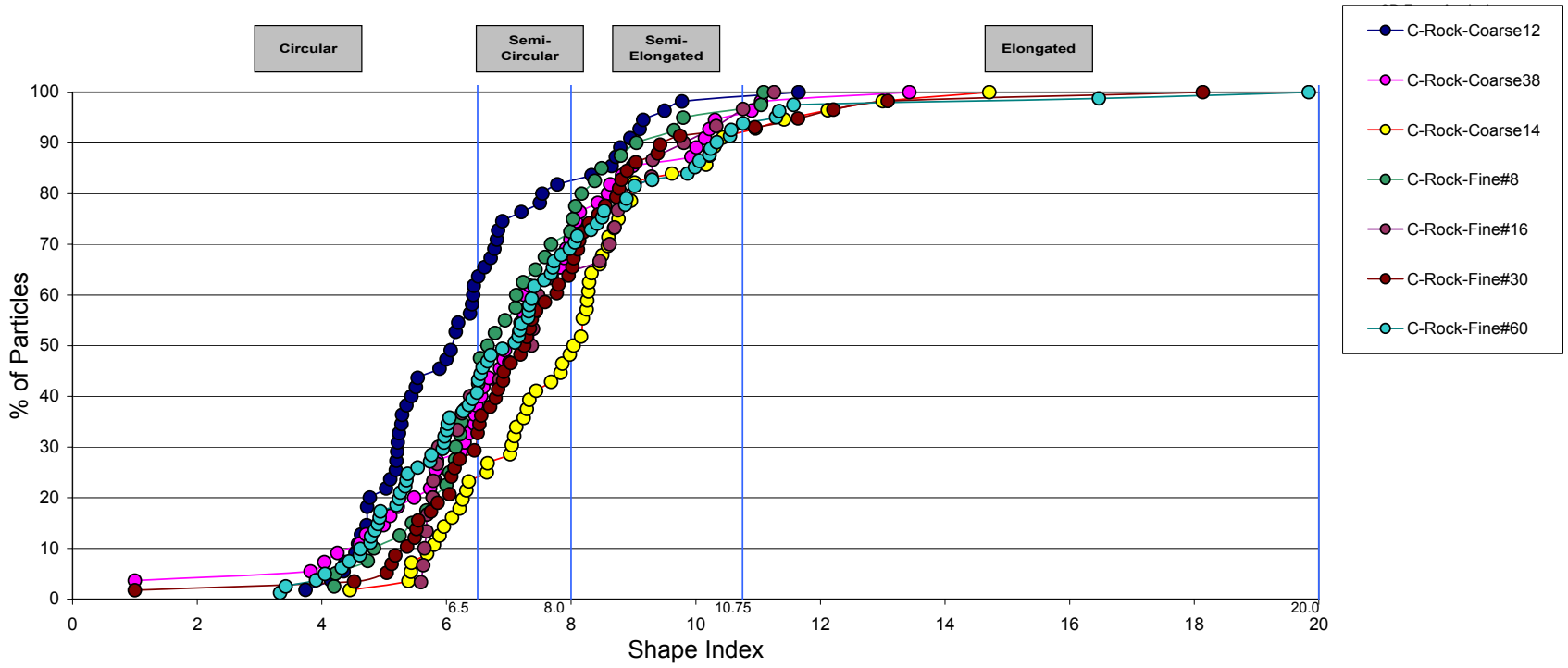

Figure D35. Shape index limestone C-Rock

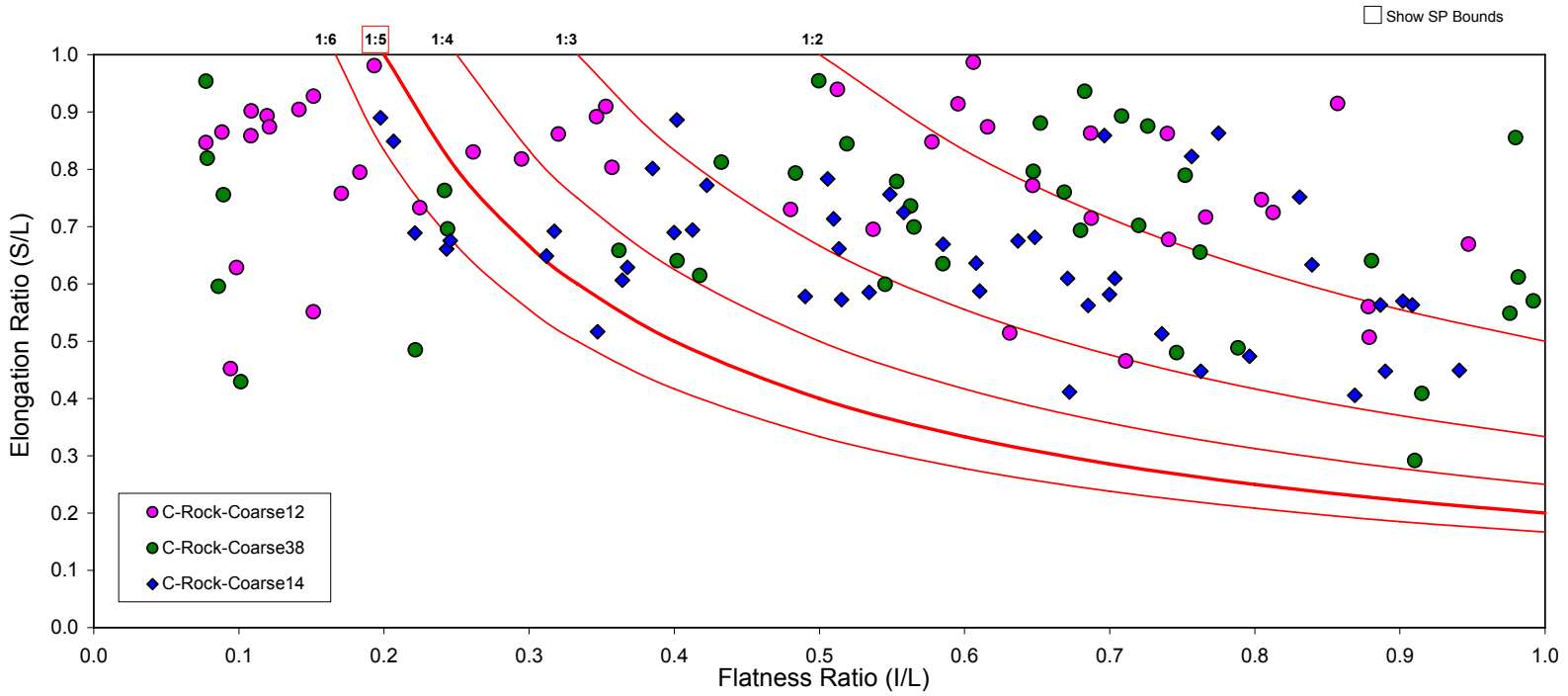

Figure D36. Flat to elongated ratio limestone C-Rock

D.2.3 C/F-Blend

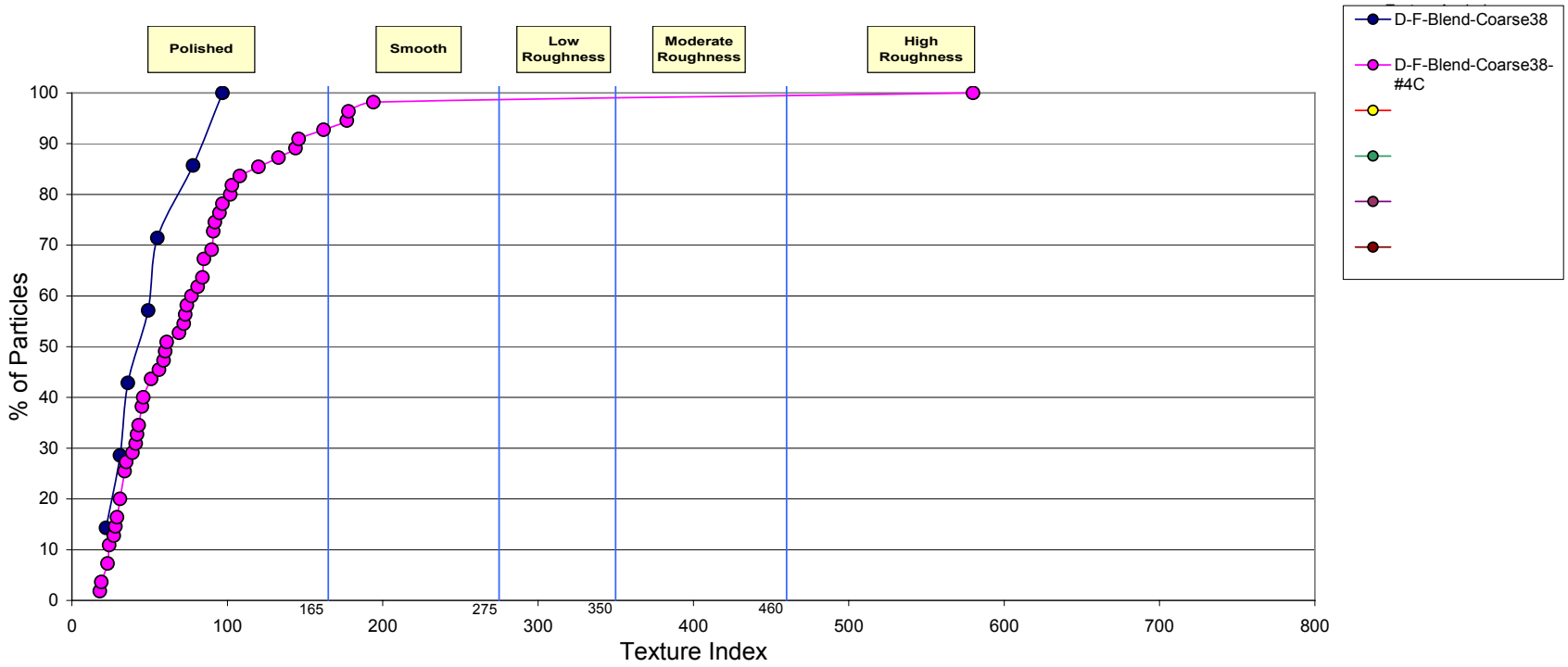

Figure D37. Texture index limestone D/F-Blend

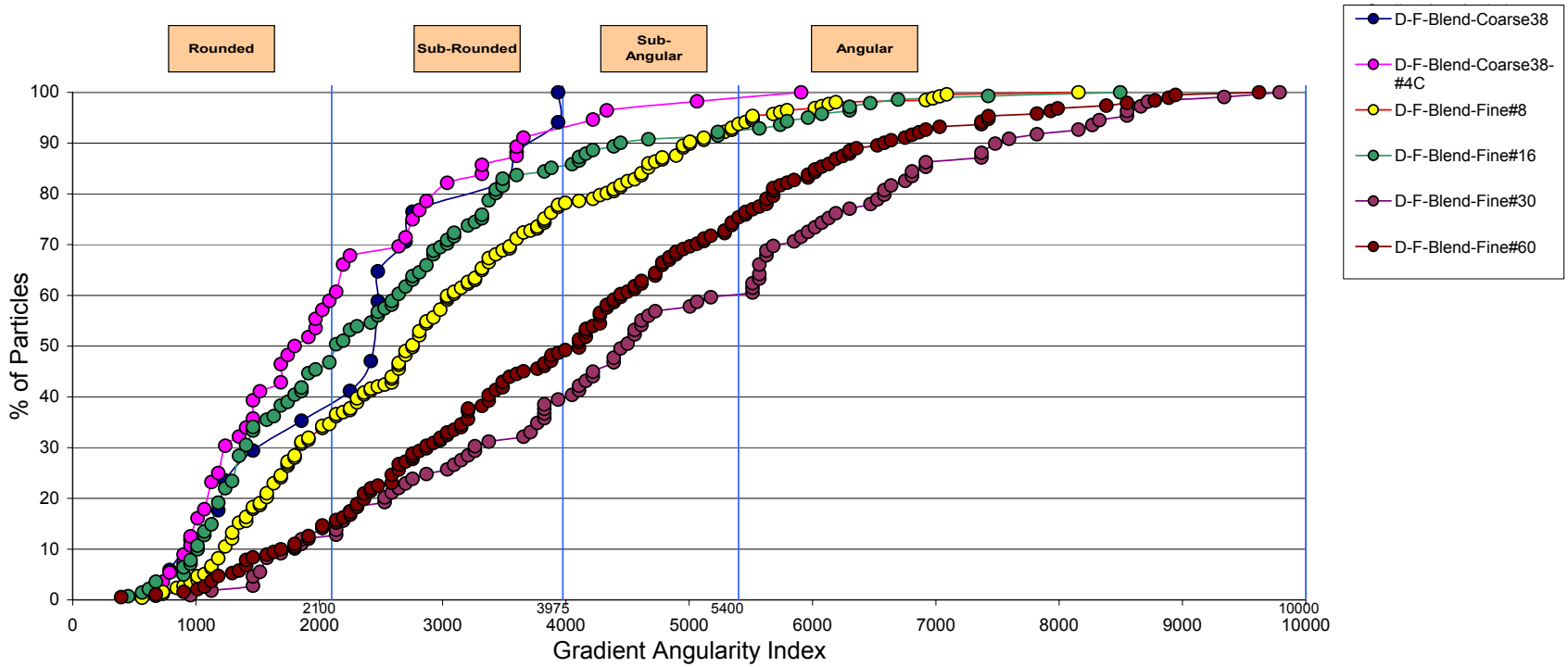

Figure D38. Gradient angularity limestone gravel D/F-Blend

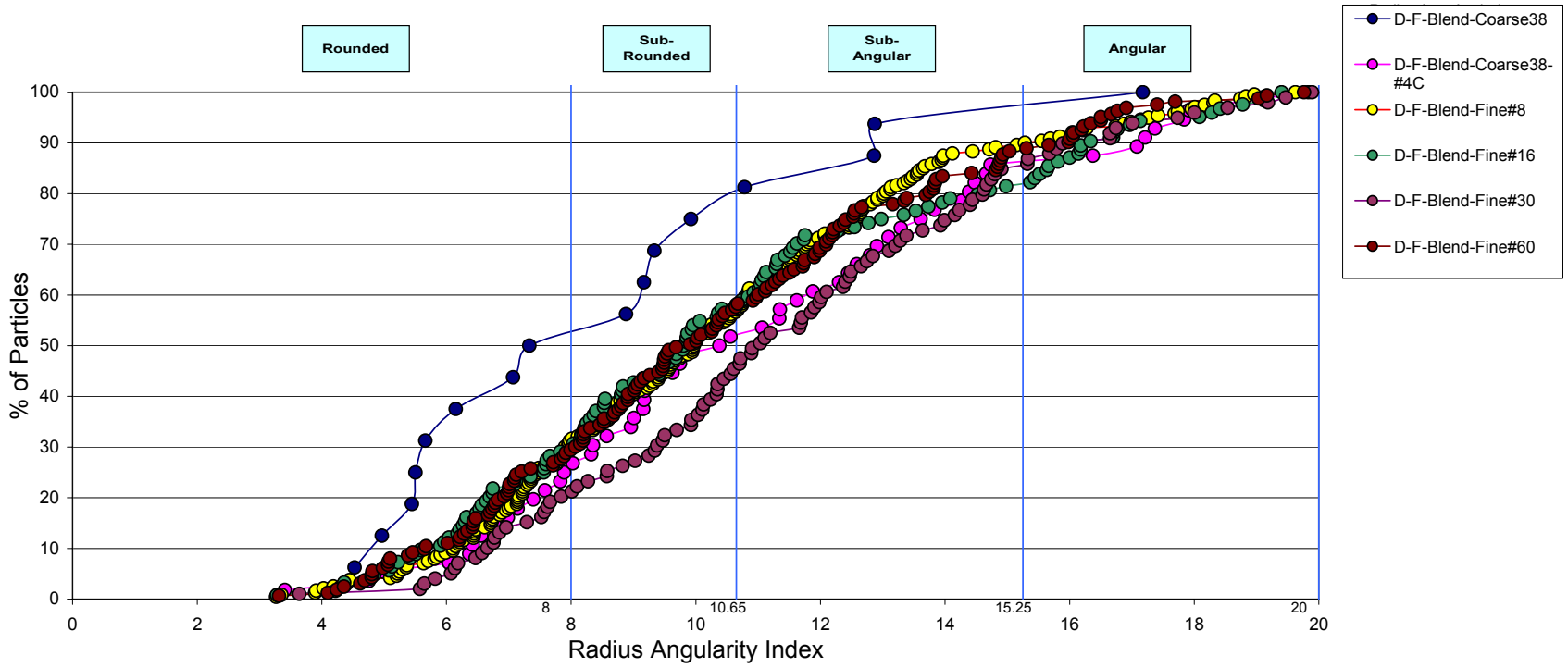

Figure D39. Radius angularity limestone gravel D/F-Blend

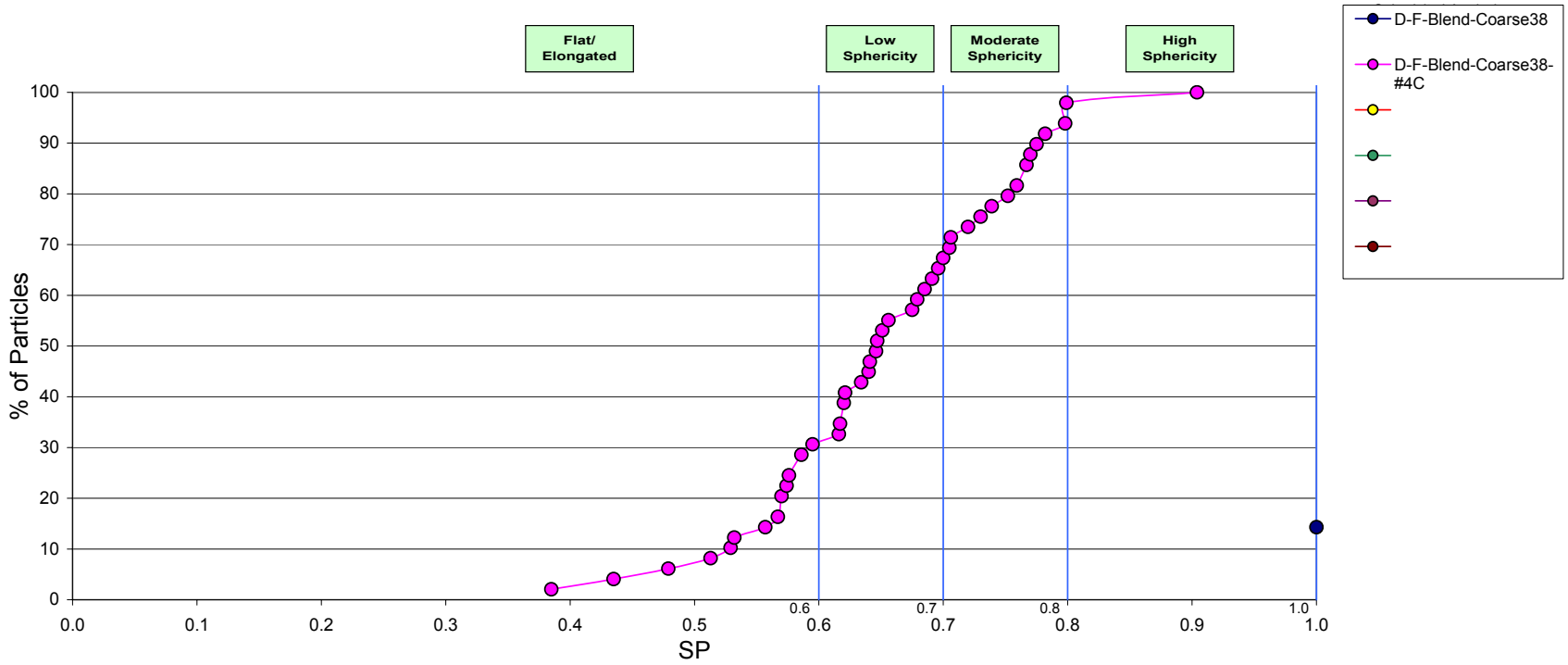

Figure D40. Sphericity limestone D/F-Blend

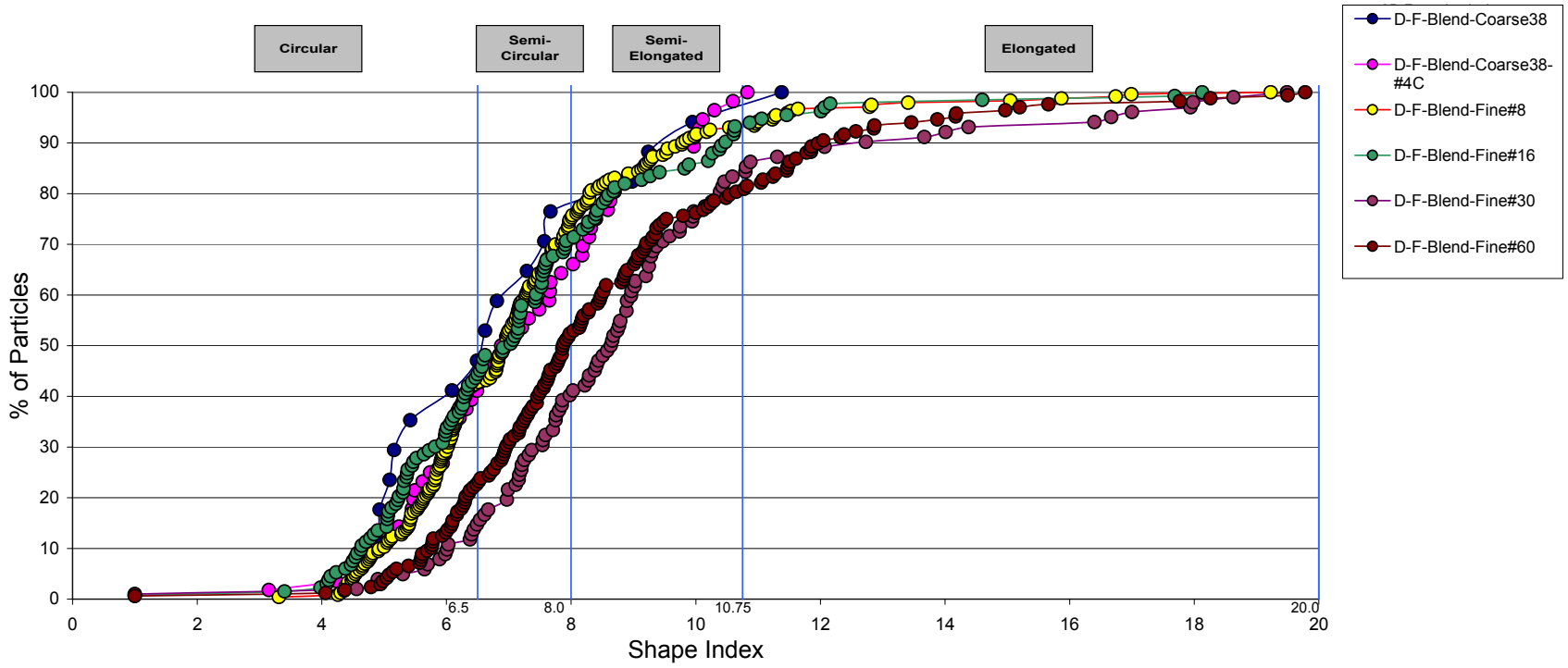

Figure D41. Shape index limestone D/F-Blend

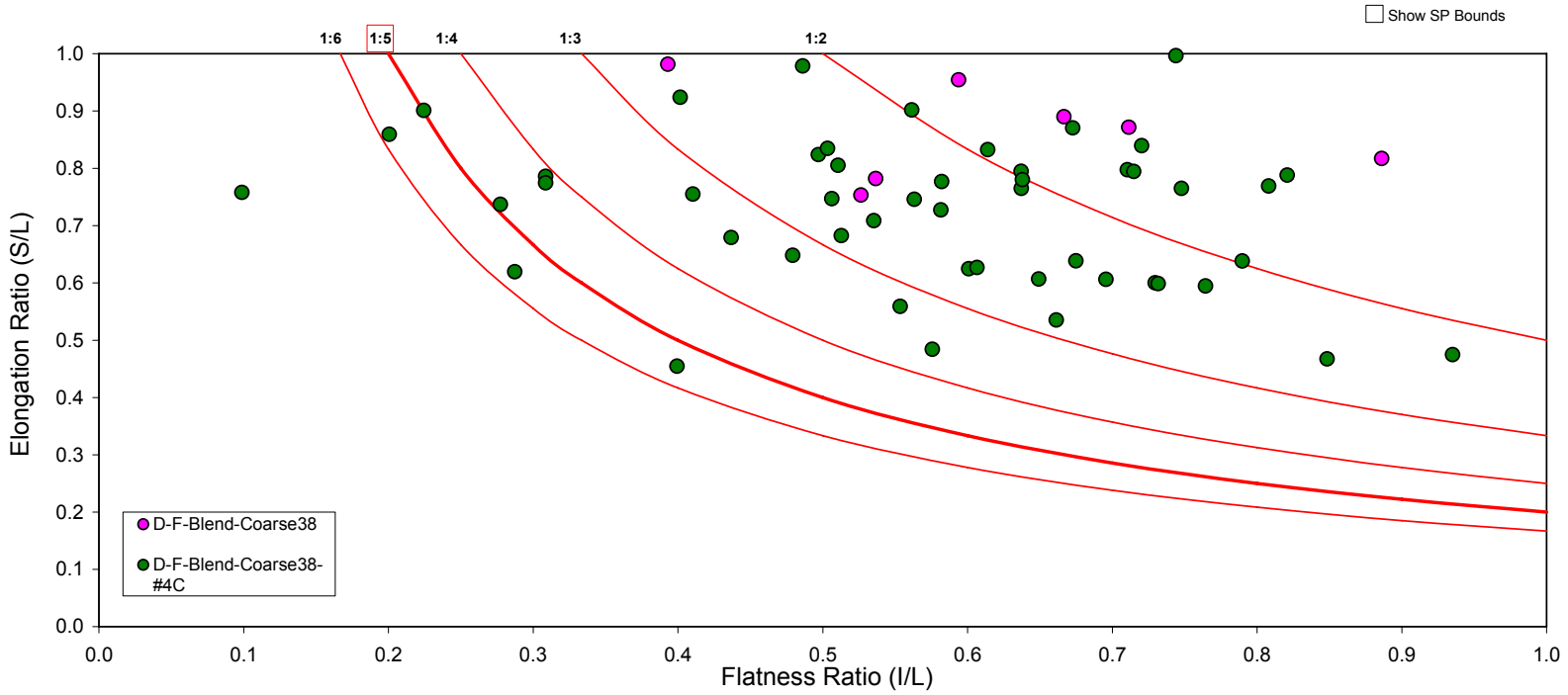

Figure D42. Flat to elongated ratio limestone D/F-Blend

D.2.4 Screenings

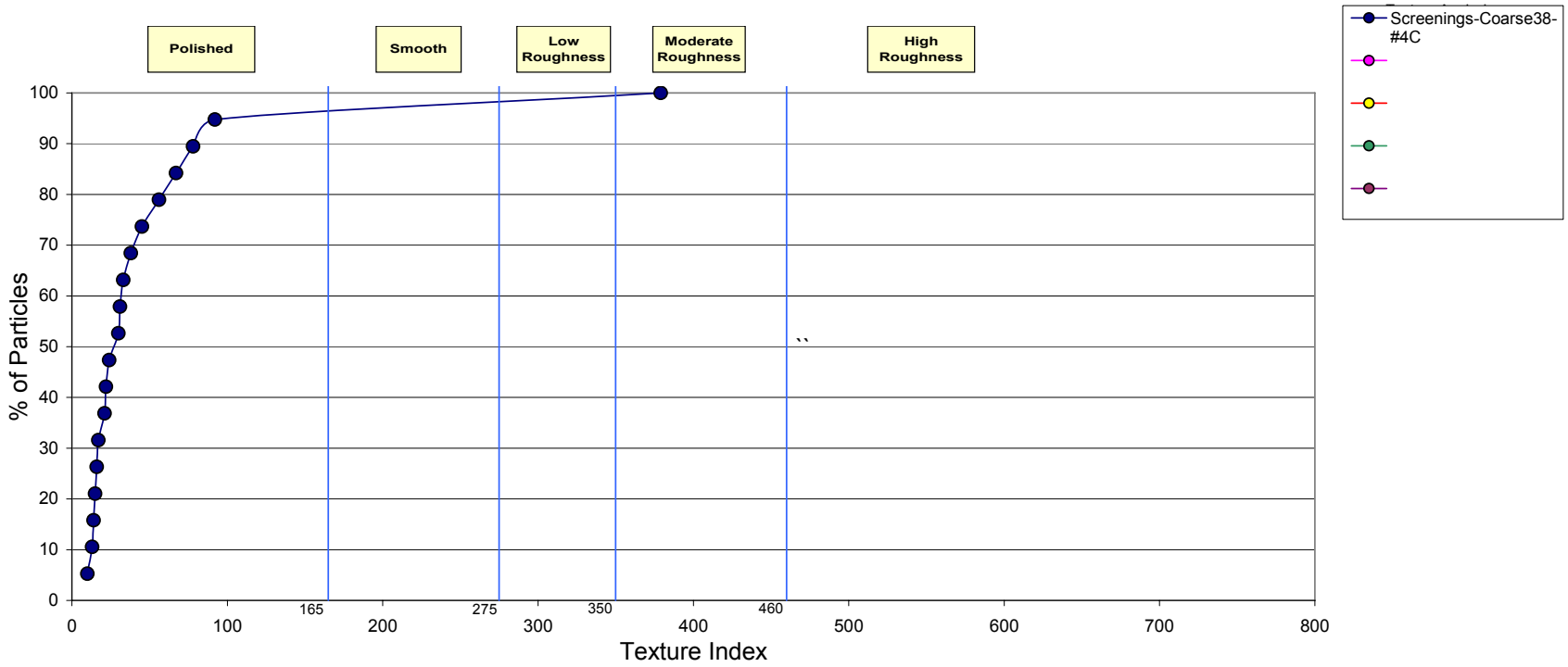

Figure D43. Texture index limestone screenings

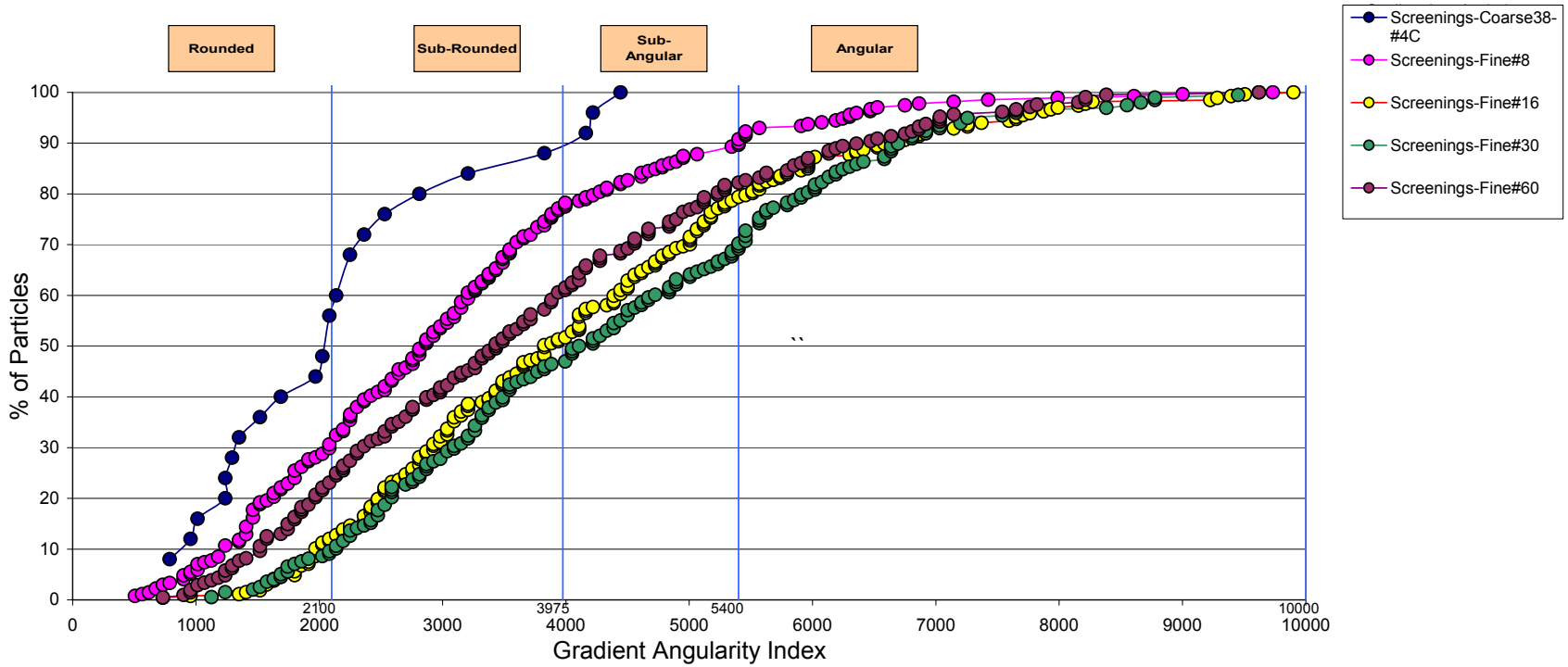

Figure D44. Gradient angularity index limestone screenings

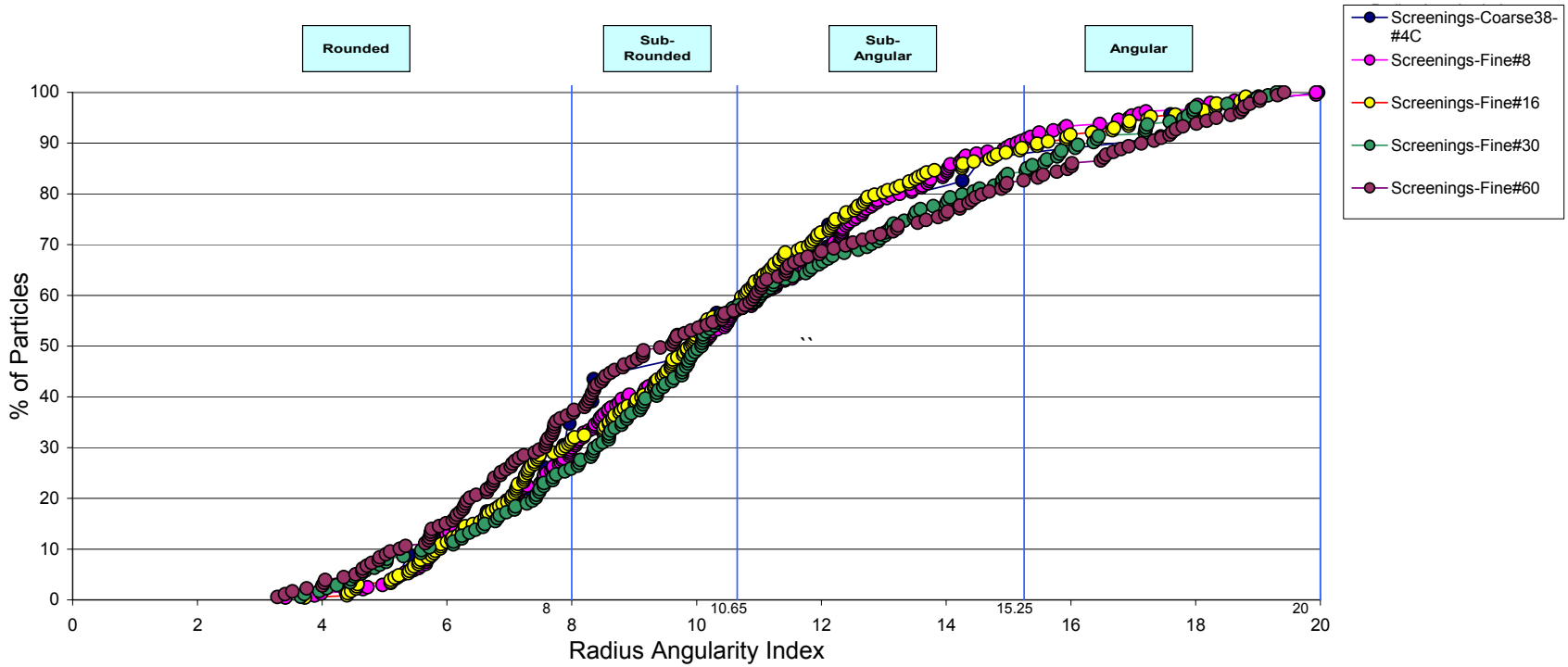

Figure D45. Radius angularity index limestone screenings

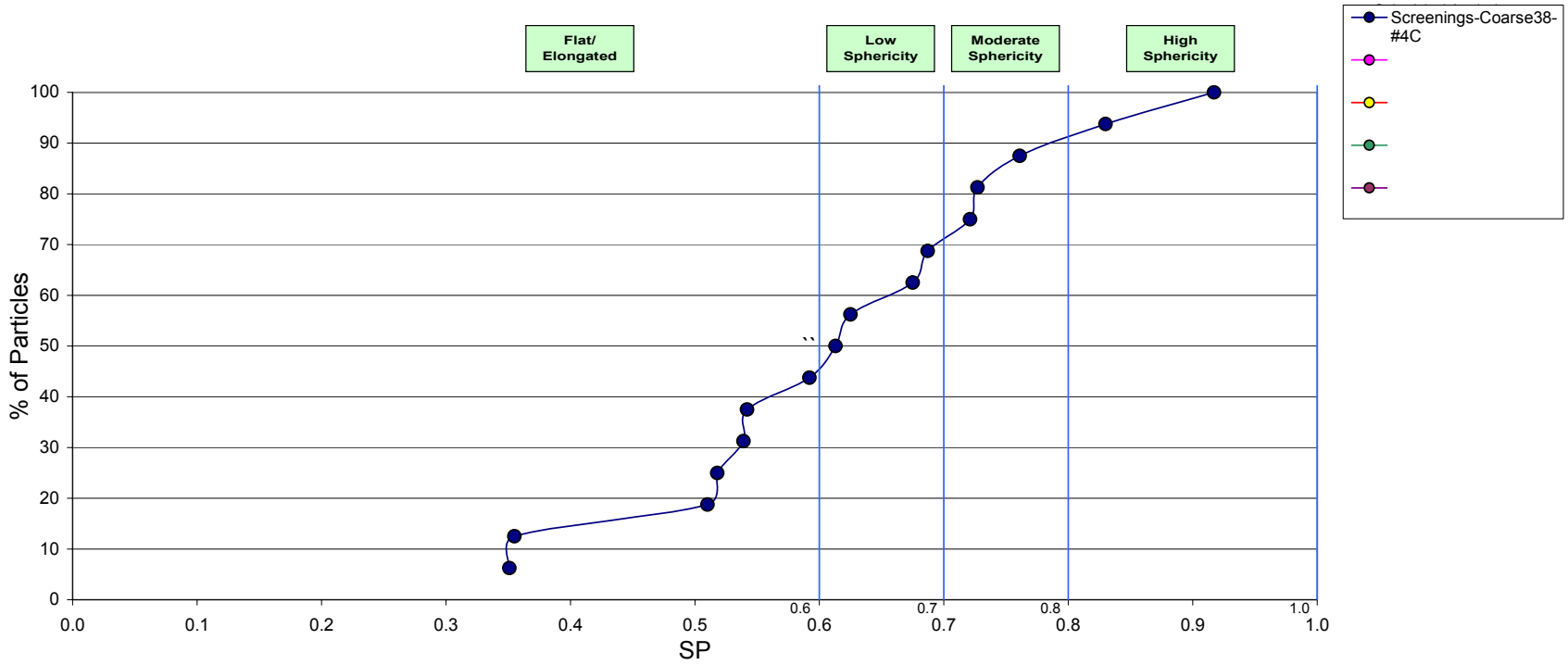

Figure D46. Sphericity limestone screenings

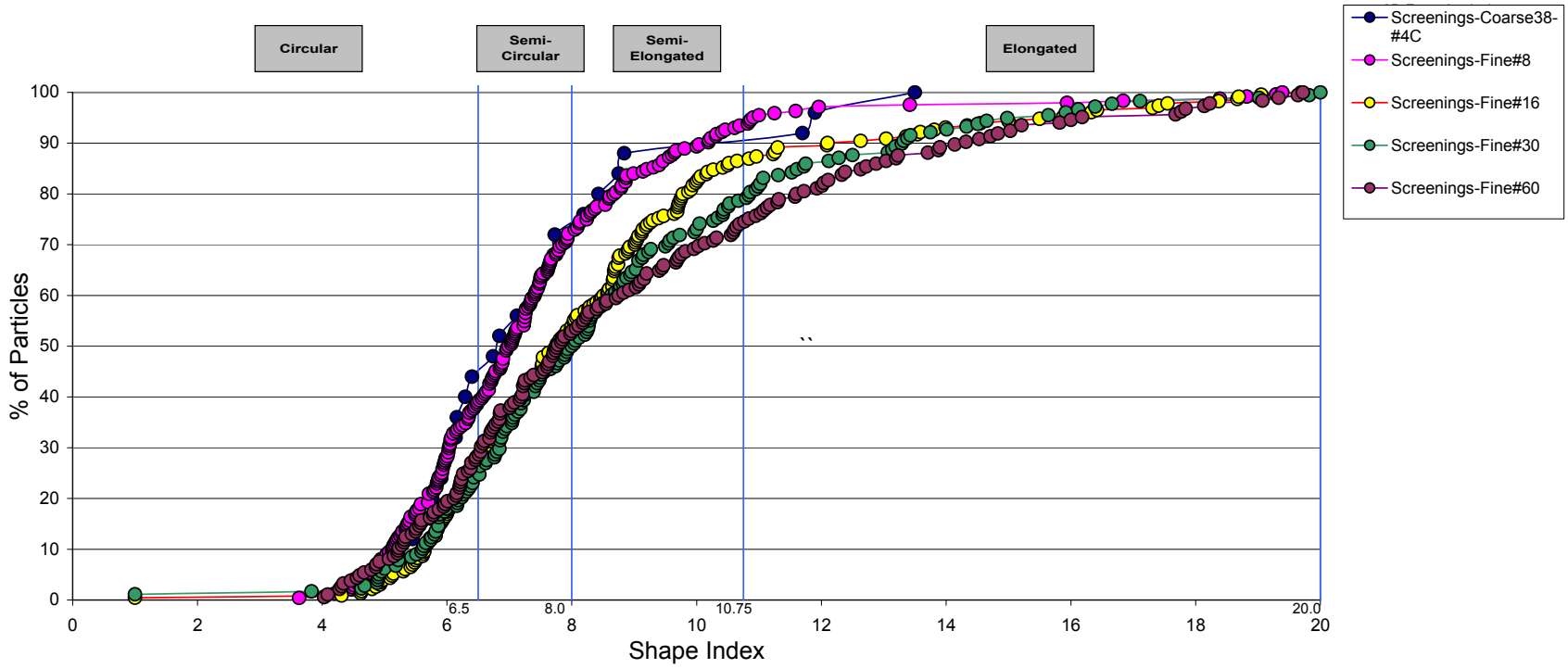

Figure D47. Shape index limestone screenings

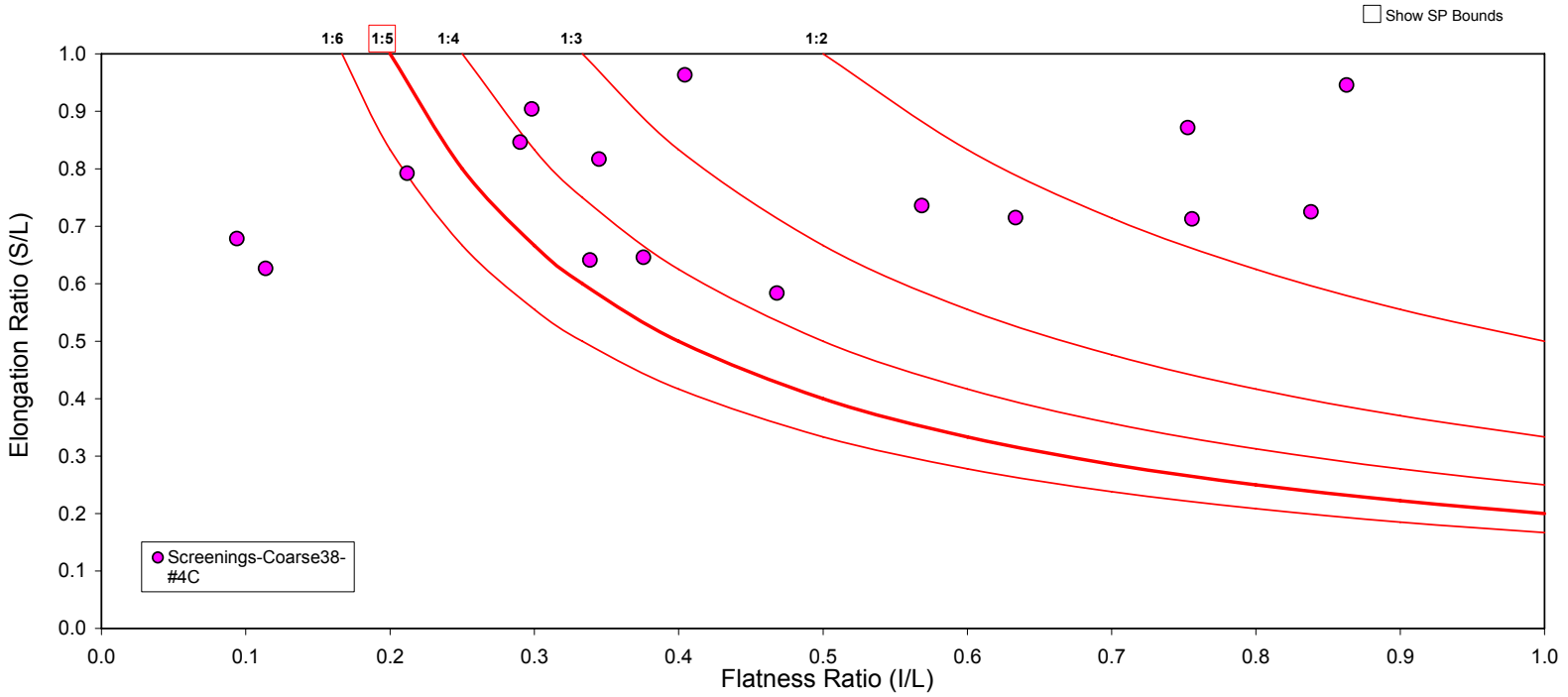

Figure D48. Flat to elongated ratio limestone screenings